frontiers | Research Topics

Compensatory growth: An adaptation to environmental stress in plants and animals

Edited by
Chao Li, Bernard Roitberg and E. Tobias Krause

Published in
Frontiers in Plant Science
Frontiers in Ecology and Evolution

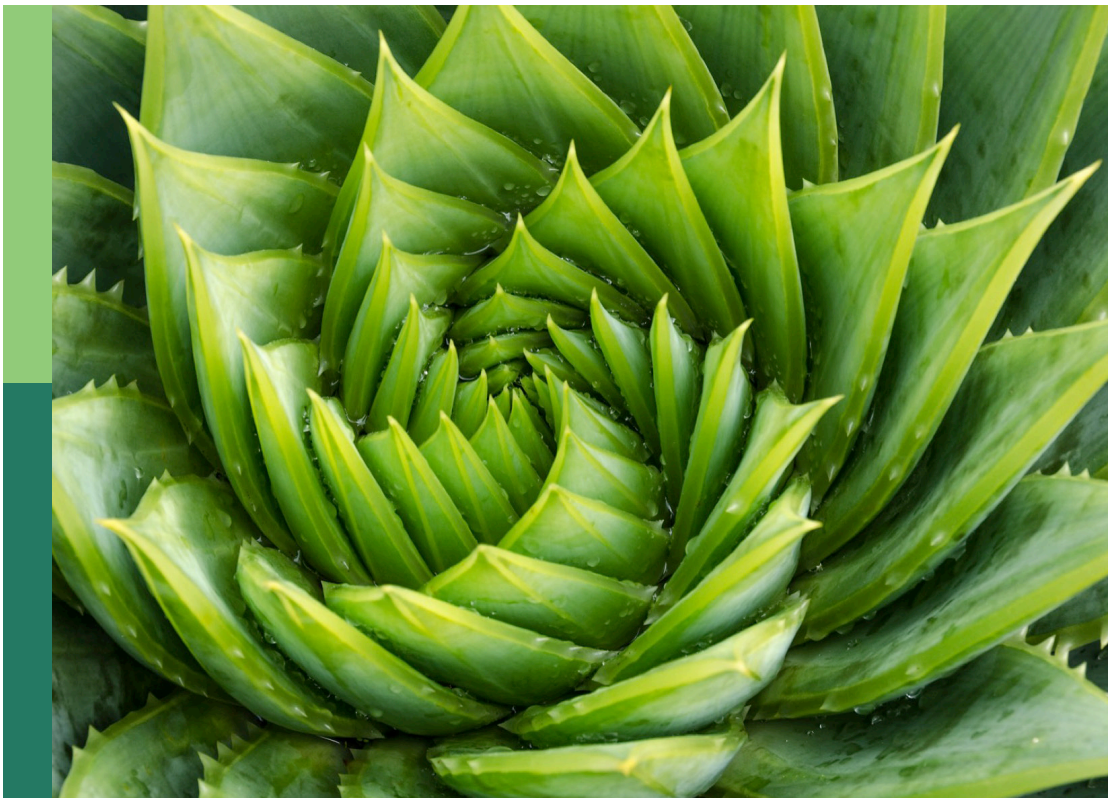

ISSN 1664-8714
ISBN 978-2-8325-4684-0
DOI 10.3389/978-2-8325-4684-0

About Frontiers

Frontiers is more than just an open access publisher of scholarly articles: it is a pioneering approach to the world of academia, radically improving the way scholarly research is managed. The grand vision of Frontiers is a world where all people have an equal opportunity to seek, share and generate knowledge. Frontiers provides immediate and permanent online open access to all its publications, but this alone is not enough to realize our grand goals.

Frontiers journal series

The Frontiers journal series is a multi-tier and interdisciplinary set of open-access, online journals, promising a paradigm shift from the current review, selection and dissemination processes in academic publishing. All Frontiers journals are driven by researchers for researchers; therefore, they constitute a service to the scholarly community. At the same time, the *Frontiers journal series* operates on a revolutionary invention, the tiered publishing system, initially addressing specific communities of scholars, and gradually climbing up to broader public understanding, thus serving the interests of the lay society, too.

Dedication to quality

Each Frontiers article is a landmark of the highest quality, thanks to genuinely collaborative interactions between authors and review editors, who include some of the world's best academicians. Research must be certified by peers before entering a stream of knowledge that may eventually reach the public - and shape society; therefore, Frontiers only applies the most rigorous and unbiased reviews. Frontiers revolutionizes research publishing by freely delivering the most outstanding research, evaluated with no bias from both the academic and social point of view. By applying the most advanced information technologies, Frontiers is catapulting scholarly publishing into a new generation.

What are Frontiers Research Topics?

Frontiers Research Topics are very popular trademarks of the *Frontiers journals series*: they are collections of at least ten articles, all centered on a particular subject. With their unique mix of varied contributions from Original Research to Review Articles, Frontiers Research Topics unify the most influential researchers, the latest key findings and historical advances in a hot research area.

Find out more on how to host your own Frontiers Research Topic or contribute to one as an author by contacting the Frontiers editorial office: frontiersin.org/about/contact

Compensatory growth: An adaptation to environmental stress in plants and animals

Topic editors

Chao Li — Canadian Forest Service, Canada

Bernard Roitberg — Simon Fraser University, Canada

E. Tobias Krause — Institute for Animal Welfare and Animal Husbandry, Friedrich-Loeffler-Institute, Germany

Citation

Li, C., Roitberg, B., Krause, E. T., eds. (2024). *Compensatory growth: An adaptation to environmental stress in plants and animals*. Lausanne: Frontiers Media SA.

doi: 10.3389/978-2-8325-4684-0

Table of contents

frontiers | Frontiers in Plant Science

TYPE Editorial
PUBLISHED 19 March 2024
DOI 10.3389/fpls.2024.1395038

OPEN ACCESS

EDITED AND REVIEWED BY
Sebastian Leuzinger,
Auckland University of Technology,
New Zealand

*CORRESPONDENCE
Chao Li
Chao.Li@NRCan-RNCan.gc.ca

RECEIVED 03 March 2024
ACCEPTED 08 March 2024
PUBLISHED 19 March 2024

CITATION
Roitberg B, Krause ET and Li C (2024) Editorial: Compensatory growth: an adaptation to environmental stress in plants and animals.
Front. Plant Sci. 15:1395038.
doi: 10.3389/fpls.2024.1395038

Editorial: Compensatory growth: an adaptation to environmental stress in plants and animals

Bernard Roitberg[1,2], E. Tobias Krause[3] and Chao Li[1]*

[1]Canadian Wood Fibre Centre, Canadian Forest Service, Edmonton, AB, Canada, [2]Department of Biological Sciences, Simon Fraser University, Burnaby, BC, Canada, [3]Institute of Animal Welfare and Animal Husbandry, Friedrich-Loeffler-Institute, Celle, Germany

KEYWORDS

adaptation, compensatory growth, catch-up growth, grassland, forest

Editorial on the Research Topic

Compensatory growth: an adaptation to environmental stress in plants and animals

Compensatory growth (CG) can be defined as increased growth rate of a previously restricted organism, and has been documented in a wide range of organisms in both the plant and animal kingdoms. Notably, CG can be expressed at the individual, population or even community level as illustrated in the research of this Research Topic. This widely-observed phenomenon has been of interest to scientists for more than a century because it directly impacts our understanding of life-history trade-offs and resource productivity, respectively. Interest in CG continues to be a stable Research Topic of interest with on average 463 paper/year in the last decade (i.e. Web of Science, search term "compensatory growth", time-period 2014-2023, minimum annual records 398, maximum 522; as of 2024-01-10).

Although compensatory growth is common, it may manifest itself in different ways from exact compensation (often referred to as catching-up growth) to under or over compensation where the comparison is with a non-restricted (i.e. control) group (Figure 1). As such, the variability in compensatory growth is as interesting as the phenomenon itself as it often has severe life-history consequences, e.g. costs on other individuals´ traits (Metcalfe and Monaghan, 2001). And, as is the case for many biological phenomena, cross-taxa consideration has the potential to explain both the inner workings and general principles associated with compensatory growth.

In this Research Topic, we have assembled 10 papers on various topics related to compensatory growth.

In Kong et al., the authors used controlled experiments to study the impact of dry-season irrigation and fertilizers on growth of *Eucalyptus* stands via enhanced litterfall decomposition. Their work demonstrates the importance of elucidating the drivers of CG, in this case, release of soil nutrients, a key limiting resource for compensatory growth in trees.

An ecosystem perspective was taken by Zhou et al. to examine how grasslands recover from drought as a form of CG. Furthermore, the authors consider both aboveground and belowground processes among plants and soil-based microorganisms as determinants of ecosystem level response, post-drought. Here, it is also important to keep in mind that CG

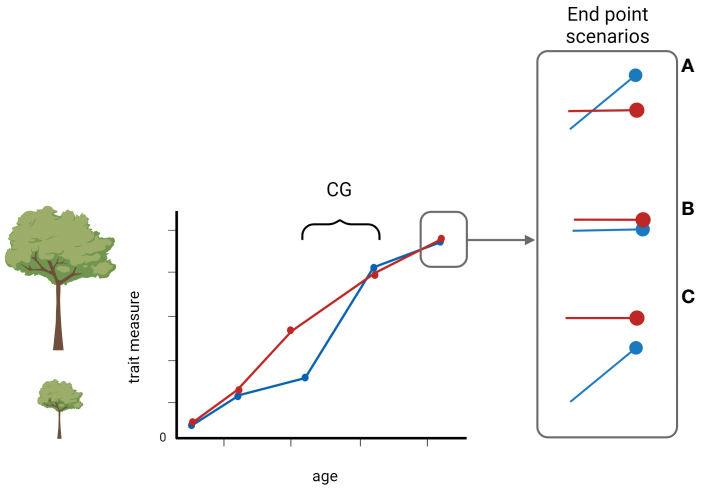

FIGURE 1
A schematic illustration of compensatory growth over time. The red line denotes normal growth, and the blue line indicates a trait of a measured unit that has experienced an unfavorable condition that resulted in a reduced growth. When the condition improved, the measured unit can display one of the three possible outcomes: **(A)** overcompensation, **(B)** exact compensation, often referred to as catch-up growth, or **(C)** undercompensation. Created with BioRender.com.

may be driven by changes in abundance of different species of grassland plants (i.e., ecosystem dynamics) or via increased performance of extant species (i.e., physiological response). There is a further attempt to consider how multiple species respond to stress and post-stress environments by Wang et al.; however, here the focus is on the impact of ammonia-oxidizing bacteria (AOB) on corn (*Zea mays*). In this case, experimentally induced increased presence of AOB, post-drought, led to greater soil nitrification and, as a result, enhanced performance of recipient corn roots and leaves, providing a mechanism to explain compensatory growth in this important crop.

Wu et al. take a mechanistic approach to explaining CG at the forest level. They studied functional traits (i.e., phenotypic traits that interact with the environment) of trees in an old-growth subtropical forest to determine how such trees respond to environmental change. Doing so provides a mechanism for explaining and predicting how forest dynamics are driven by stress (e.g. drought).

Notwithstanding that many interactions between plants and other types of organisms may be neutral or positive (e.g., pollinator-plant mutualisms), insect herbivores can stress their plant hosts by removing plant tissue or vectoring viruses. Moreover, such damage may occur at different plant stages thus adding a ontogenic slant to the problem. Bustos-Segura et al. used an experimental approach to show that lima bean plants are more likely to generate CG or tolerance in the lingo to plant-insect interactions. They found that when such damage is inflicted on seedlings that CG was more likely than when similar damage was applied to juvenile plants mirroring results found in the animal kingdom (e.g., Taborsky, 2006).

Finally, in a series of papers that relate CG to the enhancement of forest productivity since the concept of CG being introduced into forestry research to explain diverse post-thinning stand dynamics by Li et al. (2018), started from establishing a CG conceptual framework for seeking ways of enhancing forest productivity, one of the most desirable outcomes from sustainable forest management, and proposing a research roadmap by Li et al. Accordingly, Li et al. (2021) reviewed modern CG research development and examples from various fields and how different industries benefitted from CG research. Followed by presenting empirical evidence of diverse CG patterns including overcompensation in forest stands across Canada in Li et al. to support the CG conceptual framework. Further, Li et al. and Li et al. (2024) demonstrated that the outcomes of CG are predictable through a statistics-based TreeCG (Tree Compensatory Growth) model. Based on the life-history theory, the TAG (Tree Adaptive Growth) model was developed by Roitberg et al. that proved the previously overlooked overcompensation phenomenon is an expected outcome for trees, in a manner similar to other organisms despite their relatively slow growth and great longevity. As important from an applied-ecology perspective, such responses from individual trees can be scaled up to stands, demonstrating that proper pre-commercial thinning can increase productivity of forests in the long-term.

In sum, this Research Topic provides new insights on how and why CG occurs in nature and, like any good investigation, it raises new questions such as how climate change might alter such responses in the near future. What is clear, however, is that nearly all living organisms are dynamic and will respond in kind as the world changes. CG is an across taxa phenomenon, that although trivial at first glance (growing more when resources become more available after an initial shortage), has complex impact on life histories of organisms.

Author contributions

BR: Conceptualization, Writing – original draft, Writing – review & editing. EK: Conceptualization, Visualization, Writing – review & editing. CL: Conceptualization, Funding acquisition, Writing – original draft, Writing – review & editing.

Funding

The author(s) declare that financial support was received for the research, authorship, and/or publication of this article. This work was financially supported by Natural Resources Canada-Canadian Forest Service's Developing Sustainable Fibre Solutions Research Program.

Conflict of interest

The authors declare that the research was conducted in the absence of any commercial or financial relationships that could be construed as a potential conflict of interest.

The author(s) declared that they were an editorial board member of Frontiers, at the time of submission. This had no impact on the peer review process and the final decision.

Publisher's note

References

Li, C., Barclay, H., Roitberg, B., and Lalonde, R. (2021). Ecology and prediction of compensatory growth: from theory to application in forestry. *Front. Plant Sci.* 12. doi: 10.3389/fpls.2021.655417

Li, C., Barclay, H., Roitberg, B., Lalonde, B., Huang, S., Kombo, D., et al. (2024). *Realizing the full growth potential of a forest: TreeCG, a forest compensatory growth model. Fibre Fact 28* (Ottawa, Ontario, Canada: Can. Wood Fibre Cent., Can. For. Serv., Nat. Resour. Can.). Available at: https://cfs.nrcan.gc.ca/publications?id=41233&lang=en_CA.

Li, C., Huang, S., Barclay, H., and Filipescu, C. (2018). Estimation of compensatory growth of coastal Douglas-fir to precommercial thinning across a site quality gradient. *For. Ecol. Manage.* 429, 308–316. doi: 10.1016/j.foreco.2018.07.028

Metcalfe, N. B., and Monaghan, P. (2001). Compensation for a bad start: grow now, pay later? *Trends Ecol. Evol.* 16, 254–260. doi: 10.1016/S0169-5347(01)02124-3

Taborsky, B. (2006). The influence of juvenile and adult environments on life-history trajectories. *R. Soc Proc. B.* 273, 741–750. doi: 10.1098/rspb.2005.3347

frontiers in Plant Science

SYSTEMATIC REVIEW
published: 29 September 2020
doi: 10.3389/fpls.2020.575211

Forest Productivity Enhancement and Compensatory Growth: A Review and Synthesis

Chao Li[1*], *Hugh Barclay*[2†], *Bernard Roitberg*[1,3†] *and Robert Lalonde*[4]

[1] Canadian Wood Fibre Centre, Canadian Forest Service, Edmonton, AB, Canada, [2] Pacific Forestry Centre, Canadian Forest Service, Victoria, BC, Canada, [3] Department of Biological Sciences, Simon Fraser University, Burnaby, BC, Canada, [4] Department of Biology, University of British Columbia-Okanagan, Kelowna, BC, Canada

This review and synthesis article attempts to integrate observations from forestry to contemporary development in related biological research fields to explore the issue of forest productivity enhancement and its contributions in mitigating the wood supply shortage now facing the forest sector. Compensatory growth has been clearly demonstrated in the long-term precommercial thinning and fertilization trial near the Shawnigan Lake, British Columbia, Canada. This phenomenon appears similar to many observations from other biological fields. The concept of compensatory growth can be applied to forest productivity enhancement through overcompensation, by taking advantage of theories and methods developed in other compensatory growth research. Modeling technology provides an alternative approach in elucidating the mechanisms of overcompensation, which could reveal whether the Shawnigan Lake case could be generalized to other tree species and regions. A new mitigation strategy for dealing with issues related to wood supply shortage could be formed through searching for and creating conditions promoting overcompensation. A forest growth model that is state dependent could provide a way of investigating the effect of partial harvest on forest growth trajectories and stand dynamics. Results from such a study could provide cost-effective decision support tools to practitioners.

Keywords: forest growth model, overcompensation, partial harvest, plant response manipulation, wood supply

OPEN ACCESS

Edited by:
Jian-Guo Huang,
Chinese Academy of Sciences, China

Reviewed by:
Miguel Montoro Girona,
Université du Québec en Abitibi Témiscamingue, Canada
Lina Fusaro,
Italian National Research Council, Italy

****Correspondence:***
Chao Li
chao.li@canada.ca

[†]Retired

Specialty section:
This article was submitted to Functional Plant Ecology, a section of the journal Frontiers in Plant Science

Received: *22 June 2020*
Accepted: *11 September 2020*
Published: *29 September 2020*

Citation:
Li C, Barclay H, Roitberg B and Lalonde R (2020) Forest Productivity Enhancement and Compensatory Growth: A Review and Synthesis. Front. Plant Sci. 11:575211. doi: 10.3389/fpls.2020.575211

INTRODUCTION

Forest productivity has historically been a central concern in forestry, due to its close relation to timber production (Leuschner, 1984; Avery and Burkhart, 1994; Wenger, 1984) and ecosystem services such as biodiversity and wildlife habitat protection (Jenkins and Schaap, 2018; Felton et al., 2020) and carbon storage (Canadian Council of Forest Ministers, 2000; Davis et al., 2001). This concern has become urgent recently due to increasing market demands and potential climate change impact (IPCC, 2007), and enhancing concern for environmental protection (FAO, 2016). As a result, accurate estimation of forest productivity appears crucial in decisions of sustainable forest management. Here we attempt to provide a systematic review on the subject and apply the concept of compensatory growth (CG) to explain the forest dynamics after experiencing a partial mortality

caused by both anthropogenic and natural disturbances. This synthesis is aimed at offering a new approach of handling wood supply shortage related issues.

Forest Productivity

The term forest productivity has been widely used in forestry-related literature (Crow et al., 2006; Keeling and Phillips, 2007; Zhang et al., 2012; Van Bogaert et al., 2015). However, this term could mean different things to different people. Two meanings can be identified: *cumulative increase* and *net annual increase* of forest volume.

Odum (1959) distinguishes between *primary productivity* (the rate at which energy is stored by photosynthetic and chemosynthetic activity of producer organisms, chiefly green plants) and *secondary productivity* (the rate at which the carbon stored by primary producers is assimilated by animals or decomposers). Primary productivity is further divided into *gross primary productivity*, "the total rate of photosynthesis including the organic matter used up in respiration during the measurement period," and *net primary productivity* (NPP), "the rate of storage of organic matter in plant tissues in excess of the respiratory utilization by the plants during the period of measurement." In the context of a forest, NPP includes not only the biomass in trees, but also that in herbs and shrubs, although the biomass of herbs and shrubs is usually negligible compared with that of trees. These definitions have become standard in the ecological literature. Thus, the net productivity of trees (the items of interest to most foresters) usually closely approximate the NPP. The term "productivity" is noteworthy because it is a rate and involves acquisition of photosynthate per unit time.

From a forestry perspective, forest productivity is often defined as the standing forest volume at a given time t, V_t, which is the cumulative increase of stand volume since the stand was initiated (at t=t_0). It is referred to as yield in studies of forest growth and yield (Avery and Burkhart, 1994; Weetman and Mitchell, 2013). Typically, the term productivity is used to account for the accumulation of aboveground stem wood in standing trees, although it may also include below-ground accumulation. V_t will generally increase with stand age and generally a plot of volume over time has a sigmoid shape that asymptotes at the site's carrying capacity. Forest productivity is generally the basis for evaluating current forest inventory, planning bio-economy and sustainable forest management, and assessing current and future wood supply. This cumulative increase definition will be used in the current study. For carbon related studies, this definition of forest productivity is mainly concerned with carbon storage (Kurz et al., 1992; Kurz et al., 2009).

Research on forest productivity can be categorized in two ways. Most efforts have been focused on how to improve evaluation methods and accuracy of current forest productivity for a given site or forest (e.g., Martin, 1991; Huang et al., 2001). These efforts were aimed at deepening the understanding of the dynamics of ecosystems and increasing the potential of biomass production, which would improve regional carbon budgets. Such studies may also contribute to the evaluation of the effects of climate change (e.g., Biosvenue and Running, 2006). By contrast, other studies are devoted to exploring whether current forest productivity could be enhanced under normal conditions, and if so how and to what extent the enhancement could be implemented (e.g., Norby et al., 2010). Such studies enhance predictions as to future forest productivity under various conditions, including silvicultural operations.

Enhancing forest productivity will help meet the increasing wood utilization demands, especially when more frequent natural disturbances under a wide range of climate change scenarios could increase wood supply shortages (Li et al., 2000; Kirilenko and Sedjo, 2007).

Forest productivity enhancement can be viewed from two different approaches: *proactive* vs. *passive*. From a proactive perspective, the research focus is on the conditions that promote forest productivity enhancement. Here, one might view enhancement of forest productivity as a possible natural solution to resolve the issues related to wood supply shortage, because increased forest productivity would provide more wood volume being harvested for forest products such as lumber and pulp. The challenges involved with this approach include both scientific and operational investigations. From a biological and ecological view, the questions focus on what determines forest productivity, and whether and how it could be enhanced to satisfy increasing utilization demands, as well as ecosystem carbon dynamics and health and integrity as a whole. From an operational view, however, one would expect to see practical examples of forest productivity enhanced after some conditions have been applied such as silvicultural treatments. The stand volumes of the sites treated by precommercial thinning (PCT) exceeded those of control sites displayed in the long-term PCT effect studies of balsam fir in the Green River, New Brunswick (Pitt and Lanteigne, 2008) and Douglas-fir in the Shawnigan Lake trial in British Columbia (Li et al., 2018), which are examples of such treatments.

From a forest company's operational perspective, however, both the proactive approach described above and the passive approach must be taken into account. The passive approach answers the question of what to do to make the best use of current forest productivity. This approach includes full, multiple, and optimal utilization of current forest productivity through matching the right fiber attributes with the right products, in the right place at the right market time (e.g., Li, 2009), and optimization technology in the operations research could play an important role. The passive approach also involves the direct application of the basic principles of forest economics. For example, Brodie and Tedder (1982) provided an example in considering the effect of regeneration delay on harvest scheduling for both surplus and deficit forest inventory. It can also include the design, analysis, and higher-level plans such as the application of global forest product models (e.g., Buongiorno et al., 2003). This approach needs to also take into account, the risk of natural disturbances, including fires, pests, windstorms, and extreme weather conditions (e.g., Li et al., 2000; Schelhaas et al., 2003; Keane et al., 2004; Seidl et al., 2011; Gustafson and

Sturtevant, 2013; Kretchun et al., 2014; Gustafson et al., 2017; Navarro et al., 2018; Díaz-Yáñez et al., 2019; Lavoie et al., 2019), and the effects of climate change (Martin-Benito et al. 2008; He et al., 2017; Montoro Girona et al., 2019; Gustafson et al., 2020). In the current study, more attention will be paid to the proactive approach, i.e., directly working from biological and ecological enhancements, and we will leave the passive approach to others.

Limits for Forest Productivity

Forest productivity is mainly limited by factors such as resource availability to the trees on site, and physical conditions at a site (Barnes et al., 1998; Odum and Barrett, 2005; Martin-Benito et al. 2008). These resources may include light, space, soil nutrients, and water, etc. Physical conditions may include elevation, topography such as slope and aspect, climate and weather variables and their dynamic patterns over time.

The theoretical expectation of resource-dependent forest growth can be traced back to the famous Clementsian forest succession concept of "forest ecosystem change occurring over a range of decades to centuries with resulting change in composition structure, and biomass of vegetation" (Barnes et al., 1998 p. 41). Forest succession has been stated as a "universal law" that "all bare places give rise to new communities except those which present the most extreme conditions of water, temperature, light, or soil" (Clements, 1916). Its significance persists and was described by Eugene Odum (1969) as critical for human society. Despite different viewpoints, critical reviews, and new perspectives, the basic principles of forest succession theory remain unchanged in three ways: (1) succession is an orderly process that is reasonably directional and therefore predictable; (2) succession results from modification of the physical environment by the community, i.e., "community controlled"; and (3) succession will culminate in a stabilized (climax, mature) ecosystem with homeostatic properties (McIntosh, 1981). From a perspective of plant population ecology, the biomass of a population will increase with time or stand age and gradually and eventually reach a plateau or mature (climax) state.

The conventional theory of forest succession predicts the growth of a forest over time up to a level of dynamic equilibrium represented by a climax (mature) community. This general pattern, in a graphical form, can be characterized as a sigmoid shape with volume over time increasing until an asymptotic status is reached wherein the level of the plateau will be determined by the site carrying capacity, which represents the maximal capability of supporting and maintaining biomass at the site. Consequently, forest growth models at the stand level also generally have such a form. However, increasing observations of age-related decline in forest productivity suggest that forest growth patterns might not always be congruent with the predictions from forest succession theory, at the community level (e.g., Ryan et al., 1997; Binkley et al., 2002; Berger et al., 2004; Zaehle et al., 2009; Kuuluvainen and Gauthier, 2018).

Similar theories are also reflected in the study of the relationship between forest productivity and stand density, as summarized in Baskerville (1965) as follows:

"There are two principle theories dealing with the correlation of forest production to stand density. The one put forward by E. Assmann states that growth per unit area increases with increased stocking until optimum production is reached at some definable density. Beyond this point, production decreases. Assmann used basal area expressed as a percent of the basal area of fully stocked stand as his measure of density. His hypothesis was developed largely from an analysis of classical European yield tables and from observation of European thinning experiments. Assmann held that optimum production occurred within a very narrow range of densities and only on exceptionally good sites would the curve be broad, indicating roughly equivalent production across a wide range of densities.

The second general hypothesis is that put forward by C.M. Möller. He postulated that production increases with increased stocking up to the point of full occupancy of the site densities hence production should be equivalent provided the balance of nonphotosynthetic area to photosynthetic area did not exceed critical limits. Respiration would become limiting only in very high density stands where the surface area of boles and branches (the non-photosynthetic respiring area) increases greatly. Möller tested his hypothesis using Danish thinning practice in Norway spruce and beech and found it was upheld.

The two hypotheses are seen to differ only in respect to the range of densities across which production is optimum. Of critical importance therefore is the parameter of density. There is a need for a measure of stocking which is related to full occupancy (carrying capacity in the sense of population dynamics) in absolute terms. One would expect that for a given soil there must be a maximum rate at which nutrients and water can be made available to plants and that rate determines the amount and nature of roots occupying that soil. Similarly the maximum amount of foliage a given species, or combination of species, can effectively display to the sun determines the upper limit of intercepted, and hence effective radiation. The interaction of these maxima would produce the greatest dry-matter production; all other combinations would produce lesser amounts. It would be convenient to express this measure of stocking in terms of a common stand parameter such as basal area per acre."

Resource-dependent forest growth is also closely related to the concept of carrying capacity, which has been used widely in theoretical biology and population ecology for characterizing the maximal capacity of biomass that can be supported and maintained for a given site (Martire et al., 2015). Hui (2006) summarized that the carrying capacity of a biological species in an environment is the maximum population size for that species that the environment can sustain indefinitely, given the food, habitat, water, and other necessities available in the environment. In population biology, carrying capacity is defined as the environment's maximal load. It is different from the concept of population equilibrium. Its effect on population dynamics may be approximated in a logistic model, although this simplification ignores the possibility of overshoot, which real systems can exhibit. In mathematical form, the carrying capacity usually has an abbreviation of K, and it is usually called K value. Note the K value for any site likely varies over time.

In nature, the pattern of forest growth over time could be influenced by a number of factors such as site index and species (King, 1966; Means and Helm, 1985; Martin, 1991). In contrast with *K*, a quantitative parameter, the site index includes both quantitative and qualitative parameters. It is defined as the tree top height at the age of 50 years, and can be seen as a combined indicator from various nutrients, water, and site physical conditions. Site index also represents resource availability at the site when other physical site conditions are fixed. Due to differing growth and maturation requirements, different tree species could also respond to the site conditions in different manners. As a result, forest growth equations have demonstrated diverse forms in different geographical locations for different tree species. For this reason, forest growth models are site-specific and species-specific.

The concept of site index has been critical in the development of forest growth and yield models (Martin, 1991; Huang et al., 2001). The site index is a measurement commonly used by foresters to describe the productivity of a site, usually defined as dominant tree height at 50 years old (King, 1966). One example of its utility comes from the development of the TASS model in British Columbia, Canada, which stands for Tree and Stand Simulator (Mitchell, 1975). All the simulations are based on the estimated site index, and tree growth is proportional to the crown size. In other words, site index determines the upper limit of tree growth—maximized crown size—and size and shape of tree stems are determined by the realization of the maximized crown size.

Thinning Induced Compensatory Growth and Overcompensation

It has been widely observed that tree growth, in terms of diameter and total height, in PCT trials can result in increased growth rates relative to that from untreated sites in the short term (e.g., Bose et al., 2018). This is known as released growth of the remaining crop trees (Miller et al., 2007). It is easy to see that PCT reduces stand density and results in trees with larger diameters than those from untreated sites. This outcome is so common that it has been routinely applied in forestry practices to obtain tree forms that are most desirable for later processing into lumber products.

Intuitively, if this increased growth rate persists in the long term, any volume initially lost in PCT operations will be replaced over time and eventually the total stand volume will equal or even exceed stand volumes produced in untreated sites (Montoro Girona et al., 2017). Individual tree-based models (e.g., Korzukhina and Ter-Mikaelian, 1995; Battaglia and Sands, 1998; Ancelina et al., 2004) could be an interesting tool to understand this inference. This phenomenon, however, is not often reported in the literature due to the short period of observation remaining after PCT as mandated by present guidelines. For example guidelines mandate a post-PCT observation period of only 10 years for Douglas-fir (e.g., Reukema, 1975). Nevertheless, this phenomenon has been described in some long-term PCT trials such as one on balsam fir in Green River, New Brunswick, Canada, in which the stand volumes in treatment sites were about 15% higher than those from untreated sites, 42 years after the initial treatments (Pitt and Lanteigne, 2008). However, the mechanisms underlying these kinds of results are a matter of some debate. Due to its one-time measurement (i.e., measurement was made on trees at final felling), many questions could not be properly answered (re-measurement is no longer possible), and many researchers concluded that the results were simply an anomaly. Nevertheless, with the discovery from a data analysis of 40-year PCT and fertilization trial in Shawnigan Lake, British Columbia, Canada, which contained multiple measurements of the sites, it has become clear that the released growth of surviving trees can persist into the long term indeed and result in the stand volumes in treated sites that equal and exceed those from untreated sites (please see *Shawnigan Lake PCT and Fertilization Trial Overview* for a detailed overview of the case analysis). A growth response pattern to PCT is similar to the CG observed in other biological research fields; consequently, the framework of CG was used to explain the observation (Li et al., 2018). CG is a special case of growth response specifically for growth responses after thinning operations, and overcompensation has been used to describe the state when stand volumes in treated sites exceed the ones from untreated sites. CG could be extended to include shelterwood treatments (Bose et al., 2014; Pamerleau-Couture et al., 2015; Montoro Girona et al., 2016, Montoro Girona et al., 2018; Bose et al., 2020) and windstorm (Coates, 1997; Ruel et al., 2003; Montoro Girona et al., 2019).

The observed overcompensation from the Shawnigan Lake trial appears undisputable and is of great interest in terms of deepened understanding of the roles of thinning operations and search for conditions that promote forest productivity enhancement. If the role of PCT is merely for stand density management, forest productivity resulting from careful design of spacing during plantation and from PCT operations should be more or less the same. In other words, perfect design of spacing during planting should produce the same effect as without spacing in PCT operations. Harvested wood in PCT operations has no significant commercial value as lumber or generally any other forestry commodity. However, jack pine tree research (Tong and Zhang, 2005) has shown that the effects of initial spacing and the effects of subsequent PCT are probably not the same. Apparently, best results in terms of tree growth and stem quality can be expected from a narrow initial spacing during planting, followed by a later PCT.

Overcompensation is equivalent to enhanced forest productivity. In other words, if the mechanisms responsible for overcompensation can be understood, forest productivity could be enhanced through creating the right conditions, and forestry practices could benefit from applying operations that create such conditions. To reach this goal, the following questions need to be answered:

- What is/are the mechanism(s) behind CG and overcompensation?
- What factors trigger or determine the CG and overcompensation?
- Does CG aid in productive and sustainable outcomes, and can it persist over time?

- If PCT can serve as a stimulus to the remaining trees, what sorts of optimal thinning operations are needed to obtain maximized overcompensation?
- And eventually, is it possible to predict CG and overcompensation?

Objectives of This Review and Synthesis

The objectives of this review and synthesis article are twofold: to provide a conceptual framework for analyzing CG and to estimate CG contributions to forest productivity enhancement. *Forest Productivity Prediction* provides an overview of different modeling approaches and examples of characterizing forest growth. *Role of Compensatory Growth* presents a general overview of CG from different perspectives, a definition and numerical examples of CG, a brief description of CG observed from the Shawnigan Lake PCT and fertilization trial, and possible explanations of general CG from related research fields. *Possible Generalization of Overcompensation to Other Species and Geographical Regions* provides a summary of possible approaches to generalize overcompensation to other tree species and geographical regions, and the pros and cons associated with them. This article will conclude with some research recommendations.

FOREST PRODUCTIVITY PREDICTION

Forest productivity at any given site varies over time, subject to normal birth, growth, and death processes of trees (Botkin et al., 1972; Botkin, 1993; Bugmann, 2001), as well as from different natural and anthropogenic disturbance regimes including fire (Prentice et al., 1993; Li and Apps, 1995; Keane et al., 1996; Li and Apps, 1996; Li et al., 1997; Li, 2000; Li et al., 2005; Barclay et al., 2006; Li and Barclay, 2008), pest (Safranyik et al., 1999; Safranyik et al., 2001; Li et al., 2005; Hennigar et al., 2008; Li et al., 2008), climate (Allen and Breshears, 1998; Li et al., 2000) and weather such as windstorm (Ruel et al., 2003), partial harvest and fertilization (Aber et al., 1978; Aber et al., 1982), etc. Substantial initiatives and different modeling approaches have been used to predict the dynamics of forest productivity, and these efforts could be categorized into age-dependent, resource-dependent, and state-dependent forest growth models that depend on both internal and external states of trees.

Age-Dependent Forest Growth Models

Conventional age-dependent growth models are mainly empirical, data-based, statistical models commonly used for forest inventory evaluation, yield table generation, future wood supply forecast, and sustainable forest management (including harvest) planning. These models are site and species specific, and intensive field data collection, such as permanent sampling plot (PSP) and temporal sampling plot (TSP), are required to estimate parameters and improve the accuracy of the model predictions. These models predict the temporal dynamics of forest productivity and generally have a sigmoid shape wherein their saturation levels are determined by the carrying capacity of the site. These models reflect the natural courses of different stand types and provide tools for suitably estimating the productivity of natural stands.

The age-dependent forest growth models have the longest history of development and have the most mature form compared with other modeling approaches. The accuracy of model predictions has been improved over time through the enhancement of modeling systems. For example, the early growth and yield prediction system in Alberta was developed in 1984 from the phase III of the provincial AVI program (Alberta Forest Service, 1984; Huang, 1994). The system was relatively simple in equation form and provided an easy method of projecting current forest inventory into the future. It has been used in a spatially explicit model for landscape dynamics for reconstructing natural fire regimes (Li, 2000). The growth and yield prediction system (GYPSY) was developed in 2001; it provided a much more detailed and accurate description of forest growth and yield in the province for different tree species in different regions (Huang et al., 2001). The GYPSY model has been the standard growth and yield prediction system for Alberta and was further refined in 2009 (Huang et al., 2009). However, in the past two decades, increasing evidence suggested age-related decline that is inconsistent with the existing forest succession theory (e.g., Gower et al., 1996; Ryan et al., 1997; Berger et al., 2004). Some of the age-dependent forest growth models have incorporated this phenomenon (without specifying a particular mechanism), such as in Manitoba and Saskatchewan, Canada (Manitoba Conservation and Water Stewardship, 2013; Saskatchewan Ministry of Environment, 2017). These observations raised a question of their effect on the accounting of site productivity. Nevertheless, this topic is beyond the scope of the current review and synthesis.

Growth and yield prediction systems are usually region-specific and developed for difference provinces of Canada. In British Columbia, for example, The Ministry of Forests, Lands and Natural Resource Operations developed a tree level growth and yield model named TASS (Tree And Stand Simulator), which predicts the potential growth and yield of even-aged, single-species, managed stands for ten commercial tree species in British Columbia (Mitchell, 1975). A provincial system for predicting growth and yield of natural stands is also developed (Martin, 1991). These BC models are also used in Yukon for adjusted site levels. In Alberta, in addition to the GYSPY model, a Mixedwood Growth Model (MGM) is also developed (Bokalo et al., 2013). These Alberta models are also used in Northwest Territories. MGM and MGYPSY (adapted from GYPSY) are being used in Manitoba. In Ontario, Penner (2008) provided yield prediction for mixed species stands, and documented validation of empirical yield curves (Penner et al., 2008). In Quebec, a stand-level growth and yield model named NATURA-2009 is available for even-aged stands to predict the growth of merchantable trees (Pothier and Auger, 2011). For uneven-aged stands, a tree-list growth and yield model named Artemis-2009 is available (Fortin and Langevin, 2010). In New Brunswick, a stand-level growth and yield is forecasted using a tree list model

named Open Stand Model (OSM), which is similar to the Forest Vegetation Simulator (FVS) model (Dixon, 2002), but calibrated for the Acadian Forest region using the provincial permanent sample plots.

Ultimately, an age-dependent forest growth modeling system can provide estimates of forest volumes for particular tree species at specific sites at any stand age. In other words, under ideal situations, age-specific forest volumes can be calculated once the species and site conditions are known.

Resource-Dependent Forest Growth Models

Resource-dependent forest growth models are mainly useful in stand density management practices for determining how forest volumes of a stand can be altered by different stand densities. There are three main categories of these forest growth models: variable-density yield tables, stand density management diagrams, and process-based mechanistic models.

Variable-density yield tables are a conventional yield prediction method developed to account for the yield changes due to different stand densities. Such efforts can be traced back to 1940s for natural stands (e.g., Mulloy, 1944). Johnstone (1976) developed a technique to facilitate assessment of past stand development from single-examination-plot PSP data to construct the yield tables for essentially pure, natural, and unmanaged, even-aged lodgepole pine stands of Alberta. The effect of stand density on top height of trees was represented by the following equation:

$$\log_{10} TopHt = 1.0688 - 0.00276672A + 0.717922Log_{10}A \\ -0.0000371084Stems - 0.132622Log_{10}Stems \quad (1)$$

where *TopHt* is the top height defined as the arithmetic average height of the 100 largest trees per acre, *A* is the stump-height age measured at 1.0 foot above ground level, and *Stems* is the total number of living trees equal to or greater than 0.6 inch diameter at breast height (DBH) outside bark. Using this equation, the author generated several yield tables for stands ranging in age from 20 to 100 years, high- to low-productivity sites, stand densities of 500 to 2,000 stems per acre at age 70 years, and quadratic-mean diameters from 3.0 to 8.5 inches at the same age.

The stand density management diagram (SDMD) is a graphical tool for relating stand density, tree size, and stand yield. It is a graph of mean tree volume and stand density on which the maximum size-density relationship has been superimposed. The relationship is based on the concept of maximum size density as a general principle of plant population biology: in pure even-aged stands, the maximum mean tree size attainable for any density can be determined by a relationship known as the −3/2 power law:

$$Vol = \alpha Density^{-3/2} \quad (2)$$

where *Vol* is mean stand volume, *Density* is stand density, and α is a constant.

A SDMD is constructed by plotting mean tree volume against stand density on a double logarithmic scale (Drew and Flewelling, 1979). Two lines, one showing the maximum size-density relationship and another representing the lower limit of the zone of imminent competition mortality are usually included in most SDMDs. Several isolines are also drawn for stand top heights (representing height growth as a measure of site productivity) and quadratic mean diameter of a stand (representing stand diameter at a given age is altered given changes in establishment density). A crown closure line is also drawn and represents the points at which the crowns of trees in stands of different densities start to interact. These isolines can be calculated through multiple simulations using age-dependent forest growth models. For example, Farnden (1996) was able to use simulation results of a TASS model to construct SDMDs for lodgepole pine, white spruce, and interior Douglas-fir of British Columbia, Canada.

Both variable-density yield tables and stand density management diagrams are obtained from summaries of multiple simulations using empirical data-based, age-dependent, forest growth models. In other words, they are essentially an extension or application of age-dependent forest growth models.

Resource availability is a limiting factor in tree growth, and trees will likely grow faster with increased resource availability. Intuitively, therefore, trees that remain after partial harvest or other stand density management procedures would have extra resource accessibility and hence increase their growth rates. Consequently, resource-dependent forest growth models should be able to demonstrate the increased growth, either in DBH or *TopHt*, in stand dynamics after partial harvest. Such increased growth rate will inevitably result in observed CG, probably under CG, and eventually fully compensate the volume loss from the partial harvest operations. Nevertheless, it might be difficult to demonstrate overcompensation because of tree growth ceiling due to resource availability on site.

Although average stand volume can be estimated from these resource-dependent forest growth models, the effect of uneven spatial distribution of resources on the tree growth is rarely taken into account, even though this might be important in explaining the variations displayed in observations. Mechanistic modeling approaches have thus been employed to develop the TASS model (Mitchell, 1975), which is the foundation of simulating forest growth of managed stands in British Columbia, Canada.

The TASS model is also resource-dependent by way of maximal tree growth that is limited by the maximum crown development. In the model design, tree growth is assumed to be a fraction of crown development and spatial variations of resources. The TASS model appeared sensitive and capable of simulating forest dynamics after frequent small disturbance events and subsequent CG (Figures 13–16, and 18 of Mitchell, 1975), though the CG terminology was not used in the document. The simulated basal area increment from a row thinning was less than that from a checkerboard thinning regime, and various intensities of deer browsing had little effect on the final yield; in short-term simulations, their results likely describe growth during the phase of undercompensation. Nevertheless, the phenomenon of overcompensation may still

be a question of representation in the simulation results if the simulations had continued over the long term. For this reason, running long-term simulations using TASS to reproduce the Shawnigan Lake trial could serve as a test and examination.

The overcompensation phenomenon observed in the long-term PCT trial in the Green River case and the combined PCT and fertilization trial in the Shawnigan Lake case might be difficult to explain using resource-dependent forest growth models because available resources are assumed to be utilized in full by normal stands already. Therefore, we propose that a state-dependent forest growth modeling approach should be introduced.

State-Dependent Forest Growth Models

Any given organism can be described by values associated with its various states, including size, age, energy reserves, etc. The logic behind employing such variables lies in the fact that growth, for most organisms, including trees, is state dependent. For example, large trees with extensive crowns can capture more light energy than smaller trees belonging to the same species (conspecifics), but at the expense of higher maintenance costs and greater risk of mortality from wind (see Loehle, 2016). The job of a forest ecologist is to determine the key states that drive tree growth and forest productivity and there is a huge number of possible states that could be measured. For example, in a simulation model based approach, Buckley and Roberts (2006) developed a tree growth model (Deducing Emergent Structure and Physiology Of Trees or DESPOT) with at least 15 state variables to determine optimal carbon allocation to control various physiological processes to maximize net carbon gain. All of these processes and state variables have been identified as potentially important drivers of growth, and the simulations allow for interactions among them in relation to net carbon gain. As noted by Buckley and Roberts, these sorts of models will likely not produce mathematically tractable solutions but can be used to inform predictive modeling. By contrast, plant response manipulation through optimal stimuli or thinning is the state-dependent analytical approach that produced insights and predictions. One drawback is that these models are limited to just a few state variables thus requiring researchers to identify key state variables.

At the forest level, a good way of identifying and grouping states is to choose bins of appropriate size and then assign trees to these bins, across the entire forest. For example, a biologically reasonable bin size for age state would be one year; however, that fine a scale might be computationally unmanageable for forests that are tens or hundreds of years old. For tree height, bin size might be in multiples of meters. In the end, the entire population can be described by a distribution of trees across bins. Note that within a particular state (e.g., size) all individuals in a given bin are assumed identical; however, as we describe more states (e.g., now include age) the number of permutations or dimensions increases. Even in an even-aged stand, size and growth rate can be highly variable (Boyden et al., 2008). Again, computational issues arise as the number of states and bins increases; this is particularly true for analytical approaches such dynamic programming, sometimes referred to as the curse of dimensionality (Mangel and Clark, 1988).

Whether using individual based simulations or more analytically tractable state-dependent models, it is possible to calculate forest productivity by summing up a given variable across all trees in a particular forest. The key here is that carbon accumulation is not a logical phenomenon but rather the outcome of well-understood physiological processes that vary across tree states in heterogeneous forests. Interactions among these state variables and their associated physiological processes may generate emergent properties that might not be intuitive from single parameter assessments. For example, these models should generate the −3/2 power relationship without being constrained to doing so. In fact a good test of these models is to compare their predictions with real world patterns.

ROLE OF COMPENSATORY GROWTH

Compensatory Growth

Forest growth response (GR) is the term widely used in forest science for describing measured variables such as DBH and *TopHt* from treated sites, compared with those from untreated control sites, or the forest growth trajectories including those after PCT and other silvicultural treatments such as fertilization (Montoro Girona et al., 2017; Oboite and Comeau, 2019; Puhlick et al., 2019). GR appears to be a straightforward description of how forests respond to any disturbance or stimulus, and can be applied at both the individual level and the population level of trees.

While GR covers a very broad range of growth trajectories under both normal and abnormal (either advantageous or disadvantageous) environmental conditions, CG focuses on the growth trajectories after certain disadvantageous conditions (Guillet and Bergström, 2006; Rea and Massicotte, 2010; Erbilgin et al., 2014). Therefore, CG is a special case of GR. Though both GR and CG can characterize forest response to PCT, CG might be more specific and appropriate than GR; regardless, the diverse observations (with and without overcompensation) need to be examined and possible mechanisms explained. In this regard, ideas from CG research such as compensation and overcompensation could be introduced, which can serve as the starting point for exploring possible mechanisms. There are two streams of CG research: psychological behaviors (in the broad sense, see a summary by Hoffman, 2020) and ecological/biological responses.

In the field of behavioral ecology, which differs from human-based psychology, an evolutionary perspective is usually used to consider trade-offs in terms of inclusive fitness from benefit-cost analysis (Mangel and Munch, 2005; Bourke, 2011; Ferriere and Michod, 2011; Davies et al., 2012). In other words, conscious reactions need not be used but rather the focus is on responses or reactions that are selected or favored by natural selection. As such, behavioral ecologists seek behavioral strategies

that maximize an individual's lifetime reproductive success (Kalbe et al., 2008). Such strategies could include changes in growth response as a function of resource availability (Hoi et al., 2013), competition (Segers and Taborsky, 2012), or abiotic conditions (Debecker and Stoks, 2019). Thus, behavioral ecologists might ask whether facultative overcompensation, under some conditions, could confer a selective advantage (i.e., the function) over inflexible conspecifics and how such responses could be generated (i.e., the mechanism).

The phenomenon of overcompensation was probably observed first in plants in the 1920s in crops such as cotton in which removal of early reproductive organs of flower buds and squares could stimulate further growth thus generating overcompensation in the final yield. As a result, Eaton (1931) proposed this could be a means of increasing cotton yield without influencing the quality of cotton fiber. The capacity of this CG and overcompensation appeared to persist until the end of the growing season. CG was also observed in animals such as rats (Osborne and Mendel, 1915; Osborne and Mendel, 1916; Jackson, 1937) in which accelerated growth was exhibited when food intake was restored following a period of shortage. Animals later became traditional main objects of behavioral ecology research probably because of their relatively fast reaction time and short lifespan, until McNaughton (1985) who found that grazing increased grassland aboveground productivity with optimal results at intermediate grazing intensities; he concluded that CG mechanisms might be the driving forces determining plant productivity.

Given the demonstration of CG across kingdoms, questions remained as to its evolutionary advantage. Plants have received more attention in recent years, especially with the publication of a special issue of "Beyond traits: integrating behavior into plant ecology and biology" (Cahill, 2015). The main differences between animals and plants are mobility and photosynthetic ability; nevertheless, there are many similarities such as those displayed in movement of root systems and competition for nutrients and light. We might expect there to be differences in the driving mechanisms between plants and animals, but the behavioral ecology focus on the function of CG remains.

Though many behavioral ecologists focus on individuals, it is possible to scale up to the population or community level. In that regard, forests have been reported to have different capabilities of growth compensation after disturbances, such as CG after PCT operations. However, difficulties in deciding whether or not to implement PCT in forestry practice requires a better understanding with mechanistic explanations and solutions to facilitate informed management decisions. Here, practitioners could benefit from studies of the possible mechanisms of compensation and overcompensation from behavioral ecology research. With these in mind, we now describe the current understanding of CG in behavioral ecology.

The most common mechanism of CG is resource-dependent protection and defense from disturbances. Essentially, it is a survival strategy of organisms under disadvantageous conditions (Mangel and Munch, 2005). An animal's body size is usually an important characteristic influencing mating choice and reproductive success, thus increasing body size is often a surrogate for increasing life-time fitness, and is favored with the trade-off risk of being discovered and captured by predators. When disadvantageous conditions occur, nutrient intake could be reduced through lower quality or quantity of food sources with requisite decline in growth rate. When food sources are restored, animals would tend to increase nutrient intake and thus increase their growth rate to achieve normal growth. Many examples have been documented including in insects (Hoi et al., 2013; Debecker and Stoks, 2019), fish (Ali et al., 2003; Azodi et al., 2016; Gabriel et al., 2018), mammals (Bohman, 1955), birds (Wilson and Osbourn, 1960), grass (McNaughton, 1983), and livestock (Yambayamba and Price, 1991; Zubair and Leeson, 1996; Therkildsena et al., 2004). As a result, CG research is no longer a pure but also an applied science that benefits different industries including crop protection and pest management, herbivory and rangeland management, fishery management, and farm animal production. This subject goes beyond the scope of the current review, and thus can be summarized elsewhere.

Literature about CG contains some explanations for the CG phenomenon. One such hypothesis is the hypothetical growth curves of control and diet-restricted treatment groups, which represent the comparisons used in the slope analyses, where the slope of size increments in a treated group is higher than that from a control group. The situation of PCT, which is different from a normal completed CG process, is represented by the shaded area of **Figure 1** where PCT caused immediate biomass (size) removal and the effect of PCT to stand volume is readily apparent, and the CG process following PCT occurs right after the boundary between the shaded and non-shaded areas. The timing of thinning (PCT *vs.* CT) will determine the location of the boundary between the shaded and non-shaded areas, and the period required to reach full CG. Nevertheless, the final sizes of both groups are assumed to be the same, i.e., full CG.

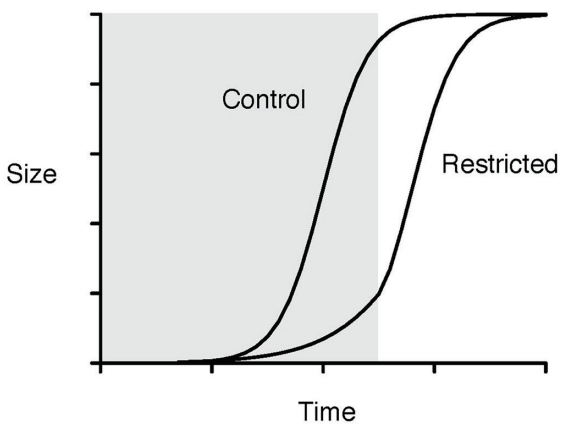

FIGURE 1 | Hypothetical growth curves of control and diet-restricted treatment groups in the slope analysis. The shaded area represents the restriction period, and the non-shaded area represents the period after restriction (redrawn from Hector and Nakagawa (2012)).

This scenario can be explained in the mathematical form of

$$Size = K/(1 + \exp(\alpha - \beta \times Time)) \quad (3)$$

where K is carrying capacity, and α and β are parameters. **Figure 2** shows the sigmoid curves with a different parameter α. A higher value of α could result in reaching the carrying capacity K earlier than with a lower value of α.

If this explanation holds, empirical evidence should be sought in the field of silvicultural research. A good example can be gleaned from our Shawnigan Lake PCT and fertilization experimental data analysis (Li et al., 2018), and this example could provide a starting point for identifying conditions of overcompensation.

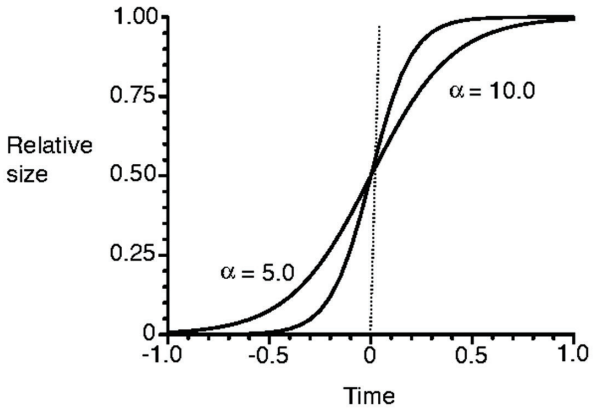

FIGURE 2 | Sigmoid curves with two different values of α (redrawn from Onoda et al. (2011)).

Shawnigan Lake PCT and Fertilization Trial Overview

The Shawnigan Lake PCT and fertilization experiment provided a good example of how CG and overcompensation occurred over time, because of the multiple measurements taken before and 1, 3, 6, 9, 12, 15, 24, 30, and 40 years after the treatments. Each measurement was conducted at each of the combinations of three levels of PCT (0, 1/3, and 2/3 basal area removal) and three levels of fertilization (0, 224, and 448 kg N/ha). Each combination had either two or four replications (Crown and Brett, 1975). Consequently, the data analysis produced a detailed characterization of how forests responded to different treatments and clearly showed the processes of CG and overcompensation over the 40-year time horizon. The relative growth of stand volumes in each combination of PCT and fertilization levels to that from the control (T0F0) appears to be the best indicator of progressive changes of CG and reaching overcompensation (**Figure 3**).

The volume-based analytical results showed that the numbers of years to reach equality of volume was dependent on the levels of fertilization and thinning intensity. For example, if the thinning intensity was fixed at 50% basal area removal, reaching full CG could require less than 30 years when 448 kg N/ha was applied, about 35 years when 224 kg N/ha was applied, and over 60 years when no fertilizer was applied. A value-based assessment could display this trend with a clearer picture: lumber value can serve as an alternative indicator of CG (unpublished results, will be presented in Li et al. in prep.). The results confirmed that favoring lumber production and overcompensation could be reached with PCT operations, and the combination of PCT and fertilization treatments should be supported in forestry practices.

We can take a step further from these primary findings to see how they can be translated to an interpolation of stand growth trajectories under different thinning intensities over time for

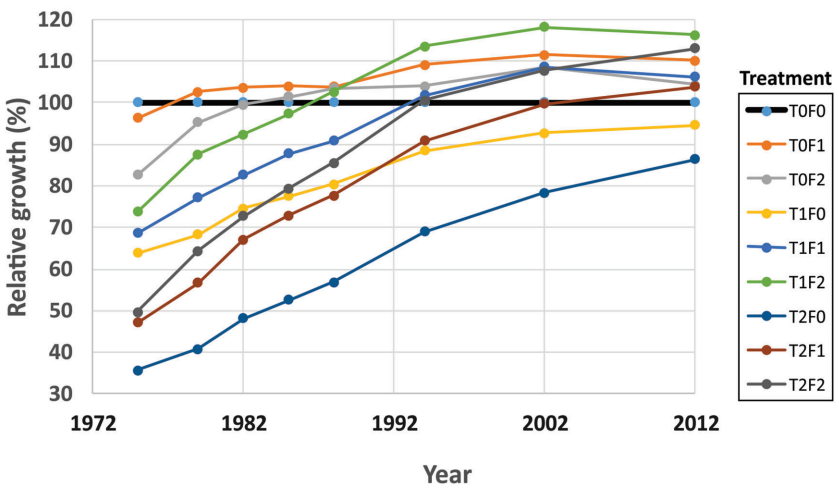

FIGURE 3 | Relative growth of stand volume over time under different treatments (redrawn from Li et al. (2018)).

each level of fertilizer application. This can be done by fitting relative volume (percent of control) using the surface fitting program TableCurve 3D, and using the equation

$$z = a + bx + cy + dx^2 + ey^2 + fxy \quad (4)$$

where x is percent of basal area removal or thinning intensity, y is year after thinning, z is relative stand volume expressed as percent of control sites, and a, b, c, d, e, and f are parameters with following values in **Table 1**:

To illustrate the fitting results, we use the fertilization level of F1 as an example (omit F0 and F2 for now), we have **Figure 4**:

For the current range of 1–40 years after treatments, we can multiply the normal growth trajectory (from control sites) by the z value to obtain altered growth trajectories. For example, applying the equation for the F1 level to the normal growth trajectory projected by using the Y-XENO model results in the growth trajectories in **Figure 5**; an economic evaluation of the Shawnigan Lake trial was carried out by Duke et al. (1989).

Removal00 means control (zero basal area removal), which is equivalent to normal growth trajectory. Removal33 and Removal66 (which represent 33 and 66% basal area removal, respectively) altered the slopes of the growth trajectories and resulted in probably reaching the status of stand maturity earlier. The figure clearly shows the shapes of altered growth trajectories by PCT treatments have a steeper slope in growth pattern than that in the normal/controlled sites. This is consistent with what Soucy et al. (2012) observed in long-term effects of thinning on growth and yield of an upland black spruce stand in Baie-Comeau, Quebec. The authors found that heavily thinned plots (50% of total basal area removal) resulted in a net stand merchantable volume increment 33% greater than that of the unthinned plots. In spite of a spruce budworm outbreak at the affected site, the heavily thinned plots maintained a superior tree growth rate and did not show senescence mortality like the other plots, allowing stand volume to catch up to that of the unthinned plots after 33 years. These provide a foundation for our scenario analysis of how future wood supply represented by regional annual allowable cut (AAC) could be affected by different shapes of growth trajectories (unpublished, to be presented elsewhere).

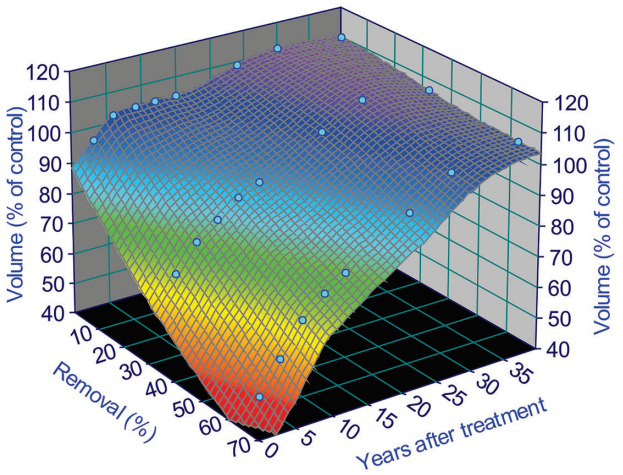

FIGURE 4 | Surface fitting results for a fertilization level of 224 kg N/ha treatments in the Shawnigan Lake trial. This relationship can only be applied from year 1 to 40 after thinning treatments, because there are no data after 40 years and any extrapolation beyond this range might result in potential bias. This is due to the uncertainties involved in the growth trajectories after 40 years, and we will deal with these uncertainties in *Extrapolation of Growth Trajectories Beyond the Periods of Current Observations*.

Definition and Numerical Examples of Compensatory Growth

With the previously mentioned analysis, we can discuss further the definition of CG and explain it using numerical examples.

According to Tuomi et al. (1994), some plants can compensate, and even overcompensate, for the loss of productivity caused by herbivory. McNaughton (1983) and later Rea and Massicotte (2010) defined CG as "exaggerated vegetative growth that results from mechanical damage to plants (e.g., cutting, animal browsing, or breakage from snow) as a physiological consequence of an increase in the root-to-shoot ratio following the loss of aboveground biomass." In general, CG has often been referred to as the process of accelerated growth of an organism following a disturbance or a period of slowed development due to unfavorable conditions such as low temperature or nutrient deprivation. In studies of fish behavior, as an example, CG has been referred to as a phase of accelerated growth when favorable conditions are restored after a period of growth depression (Ali et al., 2003).

CG is not having only a single invariant state, but a continuum ranging from negative CG when mean periodic annual increments of DBH and/or *TopHt* in treated sites, $mPAI_{Treat}$, is smaller than that from untreated sites, $mPAI_{Control}$; to no CG when $mPAI_{Treat}$ equals $mPAI_{Control}$; and to positive CG when $mPAI_{Treat}$ is bigger than $mPAI_{Control}$. Here the $mPAI$ is calculated as $mPAI_i = (Vol_{i,t_2} - Vol_{i,t_1})/(t_2 - t_1)$, where i = *Treated*, or *Control*, t_1 and t_2 are the beginning and end time of the observation period, respectively. **Figure 6** is a schematic diagram of CG continuum.

TABLE 1 | Parameters from a smooth surface fitting analysis.

Fertilization level	Parameter value					
	a	b	c	d	e	f
F0	95.82748	−0.90492	0.57782	−0.00330	−0.01314	0.02332
F1	90.13417	−0.79458	1.61649	0.00026	−0.02935	0.01884
F2	80.11890	0.03164	2.22308	−0.01263	−0.04210	0.02160

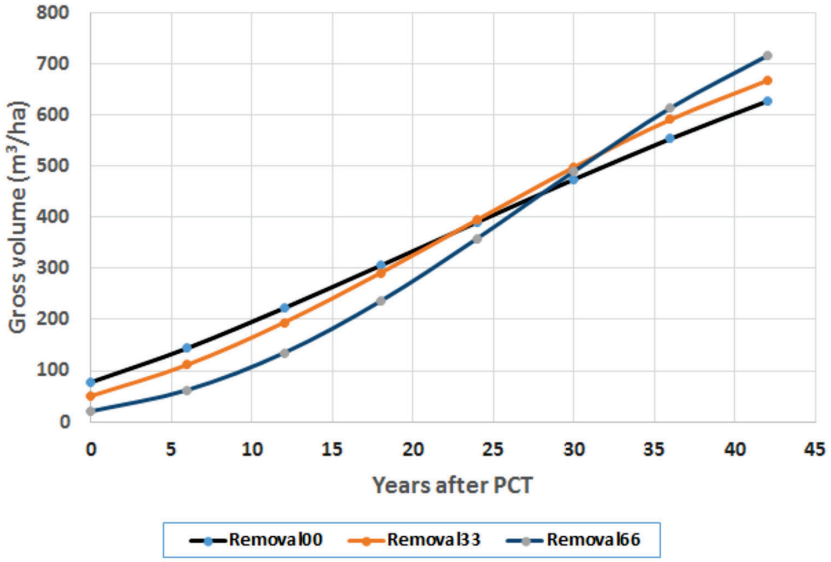

FIGURE 5 | Growth trajectories after precommercial thinning (PCT) at the fertilization level of 224 kg N/ha.

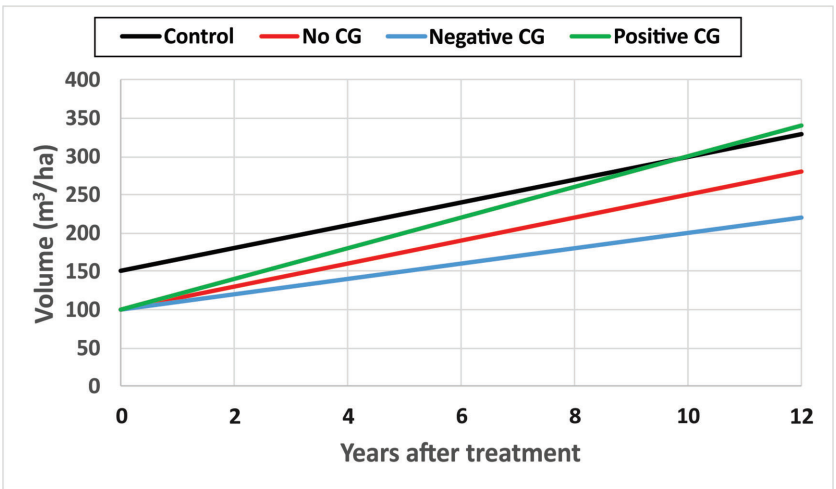

FIGURE 6 | A schematic diagram of compensatory growth (CG) continuum with hypothetical numerical examples.

Some hypothetical numerical examples are used to demonstrate different types of CG for narrative description purposes. Assuming stand volumes in an untreated site are 150 and 300 m^3/ha at year 0 and year 10 after the initial treatments as showed in black line, the $mPAI_{Control}$ will be 15 m^3/ha. If the thinning operation removed 1/3 of stand volume in the treated site and the stand volume, measured 10 years after the initial treatment, is 250 m^3/ha as shown in red line, the $mPAI_{Treat}$ will also be 15 m^3/ha. In this case, there is no CG observed since $mPAI_{Treat} = mPAI_{Control}$. However, if the stand volume measured 10 years after the initial treatment is smaller than 250 m^3/ha, say 200 m^3/ha as showed in blue line, the $mPAI_{Treat}$ will be 10 m^3/ha, and it will then be a negative CG since $mPAI_{Treat} < mPAI_{Control}$. If the stand volume measured 10 years after the initial treatment is larger than 250 m^3/ha, say 300 m^3/ha as showed in green line, the $mPAI_{Treat}$ will be 20 m^3/ha, and it will be a positive CG since $mPAI_{Treat} > mPAI_{Control}$.

The negative CG, which causes thinning shock—an unexpected result of reduction in diameter and height growth—is probably rare and short-lived, and would then shift to no CG or positive CG after that period. Harrington and Reukema (1983) provided an example of negative CG observed in a spacing

experiment through thinning on a Douglas-fir plantation in the Wind River Experimental Forest near Carson, Washington. The PCT treatments were designed for six stocking levels 875, 625, 500, 375, 250, and 125 trees per hectare (corresponding to spacings of 3.4, 4.0, 4.2, 5.0, 6.0, and 8.1 m) with a randomized block design. They found the immediate effects of the thinning treatments were detrimental including chlorotic foliage, sunscald, and snow and ice damage in the form of broken tops and branches and leaning trees. The height and diameter growth were reduced by thinning. However, the long-term (15–25 years after treatments) effects of increased growing space have been beneficial. Following the initial shock, both diameter and height growth did recover in the thinned plots. In fact, diameter and height growth are greatest at the widest spacing. Nevertheless, due to the significantly fewer trees per plot at the wide spacings, the sharp increase of basal area and cubic volume per hectare have not been great enough to offset the lesser number of trees.

Alternative explanations for the negative CG could simply mean that the organisms are constrained from catching up, for example, if trees performed better in dense groups wherein they reduce herbivory. Or there could be some limiting nutrient (e.g., N) that prevents the tree population from exceeding growth rates of non-thinned trees *via* CG. However, these phenomena will not be the focus of this current synthesis.

The example presented by Harrington and Reukema (1983) clearly showed how a negative CG translated into positive CG *via* no CG over the 25 years of observations, in which the no CG state was temporary. This has been theoretically confirmed by Jaremo and Palmqvist (2001). They presented a theoretical analysis that considers the phenotypic trait of CG ability in a context of population dynamics. Their model depicts a system of three interactors: herbivores and two different plant types referred to as ordinary and compensating. The compensating plant type has the ability to increase its intrinsic rate of biomass growth as a response to damage. This CG ability is maintained at the expense of a reduced growth rate in the absence of damage, where the ordinary plant type has the higher growth rate. Analysis of this system suggested that, even though a compensatory capacity of this kind will not imply an increase in equilibrium plant density, it will give a competitive advantage in relation to other plants in the presence of a sufficiently efficient herbivore. Invasion of compensating plants into a population of non-compensating plants is facilitated by a high CG ability and a high intrinsic rate of plant biomass increase. Conversely, an ordinary plant can invade and outcompete a compensating plant when the herbivore is characterized by a relatively low attack rate, and/or when the intrinsic growth rate of a plant is decreased.

The status of positive CG can be further distinguished as undercompensation, compensation, and overcompensation. To evaluate the exact status of positive CG, we can extrapolate the lines beyond the interception of the two straight lines. The location of the intercept indicates where the compensation happens. Before reaching the intercept, there is an indication of undercompensation, and after the interception denotes an overcompensation status, which is what the forestry practitioners seek. In the case presented by Harrington and Reukema (1983), however, overcompensation has not occurred during their 25-year observation horizon despite a transition from negative to positive CG.

Behavioral ecology views CG as a process essentially at the individual tree level. This is because natural selection operates on individuals in a population and selectively favors those individuals and those genotypes that contribute most offspring to subsequent generations. This process leads continuously to an increase in the population of those forms that contribute more offspring than their neighbors. We define "fitness" as the relative numbers of offspring left to future generations by one form compared with others. For this reason a plant might increase its fitness by reducing its number of progeny if a compensating increase in its vegetative vigor deprived its neighbors of the chance of leaving offspring (Harper, 1977). In other words, reduction of the plant numbers in a given area (e.g., a result from thinning) might not necessarily lead to the decrease of fitness, because they could potentially be compensated by increased individual plant sizes that could potentially result in more offspring compared with those from unthinned stands.

Thinning operations may alter the status of environmental conditions for surviving trees, such as reduced competitive pressure and increased availability of resources and nutrients. As a result, individual trees can devote more resources to growth because fewer reserves are required to compete with neighbors. This could be a mechanism of released growth after thinning. Nevertheless, this natural selection favored an individual-level CG process, which could eventually lead to an expression of CG at the population level, if such growth persists for a sufficient period of time.

In **Figure 6**, the status of positive CG can be demonstrated when the positive (green) and control (black) lines are extended further such as at 12 years. The partial (or insufficient) CG (or undercompensation) refers to the status of stand volumes in treated sites that are in the process of catching up with the one from untreated sites, represented as the portion of positive (green) line 1–9 years after initial treatment. In other words, the difference between stand volumes in treated and untreated sites is narrowing over time. The full CG, or compensation, denotes that no significant difference between the stand volumes in treated and untreated sites, represented as the year 10 after initial treatment where the interception of lines that represent control (black) and no CG (red) lines occur. This compensation can also be called compensation-induced equality (CIE). Overcompensation signifies that the stand volumes of treated sites exceed the one from untreated sites, represented by the portion of positive (green) line in 11–12 years after the initial treatment.

The above method can be applied to every interval between two measurements in the datasets containing multiple measurements. Resulting $mPAI_{Treat}$ and $mPAI_{Control}$ may or may not be the same over time, indicating the speed of CG process may not be invariant and could change over time.

It should be noted that the numerical examples in **Figure 6** are for illustrating the CG related concepts only, and they are not

necessarily realistic. In reality, growth rates of trees are usually much slower than the numerical examples used in **Figure 6**, which is probably the reason why the catch-up growth was not observed in short-term observations.

The framework of CG can reasonably explain the different results from short- and long-term observations, and indicate that released growth at the individual tree level is a necessary but not sufficient condition for stand volume catch up, and the sufficient condition is a time period long enough to allow the volume catch up to occur (Li et al., 2018). An advantage of the concept of CG is to allow researchers to focus on the positive CG process for potential applications in forestry practice. The CG concept is thus employed in the current study to explore and quantify how the normal growth trajectories, denoted by the untreated sites, could be altered by the CG process induced by the combinations of PCT and fertilization treatments at the Shawnigan Lake study area.

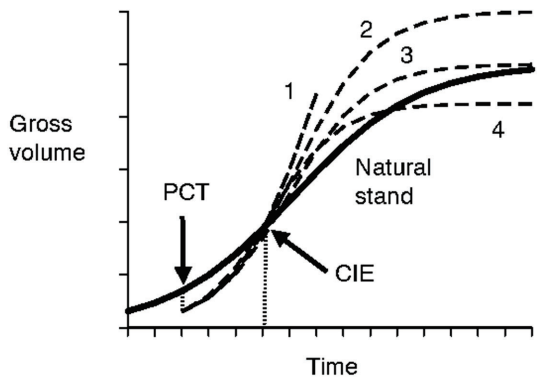

FIGURE 7 | Schematic illustration of uncertainties in long-term growth trajectories. The bold line indicates growth trajectory of natural stands. The gross volume will be reduced at the precommercial thinning (PCT) treatment, then gradually approach that of the natural stand growth curve within a certain period of time at the point of compensatory-induced-equality (CIE), and then face uncertainties with possible growth trajectories indicated by 1 (continued growth acceleration); 2 (higher maximum growth); 3 (no change to maximum growth); and 4 (lower maximum growth).

POSSIBLE GENERALIZATION OF OVERCOMPENSATION TO OTHER SPECIES AND GEOGRAPHICAL REGIONS

Though the concept of overcompensation observed at the Shawnigan Lake trial is important in relation to forest productivity enhancement and carbon accounting, two challenges remain: how to extrapolate growth trajectories beyond the periods of current observations and how to generalize overcompensation to other tree species and geographical regions.

Extrapolation of Growth Trajectories Beyond the Periods of Current Observations

The issue with the previously identified first challenge (how to extrapolate trajectories beyond the periods of current observations) lies in the uncertainties involved with growth trajectories of even longer periods of time (i.e., data from the Shawnigan Lake trial were only available for up to 40 years after the initial treatments) that have been mentioned in *Shawnigan Lake PCT and Fertilization Trial Overview*. The uncertainty could at the very least include following possibilities (**Figure 7**):

- forest productivity continues its growth increment over time due to accelerated growth rate (Huuskonen and Hynynen, 2006);
- forest productivity flattens at the same level as observed in natural stands, which is assumed to be the maximum site productivity;
- forest productivity flattens at a level higher than the observed productivity in natural stands, wherein potential maximum site productivity is higher than what has been observed in natural stands; and
- forest productivity declines gradually to a level lower than that observed in natural stands.

To deal with such uncertainties, re-measurements will be required in the years to come when taking an empirical data collection approach. For example, the Shawnigan Lake trial was initiated in 1971 and the last measurement was made in 2012, which consisted of 40 years of records. When future re-measurement becomes possible, the collected data could be used to provide an adequate answer to the uncertainty. For the Green River case, re-measuring some of the study sites is impossible because the trees have been felled, but re-measuring nearby sites with similar treatments could still provide useful information to resolve the uncertainties. The modeling approach is an alternative option, which will be discussed later in *Plant Response Manipulation Through Optimal Stimuli/Thinning Determination*.

Generalization Using CG for Other Tree Species and Geographical Regions

The other previously identified issue is to what extent the CG and overcompensation observation from a single site (Shawnigan Lake trial) could be generalized for other tree species and geographical regions. Two different approaches are available to explore the issue: empirical data collection and further analysis as well as modeling approach.

Hypothesis Testing Through Increased Empirical Data Collection and Analysis

Empirical data collection and analysis largely relies on analysis of accumulated empirical data from existing sites of long-term PCT trials for other tree species and from different geographical regions. If the hypothesis for the existence of overcompensation can be supported from these data analyses, one can comfortably generalize the overcompensation using other tree species and geographical regions.

This approach appears to be intuitively acceptable, relatively straightforward, reasonable and understandable, and easily

convincible. However, this approach is also very resource demanding in terms of both time and economic investment in a skilled workforce. Furthermore, suitable potential sites for long-term (at least 40–50 years) PCT trials need to be identified that are readily available and accessible.

Considering the long history of silviculture research, suitable potential sites could be easily identified as long as establishment measurements (before and after treatments) are available. For example, the following sites in western Canada could serve as potential sites:

- Historical thinning treatments (approximately 50 years ago) established for the coastal Douglas-fir in the Malcolm Knapp Research Forest of UBC in Maple Ridge, B.C.;
- Diverse thinning experiments 40–50 years ago launched in the mixedwood forests near Calling Lake in Northern Alberta;
- Various PCT experiments initiated in Manitoba, Canada, more than 70 years ago.

Even with sufficient financial investments, however, there might still be the possibility of insufficient suitable sites for all major tree species in all geographical regions. When this is the case, other thinning experiments need to be set up for data collection in subsequent years. These experiments will require a sufficiently long period of observations to be appropriate for the hypothesis test. Obviously, this will probably be a task to be accomplished beyond any given researcher's career limit.

With the previously described empirical data collection, the results still might be treated as anomalous or out of the ordinary due to the lack of explanatory mechanisms. Technically, this approach could still face challenges in implementation:

- Human errors or biases in the measurements spread over a long period by different researchers, with possible varying research protocols that might complicate comparative data analysis;
- Inconsistent methods of data analysis over a long period could also complicate research results. For example, different methods of estimating volumes of individual trees over the 40-year horizon resulted in significant differences in stand volumes published previously using the Shawnigan Lake trial datasets, hence infeasible data unsuitable for direct comparison;
- Experiment duration challenges include long time scale (probably more than 50 years) and uncertainties related to selection of variables to measure. In this regard, a modeling approach could probably benefit researchers through the use of simulations and a sensitivity analysis (see *Plant Response Manipulation Through Optimal Stimuli/Thinning Determination*).

Plant Response Manipulation Through Optimal Stimuli/Thinning Determination

The modeling approach proposed here takes advantage of the contemporary development from other research fields, especially from applied behavioral ecology, which has been successfully applied in other management science such as pest management in agriculture.

Different methods including chemical, physical, and biological controls have been traditionally practiced in pest management for protecting normal growth of plants. A new method of behavioral manipulation was recently added to the list (Roitberg, 2007). This new method is a result from applied behavioral ecology with the advantage of minimized environmental footprint.

In the study of thinning effect on forest productivity, thinning acts as a stimulus to forests, and how forests respond to such stimuli (i.e., forest behavior) is represented as CG. The goal of thinning operations in forestry practices is to obtain maximized forest productivity, such as the overcompensation observed in the Shawnigan Lake trial. Thus, the focus of research should be determining the optimal stimuli that can result in the maximized level of overcompensation. Such a research goal is similar to behavioral manipulation in pest management wherein optimal stimuli are supplied to reduce damage by pests or increase efficacy of natural enemies of pests. Therefore, we propose the following new state-dependent forest growth model, which is based on principles from behavioral ecology.

Without any disturbances, the stand variables could be projected according to normal growth trajectories, similar to other simulation models of stand dynamics. With a disturbance, however, the growth trajectories will be altered according to the nature of the disturbance. Huuskonen and Hynynen (2006) developed an analytic model with a logarithm form to predict diameter increment as a function of dominant height, initial stand density and the actual stem number of the growing stock, and the regeneration method. We propose that thinning (an anthropogenic disturbance) can be characterized by three components: timing, intensity, and method. In other words, any thinning regime could be expressed as a combination of these three variables, with a given forest responding to the specific variables. Here, the key issue is how a forest might respond to disturbance, and we propose that the response would be based on the state of tree (e.g., age, size, and energy reserve) and the level of stimuli (thinning). According to the first principle of evolutionary biology, the best response should have evolved over past millennia, with maximized fitness that is favored by natural selection. If this is reasonable, one should be able to calculate the best response accordingly (Smith, 1978; Parker and Smith, 1990).

Behavioral ecologists have developed an algorithm for such a calculation. For example, to investigate masting "behavior" of trees, Lalonde and Roitberg (1992) developed a method of calculating a decision matrix representing the best behavioral response to the environment under various conditions. Their conceptual framework is described below:

Most plants acquire resources as a result of photosynthesis. The rate of resource acquisition is a function of the quantity of resources previously allocated to the vegetative growth including the creation and maintenance of photosynthetic structures (e.g., leaves), support structures (lignified tissues), and uptake structures (roots). In order to accrue fitness, a plant must, at some point, divert some of its resources away from vegetative growth and toward reproduction (seeds and seed support structures). The cost of reproduction in terms of depressed capacity or vegetative investment during fruiting years is well demonstrated for masting plants, and a plant must, therefore, balance its

allocation to vegetative versus reproductive investment over its life time in order to maximize its reproductive success. This is essentially the stuff of life history theory that takes explicit recognition of state-dependent costs and benefits into account (see *State-Dependent Forest Growth Models* on state dependence). Lalonde and Roitberg thus developed a stochastic dynamic optimization model to determine how the dynamics of resource acquisition can lead to fluctuations in seed production in a long-lived perennial. The stochastics are based upon environmental inputs (e.g., light, water, nutrients) and dynamics refer to changes in values of state variables (e.g., roots and shoots) associated with plant response. The optimization equation takes the form of

$$\begin{aligned} F(V,S,t,T) = \max\{ & P_g F(V - C \times V + Q_g, S + (R_g - R_g D), t-1, T) \\ & + (1-P_g)/2 \times F(V - C \times V + Q_f, S + (R_f - R_f D), t-1, T) \\ & + (1-P_g)/2 \times F(V - C \times V + Q_b, S + (R_b - R_b D), t-1, T)\} \end{aligned} \quad (5)$$

where V is vegetative growth; S is the number of seeds that it has already produced; t is current age in relation to its maximum life span T; P_g the probability of experiencing a good growth year; C is the maintenance factor; D is a start-up cost; Q and S are resources allocated to vegetative and reproductive growth, respectively; R is current investment in seed production; and the subscript's of g, f, and b indicate good, fair, and bad growth year, respectively. This equation was solved at (t=T) for all states of vegetative and reproductive investment and then iterated backward in time (i.e., backward induction) for a 100-year life span. The results were used to construct a decision matrix that holds the calculated optimal investment level to vegetative growth and to reproduction for all possible states and times (i.e., the matrix provides an analytical solution to the problem of living in a stochastic world with known probabilities of events and related outcomes).

After the decision array was constructed, Lalonde and Roitberg (1992) were able to investigate the effect of an optimized life-history strategy on the emergent properties of the seed production population, using a stochastic simulation model. Without any further details, this outlined simulation procedure provides a new approach of developing a state-dependent forest growth model where anthropogenic disturbance (e.g. PCT) is explicitly included to predict growth response of surviving trees in a stand.

The advantage of this new modeling approach is its capability of analytically answering some key questions about the generalization of CG to other tree species and geographical regions. With parameters specific to a tree species of concern, this new model is expected to produce growth trajectories under given management scenarios such as different thinning regimes.

OVERCOMPENSATION AND WOOD SUPPLY SHORTAGE

Through vast forest areas across Canada, unfavorable climate and extreme weather conditions have caused most trees to grow slower than in many other parts of the world. Despite expectations of better-quality wood fiber resulting from slow-growing trees in general, mean annual increment (MAI) also may be lower, which would inevitably lead to insufficient wood supply for the increasing demands from markets. Consequently, balance between demands of utilization and concerns of sustainability and environment protection have become important in fulfilling goals of sustainable forest management.

Overcompensation provides enhanced forest productivity, which would have a profound effect on current and future wood supply. As a result, searching for conditions for promoting overcompensation could form a new mitigation strategy for dealing with the issues related to wood supply shortage. In other words, overcompensation adds a new pillar to the existing strategies of forest productivity:

- Borrowing some future wood supply to satisfy market opportunities: adjust harvest activities to allow fluctuation according to market demand. This appeared a good strategy from a market economic perspective; however, it could create unfavorable conditions for mill operations;
- Relaxing current harvest constraints: harvest activities would have increased flexibility and thus lead to temporal fluctuations of wood supply;
- Improving efficiency of wood utilization: this can be achieved mainly by two means: (a) produce more log volume from the same forests, such as making changes in wood utilization standards (e.g., Li et al., 2016a), produce more products without increasing the total volume of harvested wood such as optimization of sawing technology (Li et al., 2016b).
- Developing new managed forest areas: expansion of existing managed forest area through building infrastructures for accessibility and markets, this needs to be taken into account at higher levels of planning and during decision-making processes.

This new mitigation strategy differs from the above four existing strategies because of the context of enhancing forest productivity, instead of only being based on current forest productivity. This strategy aims at increasing forest productivity through overcompensation and earlier than normal achievement of stand maturity, and hence elevating regional annual allowable cut that is essentially based on the long-term average forest productivity. Such a proactive mitigation strategy could provide an environment that satisfies industrial demands without compromising the goals of sustainable forest management.

CONCLUDING REMARKS AND RECOMMENDATIONS

CG is common in organisms from both plant and animal kingdoms despite different terminologies used to describe them in the literature. CG encompasses a continuum from undercompensation to full compensation, and to overcompensation. Overcompensation is of particular interests in the field of forestry because it results in enhanced forest productivity. Studying the overcompensation mechanisms is important because it could reveal whether the Shawnigan Lake case and Green River thinning trials could be generalized to other tree species and geographical regions, and thus benefit the forest sector. Searching for and creating

conditions for promoting overcompensation could form a new mitigation strategy for dealing with issues related to wood supply shortage. Results from such studies could provide cost-effective decision support tools to forestry practitioners.

To accomplish this new mitigation strategy, we recommend to conduct several tasks: (1) further clarification of CG concept to avoid misunderstanding and misapplication in forestry practice; (2) identification of alternative indicators of CG that are compatible with forestry practice; (3) collection of empirical datasets from legacy silviculture sites; and (4) development of flexible and user-friendly tools for predicting CG for given stand types and site conditions. These tools should be state-dependent, and combined using optimization and simulation technology, an approach developed in behavioral ecology, can determine the conditions under which overcompensation could occur and then refine the model by incorporating species-specific parameters for predicting whether and how overcompensation could be expected for a region under management.

DATA AVAILABILITY STATEMENT

The data analyzed in this study is subject to the following licenses/restrictions: Datasets used in this review and synthesis paper were published in the literature. Requests to access these datasets should be directed to chao.li@canada.ca.

AUTHOR CONTRIBUTIONS

CL, HB, BR, and RL jointly conceived and wrote the paper.

FUNDING

This work was financially supported by Natural Resources Canada-Canadian Forest Service's Developing Sustainable Fibre Solutions Research Program.

ACKNOWLEDGMENTS

We are deeply indebted to many Canadian Forest Services researchers under Dr. Holger Brix for their foresight and early efforts in the sound establishment of the Shawnigan Lake silviculture experiment as well as in conducting the subsequent regular re-measurements. The authors would also thank Shongming Huang of Alberta Agriculture and Forestry for discussions related to GYPSY model, Derek Sattler of the Canadian Forest Service for providing information related to the TASS model, and Cosmin Filipescu of the Canadian Forest Service for allowing access to the Shawnigan Lake trial data. We also thank the two reviewers for their constructive comments and Brenda Laishley of the Canadian Forest Service for her critical reading and helpful comments on an earlier version of this manuscript.

REFERENCES

Aber, J. D., Botkin, D. B., and Melillo, J. M. (1978). Predicting the effects of different harvesting regimes on forest floor dynamics in northern hardwoods. *Can. J. For. Res.* 8, 306–315. doi: 10.1139/x78-046

Aber, J. D., Melillo, J. M., and Federer, C. A. (1982). Predicting the effects of rotation length, harvest intensity, and fertilization on fiber yield from northern hardwood forests in New England. *For. Sci.* 28, 31–45.

Alberta Forest Service (1984). *Alberta phase 3 forest inventory: single tree volume tables. Appendix 1* (Edmonton, AB: AB Energy Nat. Resour).

Ali, M., Nicieza, A., and Wootton, R. J. (2003). Compensatory growth in fishes: a response to growth depression. *Fish Fish.* 4, 147–190. doi: 10.1046/j.1467-2979.2003.00120.x

Allen, C. D., and Breshears, D. D. (1998). Drought-induced shift of a forest-woodland ecotone: rapid landscape response to climate variation. *Proc. Nat. Acad. Sci.* 95, 14839–14842. doi: 10.1073/pnas.95.25.14839

Ancelina, P., Courbauda, B., and Fourcaud, T. (2004). Development of an individual tree-based mechanical model to predict wind damage within forest stands. *For. Ecol. Manage.* 203, 101–121. doi: 10.1016/j.foreco.2004.07.067

Avery, T. E., and Burkhart, H. E. (1994). *Forest Measurements. 4th Ed* (Boston, MA: McGraw-Hill, Inc).

Azodi, M., Nafisi, M., Morshedi, V., Modarresi, M., and Faghih-Ahmadani, A. (2016). Effects of intermittent feeding on compensatory growth, feed intake and body composition in Asian sea bass (*Lates calcarifer*). *Iran. J. Fish. Sci.* 15, 144–156.

Barclay, H. J., Li, C., Hawkes, B., and Benson, L. (2006). Effects of fire size and frequency and habitat heterogeneity on forest age distribution. *Ecol. Model.* 197, 207–220. doi: 10.1016/j.ecolmodel.2006.03.007

Barnes, B. V., Zak, D. R., Denton, S. R., and Spurr, S. H. (1998). *Forest Ecology*. *4th ed* (New York, NY: John Wiley & Sons, Inc).

Baskerville, G. L. (1959). Establishment report – Cleaning and thinning young fir. 1959 Project M-443-59. Dept. North. Aff. Nat. Resour., For. Brnch., Mar. Distr., Fredericton, N.B., Canada.

Baskerville, G. L. (1965). Dry matter production in immature balsam fir stands. *For. Sci. Monogr.*

Battaglia, M., and Sands, P. J. (1998). Process-based forest productivity models and their application in forest management. *For. Ecol. Manage.* 102, 13–32. doi: 10.1016/S0378-1127(97)00112-6

Berger, U., Hildenbrandt, H., and Grimm, V. (2004). Age-related decline in forest production: modelling the effects of growth limitation, neighbourhood competition and self-thinning. *J. Ecol.* 92, 846–853. doi: 10.1111/j.0022-0477.2004.00911.x

Binkley, D., Stape, J. L., Ryan, M. G., Barnard, H. R., and Fownes, J. (2002). Age-related decline in forest ecosystem growth: an individual-tree, stand-structure hypothesis. *Ecosystems* 5, 58–67. doi: 10.1007/s10021-001-0055-7

Bohman, V. R. (1955). Compensatory growth of beef cattle: the effect of hay maturity. *J. Anim. Sci.* 14, 249–255. doi: 10.2527/jas1955.141249x

Boisvenue, C., and Running, S. W. (2006). Impacts of climate change on natural forest productivity–evidence since the middle of the 20th century. *Glob. Change Biol.* 12, 862–882. doi: 10.1111/j.1365-2486.2006.01134.x

Bokalo, M., Stadt, K. J., Comeau, P. G., and Titus, S. J. (2013). The validation of the Mixedwood Growth Model (MGM) for use in forest management decision making. *Forests* 4, 1–27. doi: 10.3390/f4010001

Bose, A. K., Harvey, B. D., Brais, S., Beaudet, M., and Leduc, A. (2014). Constraints to partial cutting in the boreal forest of Canada in the context of natural disturbance-based management: a review. *Forestry* 87, 11–28. doi: 10.1093/forestry/cpt047

Bose, A. K., Weiskittel, A., Kuehne, C., Wagner, R. G., Turnblom, E., and Burkhart, H. E. (2018). Tree-level growth and survival following commercial thinning of four major softwood species in North America. *For. Ecol. Manage.* 427, 355–364. doi: 10.1016/j.foreco.2018.06.019

Bose, A., Nelson, A. S., and Olson, M. (2020). Growth and mortality response of forest regeneration to partial harvesting varies by species shade tolerance. *Can. J. For. Res*. doi: 10.1139/cjfr-2020-0022

Botkin, D. B., Janak, J. F., and Wallis, J. R. (1972). Some ecological consequences of a computer model of forest growth. *J. Ecol.* 60, 849–872. doi: 10.2307/2258570

Botkin, D. B. (1993). *Forest Dynamics: An Ecological Model* (Oxford and New York: Oxford University Press), 309.

Bourke, A. G. F. (2011). The validity and value of inclusive fitness theory. *Proc. Biol. Sci.* 278 (1723), 3313–3326. doi: 10.1098/rspb.2011.1465

Boyden, S., Binkley, D., and Stape, J. L. (2008). Competition among Eucalyptus trees depends on genetic variation and resource supply. *Ecology* 89, 2850–2859. doi: 10.1890/07-1733.1

Brodie, J. D., and Tedder, P. L. (1982). Regeneration delay: economic costs and harvest loss. *J. For.* 26–28.

Buckley, T. N., and Roberts, D. W. (2006). DESPOT, a process-based tree growth model that allocates carbon to maximize carbon gain. *Tree Physiol.* 26, 129–144. doi: 10.1093/treephys/26.2.129

Bugmann, H. (2001). A review of forest Gap models. *Clim. Change* 51, 259–305. doi: 10.1023/A:1012525626267

Buongiorno, J., Zhu, S., Zhang, D., Turner, J., and Tomberlin, D. (2003). *The Global Forest Products Model* (Oxford, UK: Academic Press), 301 p.

Cahill, J. F. (2015). Introduction to the Special Issue: beyond traits: integrating behaviour into plant ecology and biology. *AoB Plants* 7, plv120. doi: 10.1093/aobpla/plv120

Canadian Council of Forest Ministers (2000). *Criteria and indicators of sustainable forest management in Canada* (Ottawa, ON: Nat. Resour. Can., Can. For. Serv).

Clements, F. E. (1916). *Plant succession: An analysis of the development of vegetation* Vol. 242 (Washington, D.C: Carnegie Inst. Publ), 512 pp.

Coates, K. D. (1997). Windthrow damage 2 years after partial cutting at the Date Creek silvicultural systems study in the interior cedar hemlock forests of northwestern British Columbia. *Can. J. For. Res.* 27, 1695–1701. doi: 10.1139/x97-132

Crow, T. R., Dey, D. C., and Riemenschneider, D. (2006). *Forest productivity: Producing goods and services for people. Gen. Tech. Rep. NC-246* (St. Paul, MN: USDA For. Serv., Nor. Cent. Res. Stat), 34 p.

Crown, M., and Brett, C. P. (1975). *Fertilization and thinning effect on a Douglas-fir ecosystem at Shawnigan Lake: An establishment report* (Victoria, BC: Environ. Can., Can. For. Serv., Pac. For. Res. Ctr.). Info Rep. BC-X-110.

Davies, N. B., Krebs, J. R., and West, S. A. (2012). *An Introduction to Behavioural Ecology. 4th ed* (Oxford: Wiley-Blackwell).

Davis, L. S., Johnson, K. N., Bettinger, P., and Howard, T. E. (2001). *Forest Management: To Sustain Ecological, Economic, and Social Values. 4th Edition* (Long Grove, Illinois: Waveland Press, Inc), 804 pp.

Debecker, S., and Stoks, R. (2019). Pace of life syndrome under warming and pollution: integrating life history, behavior and physiology across latitudes. *Ecol. Monogr.* 89, e01322. doi: 10.1002/ecm1332

Díaz-Yáñez, O., Mola-Yudego, B., and González-Olabarria, J. R. (2019). Modelling damage occurrence by snow and wind in forest ecosystems. *Ecol. Model.* 408:108741. doi: 10.1016/j.ecolmodel.2019.108741

Dixon, G. E. (2002). Essential FVS: A user's guide to the Forest Vegetation Simulator. Internal Rep. Fort Collins, CO: USDA For. Serv., For. Manag. Serv. Cent. 226p. (Revised: January 7, 2020).

Drew, T. J., and Flewelling, J. W. (1979). Stand density management: an alternative approach and its application to Douglas-fir plantations. *For. Sci.* 25, 518–532.

Duke, K. M., Townsend, G. M., and White, W. A. (1989). *An economic analysis of fertilization and thinning effects on Douglas-fir stands at Shawnigan Lake* (Victoria, BC: Ministry of Supply and Services Canada). For. Can., Pac. Yt. Reg., Pac. For. Ctr., Info. Rep. BC-X-312.

Eaton, F. M. (1931). Early defloration as a method of increasing cotton yields and the relation of fruitfulness to fiber and boll characters. *J. Agric. Res.* 42, 447–462.

Erbilgin, N., Galvez, D. A., Zhang, B., and Najar, A. (2014). Resource availability and repeated defoliation mediate compensatory growthin trembling aspen (*Populus tremuloides*) seedlings. *PeerJ* 2, e491. doi: 10.7717/peerj.491

FAO (2016). *Environmental conservation and forestry* (MYANMAR: National Action Plan for Agriculture (NAPA) Working Paper 5, Yangon). Available at: http://www.fao.org/3/a-bl825e.pdf (Accessed Aug. 12, 2020).

Farnden, C. (1996). *Stand density management diagrams for lodgepole pine, white spruce and interior Douglas-fir* (Victoria, BC: Ministry of Supply and Services Canada). Pac. For. Ctr., Can. For. Serv., Info. Rep. BC-X-360.

Felton, A., Löfroth, T., Angelstam, P., Gustafsson, L., Hjältén, J., Felton, A. M., et al. (2020). Keeping pace with forestry: Multi-scale conservation in a changing production forest matrix. *Ambio* 49, 1050–1064. doi: 10.1007/s13280-019-01248-0

Ferriere, R., and Michod, R. (2011). Inclusive fitness in evolution. *Nature* 471, E6–E8. doi: 10.1038/nature09834

Fortin, M., and Langevin, L. (2010). *ARTÉMIS-2009 : un modèle de croissance basé sur une approche par tiges indivuelles pour les forêts du Québec. Mémoire de recherche forestière n 156. Direction de la recherche forestière, Ministère des Ressources naturelles et de la Faune*. Available at: https://www.mffp.gouv.qc.ca/publications/forets/connaissances/recherche/Fortin-Mathieu/Memoire156.pdf (Accessed Aug. 12, 2020).

Gabriel, N. N., Omoregie, E., Martin, T., Kukuri, L., and Shilombwelwa, L. (2018). Compensatory growth response in *Oreochromis mossambicus* submitted to short-term cycles of feed deprivation and refeeding. *Turk. J. Fish. Aqu. Sci.* 18, 161–166. doi: 10.4194/1303-2712-v18_1_18

Gower, S. T., McMurtrie, R., and Murty, D. (1996). Aboveground net primary production decline with stand age: potential causes. *Trends Ecol. Evol.* 11, 378–382. doi: 10.1016/0169-5347(96)10042-2

Guillet, C., and Bergström, R. (2006). Compensatory growth of fast-growing willow (*Salix*) coppice in response to simulated large herbivore browsing. *Oikos* 113, 33–42. doi: 10.1111/j.0030-1299.2006.13545.x

Gustafson, E. J., and Sturtevant, B. R. (2013). Modeling forest mortality caused by drought stress: implications for climate change. *Ecosystems* 16, 60–74. doi: 10.1007/s10021-012-9596-1

Gustafson, E. J., Miranda, B. R., De Bruijn, A. M. G., Sturtevant, B. R., and Kubiske, M. E. (2017). Do rising temperatures always increase forest productivity? Interacting effects of temperature, precipitation, cloudiness and soil texture on tree species growth and competition. *Env. Model. Soft.* 97, 171–183. doi: 10.1016/j.envsoft.2017.08.001

Gustafson, E. J., Kern, C. C., Miranda, B. R., Sturtevant, B. R., Bronson, D. R., and Kabrick, J. M. (2020). Climate adaptive silviculture strategies: How do they impact growth, yield, diversity and value in forested landscapes? *For. Ecol. Manage.* 470–471, 118208. doi: 10.1016/j.foreco.2020.118208

Harper, J. L. (1977). *Population Biology of Plants* (London, England: Academic Press), 892 P.

Harrington, C. A., and Reukema, D. L. (1983). Initial shock and long-term stand development following thinning in a Douglas-fir plantation. *For. Sci.* 29, 33–46.

He, H. S., Gustafson, E. J., and Lischke, H. (2017). Modeling forest landscapes in a changing climate: theory and application. *Landsc. Ecol.* 32, 1299–1305. doi: 10.1007/s10980-017-0529-4

Hector, K. L., and Nakagawa, S. (2012). Quantitative analysis of compensatory and catch-up growth in diverse taxa. *J. Anim. Ecol.* 81, 583–593. doi: 10.1111/j.1365-2656.2011.01942.x

Hennigar, C. R., MacLean, D. A., Quiring, D. T., and Kershaw, J. A.Jr (2008). Differences in spruce budworm defoliation among balsam fir and white, red, and black spruce. *For. Sci.* 54, 158–166. doi: 10.1093/forestscience/54.2.158

Hoffman, R. (2020). *Alfred Adler"s theories of individual psychology and Adlerian therapy. Simply Psychology*. Available at: https://www.simplypsychology.org/alfred-adler.html (Accessed Aug. 12, 2020).

Hoi, A. E., Zappia, S., Phelan, C., and Roitberg, B. (2013). The confusing transition into adulthood: time allocation to the life history transition of aquatic larvae. *Evol. Ecol. Res.* 15, 959–963.

Huang, S., Morgan, D., Klappstein, G., Heidt, J., Yang, Y., and Greidanus, G. (2001). *GYPSY: A growth and yield projection system for natural and regenerated stands within an ecologically based, enhanced forest management framework* (Edmonton, AB: AB Sustain. Resour. Dev).

Huang, S., Meng, S. X., and Yang, Y. (2009). *A Growth and Yield Projection System (GYPSY) for Natural and Post-harvest stands in Alberta* (Edmonton, AB: AB Sustain. Resour. Dev).

Huang, S. (1994). *Summary of equations and estimated coefficients for ecologically based individual tree volume estimation in Alberta* (Edmonton, AB: AB Environ. Prot., Ecologically based individual tree volume estimation for major Alberta tree species. Rep), 3.

Hui, C. (2006). Carrying capacity, population equilibrium, and environment's maximal load. *Ecol. Model.* 192, 317–320. doi: 10.1016/j.ecolmodel.2005.07.001

Huuskonen, S., and Hynynen, J. (2006). Timing and intensity of precommercial thinning and their effects on the first commercial thinning in Scots pine stands. *Sil. Fen.* 40, 645–662. doi: 10.14214/sf.320

IPCC (2007). *Climate change 2007 — the physical science basis: Working Group I contribution to the fourth assessment report of the IPCC* Vol. 4. Ed. S. Solomon (United Kingdom and New York, NY, USA: Cambridge University Press).

Jackson, C. M. (1937). Recovery of rats upon refeeding after prolonged suppression of growth by underfeeding. *Anat. Rec.* 68, 371–381. doi: 10.1002/ar.1090680310

Jaremo, J., and Palmqvist, E. (2001). Plant compensatory growth: a conquering strategy in plant–herbivore interactions? *Evol. Ecol.* 15, 91–102. doi: 10.1023/A:1013899006473

Jenkins, M., and Schaap, B. (2018). *Forest Ecosystem Services. Background Analytical Study 1. Background study prepared for the thirteenth session of the United Nations Forum on Forests* (accessed Aug. 12, 2020), 41 p. Available at: https://www.un.org/esa/forests/wp-content/uploads/2018/05/UNFF13_BkgdStudy_ForestsEcoServices.pdf.

Johnstone, W. D. (1976). *Variable-density yield tables for natural stands of lodgepole pine in Alberta* (Ottawa, ON: Can. For. Serv., Dept. Fish. Environ. For. Tech. Rep), 20.

Kalbe, M., Eizaguirre, C., Dankert, I., Reusch, T. B. H., Sommerfeld, R. D., Wegner, K. M., et al. (2008). Lifetime reproductive success is maximized with optimal major histocompatibility complex diversity. *Proc. R. Soc B* 276, 925–934. doi: 10.1098/rspb.2008.1466

Keane, R. E., Morgan, P., and Running, S. W. (1996). *FIRE-BGC – A mechanistic ecological process model for simulating fire succession on coniferous forest landscapes of the northern Rocky Mountains, USDA For. Serv. Res. Paper INT-RP-484*. 122.

Keane, R. E., Cary, G. J., Davies, I. D., Flannigan, M. D., Gardner, R. H., Lavorel, S., et al. (2004). A classification of landscape fire succession models: spatial simulations of fire and vegetation dynamics. *Ecol. Model.* 179, 3–27. doi: 10.1016/j.ecolmodel.2004.03.015

Keeling, H. C., and Phillips, O. L. (2007). The global relationship between forest productivity and biomass. *Glob. Ecol. Biogeog.* 16, 618–631. doi: 10.1111/j.1466-8238.2007.00314.x

King, J. E. (1966). *Site index curves for Douglas-fir in the Pacific Northwest. Weyerhaeuser Forestry Paper No. 8*. 49 p.

Kirilenko, A., and Sedjo, R. A. (2007). Climate change impacts on forestry. *PNAS* 104, 19697–19702. doi: 10.1073/pnas.0701424104

Korzukhina, M. D., and Ter-Mikaelian, M. T. (1995). An individual tree-based model of competition for light. *Ecol. Model.* 79, 221–229. doi: 10.1016/0304-3800(94)00039-K

Kretchun, A. M., Scheller, R. M., Lucash, M. S., Clark, K. L., Hom, J., Van Tuyl, S., et al. (2014). Predicted effects of gypsy moth defoliation and climate change on forest carbon dynamics in the New Jersey Pine Barrens. *PloS One* 9, e102531. doi: 10.1371/journal.pone.0102531

Kurz, W. A., Apps, M. J., Webb, T. M., and McNamee, P. J. (1992). *The carbon budget of the Canadian forest sector: Phase I. For. Can, Nor. For. Cent., Edmonton, Alberta. Info. Rep. NOR-X-326E*. Available at: https://cfs.nrcan.gc.ca/pubwarehouse/pdfs/11881.pdf (Accessed Aug. 17, 2020).

Kurz, W. A., Dymond, C. C., White, T. M., Stinson, G., Shaw, C. H., Rampley, G. J., et al. (2009). CBM-CFS3: a model of carbon-dynamics in forestry and land-use change implementing IPCC standards. *Ecol. Model.* 220, 480–504. doi: 10.1016/j.ecolmodel.2008.10.018

Kuuluvainen, T., and Gauthier, S. (2018). Young and old forest in the boreal: critical stages of ecosystem dynamics and management under global change. *For. Ecosys.* 5, 26. doi: 10.1186/s40663-018-0142-2

Lalonde, R. G., and Roitberg, B. D. (1992). On the evolution of masting behavior in trees: predation or weather? *Am. Nat.* 139, 1293–1304. doi: 10.1086/285387

Lavoie, J., Montoro Girona, M., and Morin, H. (2019). Vulnerability of conifer regeneration to spruce budworm outbreaks in the Eastern Canadian boreal forest. *Forests* 10, 850. doi: 10.3390/f10100850

Leuschner, W. A. (1984). *Introduction to Forest Resource Management* (Malabar, Florida: Krieger Publishing Company), 298 p.

Li, C., and Apps, M. J. (1995). Disturbance impact on forest temporal dynamics. *Water Air Soil Pollut.* 82, 429–436. doi: 10.1007/BF01182852

Li, C., and Apps, M. J. (1996). Effects of contagious disturbance on forest temporal dynamics. *Ecol. Model.* 87, 143–151. doi: 10.1016/0304-3800(95)00023-2

Li, C., and Barclay, H. (2008). Fire disturbance patterns and forest age structure. *Nat. Res. Model.* 14, 495–521. doi: 10.1111/j.1939-7445.2001.tb00071.x

Li, C., Ter-Mikaelian, M., and Perera, A. (1997). Temporal fire disturbance patterns on a forest landscape. *Ecol. Model.* 99, 137–150. doi: 10.1016/S0304-3800(96)01944-8

Li, C., Flannigan, M. D., and Corns, I. G. W. (2000). Influence of potential climate change on forest landscape dynamics of west-central Alberta. *Can. J. For. Res.* 30, 1905–1912. doi: 10.1139/x00-118

Li, C., Barclay, H. J., Hawkes, B. C., and Taylor, S. W. (2005). Lodgepole pine forest age class dynamics and susceptibility to mountain pine beetle attack. *Ecol. Compl.* 2, 232–239. doi: 10.1016/j.ecocom.2005.03.001

Li, C., Hans, H., Barclay, H., Liu, J., Carlson, G., and Campbell, D. (2008). Comparison of spatially explicit forest landscape fire disturbance models. *For. Ecol. Manage.* 254, 499–510. doi: 10.1016/j.foreco.2007.07.022

Li, C., Huang, S., Barclay, H., and Sidders, D. (2016a). Effect of utilization standard on wood supply and lumber yield. *J. Sustain. For.* 35, 217–233. doi: 10.1080/10549811.2016.1144514

Li, C., Huang, S., Barclay, H., and Sidders, D. (2016b). Modeling lumber yield of white spruce in Alberta, Canada: a comparative approach. *J. For. Res.* 21, 271–279. doi: 10.1007/s10310-016-0544-3

Li, C., Huang, S., Barclay, H., and Filipescu, C. N. (2018). Estimation of compensatory growth of coastal Douglas-fir following pre-commercial thinning across a site quality gradient. *For. Ecol. Manage.* 429, 308–316. doi: 10.1016/j.foreco.2018.07.028

Li, C. (2000). Reconstruction of natural fire regimes through ecological modelling. *Ecol. Model.* 134, 129–144. doi: 10.1016/S0304-3800(00)00290-8

Li, C. (2009). Toward full, multiple, and optimal wood fibre utilization: A modeling perspective. *For. Chron.* 85, 377–381. doi: 10.5558/tfc85377-3

Loehle, C. (2016). Biomechanical constraints on tree architecture. *Trees* 30, 2061–2070. doi: 10.1007/s00468-016-1433-2

Mangel, M., and Clark, C. (1988). *Dynamic Modeling in Behavioral Ecology* (Princeton: N. J. PU Press).

Mangel, M., and Munch, S. B. (2005). A life-history perspective on short- and long-term consequences of compensatory growth. *Am. Nat.* 166, E155–E176. doi: 10.1086/444439

Manitoba Conservation and Water Stewardship (2013). *Wood supply analysis report: forest management unit 24*. Available at: https://www.gov.mb.ca/sd/forestry/pdf/wood-supply/pineland_wood_supply_analysis_report_2013.pdf (Accessed June 18, 2020).

Martin, P. (1991). *Growth and yield prediction systems. Special Report Series 7* (BC Ministry of Forests), 31 p.

Martin-Benito, D., Cherubini, P., Rio, M., and Canellas, I. (2008). Growth response to climate and drought in Pinus nigra Arn. trees of different crown classes. *Trees* 22, 363–373. doi: 10.1007/s00468-007-0191-6

Martire, S., Castellani, V., and Sala, S. (2015). Carrying capacity assessment of forest resources: enhancing environmental sustainability in energy production at local scale. *Resour. Conserv. Recycl.* 94, 11–20. doi: 10.1016/j.resconrec.2014.11.002

McIntosh, R. P. (1981). "Succession and ecological theory," in *Forest Succession: Concepts and Application*. Eds. D. C. West, H. H. Shugart and D. B. Botkin (New York, NY: Springer-Verlag), 10–23.

McNaughton, S. J. (1983). Compensatory plant growth as a response to herbivory. *Oikos* 40, 329–336. doi: 10.2307/3544305

McNaughton, S. J. (1985). Ecology of a grazing ecosystem: the Serengeti. *Ecol. Monogr.* 55, 259–294. doi: 10.2307/1942578

Means, J. E., and Helm, M. E. (1985). *Height growth and site index curves for Douglas-fir on dry sites in the Willamette National Forest* (Res. Pap. PNW-341. Portland, OR: USA For. Serv., Pac. NW For. Range Exp. Stat), 17 p.

Miller, G. W., Stringe, J. W., and Mercker, D. C. (2007). *Technical guide to crop tree release in hardwood forests. Professional Hardwood Notes* (University of Tennessee Extension PB1774). Available at: https://www.nrs.fs.fed.us/pubs/jrnl/2007/nrs_2007_miller_001.pdf (Accessed Aug. 12, 2020).

Mitchell, K. J. (1975). Dynamics and simulated yield of Douglas-fir. *For. Sci. Monogr.* 17, 39.

Montoro Girona, M., Morin, H., Lussier, J. M., and Walsh, D. (2016). Radial growth response of black spruce stands ten years after experimental shelterwoods and seed-tree cuttings in boreal forest. *Forests* 7, 240. doi: 10.3390/f7100240

Montoro Girona, M., Rossi, S., Lussier, J.-M., Walsh, D., and Morin, H. (2017). Understanding tree growth responses after partial cuttings: A new approach. *PloS One* 12 (2), e0172653. doi: 10.1371/journal.pone.0172653

Montoro Girona, M., Lussier, J. M., Morin, H., and Thiffault, N. (2018). Conifer regeneration after experimental shelterwood and seed-tree treatments in boreal forests: finding silvicultural alternatives. *Front. Plant Sci.* 9, 1145. doi: 10.3389/fpls.2018.01145

Montoro Girona, M., Morin, H., Lussier, J. M., and Ruel, J. C. (2019). Post-cutting mortality following experimental silvicultural treatments in unmanaged boreal forest stands. *Front. For. Glob. Change* 2, 4. doi: 10.3389/ffgc.2019.00004

Mulloy, G. A. (1944). *Empirical stand density yield tables* (Can. Dept. Mines Resour., Dom. For. Serv., Silvic. Res. Note 73), 22 p.

Navarro, L., Morin, H., Bergeron, Y., and Girona, M. M. (2018). Changes in spatiotemporal patterns of 20th century spruce budworm outbreaks in eastern Canadian boreal forests. *Front. Plant Sci.* 9, 1905. doi: 10.3389/fpls.2018.01905

Norby, R. J., Warren, J. M., Iversen, C. M., Medlyn, B. E., and McMurtriec, R. E. (2010). CO_2enhancement of forest productivity constrained by limited nitrogen availability. *Proc. Natl. Acad. Sci.* 107, 19368–19373. doi: 10.1073/pnas.1006463107

Oboite, F. O., and Comeau, P. G. (2019). Release response of black spruce and white spruce following overstory lodgepole pine mortality due to mountain pine beetle attack. *For. Ecol. Manage.* 432, 446–454. doi: 10.1016/j.foreco.2018.09.029

Odum, E. P., and Barrett, G. W. (2005). *Fundamentals of Ecology. 5th ed* (Belmont, CA: Thomson Brooks/Cole).

Odum, E. P. (1959). *Fundamentals of Ecology* (Philadelphia, PA: W.B. Saunders).

Odum, E. P. (1969). The strategy of ecosystem development. *Science* 164, 262–270. doi: 10.1126/science.164.3877.262

Onoda, T., Yamamoto, R., Sawamura, K., Inoue, Y., Matsui, A., Miyake, T., et al. (2011). Empirical growth curve estimation using sigmoid sub-functions that adjust seasonal compensatory growth for male body weight of thoroughbred horses. *J. Equine Sci.* 22, 37–42. doi: 10.1294/jes.22.37

Osborne, T. B., and Mendel, L. B. (1915). The resumption of growth after long continued failure to grow. *J. Biol. Chem.* 23, 439–454.

Osborne, T. B., and Mendel, L. B. (1916). Acceleration of growth after retardation. *Am. J. Physiol. – Leg. Cont.* 40, 16–20. doi: 10.1152/ajplegacy.1916.40.1.16

Pamerleau-Couture, E., Krause, C., Pothier, D., and Weiskittel, A. (2015). Effect of three partial cutting practices on stand structure and growth of residual black spruce trees in north-eastern Quebec. *Forestry* 88, 471–483. doi: 10.1093/forestry/cpv017

Parker, G., and Smith, J. M. (1990). Optimality theory in evolutionary biology. *Nature* 348, 27–33. doi: 10.1038/348027a0

Penner, M., Woods, M., Parton, J., and Stinson, A. (2008). Validation of empirical yield curves for natural-origin stands in boreal Ontario. *For. Chron.* 84, 704–717. doi: 10.5558/tfc84704-5

Penner, M. (2008). Yield prediction for mixed species stands in boreal Ontario. *For. Chron.* 84, 1–7. doi: 10.5558/tfc84046-1

Pitt, D., and Lanteigne, L. (2008). Long-term outcome of precommercial thinning in northwestern New Brunswick: growth and yield of balsam fir and red spruce. *Can. J. For. Res.* 38, 592–610. doi: 10.1139/X07-132

Pothier, D., and Auger, I. (2011). *NATURA-2009: un modèle de prévision de la croissance à l''échelle du peuplement pour les forêts du Québec. Mémoire de recherche forestière n 163. Direction de la recherche forestière, Ministère des Ressources naturelles et de la Faune*. Available at: http://www.mffp.gouv.qc.ca/publications/forets/connaissances/recherche/Auger-Isabelle/Memoire163.pdf (Accessed Aug. 12, 2020).

Prentice, I. C., Sykes, M. T., and Cramer, W. (1993). A simulation model for the transient effects of climate change on forest Landscapes. *Ecol. Model.* 65, 51–70. doi: 10.1016/0304-3800(93)90126-D

Puhlick, J. J., Kuehne, C., and Kenefic, L. S. (2019). Crop tree growth response and quality after silvicultural rehabilitation of cutover stands. *Can. J. For. Res.* 49, 670–679. doi: 10.1139/cjfr-2018-0248

Rea, R. V., and Massicotte, H. B. (2010). Viewing plant systematics through a lens of plant compensatory growth. *Am. Biol. Teach.* 72, 541–544. doi: 10.1525/abt.2010.72.9.4

Reukema, D. L. (1975). *Guidelines for precommercial thinning of Douglas-fir. General Technical Report PNW 30* (Portland, OR: USDA For. Serv., PNW, For. Rng. Exp. Sta. P), 10.

Roitberg, B. D. (2007). Why pest management needs behavioral ecology and vice versa. *Entomol. Res.* 37, 14–18. doi: 10.1111/j.1748-5967.2007.00045.x

Ryan, M. G., Binkley, D., and Fownes, J. H. (1997). Age-related decline in forest productivity: pattern and process. *Adv. Ecol. Res.* 27, 213–262.

Ruel, J. C., Raymond, P., and Pineau, M. (2003). Windthrow after shelterwood cutting in balsam fir stands. *Northern J. Appl. Forest.* 20, 5–3.

Safranyik, L., Barclay, H. J., Thomson, A. J., and Riel, W. G. (1999). A population dynamics model for the mountain pine beetle, Dendroctonus ponderosae Hopk. Coleoptera: Scolytidae. (Victoria, BC: Natural Resources Canada, Canadian Forest Service, Pacific Forestry Centre). Information Report BC-X-386. 35 p

Safranyik, L., Linton, D. A., Shore, T. L., and Hawkes, B. C. (2001). The effects of prescribed burning on mountain pine beetle in lodgepole pine. (Victoria, BC: Natural Resources Canada, Canadian Forest Service, Pacific Forestry Centre). Information Report BC-X-391. 9 p.

Saskatchewan Ministry of Environment (2017). *Island Forests 2018–2038 Forest Management Plan Volume II* (Regina, SK: Saskatchewan Ministry of Environment). Available at: http://publications.saskatchewan.ca/api/v1/products/85384/formats/98889/download (Accessed June 18, 2020).

Schelhaas, M. J., Nabuurs, G. J., and Schuck, A. (2003). Natural disturbances in the European forests in the 19th and 20th centuries. *Glob. Change Biol.* 9, 1620–1633. doi: 10.1046/j.1365-2486.2003.00684.x

Segers, F. H., and Taborsky, B. (2012). Competition level determines compensatory growth abilities. *Beh. Ecol.* 23, 665–671. doi: 10.1093/behaveco/ars013

Seidl, R., Fernandes, P. M., Fonseca, T. F., Gillet, F., Jönsson, A. M., Merganičová, K., et al. (2011). Modelling natural disturbances in forest ecosystems: a review. *Ecol. Model.* 222, 903–924. doi: 10.1016/j.ecolmodel.2010.09.040

Smith, J. M. (1978). Optimization theory in evolution. *Ann. Rev. Ecol. Syst.* 9, 31–56. doi: 10.1146/annurev.es.09.110178.000335

Soucy, M., Lussier, J. M., and Lavole, L. (2012). Long-term effects of thinning on growth and yield of an upland black spruce stand. *Can. J. For. Res.* 42, 1669–1677. doi: 10.1139/x2012-107

Therkildsena, M., Vestergaarda, M., Buska, H., Jensena, M. T., BRiisa, B., Karlssona, A. H., et al. (2004). Compensatory growth in slaughter pigs—in vitro muscle protein turnover at slaughter, circulating IGF-I, performance and carcass quality. *Live. Prod. Sci.* 88, 63–75. doi: 10.1016/j.livprodsci.2003.10.009

Tong, Q. J., and Zhang, S. Y. (2005). Impact of initial spacing and precommercial thinning on jack pine tree growth and stem quality. *For. Chron.* 81, 418–428. doi: 10.5558/tfc81418-3

Tuomi, J., Nilsson, P., and Åström, M. (1994). Plant Compensatory Responses: Bud Dormancy as an Adaptation to Herbivory. *Ecology* 75, 1429–1436. doi: 10.2307/1937466

Van Bogaert, R., Gauthier, S., Raulier, F., Saucier, J. P., Boucher, D., Robitaille, A., et al. (2015). Exploring forest productivity at an early age after fire: a case study at the northern limit of commercial forests in Quebec. *Can. J. For. Res.* 45, 579–593. doi: 10.1139/cjfr-2014-0273

Weetman, G. F., and Mitchell, S. J. (2013). "Silviculture," in *Forestry Handbook for British Columbia, 5th Edition*. Eds. S. B. Watts and L. Tolland (Vancouver, BC: The Forestry Undergraduate Society, Faculty of Forestry, UBC), 394–431.

Wenger, K. F. (1984). *Forestry Handbook. 2nd ed* (New York, NY: John Wiley & Sons, Inc).

Wilson, P. N., and Osbourn, D. F. (1960). Compensatory growth after undernutrition in mammals and birds. *Biol. Rev.* 35, 324–363. doi: 10.1111/j.1469-185X.1960.tb01327.x

Yambayamba, E., and Price, M. A. (1991). Growth performance and carcass composition in beef heifers undergoing catch-up (compensatory) growth. *Can. J. Anim. Sci.* 71, 1021–1029. doi: 10.4141/cjas91-123

Zaehle, S., Sitch, S., Prentice, I. C., Liski, J., Cramer, W., Erhard, M., et al. (2009). The importance of age-related decline in forest NPP for modeling regional carbon balances. *Ecol. Appl.* 16, 1555–1574. doi: 10.1890/1051-0761(2006)016[1555:TIOADI]2.0.CO;2

Zhang, Y., Chen, H. Y., and Reich, P. B. (2012). Forest productivity increases with evenness, species richness and trait variation: a global meta-analysis. *J. Ecol.* 100, 742–749. doi: 10.1111/j.1365-2745.2011.01944.x

Zubair, A., and Leeson, S. (1996). Compensatory growth in the broiler chicken: A review. *Worlds Poult. Sci. J.* 52, 189–201. doi: 10.1079/WPS19960015

Conflict of Interest: The authors declare that the research was conducted in the absence of any commercial or financial relationships that could be construed as a potential conflict of interest.

frontiers | Frontiers in Plant Science

ORIGINAL RESEARCH
published: 06 May 2022
doi: 10.3389/fpls.2022.907598

Detecting Compensatory Growth in Silviculture Trials: Empirical Evidence From Three Case Studies Across Canada

Chao Li[1], Hugh Barclay[2†], Shongming Huang[3], Bernard Roitberg[1,4†], Robert Lalonde[5] and Nelson Thiffault[6]*

[1]Canadian Wood Fibre Centre, Canadian Forest Service, Edmonton, AB, Canada, [2]Pacific Forestry Centre, Canadian Forest Service, Victoria, BC, Canada, [3]Alberta Agriculture, Forestry and Rural Economic Development, Edmonton, AB, Canada, [4]Department of Biological Sciences, Simon Fraser University, Burnaby, BC, Canada, [5]Department of Biology, University of British Columbia, Okanagan, BC, Canada, [6]Canadian Wood Fibre Centre, Canadian Forest Service, Québec City, QC, Canada

Compensatory growth (CG) appears common in biology and is defined as accelerated growth after experiencing a period of unfavorable conditions. It usually leads to an increase in biomass that may eventually equal or even surpass that of sites not experiencing disturbance. In forestry, with sufficient time the stand volume lost in a disturbance such as a thinning operation could match or even exceed those from undisturbed sites, respectively called exact and overcompensation. The forest sector could benefit from enhanced productivity and associated ecosystem services such as carbon storage through overcompensation. Therefore, detection of CG in different types of forests becomes important for taking advantage of it in forest management. However, compensatory growth has not been reported widely in forestry, partially due to the paucity of long-term observations and lack of proper indicators. Legacy forest projects can provide a suitable data source, though they may be originally designed for other purposes. Three case studies representing different data structures of silviculture trials are investigated to evaluate if compensatory growth is common in forest stands. Our results showed that compensatory growth occurred in all three cases, and thus suggested that the compensatory growth might indeed be common in forest stands. We found that the relative growth (RG) can serve as a universal indicator to examine stand-level compensatory growth in historical long-term silviculture datasets. When individual tree-based measurements are available, both volume and value-based indicators can be used in detecting compensatory growth, and lumber value-based indicators could be more sensitive in detecting overcompensation.

Keywords: density management, overcompensation, plantation spacing, thinning operation, wood fiber value simulation model

OPEN ACCESS

Edited by:
Runguo Zang,
Chinese Academy of Forestry, China

Reviewed by:
Tonggui Wu,
Chinese Academy of Forestry, China
Rongzhou Man,
Ontario Ministry of Northern Development, Mines, Natural Resources and Forestry, Canada

****Correspondence:***
Chao Li
chao.li@nrcan-rncan.gc.ca

[†]Retired

Specialty section:
This article was submitted to Functional Plant Ecology, a section of the journal Frontiers in Plant Science

Received: *29 March 2022*
Accepted: *19 April 2022*
Published: *06 May 2022*

Citation:
Li C, Barclay H, Huang S, Roitberg B, Lalonde R and Thiffault N (2022) Detecting Compensatory Growth in Silviculture Trials: Empirical Evidence From Three Case Studies Across Canada. Front. Plant Sci. 13:907598. doi: 10.3389/fpls.2022.907598

INTRODUCTION

Forest productivity representing long-term potential in forest dynamics is one of the major concerns and indicators in achieving sustainable forest management (Crow et al., 2006). It is also positively correlated with many ecosystem services such as carbon sequestration and storage (Kurz et al., 1992, 2009; Pöyry, 2018). Enhancement of forest productivity will thus

not only produce more wood for necessities of human society, but also present a natural remedy against climate change through altering regional carbon budgets. Exploring the conditions under which enhanced forest productivity could occur is important in this regard.

Considerable efforts have been devoted to enhancing forest productivity through silviculture (Natural Resources Canada, 1995; D'Amato et al., 2017), among which is stand density management that aims at determining the optimal stand density leading to maximizing management goals (Drew and Flewelling, 1979; Newton, 1997). Numerous experiments have been conducted to determine the effectiveness of density management for identifying best practices. Diverse results have also been reported in the literature: some are consistent, but others appear inconsistent. For example, there is a consensus that precommercial thinning (PCT) can result in faster growth of diameter and height in trees than that from untreated sites (e.g., Smith, 1986; Weetman and Mitchell, 2013). Bose et al. (2018) showed that in four major softwood species in North America [i.e., loblolly pine (*Pinus taeda* L.), coastal Douglas-fir (*Pseudotsuga menziesii* Mirbel), red spruce (*Picea rubens* Sarg.), and balsam fir (*Abies balsamea* L.)], tree volume growth was 31% higher in thinned stands relative to unthinned stands on average, irrespective of species and tree size. However, in long-term observations at the stand level, consequences of PCT are inconsistent: some appeared to have lower stand productivity compared to controls (e.g., Harrington and Reukema, 1983), but the reverse has also being reported (e.g., Warrack, 1979; Pitt and Lanteigne, 2008; Schütz et al., 2015). These inconsistent results unavoidably create difficulties in management decisions. Here, the great puzzle is how such inconsistent and diverse results occur.

The framework of compensatory growth (CG) might help explaining these inconsistent results. For example, Li et al. (2018) evaluated the different growth responses, including overcompensation, from the Shawnigan Lake PCT and fertilization trial in British Columbia (Canada), in which stand gross volumes from most treated sites exceeded those from controls 40 years after initial treatments. A descriptive model was then developed to predict the number of years required to reach an exact compensation, or the compensatory-induced-equity (CIE), under different combinations of PCT and fertilization. This unique dataset offers the opportunity to generalize the results to other species, site conditions, and geographical regions (Li et al., 2020).

Compensatory growth was defined as "the ability of an organism to grow at an accelerated rate following a period of food shortage or a decline in reproductive weight" (Mangel and Munch, 2005), and is widely observed in plants and animals as reviewed by Li et al. (2021). Despite the concept of CG being relatively new in tree biology and forestry, it has been commonly reported for other organisms; the earliest observations can be traced back about a century ago in rats and cotton crops (Osborne and Mendel, 1915, 1916; Eaton, 1931). It has also been observed in grasslands (McNaughton, 1985), fishes (Ali et al., 2003), fast-growing willow (Guillet and Bergström, 2006), balsam fir (Pitt and Lanteigne, 2008), aspen (*Populus tremuloides* Michx.) seedlings (Erbilgin et al., 2014), and Douglas-fir (Schütz et al., 2015; Li et al., 2018). In forestry, CG of trees is a special case of growth response that characterizes the process of released growth of crop trees after thinning operations, or other partial disturbances that maintain a forest cover. It reflects the accelerated growth induced by the redistribution of space, light, nutrients, and water to the trees surviving from the disturbance (e.g., thinning). Nevertheless, the CG process has not been shown to display a single fixed pattern; it appears to depend on species, social environment, seasonal development, temperature, environmental resource availability, and physiological factors such as internal state and age (Mangel and Munch, 2005).

Three main types of CG have been demonstrated along a continuum: (1) under compensation, in which stand volumes of treated sites are lower than those from control sites; (2) exact compensation, or CIE, in which stand volumes of treated sites are the same as those from control sites; and (3) overcompensation, in which stand volumes of treated sites are higher than those from control sites (Belsky, 1986; Maschinski and Whitham, 1989; Whitham et al., 1991; Li et al., 2020, 2021). In the short term, CG is expressed as an accelerated annual increment of diameter and height after thinning operations. When this trend persists for a longer term, overcompensation, the most desirable outcome from silviculture research, becomes possible, as observed for the costal Douglas-fir in the Shawnigan Lake trial (Li et al., 2018). Thus, when accelerated growth occurs over a certain period, under compensation may proceed to exact compensation, and later to overcompensation.

Compensatory growth can be seen as a component of the total Density-Dependent (D-D) response to disturbances such as fire, insect attack, death of senescent trees, and PCT. The D-D response indicates that population size may oscillate back and forth across the mean population size at carrying capacity for some time (Varley et al., 1973) when the response is over-compensatory. For trees, the status of volume can change from under-compensation to CIE, and later to over-compensation, so that the age and status of the tree's growth cycle need to be specified. From an evolutionary biology perspective, CG can also be related to the concept of life-history theory (LHT), which "attempts to understand how natural selection designs organisms to achieve reproductive success, given knowledge of how selective factors in the environment (i.e., extrinsic mortality) and factors intrinsic to the organism (i.e., trade-offs, constraints) affect survival and reproduction" (Fabian and Flatt, 2012). LHT starts with the basic principle of evolutionary biology that natural selection favors the strategies of organisms that maximize reproductive success. One can then use LHT to find the optimal resource or energy allocation strategy among growth, reproduction, and maintenance of individual trees. Nevertheless, the concept of CG appears straightforward and easy to understand without requiring specific knowledge of a given speciality.

Li et al. (2021) summarized possible gains that different industries can benefit from with CG research: (1) increased

productivity directly from overcompensation; and (2) indirectly from reduced costs associated with production and related operations. To determine the best strategy for taking advantage of CG research, forest managers and researcher need to understand the CG patterns and status of managed forests. For example, if overcompensation can be expected, the direct benefit should be targeted first, due to enhanced productivity that will benefit both increased wood supply and improved ecosystem services, without excluding the benefits from the indirect aspects. From an interdisciplinary point of view, there is a possibility of higher productivity potential from observed productivity of natural stands, if manipulated properly (Li et al., 2021). Therefore, detecting CG patterns and status in forests, especially determining whether overcompensation is reachable, is important for the forest sector in designing future research focus.

Despite the fact that CG has been reported as a common phenomenon in both plants and animals, and that different industries have benefitted greatly from CG research, direct evidence of CG in tree biology and forestry has not been as widely reported as in other fields, and the beneficial applications of CG research results are still limited. It may be unrealistic or infeasible to rely on efforts of designing and implementing new experiments for answering related questions, due to the long lifespan of trees, especially in sub-boreal and boreal ecosystems (several decades). However, revisiting datasets from historical long-term legacy projects might provide useful clues, though these experiments were not originally designed for this purpose. Owning to the different purposes of these trials, different data structures could provide different measured variables at different measurement intervals. Therefore, finding the common variables, either measured or derived, as indicators of CG is a major task in detecting CG in different tree species and different regions.

We hypothesized that CG is common at tree and stand levels. If this hypothesis were true, one could expect that plenty of empirical evidence should exist in historical forestry datasets. To examine this hypothesis, proper methodology needs to be developed to detect CG from historical datasets. The research questions raised here include "what indicators could be used for identifying CG?", and "which one can serve as a universal indicator of CG?" In this study, we use three published datasets as case studies to identify and demonstrate potential indicators of CG, in addition to stand gross volume, and to identify a universal indicator that could be used for detecting CG from a wide range of historical forestry datasets.

Historical silviculture datasets usually include stand variables, which are calculated from tree data, the standard format for silviculture research. We will show that relative growth (RG) can serve as a universal CG indicator for both tree and stand level variables. When tree level variables are available, many can serve as indicators of CG, although value-based indicators might be more sensitive to overcompensation than volume-based indicators.

MATERIALS AND METHODS

Study Areas and Data Sources

Figure 1 illustrates the locations of our three case studies. Key information about the case studies is summarized in **Table 1**.

The MacKay Thinning Experiment

Lodgepole pine (*Pinus contorta* Douglas) is a major economic species on the eastern slopes of the Canadian Rocky Mountains; it is commonly grown over rotations of 70–150 years (Stewart et al., 2006). Since 1938, the Canadian Forest Service (CFS) has established dozens of silvicultural field studies involving this species, ranging from simple trials of a single thinning prescription, to complex levels of growing stock installations replicated on sites of differing productivity or aspect, to factorial experiments of thinning and fertilization. Although most of these studies have been discontinued, a number of them remain undisturbed and adequately documented to justify their continuation as active research sites for intensive management of the foothills lodgepole pine resource (see **Figure 1** and **Table 1** for location and summary info).

Stewart and Salvail (2017) evaluated the effects of different PCT treatments on the growth of lodgepole pine using four study sites, including the MacKay thinning experiment established almost 70 years ago. The MacKay thinning experiment dataset contains the complete records of untreated plots corresponding to different treatments that allows calculation of relative volume growth at each measurement.

The original objective of the experiment was to determine whether PCT of lodgepole pine could improve merchantable volume and quality at a young age and, in turn, shorten rotation and increase annual allowable cuts. Only stand density, mean diameter at breast height (DBH; 1.3 m), tree height (TH), and stand volume data were used in the current analysis.

The Petawawa Research Forest Experiment

Red pine (*Pinus resinosa* Aiton) is a widely planted species across North America exhibiting a faster growth rate compared with most native tree species in northern United States and southeastern Canada (Thiffault et al., 2021). Forest managers generally recognize that high planting densities can result in greater volume production at stand level, but that maximized individual tree size can be achieved at lower densities. Optimum planting densities and thinning intensities can be derived from density management diagrams, which are based on assumptions derived from the observations of unmanaged stands. However, empirical data from real stand density management treatments are expected to provide objective observations from managed stands (see **Figure 1** and **Table 1** for location and summary info).

Commercial thinning (CT) has recently attracted attention as one possible way of dealing with wood supply shortage, because it provides a means to utilize wood supply from immature stands and take advantage of low stumpage price. Compared with PCT, CT is an operation with notable immediate economic gain from harvested wood. CT can be applied

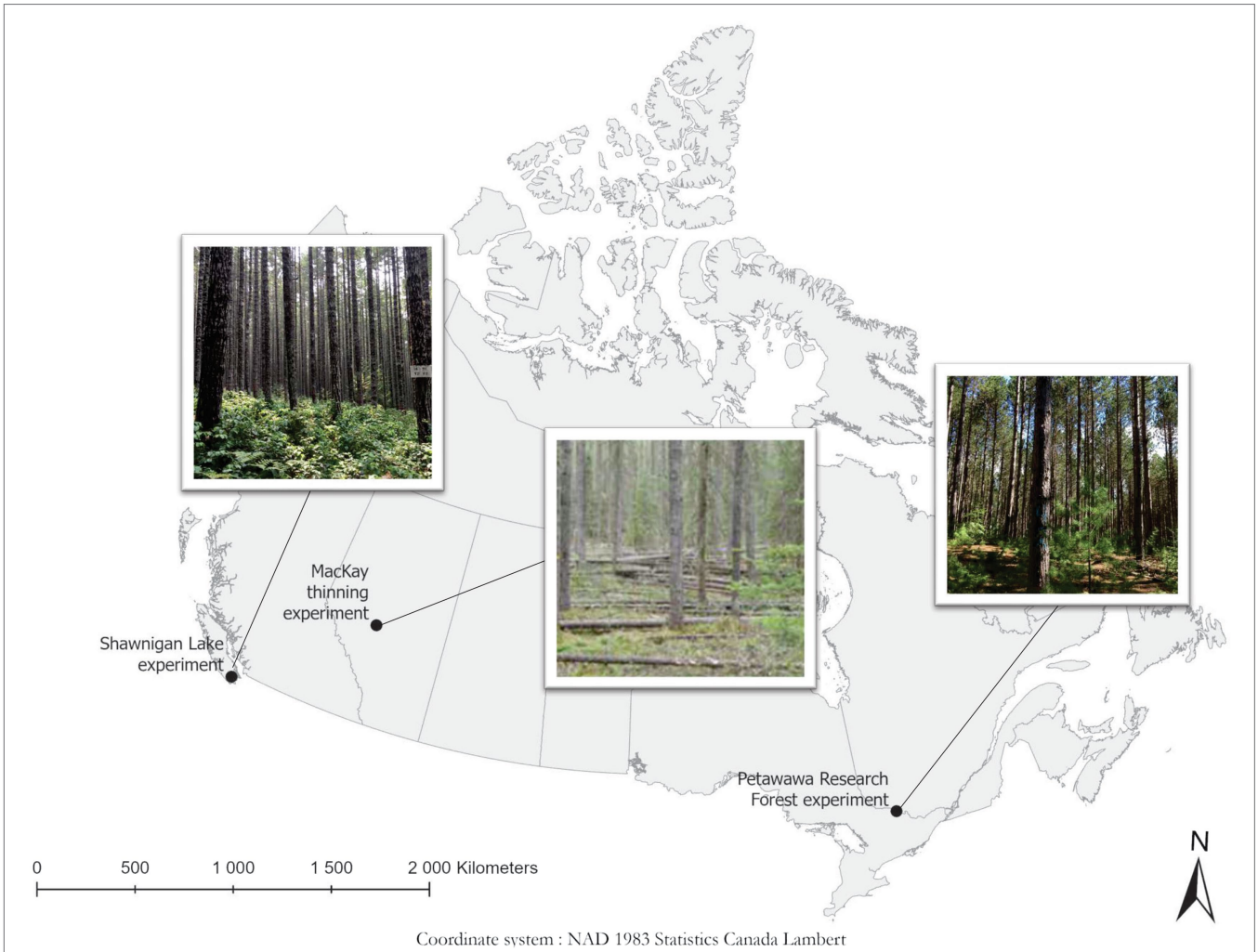

FIGURE 1 | Locations of the three case studies in Canada, with a photograph of a thinned plot from each site. Photos of Shawnigan and Petawawa are from N. Thiffault. The photo of MacKay is from B. Joss and J. Salvail, as used in Stewart and Salvail (2017).

multiple times for a stand to reach enhanced total stand productivity, which is calculated as the sum of final standing volume and cumulative volume harvested from multiple CT operations. Multiple CTs usually result in chainsaw shape for standing volume over time (Nyland, 1996). The chainsaw shape of stand productivity shows CG processes with multiple reductions caused by each of the CT operations. The key question is whether cumulative compensation overtakes or even exceeds the growth observed in control sites. Theoretically, thinning keeps the remaining trees vigorous and less prone to breakage, therefore when performed appropriately, the cumulative stand productivity from the CT stands could exceed that from control.

A recently published red pine dataset regarding a 30-year multiple CT trial under different spacing regimes (supplemental materials of Thiffault et al., 2021) was used for our second case study. The dataset contained mainly stand density, gross volume, and basal area at the stand level. The paired volume data structure allowed calculation of relative volume growth.

Shawnigan Lake Experiment

Coastal Douglas-fir is a long-lived species in northwest coast areas of North America; it can typically live more than 750 years in the absence of high-intensity fires or storms, and some have been known to live well over 1,000 years. Douglas-fir has also a long silviculture history in the region because of its high-value timber at minimum direct cost (Curtis et al., 1998). Plantation and silviculture of coastal Douglas-fir have been common in the Pacific Northwest (PNW) of United States and western Canada (see **Figure 1** and **Table 1** for location and summary info).

The original objective of the trial was to better understand tree growth processes and develop effective and environmentally acceptable thinning and fertilization practices for increasing wood yields (Crown and Brett, 1975). Only the measurements at 40-year after initial treatments were used in our current study.

TABLE 1 | Summary of the three case studies in Canada.

Case study	Location	Size of study site	Species	Year of establishment	Site index at age 50	Experiment design	Reference
MacKay thinning experiment	Foothill Alberta (lat. 53°32.7′′N; long. 115°32.3′′W)	1.5 ha	Lodgepole pine (*Pinus contorta* Douglas)	1954	18 m	Thinning at 22-year old stands of fire origin; treatments of spacing density of 4,330, 2,990, 1,680, and 750 stems/ha and a control arranged in a randomized complete block design with multiple replicates; measured in 1954, 1960, 1969, 1979, 1989, 1996, 2003, 2008, and 2013 with a measurement plot size of 0.08 ha each in block A, B, and C, and of 0.30 ha in block D; measured for DBH; 1.3 m for all living trees.	Stewart et al., 2006; Stewart and Salvail, 2017
Petawawa research forest experiment	Petawawa Research Forest in Chalk River, Ontario, Canada (lat. 46°00′0′′N; long. 77°26′0′′W)	10 stands of about 1.6 ha each	Red pine (*Pinus resinosa* Aiton)	1953	24 m	Established on abandoned farmland; a factorial design of six initial spacings of 1.2, 1.5, 1.8, 2.1, 2.4, and 3.0 m were randomly allocated to 10 stands; In 1962, two 0.101 ha sampling plots were established for each spacing and measured periodically; repeated commercial thinning in 1992, 2002, and 2013, bringing BA down to the same original residual BA target value of 37.9 m^2/ha; DBH and TH before each of the thinning entries were measured for the permanent sampling plots (0.08–0.101 ha) established in each spacing-thinning treatment combination; DBH was measured for every tree in each sample plot, but TH was only measured for a subsample of trees (19–76% of live stems) through a range of diameters.	Thiffault et al., 2021
Shawnigan lake experiment	Shawnigan Lake, BC (lat. 48°38′13′′N; long. 123°43′16′′W)	50 ha	Coastal Douglas-fir (*Pseudotsuga menziesii* Mirbel)	1971–1972	21 m	Thinning and fertilization treatments on 23-year old plantation with averaged 7.6 cm DBH and 8.6 m TH; a randomized 3 × 3 factorial design comprising three levels of thinning (T0, T1, and T2 corresponding to 0, 1/3, and 2/3 BA removal, respectively) and three levels of fertilization (F0, F1, and F2 corresponding to 0, 224, and 448 kg N/ha of fertilizer, respectively); multiple replications measured in plots with a size of 0.0405 ha each, surrounded by a 15-m-wide treated buffer; measured in 1, 3, 6, 9, 12, 15, 24, 32, and 40 years after initial treatments.	Crown and Brett, 1975; Omule et al., 2011; Li et al., 2018

DBH, diameter at breast height (1.3 m); TH, tree height; and BA, basal area.

Evaluation Methods

Relative Growth

Relative growth was used as an indicator of the status of CG defined as the ratio of estimated variables from treated site, V_{treated}, to untreated site, $V_{\text{untreated}}$ (Li et al., 2018). The ratio is presented as a percentage:

$$RG = \left(V_{Treated} / V_{Untreated}\right) \times 100\% \quad (1)$$

A CIE is indicated when RG is 100%, i.e., the variable measured from the treated site equals to the one from the untreated site. Overcompensation is denoted when RG is greater than 100%, and undercompensation occurs when RG is less than 100%. Therefore, the status of CG can be seen as a point within a continuum as defined in Maschinski and Whitham (1989) and Whitham et al. (1991). In the current study, RG was used to measure the status of CG in volume- and value-based measurements.

Other alternative indicators could also be developed, such as the changes in mean periodic annual increment (mPAI), as suggested in Li et al. (2020). However, here we focus on the relative growth because of its simplicity and ease of calculation.

WFVSM Model

The Wood Fiber Value Simulation Model (WFVSM) was used to calculate both volumes and values of a forest inventory consisting of tree-based records (Li et al., 2017). A brief description of data flow and analytical procedure of WFVSM is as follows: the records are first categorized by species groups of softwood and hardwood, and followed by volume and value calculations for trees harvested for segregation to different types of treatment centers for different products, which include sawmill, pulp mill, veneer mill, plywood mill, biomass, bioenergy (heating values and electricity), carbon content, and some wood fiber attributes. These calculations were based on published relationships (e.g., Briggs, 1994), except for sawmill output, which was simulated using an industrial sawmill operation software, Optitek (Li et al., 2013; FPInnovations, 2014).

Optitek was originally designed for simulating every step of operations in a real sawmill when profiles of individual logs are scanned into the computer system as images. It also has an input option for an artificial log consisting of variables including log length and sweep, and diameters at both large and small ends. Taper equation of Kozak (1988) was used to calculate the diameters at both large and small ends for each log. The eight parameters of the Kozak equation for coastal Douglas-fir were obtained from the Forest Inventory Zones A, B, and C of British Columbia (BC Ministry of Forests, Lands and Natural Resource Operations, 2014).

A look-up-table was constructed for coastal Douglas-fir through multiple simulations using Optitek. Each row of the table represents a summarized sawmill output for a possible combination of DBH (at the interval of 1 cm) and TH (at the interval of 1 m). All the values including volumes and monetary values of lumber, chip, sawdust, and shavings, as well as planing and fixed costs are among the tallied simulation results.

The estimation of the values of each treated and untreated plot can then be guided by basic principle of forestry economics (Pearse, 1990):

$$V_{Net} = V_{Revenue} - V_{Cost} \quad (2)$$

where V_{Net} is the net value, V_{Revenue} is the revenue, and V_{Cost} is the associated cost. Both V_{Revenue} and V_{Cost} can be generated from different utilization of harvested wood, such as sawmill, pulp mills, veneer mills, plywood mills, and bio-refineries, as well as when harvested wood is used as a source of biomass, and carbon capture. In the sawmill operation, for instance, V_{Revenue} can be expressed as

$$V_{Revenue} = V_{Lumber} + V_{Chip} + V_{Sawdust} + V_{Shavings} + V_{Bark} \quad (3)$$

where V_{Lumber}, V_{Chip}, V_{Sawdust}, V_{Shavings}, and V_{Bank} are values of lumber, chips, sawdust, shavings, and bark, respectively. V_{Cost} can be estimated as

$$V_{Cost} = V_{Drying} + V_{Planing} + V_{Fixed} \quad (4)$$

where V_{Drying}, V_{Planing}, and V_{Fixed} are the costs of drying, planing, and fixed cost. Substituting Eqs. 3 and 4 into Eq. 2, we then have

$$V_{Net} = \left(V_{Lumber} + V_{Chip} + V_{Sawdust} + V_{Shavings} + V_{Bark}\right) - \left(V_{Drying} + V_{Planing} + V_{Fixed}\right) \quad (5)$$

Statistical Analysis

The scattered RG data for different variables were smoothed as a surface to represent the trend of RG under different thinning (including PCT or CT) and fertilization treatments when applicable, using TableCurve 3D (SYSTAT Software Inc., 2002).

A two-way ANOVA (McDonald, 2014) was used to investigate whether the average stand commodity values could be significantly influenced by different levels of thinning and fertilization, as well as their interactions for the Shawnigan Lake dataset. ANOVAs were conducted using the car package in R v. 4.0.4 (Fox and Weisberg, 2019). We used $p < 0.01$ as a significance threshold.

RESULTS AND DISCUSSION

Case Study 1 (Lodgepole Pine): Volume-Based Indicators Using Stand Level Data

Many documented long-term silviculture trials have been designed for studying density management, because density is perhaps the easiest variable to control in a forest stand. A common indicator used in reporting results from such trials is the gross volume at the stand level, which allows

TABLE 2 | Stand density, mortality, and maximal relative volume growth of the MacKay thinning trial in Alberta, Canada, in which naturally regenerated lodgepole pine (*Pinus contorta* Douglas) stands were submitted to a gradient of pre-commercial thinning intensity.

Treatment code*	Stand density (Stems/ha)		Mortality (%)			Max relative volume growth (%)
	1954	2013	Total	Thinning	Nature	
A1	4,330	1,593	85	60	25	104
A2	2,990	1,173	89	72	17	116
A3	1,680	840	92	84	8	97
A4	2,990	1,124	90	72	17	107
A6	10,762	2,462	77	–	77	100
B1	4,330	1,494	87	64	24	100
B2	2,990	1,082	91	75	16	86
B3	1,680	1,074	91	86	5	85
B4	2,990	1,396	88	75	13	98
B6	11,887	2,850	76	–	76	100
C1	4,330	1,457	85	56	29	109
C2	2,990	1,334	86	69	17	125
C3	1,680	1,037	89	83	7	102
C4	2,990	1,569	84	69	15	103
C6	9,762	2050	79	–	79	100
D1	750	602	94	92	2	95

Maximum relative volume growth after a 60-year experimental period was calculated as the ratio of the volume obtained in the treated vs. control stands (see Eq. 1).
**Treatment code represents the combination of block name and plot number at the MacKay thinning trial.*

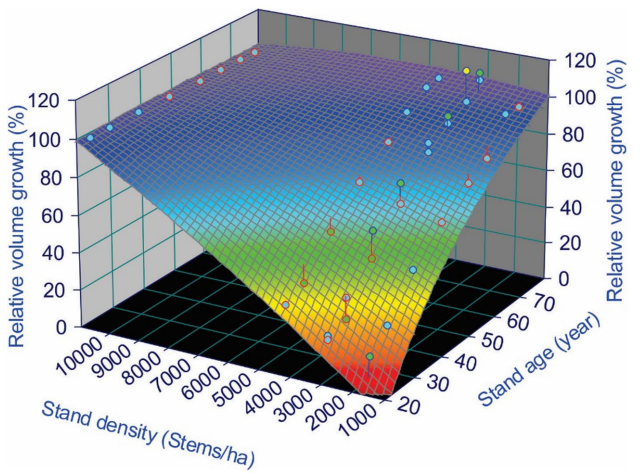

FIGURE 2 | Compensatory growth (CG) of lodgepole pine (*Pinus contorta* Douglas) in Block A of the MacKay thinning trial in Alberta, Canada, expressed as relative volume growth under different stand densities over a 60-year experimental period. Maximum relative volume growth was calculated as the ratio of the volume obtained in the treated vs. control stands (see Eq. 1).

comparing the observations from treated vs. untreated sites. They represent an excellent data source for examining whether CG is expressed in forests. The relative volume growth represented in Equation 1 can be used to detect whether or not stands displayed CG, as demonstrated here.

The initial stand density in the study area varied between 9,763 and 11,888 stems/ha. These initial densities were much higher than for some other tree species, such as coastal Douglas-fir from the Shawnigan Lake trial (3,950 stems/ha, see the case study #3 below). In Blocks A, B, and C, six plots were established (thinned to a density of 4,330 stems/ha in plot 1; 2,990 stems/ha in plot 2, 4, and 5; and 1,680 stems/ha in plot 3). Block D had one plot thinned to a density of 750 stems/ha. As a result, the numbers of trees removed at the beginning for spacing design were very high (55–93%). In the control plots (plot 6 in Block A, B, and C), self-thinning was important (76–79% over 60 years). This suggested that thinning removed large numbers of trees that might otherwise have been lost in self-thinning, such as reported by Thiffault et al. (2021). Since plot 5 was thinned twice, the measurement was not included in the current study for the purpose of comparison.

Table 2 shows some statistics from the MacKay trial dataset. Among the 13 plots (except three control plots), eight of them reached relative volume growth of over 100% (exact or overcompensation), and five were below 100% (under compensation). Unless the stand density was too low to use the available resources efficiently, there is no reason to expect these plots will not catch-up with the control given sufficient time, since they already reached 85–97% of gross volumes of the control plots.

A 3D surface plot using a smoothing function for relative volume growth under different stand densities and ages shows the trend of CG that occurred over the study area. From **Table 2**, we observe that almost all plots from Block C reached exact or overcompensation, and that all plots from Block B were below 100% compensation. Plots from Block A were a mix of under, exact and overcompensation. Therefore, as an example of such a 3D surface plot, **Figure 2** shows the data from the Block A of the MacKey thinning trial.

Figure 2 shows a clear CG pattern, in which relative volume growth was low immediately after the PCT treatments (age 20 years), but gradually approached control over time. Around 60 years after the PCT, plots with a stand density of 4,330 and

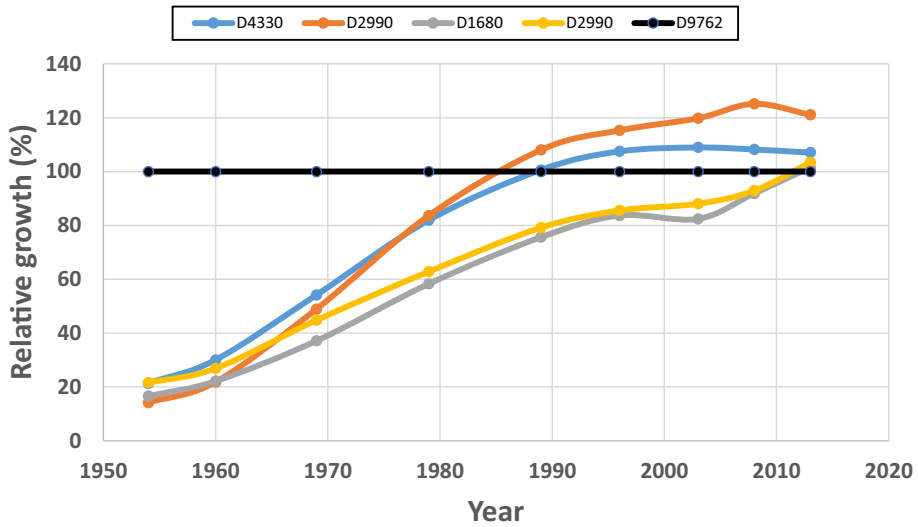

FIGURE 3 | Compensatory growth patterns for different sample plots within Block C of the MacKay thinning trial in Alberta, Canada, expressed as relative volume growth under different stand densities. Maximum relative volume growth was calculated as the ratio of the volume obtained in the treated vs. control stands (see Eq. 1). Data shows that plots with a same stand density can reach compensatory-induced-equity (CIE) by different paths.

2,990 stems/ha reached CIE, but for plots with stand density of 1,680 stems/ha, the RG was still below 100% (undercompensation).

We also observed different CG patterns among individual plots, though they are physically located very close. For example, **Figure 3** illustrates data from Block C, in which two plots with a same stand density (2,990 stems/ha) reached CIE from different paths; one plot reached CIE 25 years earlier than the other one. This stressed the need to pay attention to the different growth rates, or the different responses to partial mortality, among individual trees.

Case Study 2 (Red Pine): Relative Volume Indicator Using Metadata

There is much empirical evidence to support the theoretical expectation that thinning maintains remaining trees that are vigorous and less prone to breakage at the individual tree level (e.g., Reukema and Bruce, 1977; Greene and Emmingham, 1986; Kim et al., 2016; Gauthier and Tremblay, 2019; Gupta et al., 2020; Bjelanovic et al., 2021). However, empirical evidence supporting the expectation of overcompensation are scares. There are few long-term datasets from CT trials to support it.

Plotting raw data of gross volume over time from the red pine experiment displays the shapes of stand growth trajectories of both thinned and unthinned plots under different spacing regimes. One might expect that all thinned plots will show a "Chainsaw" shape (see **Figure 4**). When displayed in cumulative stand productivity, which is the standing volume plus harvested volumes previously, this allows a comparison with stand volumes from unthinned plots. This comparison could be better represented with relative volume growth.

As reported by Thiffault et al. (2021), the stand volumes between treated and untreated plots at the beginning of the CT trial were different; thus, we scaled stand volumes to the same level at the beginning of each spacing treatment for an easy comparison. Two points can be observed from **Figure 4**:

1. As expected, the normal (solid lines) and "Chainsaw" (dashed lines) shapes of standing volumes from unthinned and thinned plots, respectively, are evident in **Figure 4A**. The Chainsaw shape illustrates that standing volume declined right after each thinning operation, and then gradually increased until the next thinning operation for a similar cyclic fluctuation. However, it is still difficult to judge if the increase of standing volume reached a level of overcompensation.
2. The relative productivity (cumulative volume growth) under different spacing regimes (**Figure 4B**) clearly indicate overcompensation when spacing was narrower than 1.8 m, and under compensation when spacing was wider than 2.1 m. This appears consistent with what was reported by Thiffault et al. (2021), who showed that cumulative harvested and standing volume in narrow spacing treatments exceeded that from corresponding control plots. Thiffault et al. (2021) explained this as being too low stand density that resulted in insufficient utilization of available resources. Nevertheless, relative productivity further displays different CG patterns under different spacing regimes.

The second point above may also provide a possible explanation for the so-called "initial shock," a negative impact of a thinning operation, of the coastal Douglas-fir after a thinning operation reported in Harrington and Reukema (1983), in which stand volumes in thinned stands were observed as reduced compared with unthinned stands, 25 years later. The initial shock could be caused by sudden exposure to high wind and light, leading to moisture stress and, greater allocation of growth to roots. There is also likely mechanical damage to

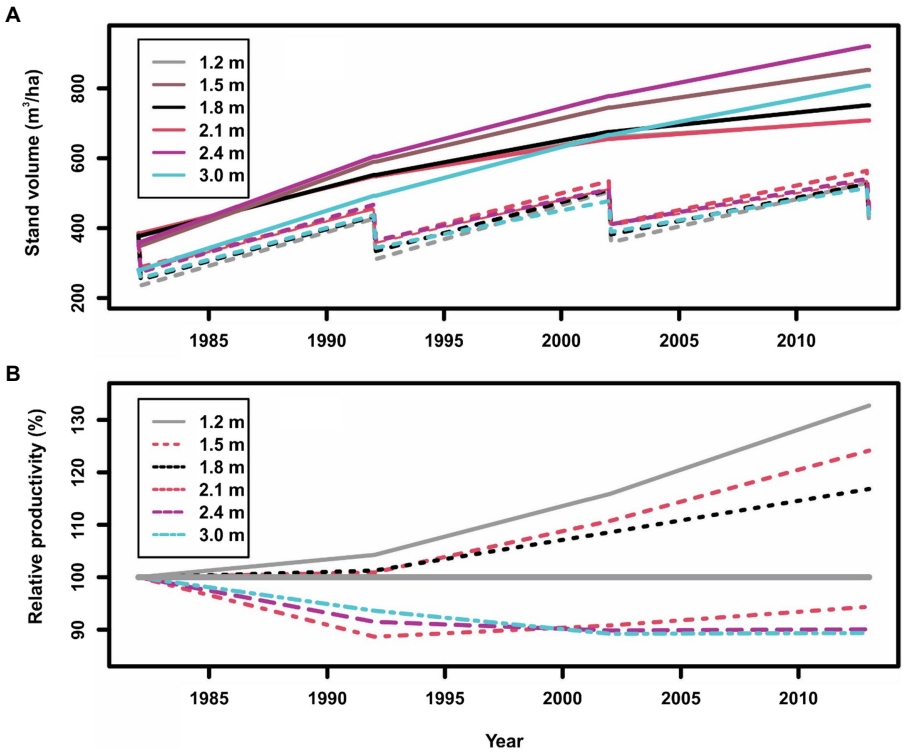

FIGURE 4 | Stand gross volumes (**A**: in which solid lines indicate control plots, and dashed lines indicate thinned plots) and relative productivity (volume growth) (**B**: in which the line of 100% indicates the control plots, >100% indicates overcompensation, and <100% indicates under compensation) of planted red pine (*Pinus resinosa* Aiton) under different spacing regimes created by initial planting density and thinning in Chalk River, Ontario, Canada.

roots of residual trees during harvest; however, it could also probably caused by too wide spacings (3.4–8.1 m, corresponding to 875–125 stems/ha) for poor site conditions (height at 100 years = 24 m).

In addition in displaying diverse CG patterns in the red pine plantations, this case study also provides an empirical evidence of how proper CT regimes can enhance stand productivity. It appears that an increase in stand density could result in more enhanced stand productivity; however, a question remains on whether maximal stand productivity could be reached when stand density increases to a maximum. This CT trial could not provide a full answer to this question, as the maximal stand density was only covered until 6,944 stems/ha.

Case Study 3 (Douglas-fir): Volume and Value-Based Indicators Using Tree Data

The Shawnigan Lake trial has tree-based records for all treated and control plots, with multiple measurements over 40-years. The dataset has spawned a large number of publications over the past 4 decades from a variety of perspectives and specific analyses. Earlier results have shown that increased growth has been happening in some treatments. For example, Brix (1993) showed that 15 years after the initial treatment, stand volume in some treatments exceeded those from control plots. Using the volume estimates from these reports, Li et al. (2018) used relative volume growth to demonstrate that the volumes in more than half of the treated plots had reached exact compensation by 24 years after the initial treatments (measured in 1994). Around 40 years after initial treatments, most of treatment plots have reached overcompensation, except plots without fertilization. This illustrated how the CG process happened over the 40-year's horizon, from under compensation to CIE and to overcompensation, and how diverse CG patterns resulted from the different treatments.

Furthermore, a two-way ANOVA analysis on the 40 year data indicated that fertilization contributed significantly to stand volume differences ($p = 0.015$), whereas thinning ($p = 0.616$) and the fertilization × thinning did not ($p = 0.587$; Li et al., 2018). This result suggested that fertilization was the major factor behind the diverse CG patterns.

In the current study, we aimed at making full use of tree level records from the 2012 measurements to evaluate different value-based estimates as additional indicators of CG, and compare them with gross volume results for examining their relative sensitivity in detecting overcompensation.

Commodity Value-Based CG Indicator

Commodity values are the most direct and explicit way of representing wood value potential for a given forest inventory.

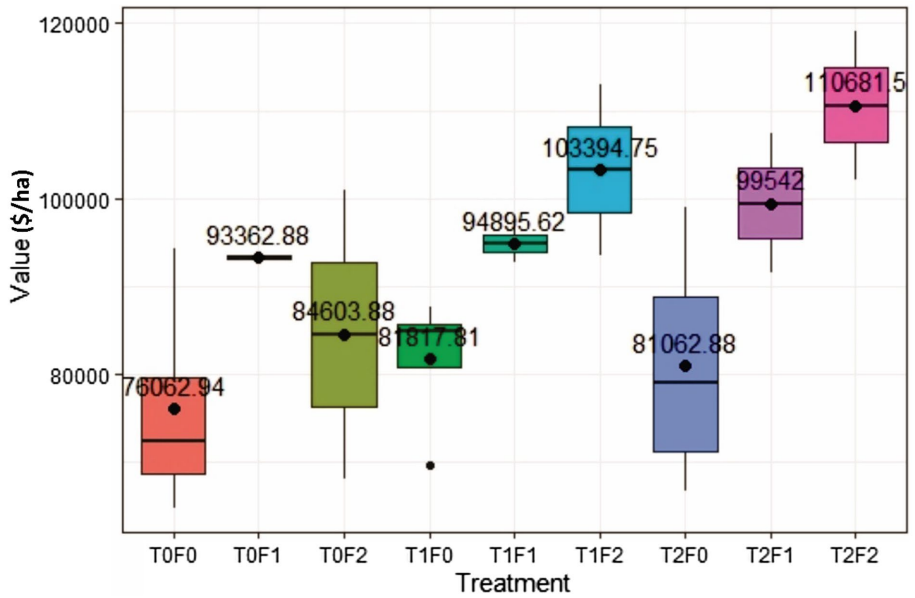

FIGURE 5 | Simulated lumber value recovery for Douglas-fir (*Pseudotsuga menziesii* Mirbel) trees as a function of different combinations of pre-commercial thinning (PCT) and fertilization, 40 years after initial treatments at the Shawnigan Lake trial in British Columbia, Canada. T0, T1, and T2 correspond to 0, 1/3, and 2/3 basal area removal, respectively. F0, F1, and F2 correspond to 0, 224, and 448 kg N/ha fertilization with urea, respectively.

TABLE 3 | Two-way ANOVA results for lumber value recovery of Douglas-fir (*Pseudotsuga menziesii* Mirbel) trees under different treatments, 40 years after application at the Shawnigan Lake trial in British Columbia, Canada.

Effects (fixed)	DF	Sum Sq	Mean Sq	*F* value	Pr(>F)
Thinning	2	484,605,043	242,302,522	1.561	0.242
Fertilization	2	2,004,875,596	1,002,437,798	6.458	0.009**
Thinning × Fertilization	4	359,216,108	89,804,027	0.579	0.683
Residuals	15	2,328,232,519	155,215,501		

*DF = degrees of freedom. **Significant at $\alpha = 0.01$.*

For a volume-based commodity such as pulp, one could expect that the value recovery is proportional to volume recovery. However, for a dimensional commodity such as lumber, the situation could differ.

Lumber value recovery from all treated sites exceeded that from the untreated site (T0F0; no thinning and no fertilization), ranging from $4,999 to $34,618/ha on average 40 years after treatments (**Figure 5**).

The two-way ANOVA (**Table 3**) showed that fertilization increased stand lumber value recovery significantly. Pre-commercial thinning and the fertilization × thinning interactions did not influenced stand lumber value. A commodity value-based assessment displayed the same trend to that from a volume-based assessment (Li et al., 2018). In other words, fertilization could have contributed more in lumber value recovery increase than that of PCT, which is also consistent with the results from another fertilization study conducted in the same region (Cosmin Filipescu, Pers. Comm. Canadian Forest Services, Jan., 2020). Since fertilization has been treated as a surrogate of site quality, the ANOVA results also suggested that acceleration of the CG process could be expected with improved site quality.

A commodity value-based CG indicator in monetary term is easy to understand and effective in decision support; however, this indicator could be influenced by market fluctuations in commodity price. For example, lumber value per thousand board feet (Mfb) can change quickly and with great amplitude. The lumber value used in the current Optitek simulation was set as $400/Mfb, although in the real market it can be as high as $1,600/Mfd when market demand is high, and as low as $250/Mfd when market conditions are unfavorable. As a result, one could expect that relative value could improve representation.

Relative Value-Based CG Indicator

Figure 5 shows that PCT increased lumber value recovery, and that fertilization amplified the impact significantly (**Table 3**). Different from gross volume-based assessment in Li et al. (2018), lumber value recovery from unfertilized sites also exceeded those from control sites ($5,000/ha for T1F0 and $4,999/ha for T2F0). This surprising result could be explained by the changing percentage of small and large dimension lumber (**Figure 6**), in which increased percentage of large

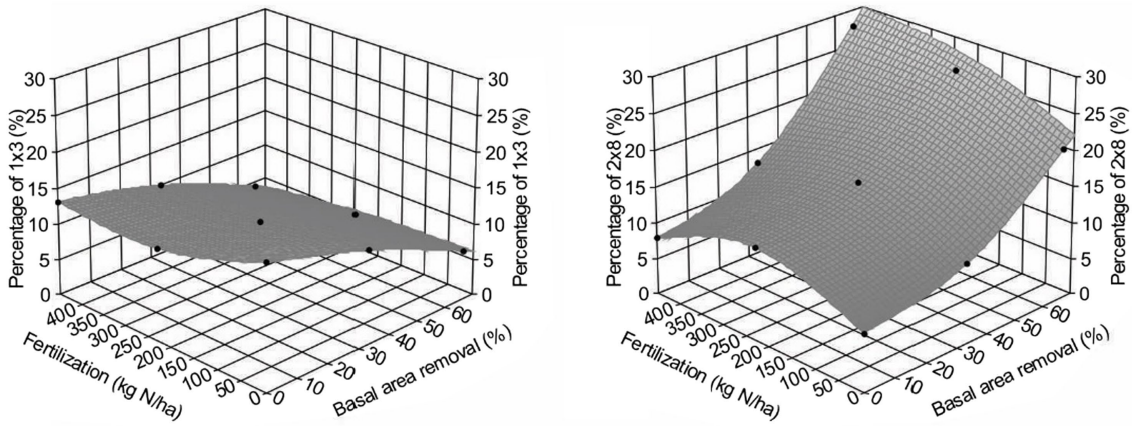

FIGURE 6 | Effect of different treatments combinations on the percentage of small (left, represented by 1 inches × 3 inches lumber) and large (right, represented by 2 inches × 8 inches lumber) dimension lumbers of Douglas-fir (*Pseudotsuga menziesii* Mirbel) trees, 40 years after application at the Shawnigan Lake trial in British Columbia, Canada.

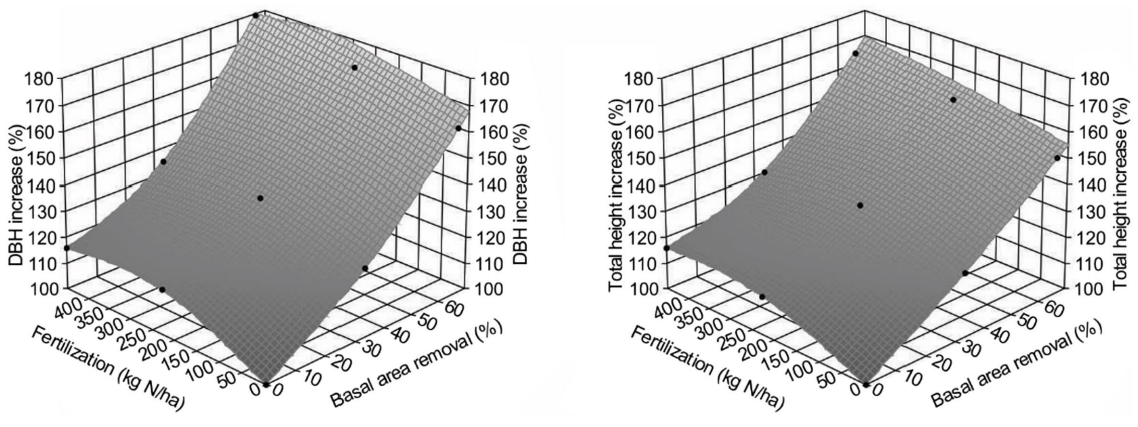

FIGURE 7 | Effect of different treatments combinations on average increase of diameter at breast height (DBH; 1.3 m; left) and total height (right) for Douglas-fir (*Pseudotsuga menziesii* Mirbel) trees, 40 years after application at the Shawnigan Lake trial in British Columbia, Canada.

dimension lumber (usually worth more than small dimension lumber) under increased PCT intensity resulted in the total value recovery increase unproportioned to volume. This non-intuitive result could also be further explained by the changes in average tree size under PCT and fertilization (**Figure 7**); trees with larger sizes favor the production of large dimension lumbers.

Given the above, we estimated the trend of how lumber value recovery would change across different treatments by using the WFVSM model. The results (**Figure 8**) indicated that the lumber value recovery will likely increase with increasing PCT intensity and fertilization. Although relative total sawmill value recovery may not be as high as the lumber value recovery, the trend should be similar, as total production costs will also increase with the increasing PCT intensity and fertilization. As a result, the net value recovery from the sawmill operation will have a very similar pattern compared with the lumber value recovery.

The indicator of relative value recovery enables comparison with relative volume growth for identifying whether lumber value recovery based assessment would be more sensitive in detecting overcompensation than that of volume-based assessment.

Comparison Between Relative Volume and Value-Based Indicators

When we compared volume-based assessment as summarized in Li et al. (2018), all value-based relative growth indicators exceeded 100% (i.e., overcompensation) and are higher than those from volume-based assessment (**Figure 9**). This suggests that value-based indicator might be more sensitive than volume-based assessment in detecting overcompensation.

Overall, this case study shows that PCT triggered CG processes and eventually overcompensation, and that relative growth indicators allowed displaying diverse CG pattern depending largely on the level of fertilization or site quality.

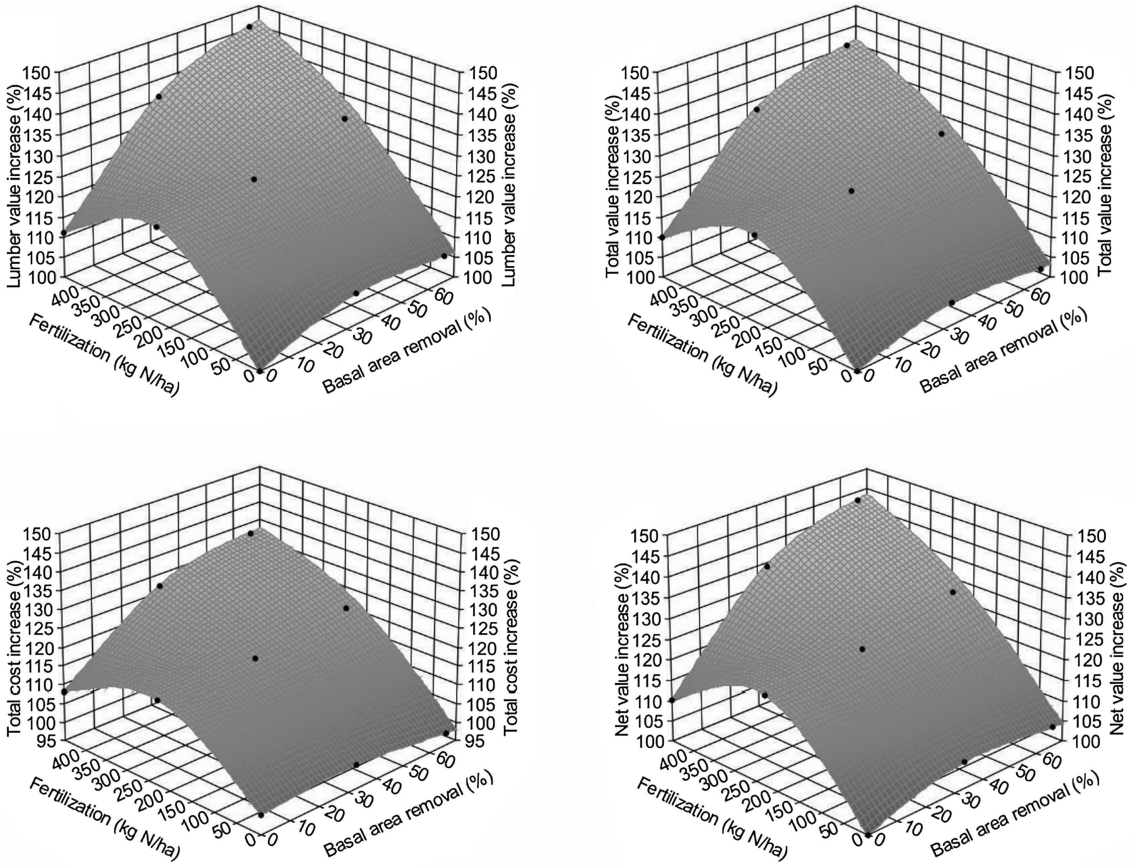

FIGURE 8 | Increase of lumber value recovery (upper left), total value recovery (upper right), total operational cost (lower left), and net value recovery (lower right) for Douglas-fir (*Pseudotsuga menziesii* Mirbel) trees, 40 years after different treatment combinations relative to the untreated sites at the Shawnigan Lake trial in British Columbia, Canada.

The intensity of PCT was employed as an independent variable for predicting the time required to reach CIE.

Lessons From Three Canadian Case Studies

Detection of CG patterns and status is a pre-condition for designing and taking full advantage of CG phenomenon in silviculture and forest management. For example, the capacity for predicting long-term stand growth trajectories under various partial mortality scenarios could provide decision support for designing the best silviculture prescription. Forecasting levels of enhanced long-term productivity may provide a solid foundation for increasing regional annual allowable cut, thus supporting consistent wood supply as a key component of sustainable forest management (e.g., Pinno et al., 2021).

Compensatory growth appears to be a common phenomenon across taxa (Li et al., 2021). The case studies we present here suggest that CG also commonly exists in a range of tree species. The possible reasons for its not having been reported widely in the literature can be attributed to:

- Long lifespan of trees: This makes the detection of CG difficult due to the scarcity of appropriate data. This problem is not present for short lifespan species such as annual plants, animals in farm, fishery, and aquaculture, for which experimental approaches to detect CG are relatively easy to implement.
- Lack of proper methods or indicators in CG detection: researchers usually report the absolute values in stand volume; however, the comparison of results can be misleading if volumes are calculated using different methods (Li et al., 2015). RG could avoid this difficulty but is rarely used.
- Research focus and terminology: overcompensation is highly desirable in the forest sector; however, the topic is seldom an explicit research focus, primarily due to the paucity of long-term observations. The red pine dataset presented in our second case study (the red pine experiment) illustrates that CT is probably a worthy treatment to take advantage of the volume that would be loss to natural mortality otherwise (Thiffault et al., 2021). While CG was indeed documented in their study, it was not termed so.

The three case studies described here consist of three data structures (stand level density management, paired CT results, and individual level of tree records), showing that detection of

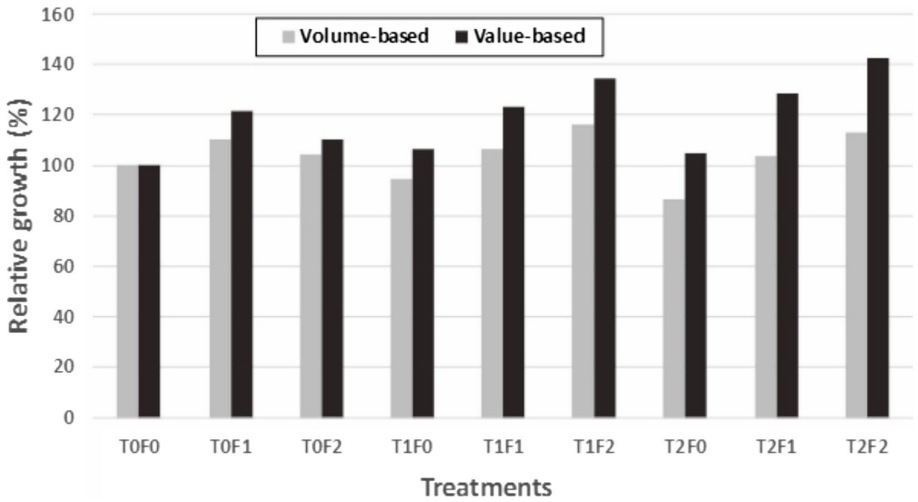

FIGURE 9 | Commodity value-based vs. volume-based growth estimates for Douglas-fir (*Pseudotsuga menziesii* Mirbel) trees relative to untreated sites (as 100%) for different treatment combinations, 40 years after application at the Shawnigan Lake trial in British Columbia, Canada.T0, T1, and T2 correspond to 0, 1/3, and 2/3 basal area removal, respectively. F0, F1, and F2 correspond to 0, 224, and 448 kg N/ha fertilization with urea, respectively.

CG patterns might not require high-resolution datasets, though tree records could provide more options of CG indicators. Our results show that revisiting historical datasets from long-term legacy silviculture trials, even those designed for other purposes, and using a universal indicator of RG can enable detecting CG patterns (**Figure 2**) and different status (**Table 2**), without having to wait for newly designed experiments to be completed. However, when tree-level data are available, both volume and value-based indicators could be used, and lumber value related indicators are more sensitive to overcompensation (**Figure 9**).

Insufficient replicates might influence the ability to generalize conclusions. For example, **Figure 3** shows different paths to CIE for two plots with a same stand density located close to each other. Though this can be attributed to different individual responses to the same disturbance, it also suggests that enough replications is necessary for avoiding inaccurate general conclusions.

Also, a lack of coverage of a large gradient of site quality might pose challenges, because different site conditions may alter the number of years necessary to reach CIE. For example, the datasets used in the first (MacKay experiment) and third (Shawnigan Lake experiment) case studies reported here originate from poor sites, while the dataset from the second (Petawawa Research Forest experiment) case study originates from a good site, exhibiting a top performance for the species. They are theoretically unsuitable for a direct comparison, thus creating difficulties for developing a generalized equation for predicting the number of years to reach CIE. Nevertheless, it suggests that the probability of forest productivity to be enhanced by PCT or CT could be higher on good sites than on poor sites.

Despite these limitations, historical legacy projects are interesting data sources for detecting CG in forests stands. Furthermore, our analyses also suggest that a modeling approach might be a more favorable way than a strictly experimental approach to improve our understanding of CG and our capacity to predict CG in forest ecosystems.

CONCLUSION AND RECOMMENDATIONS

Our three case studies using historical legacy silviculture datasets suggest that CG might be common in tree biology and forestry. Relative growth could serve as a universal indicator for detecting CG in forest ecosystems; when tree data are available, both volume- and value-based indicators can be used for this purpose, and lumber-value related indicators could be more sensitive to overcompensation than other indicators. However, assessment could be complicated by other factors that influence forest productivity, such as age structure of stands and species composition.

Due to the long lifespan of trees, experimental approaches might not be as efficient in detecting CG as for other plants and animals with shorter lifespan. Therefore, a modeling approach could be employed to accelerate our understanding and prediction of CG in tree biology and forestry for decision support in forestry practice.

DATA AVAILABILITY STATEMENT

The data analyzed in this study is subject to the following licenses/restrictions: Permission of the datasets used in this study obtained from data providers. Requests to access these datasets should be directed to Jim Stewart; NT; and Cosmin Filipescu.

AUTHOR CONTRIBUTIONS

CL, HB, and SH: research design, data analysis, and draft writing. CL, HB, SH, BR, RL, and NT: review and editing. All authors contributed to the article and approved the submitted version.

FUNDING

This work was financially supported by Natural Resources Canada-Canadian Forest Service's Developing Sustainable Fibre Solutions Research Program.

ACKNOWLEDGMENTS

The authors thank Jim Stewart of the Canadian Forest Service for supplying the lodgepole pine dataset and reading through an earlier version of this manuscript; Cosmin Filipescu of the Canadian Forest Service for supplying the costal Douglas-fir dataset; Myriam Madore of the Canadian Forest Service for helping with **Figure 1**; Richard Krygier of the Canadian Forest Service for validating **Figure 5**; and Dan Mazerolle of the Canadian Forest Service for providing related information and constructive discussion. We express our gratitude to Jared Salvail, Michael Hoepting, and Jeff Fera of the Canadian Forest Service for the field data collection and compilation of the lodgepole pine and red pine trials. We also thank the critical reading and constructive suggestions from the two peer-reviewers on an earlier version of this manuscript.

REFERENCES

Ali, M., Nicieza, A., and Wootton, R. J. (2003). Compensatory growth in fishes: a response to growth depression. *Fish Fish.* 4, 147–190. doi: 10.1046/j.1467-2979.2003.00120.x

BC Ministry of Forests, Lands and Natural Resource Operations (2014). CGNF Compilation Standards for the Coast Forest Area. Timber Pricing Branch, Victoria, BC. Available at: https://www2.gov.bc.ca/assets/gov/farming-natural-resources-and-industry/forestry/timber-pricing/timber-cruising/cgnf-compilation-standards/2014_cgnf_comp_master.pdf (Accessed April 3, 2018).

Belsky, A. J. (1986). Does herbivory benefit plants? A review of the evidence. *Am. Nat.* 127, 870–892. doi: 10.1086/284531

Bjelanovic, I., Comeau, P., Meredith, S., and Roth, B. (2021). Precommercial thinning increases spruce yields in boreal mixedwoods in Alberta, Canada. *Forests* 12:412. doi: 10.3390/f12040412

Bose, A. K., Weiskittel, A., Kuehne, C., Wagner, R. G., Turnblom, E., and Burkhart, H. E. (2018). Tree-level growth and survival following commercial thinning of four major softwood species in North America. *For. Ecol. Manag.* 427, 355–364. doi: 10.1016/j.foreco.2018.06.019

Briggs, D. G. (1994). *Forest Products Measurement and Conversion Factors: With Special Emphasis on the U.S. Pacific Northwest*. Seattle, WA, USA: College of Forest Resources, University of Washington.

Brix, H. (1993). Fertilization and thinning effect on a Douglas-fir ecosystem at Shawnigan Lake: a synthesis of project results. Forestry Canada, Pacific Forestry Centre, Victoria, B.C., FRDA Report 196.

Crow, T. R., Dey, D. C., and Riemenschneider, D. (2006). Forest productivity: producing goods and services for people. General Technical Report. NC-246. St. Paul, MN: USDA Forest Service, North Central Research Station. 34.

Crown, M., and Brett, C. P. (eds.) (1975). Fertilization and thinning effect on a Douglas-fir ecosystem at Shawnigan lake: an establishment report. Environment Canada, Canadian Forest Services, Pacific Forest Research Center, Victoria, BC. Information Report. BC-X-110.

Curtis, R. S., DeBell, D. S., Harrington, C. A., Lavender, D. P., Clair, J. B., Tappeiner, J. C., et al. (1998). Silviculture for multiple objectives in the Douglas-fir region. General Technical Report. PNW-435. USDA Forest Service Pacific Northwest Research Station, Portland, OR. 123.

D'Amato, A. W., Jokela, E. J., O'Hara, K. L., and Long, J. N. (2017). Silviculture in the United States: an amazing period of change over the past 30 years. *J. For.* 116, 55–67. doi: 10.5849/JOF-2016-035

Drew, T. J., and Flewelling, J. W. (1979). Stand density management: an alternative approach and its application to Douglas-fir plantations. *For. Sci.* 25, 518–532.

Eaton, F. M. (1931). Early defloration as a method of increasing cotton yields and the relation of fruitfulness to fiber and boll characters. *J. Agric. Res.* 42, 447–462.

Erbilgin, N., Galvez, D. A., Zhang, B., and Najar, A. (2014). Resource availability and repeated defoliation mediate compensatory growth in trembling aspen (*Populus tremuloides*) seedlings. *PeerJ* 2:e491. doi: 10.7717/peerj.491

Fabian, D., and Flatt, T. (2012). Life history evolution. *Nat. Educ. Knowl.* 3:24.

Fox, J., and Weisberg, S. (2019). *An {R} Companion to Applied Regression. 3rd Edn*. Thousand Oaks CA: Sage.

FPInnovations (2014). *User's Manual Optitek 10*. Quebec: FPInnovations.

Gauthier, M. M., and Tremblay, S. (2019). Late-entry commercial thinning effects on *Pinus banksiana*: growth, yield, and stand dynamics in Québec, Canada. *J. For. Res.* 30, 95–106. doi: 10.1007/s11676-018-0778-3

Greene, S. E., and Emmingham, W. H. (1986). Early lessons from commercial thinning in a 30-year-old sitka spruce-Western hemlock forest. USDA Forest Service—Research Note PNW-448. Pacific Northwest Research Station, Portland, OR.

Guillet, C., and Bergström, R. (2006). Compensatory growth of fast-growing willow (*Salix*) coppice in response to simulated large herbivore browsing. *Oikos* 113, 33–42. doi: 10.1111/j.0030-1299.2006.13545.x

Gupta, S. D., Pinno, B. D., and McCready, T. (2020). Commercial thinning effects on growth, yield and mortality in natural lodgepole pine stands in Alberta. *For. Chron.* 96, 111–120. doi: 10.5558/tfc2020-016

Harrington, C. A., and Reukema, D. (1983). Initial shock and long-term stand development following thinning in a Douglas-fir plantation. *For. Sci.* 29, 33–46.

Kim, M., Lee, W. K., Kim, Y. S., Lim, C. H., Song, C., Park, T., et al. (2016). Impact of thinning intensity on the diameter and height growth of *Larix kaempferi* stands in Central Korea. *For. Sci. Tech.* 12, 77–87. doi: 10.1080/21580103.2015.1075435

Kozak, A. (1988). A variable-exponent taper equation. *Can. J. For. Res.* 18, 1363–1368. doi: 10.1139/x88-213

Kurz, W. A., Apps, M. J., Webb, T. M., and McNamee, P. J. (1992). The carbon budget of the Canadian forest sector: Phase I. Forest Canada, Northern Forestry Centre, Edmonton, Alberta. Information Report. NOR-X-326E. Available at: https://cfs.nrcan.gc.ca/pubwarehouse/pdfs/11881.pdf (Accessed August 17, 2020).

Kurz, W. A., Dymond, C. C., White, T. M., Stinson, G., Shaw, C. H., Rampley, G. J., et al. (2009). CBM-CFS3: a model of carbon-dynamics in forestry and land-use change implementing IPCC standards. *Ecol. Model.* 220, 480–504. doi: 10.1016/j.ecolmodel.2008.10.018

Li, C., Barclay, H., Hans, H., and Sidders, D. (2015). Estimation of log volumes: a comparative study. Natural Resources Canada, Canadian Forest Services, Canadian Wood Fibre Center, Information Report. FI-X-11. Edmonton, Alberta, Canada. 10.

Li, C., Barclay, H., Huang, S., Hans, H., and Ghebremusse, S. (2013). Sensitivity of predictions of merchantable tree height, log production, and lumber recovery to tree taper. *For. Chron.* 89, 741–752. doi: 10.5558/tfc2013-136

Li, C., Barclay, H., Huang, S., and Sidders, D. (2017). Wood fibre value simulation model: a new tool to assist measuring changes in forest landscapes by evaluating forest inventory. *Landsc. Ecol.* 32, 1517–1530. doi: 10.1007/s10980-016-0406-6

Li, C., Barclay, H., Roitberg, B., and Lalonde, R. (2020). Forest productivity enhancement and compensatory growth: a review and synthesis. *Front. Plant Sci.* 11:575211. doi: 10.3389/fpls.2020.575211

Li, C., Barclay, H., Roitberg, B., and Lalonde, R. (2021). Ecology and prediction of compensatory growth: from theory to application in forestry. *Front. Plant Sci.* 12:655417. doi: 10.3389/fpls.2021.655417

Li, C., Huang, S., Barclay, H., and Filipescu, C. N. (2018). Estimation of compensatory growth of coastal Douglas-fir following pre-commercial thinning across a site quality gradient. *For. Ecol. Manag.* 429, 308–316. doi: 10.1016/j.foreco.2018.07.028

Mangel, M., and Munch, S. B. (2005). A life-history perspective on short- and long-term consequences of compensatory growth. *Am. Nat.* 166, E155–E176. doi: 10.1086/444439

Maschinski, J., and Whitham, T. G. (1989). The continuum of plant responses to herbivory: the influence of plant association, nutrient availability and timing. *Am. Nat.* 134, 1–9. doi: 10.1086/284962

McDonald, J. H. (2014). *Handbook of Biological Statistics*. *3rd Edn.* Baltimore, MD: Sparky House Publishing.

McNaughton, S. J. (1985). Ecology of a grazing ecosystem: the Serengeti. *Ecol. Monogr.* 55, 259–294. doi: 10.2307/1942578

Natural Resources Canada (1995). Silviculture Terms in Canada. 2nd Ed. Policy, Economics and International Affairs Directorate, Canadian Forest Services, Natural Resources Canada, Ottawa, ON. 109.

Newton, P. F. (1997). Stand density management diagrams: review of their development and utility in stand-level management planning. *For. Ecol. Manag.* 98, 251–265. doi: 10.1016/S0378-1127(97)00086-8

Nyland, R. D. (1996). *Silviculture: Concepts and Applications*. New York. NY: The McGraw-Hill Companies, Inc., 633.

Omule, A. Y., Mitchell, A. K., and Wagner, W. L. (2011). Fertilization and thinning effects on a Douglas-fir ecosystem at Shawnigan Lake: 32-year growth response. Natural Resources Canada, Canadian Forest Service, Canadian Wood Fibre Centre. Information Report FI-X-005. Available at: http://cfs.nrcan.gc.ca/pubwarehouse/pdfs/32164.pdf> (Accessed April 3, 2018).

Osborne, T. B., and Mendel, L. B. (1915). The resumption of growth after long continued failure to grow. *J. Biol. Chem.* 23, 439–454. doi: 10.1016/S0021-9258(18)87585-8

Osborne, T. B., and Mendel, L. B. (1916). Acceleration of growth after retardation. *Am. J. Phys.* 40, 16–20. doi: 10.1152/ajplegacy.1916.40.1.16

Pearse, P.H. (1990). *Introduction to Forestry Economics*. Vancouver: University of British Columbia Press.

Pinno, B. D., Thomas, B. R., and Lieffers, V. J. (2021). Wood supply challenges in Alberta—growing more timber is the only sustainable solution. *For. Chron.* 97, 106–108. doi: 10.5558/tfc2021-013

Pitt, D., and Lanteigne, L. (2008). Long-term outcome of precommercial thinning in northwestern New Brunswick: growth and yield of balsam fir and red spruce. *Can. J. For. Res.* 38, 592–610. doi: 10.1139/X07-132

Pöyry (2018). Assessment of the benefits of sustainable forest management. Final report for Drax Power Limited. 59. Available at: https://www.drax.com/wp-content/uploads/2018/11/ASSESSMENT-BENEFITS-SUSTAINABLE-FOREST-MANAGEMENT-Poyry-report-for-Drax.pdf (Accessed September 10, 2021).

Reukema, D. L., and Bruce, D. (1977). Effects of thinning on yield of Douglas-fir: concepts and some estimates obtained by simulation. USDA Forest Services. GTR-PNW-58. Pacific Northwest Forest and Range Experiment Station, Portland, OR.

Schütz, J. P., Ammann, P. L., and Zingg, A. (2015). Optimising the yield of Douglas-fir with an appropriate thinning regime. *Euro. J For. Res.* 134, 469–480. doi: 10.1007/s10342-015-0865-3

Smith, D. M. (1986). *The Practice of Silviculture*. *8th Edn*. Toronto, ON: John Wiley & Sons.

Stewart, J. D., Jones, T. N., and Noble, R. C. (2006). Long-term lodgepole pine silviculture trials in Alberta: history and current results. Natural Resources Canada, Canadian Forest Services, Northwest Forestry Center, Edmonton, AB, and Foothills Model Forest, Hinton, AB.

Stewart, J. D., and Salvail, J. C. (2017). Evaluation of precommercial thinning of lodgepole pine from long-term research installations in Alberta. Natural Resources Canada, Canadian Forest Services, Canadian Wood Fibre Center, Information Report. FI-X-16. 62.

SYSTAT Software Inc. (2002). *TableCurve 3D User's Manual. Version 4.0 for Windows*. Chicago, IL: Author.

Thiffault, N., Hoepting, M. K., Fera, J., Lussier, J. M., and Larocque, G. R. (2021). Managing plantation density through initial spacing and commercial thinning: yield results from a 60-year-old red pine spacing trial experiment. *Can. J. For. Res.* 51, 181–189. doi: 10.1139/cjfr-2020-0246

Varley, C. G., Gradwell, G. R., and Hassell, M. P. (1973). *Insect Population Ecology: An Analytical Approach*. Berkeley and Los Angeles, California: University of California Press, 212.

Warrack, G. C. (1979). Successive thinnings in a natural stand of Douglas-fir over a fifty year period. 11. British Columbia Ministry of Forests Research Note No. 87, Victorial, B.C.

Weetman, G. F., and Mitchell, S. J. (2013). "Silviculture," in *Forestry Handbook for British Columbia*. *5th Edn.* eds. S. B. Watts and L. Tolland. (Vancouver, BC, Canada: The Forestry Undergraduate Society, Faculty of Forestry, University of British Columbia), 394–431.

Whitham, T. G., Maschinski, J., Larson, K. C., and Paige, K. N. (1991). "Plant responses to herbivory: the continuum from negative to positive and underlying physiological mechanism," in *Plant-Animal Interactions: Evolutionary Ecology in Tropical and Temperate Regions*. eds. P. W. Price, T. M. Lewinsohn, G. W. Fernandes and W. W. Benson (New York: John Wiley & Sons), 227–256.

Conflict of Interest: The authors declare that the research was conducted in the absence of any commercial or financial relationships that could be construed as a potential conflict of interest.

Publisher's Note: All claims expressed in this article are solely those of the authors and do not necessarily represent those of their affiliated organizations, or those of the publisher, the editors and the reviewers. Any product that may be evaluated in this article, or claim that may be made by its manufacturer, is not guaranteed or endorsed by the publisher.

frontiers | Frontiers in Ecology and Evolution

ORIGINAL RESEARCH
published: 26 May 2022
doi: 10.3389/fevo.2022.919571

Effects of Fertilization and Dry-Season Irrigation on Litterfall Dynamics and Decomposition Processes in Subtropical *Eucalyptus* Plantations

*Jiejun Kong[1], Yubiao Lin[1], Feng Huang[1], Wenquan Liu[1], Qian He[1], Yan Su[1], Jiyue Li[1], Guangyu Wang[2] and Quan Qiu[1,2]**

[1] Guangdong Key Laboratory for Innovative Development and Utilization of Forest Plant Germplasm, College of Forestry and Landscape Architecture, South China Agricultural University, Guangzhou, China, [2] Faculty of Forestry, University of British Columbia, Vancouver, BC, Canada

OPEN ACCESS

Edited by:
Bernard Roitberg,
Simon Fraser University, Canada

Reviewed by:
César Marín,
Santo Tomás University, Chile
Xia Zhichao,
Hangzhou Normal University, China

***Correspondence:**
Quan Qiu
qqiu@scau.edu.cn

Specialty section:
This article was submitted to Ecophysiology, a section of the journal Frontiers in Ecology and Evolution

Received: *13 April 2022*
Accepted: *06 May 2022*
Published: *26 May 2022*

Citation:
Kong J, Lin Y, Huang F, Liu W, He Q, Su Y, Li J, Wang G and Qiu Q (2022) Effects of Fertilization and Dry-Season Irrigation on Litterfall Dynamics and Decomposition Processes in Subtropical Eucalyptus Plantations. Front. Ecol. Evol. 10:919571. doi: 10.3389/fevo.2022.919571

Nutrient management in *Eucalyptus* plantations is critical for wood production and sustainable development. The biogeochemical mechanisms in *Eucalyptus* plantations are not fully understood due to changes in the spatiotemporal pattern of precipitation and plantation management. The nutrients released from litterfall are important sources of soil nutrition. We measured the seasonal production of various litterfall types and the proportions of their released nutrients in *Eucalyptus urophylla* × *E. grandis* plantations under compound fertilization, dry-season irrigation, and a combined compound fertilization and dry-season irrigation treatment. Our results showed that fertilization increased aboveground biomass and annual litterfall production (except leaf), and that the peak of litterfall production occurred in the rainy season. We found that the decomposition rates of leaf were significantly higher than that of twig, which were mainly controlled by stoichiometric characteristics, followed by soil enzyme activity (β-glucosidase, urease, and polyphenol oxidase). Fertilization decreased the carbon: nitrogen ratio and carbon: phosphorus ratio in litter, and increased soil enzyme activities, which accelerates litter decomposition and nutrient release. Dry-season irrigation increased litter decomposition and only affected the proportion of released potassium by changing the carbon: potassium ratio. Fertilization and dry-season irrigation accelerated the nutrient cycle to enhance compensatory growth. These results help to comprehend the effects of forest management on litterfall dynamics and decomposition processes in *Eucalyptus* plantations with seasonal drought.

Keywords: fertilization, irrigation, *Eucalyptus*, litterfall production, decomposition rate, nutrient release

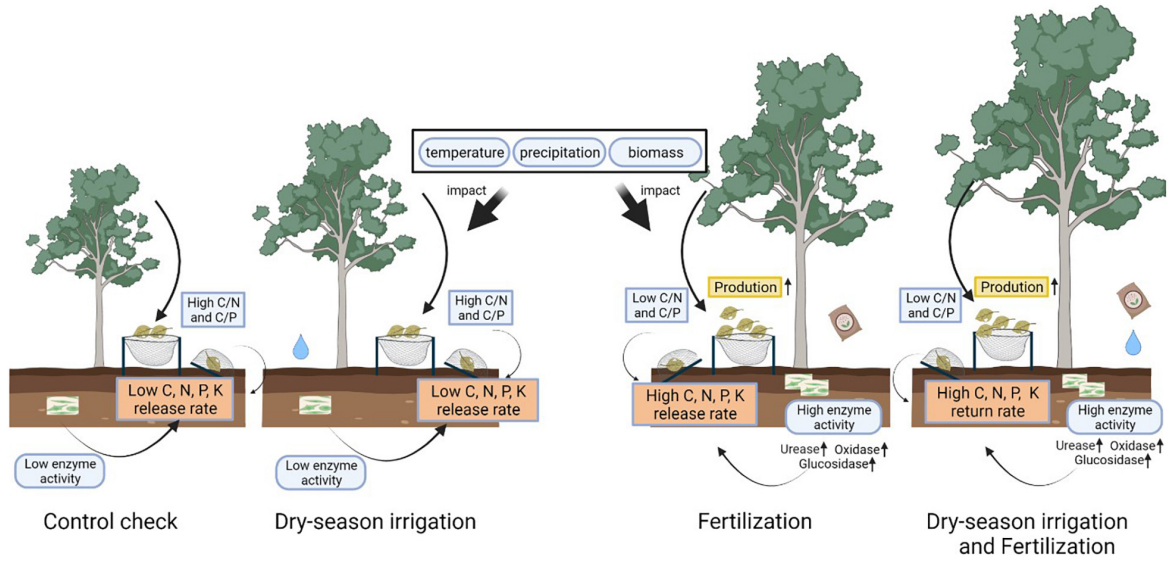

GRAPHICAL ABSTRACT 1 | Response of litterfall production and decomposition to fertilization and dry-season irrigation.

INTRODUCTION

Litterfall periodically falls to the forest floor and transfers carbon (C) and nutrients into the soil, providing an important biogeochemical process in forest ecosystems (Da Silva et al., 2018; Ni et al., 2021). In tropical forests, over 50% of aboveground net primary productivity is converted to litterfall which transfers nutrient resources to the forest floor, which is beneficial to the sustainable development of forest ecosystems (Camargo et al., 2015; Yin et al., 2019). Additionally, litter in the soil surface can maintain soil fertility by mitigating erosion (Wang et al., 2020) and providing an active environment for soil animals and microorganisms (Cajaiba et al., 2017; Dong et al., 2021). Global climate change has impacted the global hydrological cycle by changing the spatiotemporal pattern of precipitation, water availability, air temperature, air humidity, etc. (Dai, 2013; Dubreuil et al., 2019). Drought can change the nutrient cycle by increasing litterfall production and inhibiting its decomposition rate (Paudel et al., 2015; Yu et al., 2019b). The seasonal drought caused by changes in precipitation pattern (Zhou et al., 2011) in southern China has affected the ecosystem nutrient cycle (Dawoe et al., 2010; Yu et al., 2019b).

Numerous studies show that the shedding process of the aboveground parts of vegetation is affected by vegetation type, species composition, topography, climate, and the physical and chemical properties of soil (Blanco et al., 2008; Tang et al., 2010; Camargo et al., 2015; Kamruzzaman et al., 2019; Gonzalez et al., 2020; Zhu et al., 2021). In the tropical/subtropical forest with seasonal drought, the peak of litterfall production generally occurs in the dry season, which is highly correlated with precipitation (Chave et al., 2010; Paudel et al., 2015). Falling leaves are an important part of litterfall and respond rapidly to environmental changes (Liu et al., 2004). In order to avoid the risk of drought, plants will increase litter production to decrease the loss of water, especially *via* leaf removal (Liu et al., 2015). In addition, nutrient deficits limit plant growth, resulting in the reduction of litterfall production (Wright et al., 2011). After falling from the plant, litter decomposes in the surface soil and releases nutrients to form organic matter, which is vital to maintaining soil fertility (Cotrufo et al., 2015). Litter decomposition is primarily determined by litter quality, decomposer biodiversity, decomposer activity, and environmental factors. Firstly, different indicators of litter quality determine the decomposability of substrate. The easily decomposed litter is characterized by high nutrient content [nitrogen (N) and/or phosphorus (P)], low stoichiometric characteristics (C:N and/or C:P), and lower recalcitrant polymer content (lignin or holocellulose) (Adair et al., 2008; Mora-Gómez et al., 2020; Hou et al., 2021). Generally, higher contents of soil nutrients were accompanied with high litter quality (Ge et al., 2013). Secondly, environmental factors affect litter decomposition through biodiversity and the activity of soil decomposers. For example the decrease of soil water content caused by drought can reduce the litter decomposition rates by changing the composition of the microbial community and decreasing microbial activity (Petraglia et al., 2019; Liu et al., 2021). Therefore, climate change and forest management (fertilization) not only change the nutrient input from litterfall production, but also affect the released nutrient proportions through litterfall decomposition. Combining litter production and decomposition to assess the nutrient return from litterfall would further realize the variations of soil fertility under the environmental changes.

With its fast growth and high yield, *Eucalyptus* is widely planted in southern China, covering an area of 4.5 million ha (Xie et al., 2017). Due to the soil in southern China being impoverished (Zhen et al., 2005), compound fertilizers have been applied to meet the fast-growing requirements in

the conventionally managed *Eucalyptus* plantations (Lu et al., 2020). Affected by the fast-growing characteristics and short rotation, the harvesting of *Eucalyptus* plantations leads to high nutrient export, and results in the decrease of soil fertility (Menegale et al., 2016; Lu et al., 2020). As defined by Li et al. (2020), compensatory growth refers to an organism's accelerated growth following a disturbance or a period of slow growth caused by unfavorable environmental conditions, such as low temperature or nutrient deprivation. After alleviating nutrient deprivation, compensatory growth caused by fertilization leads to an increase in litterfall production by increasing aboveground biomass (Wright et al., 2011). Moreover, increased litter quality under fertilization positively governs the litter decomposition rates (Hou et al., 2021). Due to *Eucalyptus*' high transpiration, fertilizing its plantation will increase transpiration, which reduces soil water content (Hua et al., 2021). The decrease of soil water content has negative effects on aboveground biomass and soil microbial community in *Eucalyptus* plantations, increasing the litterfall production and reducing the litterfall decomposition (Ribeiro et al., 2002; Nouvellon et al., 2012). Consequently, the reduced growth, increased litterfall production, and decreased decomposition rate are offset or reversed under sufficient water supply. Aboveground biomass is subjected to decreases *via* drought stress and increases *via* fertilization. These changes in aboveground biomass can affect the light environment and litter decomposition under the canopy, resulting in further alterations in plantation nutrient cycles (Wright et al., 2011; Liu et al., 2015; Almagro et al., 2017). Nevertheless, the effects of seasonal drought and variations in growth patterns under fertilization on litter deposition are not fully understood. Therefore, exploring the effects of dry season irrigation on nutrient inputs from litterfall in the early growth stage can provide better supporting data for improving nutrient management to ensure healthy growth in the early stage of *Eucalyptus* plantations under seasonal drought.

In this study, *Eucalyptus urophylla* × *E. grandis*, the high-productivity genotypes mainly planted in southern China, was selected to examine the variations of litterfall patterns and decomposition processes under dry-season irrigation and fertilization. The following hypotheses are proposed: (1) the peak of litterfall production occurs in the dry season; (2) fertilization increases the litterfall production, and irrigation decreases the litterfall production; (3) fertilization and irrigation accelerate litter decomposition by increasing litter quality and enzyme activity; (4) fertilization and irrigation promote nutrient release through enhancing soil enzyme activity; and (5) fertilization and irrigation enhance compensatory growth. This research aims to improve forest productivity in *Eucalyptus* plantations through the enhancement of water and fertilizer management.

MATERIALS AND METHODS

Study Site

The experimental site is located at the Zengcheng Teaching and Research Bases of South China Agricultural University, Guangzhou (23°14′48N, 113°38′20E), which belongs to a subtropical monsoon climate. According to the data of the Zengcheng meteorological observatory from 1981 to 2010, the annual average temperature is 21.91°C and the annual average precipitation is 2004.4 mm. The seasonal drought in the study site is obvious as its rainfall between October and March only is accounted for 14% of the whole year. The monthly precipitation and the mean air temperature during the experiment are shown in **Figure 1**.

Experimental Design

Eucalyptus urophylla × *E. grandis* was selected as experimental materials and its seedlings (approx. 20 – 35 cm tall) were planted in April 2017 at a density of 3 × 2 m. The forestland was 0.536 ha in total and divided into five terraces with horizontal terraced land preparation method. Each terrace had four treatments (one plot per treatment), which were randomly arranged from 20 to 92 trees for each plot. A total of 20 plots were employed in the present study, and their shapes were described in Yu's study (Yu et al., 2019a). The experiment was set up as a completely random block design of water and fertilizer. There were four treatments in total: (1) no dry-season irrigation and no fertilizer (CK), (2) dry-season irrigation but no fertilizer (W), (3) no dry-season irrigation but fertilizer (F), and (4) dry-season irrigation and fertilizer. Dry-season irrigation was carried out only from October to March with drip irrigation equipment. Following Yu's observation (Yu et al., 2019a), the irrigation was given 8 h/week at 4 L/h to ensure the soil relative water content of the soil from 40 cm depth and 40 cm away from the trees was maintained at 90% for 3 days. The fertilizer addition refers to the added amount of *Eucalyptus* production in southern China (Ministry of Forestry of the People's Republic of China, 2015). As of July 2020, fertilizer was applied 4 times: base fertilizer, first extra fertilizer, second additional fertilization, and third additional fertilization. The base fertilizer was applied at 400 g/hole in March 2017, which includes N: 24 g, P_2O_5: 72 g, and K_2O: 24 g. The first extra fertilizer was applied at 400 g/hole

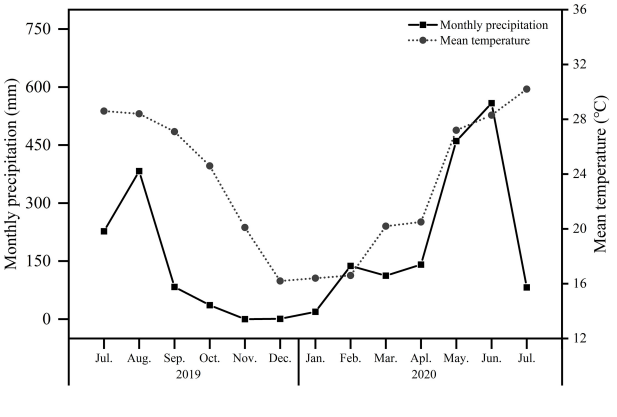

Figure 1 | Monthly precipitation and mean temperature during the experimental period from July 2019 to July 2020. The dot with the broken line represented the mean temperature and the square with solid line indicated the monthly precipitation.

for F and WF treatments in July 2017, including N: 45 g, P_2O_5: 21 g, and K_2O: 24 g. The second and third additional fertilization for F and WF treatments were, respectively, carried out at 400 g/hole in July 2018 and July 2019, each of which included N: 60 g, P_2O_5: 28 g, and K_2O: 32 g. The initial soil nutrient concentrations (40 cm) were total nitrogen (TN): 0.34 g/kg, total phosphorus (TP): 0.16 g/kg, total potassium (TK): 8.82 g/kg, alkaline hydrolysis nitrogen (AHN): 30.74 mg/kg, available phosphorus (AP): 0.30 mg/kg, and rapidly available potassium (AK): 10.42 mg/kg.

Growth Traits

The diameter at breast height (DBH) and height of all *E. urophylla* × *E. grandis* were measured in July 2019 and July 2020. The number of measurements for each treatment were 150 (CK), 189 (W), 146 (F), and 168 (WF). In July 2020, 5 standard trees of each treatment fell to estimate the aboveground biomass. The aboveground part was broken down into stem, twig, leaf, and fruit. All the materials were dried and weighed to calculate the biomass of each organ under various treatments.

Litterfall Deposition and Decomposition

In July 2019, 5 collectors were set in each block using five-point sampling method to measure litterfall deposition, 1 m × 1 m (1 m^2) in size, made from mesh gauze (2 mm diameter), with collectors installed at a height of 1 m above the ground to ensure the separation of the mesh gauze from the surface. The litterfall was collected monthly (the end of each month) and classified into organs: leaf, twig, fruit, and bark. The litterfall deposition was monitored from August 2019 to July 2020. All samples were dried in an oven at 65°C to constant weight and then weighed.

In July 2019, fresh litterfall was collected from the plantation's floor and air-dried to constant weight in a laboratory. Portions of 10 g of leaves and twig samples (cut into 10 cm length) were separately packed in corrosion-resistant plastic bags with 2 mm^2 mesh and measuring 25 cm × 25 cm. A 20 leaf bags and 20 twig bags were placed under the litter layer in each plot using five-point methods at the end of July. We planned for 4 successive harvests in each plot during the experiment: 5 leaf bags and 5 twig bags in each plot were collected at 3, 6, 9, 12 months after placing litter bag to measure litter decomposition. After collection, the materials contained in the plastic bags were cleaned with a brush to remove the attachments like weed and soil particles. Afterward, the materials were dried in an oven at 65°C to constant weight (M_t). Leaves and twig litter for each treatment were oven-dried to constant weight at 65°C to determine the ratio between air-dried mass and oven-dried. Then, the ratio was used to convert the weight of initial air-dried litter to the weight of oven-dried litter (M_0). The nutrient content of the original samples (C_0) and 12 months decomposed samples (Ct) for each treatment were analyzed. Samples for chemical analysis were ground and passed through a 0.5 mm sieve for testing the concentrations of C, nitrogen (N), phosphorus (P), and potassium (K) (refer to soil chemical analysis methods). The mass loss rate (L), proportion of nutrient released (F′), and Olson model were calculated as follows:

$$L = [(M_0 - M_t)/M_0] \times 100\%$$

$$F' = 100\% - (C_t \times M_t)/(C_0 \times M_0) \times 100\%$$

Olson negative exponential decay model: $y = a \times e^{-kt}$

In the Olson model: y means the remaining mass rate of litter; a means the fitting parameter; k means the annual decomposition coefficient; t means the decomposition time.

Environmental Factors

The soil water content (SWC) was measured at the end of each month with 15 repeats for each treatment. Soil samples 40 cm deep (40 cm away from the trees) were obtained with a soil drill in three random places of each block. The soil samples were collected in an aluminum box to be weighed and dried at 105°C to constant weight in an oven. Then record the dry weight to compute the SWC. SWC (%) = (fresh weight – dry weight)/(dry weight – box weight) × 100%. The relative soil water content (SWC_r) = SWC/field moisture capacity. The field moisture capacity was measured with cutting ring methods (Ministry of Agriculture of the People's Republic of China, 2010). In July 2019, soil field water-holding capacity of 0 – 20 cm and 20 – 40 cm was measured for each plot. One profile was sampled for each plot, with disturbed and undisturbed soil samples collected from the top soil to 10 and 30 cm. Three undisturbed soil samples were collected from each soil layer with a cutting ring (70 mm diameter and 52 mm height). The disturbed soil samples were collected from the soil around the cutting ring and air dried for 3 days in a laboratory. The undisturbed soil samples were placed in a tray filled with water to a level of 2 – 5 mm below the upper rim of the cutting ring. After air dried for 3 days, the disturbed soil samples sifted by 2 mm sieve and filled with a cutting ring. Next, the undisturbed soil samples were soaked for 24 h, and then put on sand. After the undisturbed soil samples were saturated, the samples were placed on the cutting ring of disturbed soil samples. In order to ensure that the two cutting rings were contacted tightly, a 2 kg brick was placed on the top of the undisturbed soil samples. After the samples were stand for 8 h, 20 – 30 g soil samples from the cutting ring of the wet undisturbed soil samples were collected into an aluminum box of known weight (m_0), and then weighed immediately (m_1). Finally, the samples in the aluminum box were dried to constant weight (m_2) in an oven of 105°C. The formula for field water-holding capacity (FC) is: FC = (m_1 – m_2) × 1,000/(m_2 – m_0).

The soil nutrient content was measured once in the dry season (January 2020) and the rainy season (July 2020) with five repeats for each treatment. In each block, a bag of soil samples (0 – 10 cm depth) was taken from 5 places under the litter bags. The soil samples were air-dried for 3 days in the laboratory and then sifted in a mill with 2 mm sieve for testing the concentrations of C, TN, TP, TK, AHN, AP, and AK. Chemical analysis was referenced standard analysis methods (Lu, 2000; Carter and Gregorich, 2007). Organic carbon concentration was determined with the traditional potassium dichromate heating oxidation –

volumetric method (Carter and Gregorich, 2007). After sulfuric acid and hydrogen peroxide digestion, the TN concentration was determined by the distillation titration method (Lu, 2000). TP concentration was determined by the vanadium molybdate yellow colorimetric method after digesting with sulfuric acid and hydrogen peroxide (Lu, 2000). TK concentration was determined by flame photometer method after digesting with sulfuric acid and hydrogen peroxide (Lu, 2000). Hydrolytic reduction was carried out in sodium hydroxide and ferrous sulfate solutions, and then the AHN concentration was determined by sulfuric acid titration with boric acid as an indicator (Lu, 2000). After soaking with HCI-HF reagent, AP was determined by the molybdenum antimony colorimetric method. The sample was extracted with ammonium acetate and the AK was determined by flame photometer method (Lu, 2000).

Soil Enzyme Activity

The samples of soil enzyme were collected in January 2020 with 5 repeats for each treatment. In each block, a bag of soil samples (0 – 10 cm depth) was taken from 5 places under the litter bags and stored in an cryogenic container. The soil samples were sifted in a mill with 1 mm sieve in a laboratory. The samples were stored at 4°C and measured within 1 week.

Soil enzyme activity analysis was referenced standard analysis methods. Enzyme activity is expressed as the mass of specific product generated per unit of dry soil weight per unit time. Acid phosphatase activity was analyzed using *p*-nitrophenyl-phosphate as substrate, and then using a spectrophotometer to measure absorbance at 410 nm to calculate activity (Santos et al., 2018). β -glucosidase activity was analyzed using sodium acetate (pH 5.5) as buffer and using 4-nitrophenyl β-D-glucopyranoside as substrate, and then using a spectrophotometer to measure absorbance at 410 nm to calculate activity (Santos et al., 2018). Urease activity was measured by phenol-sodium hypochlorite colorimetric and assayed at 540 nm, using urea as substrate (Zhen et al., 2019). Using the phenolic amino acid L-3,4-dihydroxy phenylalanine (L-DOPA) as the substrate, polyphenol oxidase activity was analyzed by spectrophotometer at 475 nm (Prosser et al., 2011). Cellulase activity was determined by 3,5-Dinitrosalicylic acid colorimetry Method. The amount of glucose released over 72 h was assayed colorimetrically at 540 nm (Guan, 1986).

Data and Statistical Analysis

Excel 2021 was used for data sorting, SPSS 22.0 was used for ANOVA analysis, Duncan's multiple comparison analysis, Pearson correlation analysis, and Olson negative exponential decay model. Origin 2021 software was used for principal component analysis (PCA) and making figures.

The annual litterfall production (total or each type) was calculated by adding up the amount of monthly litterfall production in each block. After using Grubbs method to delete outliers, one-way ANOVA following Duncan's multiple comparison analysis (normal distribution and variance homogeneity of the data have tested) was used to test the effects of treatment on litterfall production, aboveground biomass, percentages of litter remaining mass, C and nutrient concentrations, proportion of C and nutrient released, and soil enzyme activity. Pearson correlation coefficients were estimated between environmental factors and monthly litterfall productions, litter remaining mass, and soil/litter chemical traits, litter nutrient released proportion and soil/litter chemical traits. The Pearson correlation analysis, Olson negative exponential decay model, and PCA were made using the average per plot ($n = 5$).

RESULTS

Biomass

Fertilization increased the biomass of leaf, twig, and stem 3 years after plantation (**Table 1**), while dry-season irrigation increased the biomass of stem ($P < 0.05$). The biomass of stem under dry-season irrigation showed further increase by 14.7% on the basis of fertilization treatment ($P < 0.05$).

Litterfall Deposition

In *E. urophylla* × *E. grandis* plantations under different treatments, the average litterfall productions ranged from 6852.8 kg/ha/yr under CK treatment to 8720.3 kg/ha/yr under WF treatment (**Figure 2**). The total litterfall productions with fertilizer addition (F and WF) were higher than that with no fertilizer ($P < 0.05$). Dry-season irrigation had no effect on litterfall production ($P > 0.05$). Dry-season irrigation increased litterfall production but without forming significant differences. The leaf fraction showed the highest contribution in total litterfall production (average 4733.9 kg/ha/yr), without statistical differences between various treatments. The second largest contribution to total litterfall production was twig (average 1517.5 kg/ha/yr). Fertilization increased the twig (61–71%) and fruit (77–93%) production, while the twig and fruit production did not differ under dry-season irrigation. Barks were significantly different between fertilization and non-fertilization. The PCA depicted similarities/differences between treatments: there were obvious differences between fertilizer (F and WF) and no fertilizer (CK and W), and a small difference between dry-season irrigation and no dry-season irrigation (**Figure 3**).

The litterfall production of all treatments followed a seasonal pattern throughout the experimental period (**Figure 4**). The deposition over 72% occurred in the rainy season (from April to September), strongly affected by the leaf and twig productions

TABLE 1 | Aboveground biomass of *E. urophylla* × *E. grandis* 3 years after plantation.

Treatment	Leaf (kg/tree)	Twig (kg/tree)	Stem (kg/tree)
CK	1.108 ± 0.064b	1.481 ± 0.053b	11.310 ± 0.609c
W	1.221 ± 0.122b	1.664 ± 0.152b	13.973 ± 0.515c
F	2.165 ± 0.163a	4.187 ± 0.355a	37.602 ± 1.313b
WF	2.362 ± 0.209a	3.767 ± 0.444a	43.127 ± 1.205a

Means ± standard error (SE) were shown (n = 5). The letter after the numbers represented the Duncan's multiple comparison results. Different lower-case letters indicate differences between various treatments.

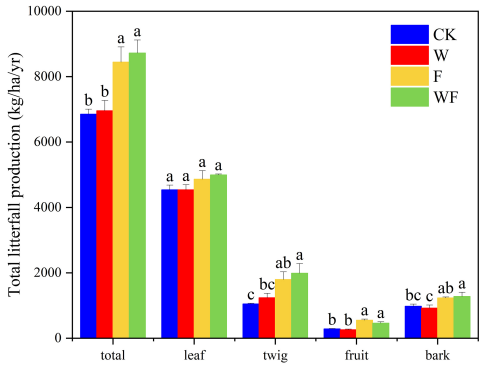

Figure 2 | Total litterfall production and components (kg/ha/yr) of *E. urophylla* × *E. grandis* from August 2019 to July 2020. The bars in different colors, respectively, indicated CK, W, F, and WF treatment. The error bars indicated SE. The values followed by the different letters are significantly different according to one-way ANOVA ($P < 0.05$).

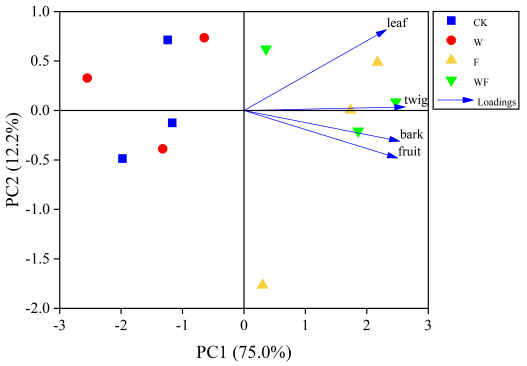

Figure 3 | Principal component analysis (PCA) of annual litterfall production (leaf, twig, fruit, and bark) under different treatments.

(**Supplementary Figure 1**). The productions of leaf, twig, and bark peaked in May and fruit in July. In particular, fruit and bark fall rarely occur during the dry season, while leaf and twig are maintained at a low level (**Figure 4** and **Supplementary Figure 1**). In Pearson correlation analysis, litterfall deposition showed positive correlations with temperature and precipitation (**Table 2**). Temperature had positively correlated with twig and fruit production ($P < 0.05$), which was not affected by dry-season irrigation and fertilization. Precipitation had positively correlations with total, leaf, twig, and bark production, but the correlation with leaf production disappeared under dry-season irrigation and fertilization.

Litter Decomposition

The Olson negative exponential decay model adequately described the decomposition rates of leaf and twig under different treatments, with R^2 values ranging from 0.70 to 0.98 (**Table 3**). The decomposition rates of the twig were lower than that of the leaf. In the first 90 days, the rates of decomposition under all treatments were more intense than in other periods (**Figure 5**). After 360 days of decomposition, the average litter decomposition rates of leaf and twig for all treatments were 30 and 12%. Different treatments had significant influences on litter decomposition. Fertilization and dry-season irrigation were beneficial to leaf and twig decomposition (**Figure 5**), of which under WF treatment attained the highest rates of decomposition with 34% (leaf) and 15% (twig), respectively, after 360 days ($P < 0.05$). According to the Olson model, the time required to decompose 95% of leaf and twig had been, respectively, reduced by 16.8 to 34% and 20.8 to 43.8% under fertilization and dry-season irrigation. In the experimental period, the remaining mass negatively correlated with initial C, N, P, and K concentration, and positively correlated with C/N, C/P, and C/K (**Table 4**). In addition, leaf decomposition was related to the activity of β -glucosidase, Urease, and Polyphenol oxidase in the dry season ($P < 0.05$), while twig decomposition was related to the activity of Urease and Polyphenol oxidase (**Table 5**).

Nutrients Released

Most of initial litter C and nutrient concentrations were influenced by fertilization, but not by dry-season irrigation (**Table 6**). Initial foliar C concentrations increased by 2.6 – 2.7% under fertilization ($P < 0.05$). Affected by the increase of P concentrations in leaf (26.1 – 27.8%) and twig (48.6 – 65.6%), C/P under fertilization were decreased (leaf, 18.8 – 20.1%; twig, 30.4 – 37.3%). Compared to CK, dry-season irrigation increased foliar K concentration by 55.9 – 58.5%, while fertilization increased the K concentrations of twig by 27.0 – 39.7% ($P < 0.05$). After decomposing 360 days, C, N, and P concentrations greatly decreased, and their difference narrowed between treatments. Meanwhile, the K concentration of twigs decreased immensely, but foliar K concentrations change little.

After 360 days of decomposition, the quantities of C, N, P, and K in leaf and twig decreased for both treatments (**Figure 6**). In leaf litter, the released proportions of N (16.2 – 18.2%) and P (22.7 – 31.5%) under fertilization were higher than that under non-fertilization ($P < 0.05$). Compared to non-fertilization, fertilization increased the C release proportion by 111.2 – 145.4%, N release proportion by 46.6 – 72.9%, and P release proportion by 121.5 – 136.4% of twig ($P < 0.05$), respectively. In particular, the C/N of WF in leaf litter was higher than that of CK (22.4%) and the C/P of WF in twig litter was higher than that of CK (49.7%) and W (34.3%). The released proportions of K were different from that of C, N, and P. Fertilization and dry-season irrigation promoted the release of foliar K, and the effect of dry-season irrigation was greater than fertilization. The release of twig K was inhibited by dry-season irrigation, but the combination of dry-season irrigation and fertilization promoted the release of twig K ($P < 0.05$).

DISCUSSION

Litterfall Production Under Different Treatments

Litterfall production generally exhibits seasonal patterns, which varies with forest types and environmental factors

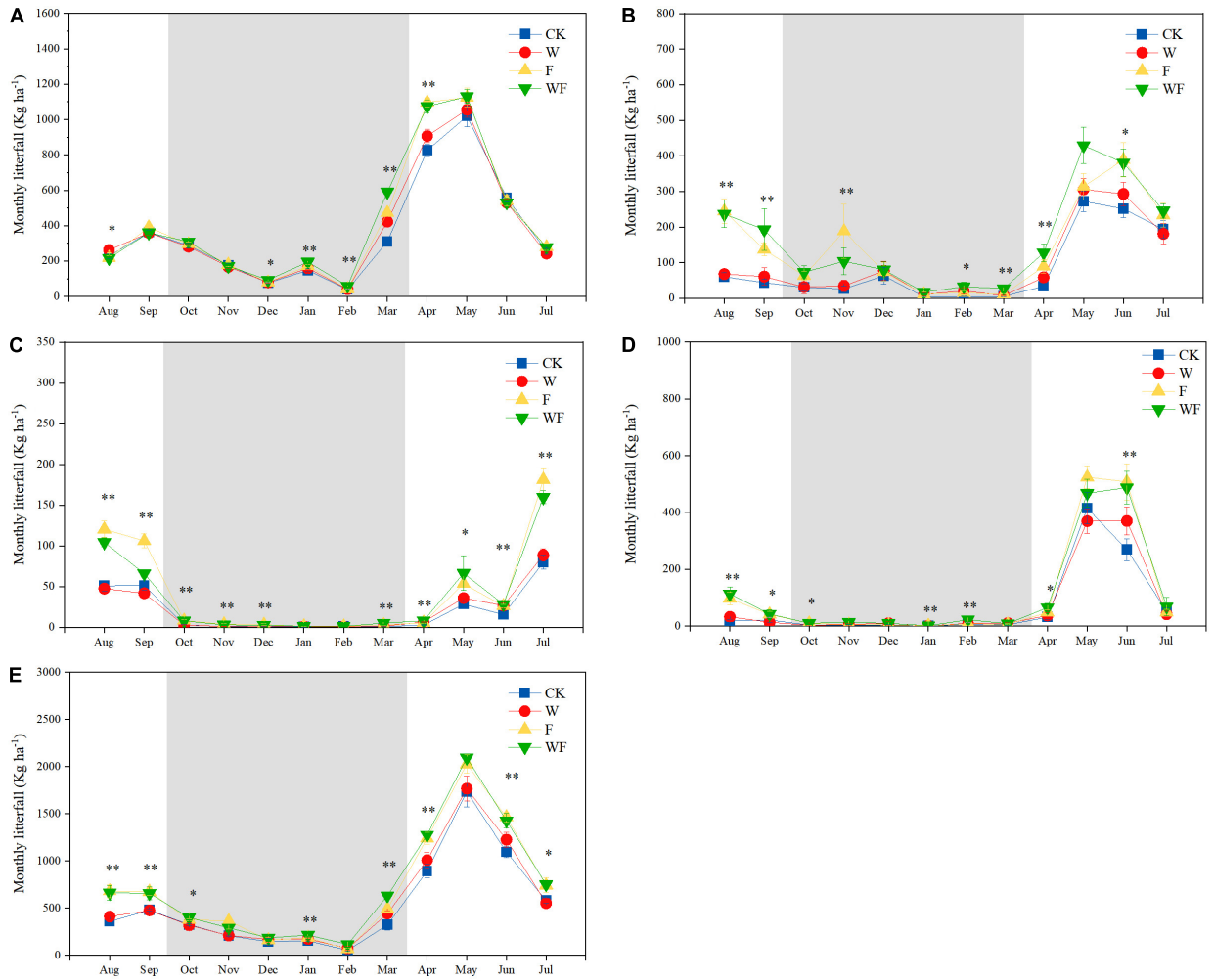

Figure 4 | Monthly leaf **(A)**, twig **(B)**, fruit **(C)**, bark **(D)**, and total **(E)** litter deposition of *E. urophylla* × *E. grandis* from August 2019 to July 2020. The gray areas represent the months in the dry season. The *P-value* showed the results from one-way ANOVA testing for the effects of dry-season irrigation and fertilization, $^{*}P < 0.05$, $^{**}P < 0.01$.

TABLE 2 | Analysis of the correlation between environmental factors and monthly litterfall productions from August 2019 to July 2020.

Treatment	Variables	Total	Leaf	Twig	Fruit	Bark
CK	Temperature	–	–	0.627*	0.802**	–
	Precipitation	0.734**	0.589*	0.728*	–	0.799**
W	Temperature	–	–	0.632*	0.830**	–
	Precipitation	0.759**	–	0.772**	–	0.863**
F	Temperature	0.604*	–	0.773**	0.779**	–
	Precipitation	0.776**	–	0.784**	–	0.893**
WF	Temperature	–	–	0.792**	0.800**	–
	Precipitation	0.765**	–	0.830**	–	0.909**

*Correlations coefficients by Pearson correlation are shown, – P > 0.05, *P < 0.05, **P < 0.01.*

TABLE 3 | Decomposition equations of Olson negative exponential decay model of leaf and twig for all treatments.

Fraction	Treatment	Equation	R^2	*k*	$t_{0.5}$(a)
Leaf	CK	$Y = 92.666e^{-0.238t}$	0.7086	0.238	2.91
	W	$Y = 91.968e^{-0.286t}$	0.7405	0.286	2.42
	F	$Y = 92.462e^{-0.314t}$	0.7936	0.314	2.21
	WF	$Y = 92.632e^{-0.362t}$	0.8404	0.326	1.91
Twig	CK	$Y = 98.96e^{-0.114t}$	0.961	0.114	6.08
	W	$Y = 99.467e^{-0.144t}$	0.9753	0.144	4.81
	F	$Y = 99.78e^{-0.19t}$	0.9741	0.190	3.65
	WF	$Y = 99.84e^{-0.203t}$	0.9857	0.203	3.41

k, the annual decomposition coefficient in Olson model; $t_{0.5}$, time to decompose 50% of the litter; $t_{0.95}$, time to decompose 95% of the litter.

(Staelens et al., 2011; Zhang et al., 2014). The litterfall in the present study was collected from the *E. urophylla* × *E. grandis* plantation after 3 years of fertilization and dry-season irrigation. On average, the litterfall productions observed in the present study (6.85 to 8.72 Mg/ha/yr) are close to values of mature *Eucalyptus* plantations (3.57–6.04 Mg/ha/yr) in Brazil

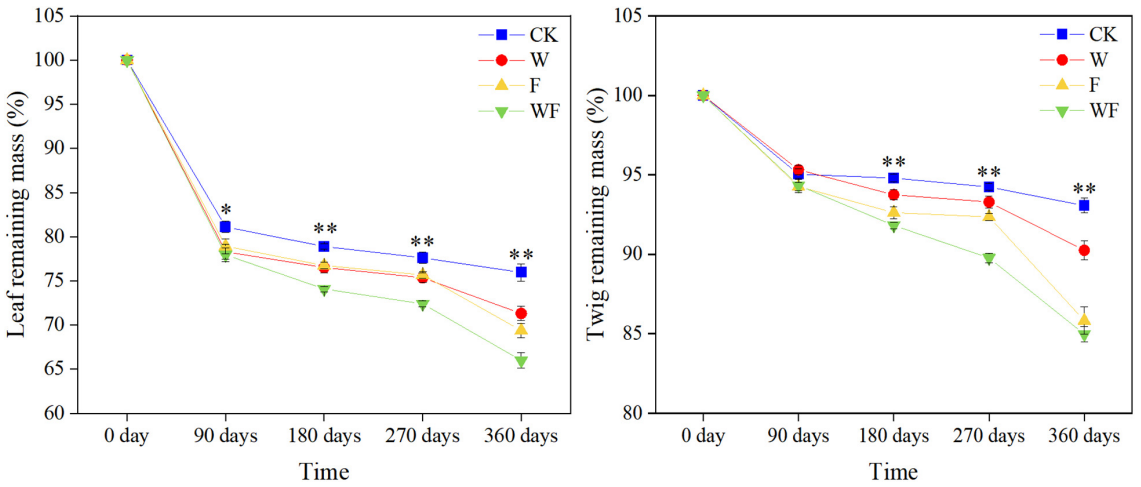

Figure 5 | Percentages of remaining mass in leaf and twig under different treatments during the experimental period. The *P-value* showed the results from one-way ANOVA testing for the effects of dry-season irrigation and fertilization, $*P < 0.05$, $**P < 0.01$.

TABLE 4 | Pearson correlation analysis between litter remaining mass (leaf and twig) and initial chemical traits.

Time	Initial C	Initial N	Initial P	Initial K	Initial C/N	Initial C/P	Initial C/K
90 days	−0.890**	−0.941**	−0.860**	−0.796**	0.905**	0.873**	0.875**
180 days	−0.914**	−0.964**	−0.902**	−0.818**	0.919**	0.890**	0.911**
270 days	−0.910**	−0.960**	−0.900**	−0.817**	0.921**	0.895**	0.907**
360 days	−0.874**	−0.931**	−0.886**	−0.821**	0.889**	0.898**	0.895**

Correlation coefficients of Pearson correlation are shown (n = 20), $**P < 0.01$.

TABLE 5 | Pearson correlation analysis between the percentage of remaining mass and enzyme activity of surface soil (10 cm) in the dry season.

Litter	Acid phosphatase	β -glucosidase	Urease	Polyphenol oxidase	Cellulase
Leaf	–	−0.568**	−0.611**	−0.544*	–
Twig	–	–	−0.473**	−0.608**	–

Correlation coefficients of Pearson correlation are shown (n = 20), $*P < 0.05$, $**P < 0.01$.

(Barlow et al., 2007; Ribeiro et al., 2018), but higher than that of a *E. urophylla* × *E. grandis* plantation (3.09 Mg/ha/yr) in southern China (Liu et al., 2009). In comparison with other studies demonstrating that litterfall production did not change with biomass (Demessie et al., 2012; Xu et al., 2019), the increases of litterfall production in our research are caused by increased biomass (**Table 1** and **Supplementary Table 1**). Our results indicate a higher leaf production, followed by twig, bark, and fruit, which was consistent with the pattern observed in other studies (Da Silva et al., 2018; De Queiroz et al., 2019). Fertilization increases all types of litterfall production except for leaf, but dry-season irrigation had little effect on these (**Figure 2**). This difference may be related to the fact that fertilization greatly increased aboveground biomass, while dry-season irrigation did not.

The value of litterfall production in tropical/subtropical forests is known to follow a seasonal pattern. Affected by environmental factors and forest types, the monthly dynamics of litterfall showed unimodal, bimodal, and irregular models (Zhang et al., 2014). The variations of total litterfall, leaf, and twig under different treatments show bimodal models, which was consistent with the studies in tropical forests (De Queiroz et al., 2019; Zhu et al., 2021). Our results show leaf litter dominated the temporal dynamics of litterfall. Previous studies have indicated that the peak of leaf abscissions of seasonally dry forests occurred in the dry season, which is the physiological mechanism of drought adaptation (Chave et al., 2010; Zhu et al., 2019, 2021). However, our results indicating that the peak of litterfall production occurred in the mid-rainy season were contrary to our hypothesis, but consistent with other studies of *Eucalyptus* (Barlow et al., 2007; Cizungu et al., 2014). Although drought stress was observed during dry season in our plantation (Hua et al., 2021), litterfall productions remained at a low level during the dry season. Moreover, dry-season irrigation and fertilization only weaken the correlation between leaf production and precipitation. Litterfall production mainly affected by precipitation (**Table 2**) may be caused by the heavy rainfall and powerful wind events

TABLE 6 | C and nutrient concentrations, C/N and C/P ratio of leaf and twig litter under various treatments after 0 and 360 days decomposition.

Time	Litter	Treatment	C(g/kg)	N(g/kg)	P(g/kg)	K(g/kg)	C/N	C/P	C/K
0 day	Leaf	CK	528.100 ± 3.799*bc*	8.394 ± 0.443*a*	0.314 ± 0.014*b*	2.044 ± 0.246*b*	63.647 ± 3.528*a*	1695.761 ± 74.512*a*	274.92 ± 34.63*a*
		W	520.700 ± 5.201*c*	8.418 ± 0.535*a*	0.299 ± 0.013*b*	3.187 ± 0.334*a*	62.846 ± 3.939*a*	1757.545 ± 81.169*a*	169.86 ± 15.62*b*
		F	542.320 ± 5.106*a*	9.308 ± 0.469*a*	0.396 ± 0.014*a*	2.451 ± 0.344*ab*	58.779 ± 2.535*a*	1377.602 ± 54.641*b*	241.21 ± 36.75*ab*
		WF	534.820 ± 2.270*ab*	9.312 ± 0.479*a*	0.382 ± 0.011*a*	3.239 ± 0.380*a*	57.990 ± 2.750*a*	1404.272 ± 44.885*b*	178.14 ± 28.36*b*
	twig	CK	478.520 ± 3.969*a*	2.158 ± 0.233*a*	0.070 ± 0.006*b*	0.277 ± 0.039*b*	232.219 ± 24.836*a*	7102.376 ± 685.106*a*	1854.55 ± 236.70*ab*
		W	473.200 ± 6.498*a*	1.940 ± 0.172*a*	0.061 ± 0.003*b*	0.253 ± 0.038*b*	250.992 ± 20.163*a*	7806.175 ± 415.882*a*	2018.45 ± 247.97*a*
		F	480.080 ± 4.888*a*	2.426 ± 0.237*a*	0.104 ± 0.014*a*	0.387 ± 0.033*a*	206.438 ± 21.850*a*	4945.722 ± 678.118*b*	1274.75 ± 110.48*b*
		WF	481.520 ± 4.256*a*	2.380 ± 0.131*a*	0.101 ± 0.009*a*	0.352 ± 0.023*ab*	204.784 ± 11.576*a*	4892.228 ± 875.848*b*	1394.02 ± 109.10*b*
360 days	Leaf	CK	406.960 ± 21.664*a*	5.590 ± 0.205*a*	0.195 ± 0.011*a*	2.410 ± 0.254*a*	72.617 ± 1.540*b*	2100.258 ± 103.828*a*	181.30 ± 29.90*a*
		W	421.340 ± 18.117*a*	5.342 ± 0.180*a*	0.214 ± 0.021*a*	2.173 ± 0.182*a*	79.622 ± 5.986*ab*	2035.755 ± 198.742*a*	198.89 ± 17.41*a*
		F	427.860 ± 17.728*a*	5.586 ± 0.187*a*	0.202 ± 0.009*a*	2.330 ± 0.183*a*	76.790 ± 3.415*ab*	2120.778 ± 90.760*a*	190.12 ± 20.97*a*
		WF	458.580 ± 8.571*a*	5.192 ± 0.251*a*	0.203 ± 0.005*a*	2.303 ± 0.090*a*	88.910 ± 3.457*a*	2270.009 ± 62.744*a*	201.46 ± 10.26*a*
	twig	CK	492.720 ± 2.716*a*	1.480 ± 0.073*a*	0.053 ± 0.002*ab*	0.155 ± 0.024*bc*	336.759 ± 17.874*a*	9363.232 ± 376.895*a*	3408.70 ± 399.50*ab*
		W	492.820 ± 4.537*a*	1.800 ± 0.280*a*	0.059 ± 0.010*a*	0.203 ± 0.028*ab*	292.556 ± 30.529*a*	9425.894 ± 1540.137*a*	2588.11 ± 311.20*bc*
		F	501.900 ± 2.598*a*	1.410 ± 0.151*a*	0.045 ± 0.005*ab*	0.252 ± 0.028*a*	374.234 ± 44.413*a*	11726.384 ± 1290.593*a*	2102.97 ± 248.75*c*
		WF	494.380 ± 2.876*a*	1.266 ± 0.129*a*	0.037 ± 0.004*b*	0.119 ± 0.012*c*	408.203 ± 43.970*a*	14033.825 ± 1632.545*a*	4289.03 ± 376.50*a*

Means ± SE were shown (n = 5). The letter after the numbers represented the Duncan's multiple comparison results. Different letters indicated significant differences between various treatments.

in the rainy season shaking off the dead hanging tissues (Dawoe et al., 2010).

Litter Decomposition Under Various Treatments

Litter decomposition is an important process of nutrient cycling in ecosystems (Yin et al., 2019). The decomposition of litter is mainly related to the initial nutrient concentrations (**Table 4**), which is consistent with previous studies that show decomposition rate is primarily determined by its traits. High nutrient concentration and corresponding low carbon: nutrient ratio increases litter attractiveness to microorganisms, which enhances the biodiversity and the activity of soil decomposers, resulting in higher decomposition rates (Zhang et al., 2019; Rawat et al., 2020). Since soil is the main source of plant nutrients, element concentrations in plants are affected by soil chemical properties (Bai et al., 2019). Fertilization increases the initial litter N, P, and K concentrations and decreases the C/N and C/P, while dry-season irrigation has little effect (**Table 6**). Low C/N and C/P indicates low recalcitrant substrate content and high nutrient content, facilitates microbial activity (Yin et al., 2019; Hou et al., 2021), and degrades organic matter (Zhang et al., 2019; Mora-Gómez et al., 2020). Meanwhile, the organic compounds from litter can influence the diversity and composition of microbial communities, further affecting the decomposition rates (McBride et al., 2020). In the present study, the average decomposition rate of leaf (30%) is much higher than that of twig (14%; **Table 3**). Compared to twig, the C/N and C/P of leaf are lower (**Table 6**), which is beneficial to decomposition (Zhang et al., 2019).

Generally, soil microbes secrete enzymes related to their nutrient demands, and enzyme activity is highly correlated with microbial activity (Frey et al., 2004; Li, 2006; Santos et al., 2018). Fertilization increased the activities of β -glucosidase, urease, and polyphenol oxidase, but not acid phosphatase and urease (**Supplementary Table 2**), indicating that N concentration limits microbial metabolism (Antonious, 2009; Wang et al., 2011). After fertilization, increased polyphenol oxidase activity was conductive to decompose recalcitrant polymers (such as lignin) of litterfall (Allison et al., 2008). Instead of cellulase, microbes in the soil of *E. urophylla* × *E. grandis* tend to secrete β -glucosidase to break down cellulose. Dry-season irrigation has little effect on soil enzyme activities during the dry season, which might be related to no differences in surface SWC_r caused by high evaporation (**Supplementary Tables 2**, **3**). Contrary to most previous studies (Salazar et al., 2011; Wang et al., 2012), the variation of soil enzyme activities is driven by foliar litter quality rather than soil nutrient (**Supplementary Tables 4**, **5**). The increased soil enzyme activities under fertilization may be caused by diverse substrate availability (Christina and John, 2000; Hu et al., 2006).

Our results indicate that decomposing 50% of leaf litter takes 2.9 years (**Table 3**), longer than that (2.1 years) in tropical forests (De Queiroz et al., 2019). Compared to other *Eucalyptus* species, the higher C/N may be the main reason for the slow decomposition rate of *E. urophylla* × *E. grandis* litter (Demessie et al., 2012; Cizungu et al., 2014). Fertilization

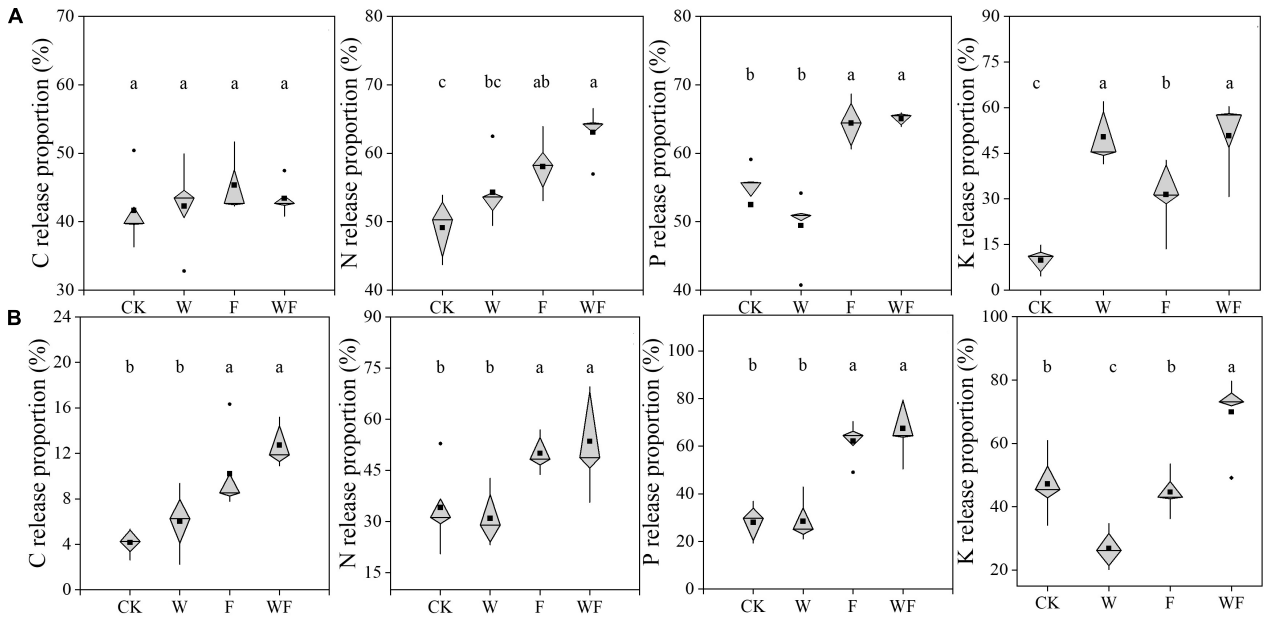

Figure 6 | The proportions of nutrient released to soil from leaf **(A)** and twig **(B)** litter bags after 360 days (n = 5). Data were shown as boxplots. The center line of the box represents the median, the box represents the inter -quartile range (IQR), the whiskers extend 1.5 times IQR, black dot represents the value outside 1.5 the IQR, and black square represents the mean value. The letters over the boxes represented the Duncan's multiple comparison results. Different lowercase letters indicated significant differences between various treatments ($P < 0.05$).

and dry-season irrigation accelerate litter decomposition rates, which is consistent with other studies (Sanaullah et al., 2012; Petraglia et al., 2019; Liu et al., 2021). By contrast with dry-season irrigation, fertilization had greater influences on the decomposition of low quality litter (Liu et al., 2006). After litter quality was increased by fertilization, dry-season irrigation further increased the decomposition rate. In the present study, fertilization stimulates litter decomposition by increasing litter quality and soil enzyme activities (Zhong et al., 2017; Hou et al., 2021; Liu et al., 2021). However, dry-season irrigation promoted litter decomposition with relatively little effect on litter quality or soil enzymes, contrary to previous studies (Prieto et al., 2019; Malik et al., 2020). The promotion of litter decomposition by dry season irrigation may be due to an increase in soil water content, which promotes soluble fraction leaching (Schreeg et al., 2013). These findings may only indicate the short-term effects of dry-season irrigation on litterfall decomposition, and further investigation should be conducted to uncover the underlying mechanisms.

Nutrient Release

In the present study, most leaf nutrients are released under different treatments after decomposing for 360 days, which was similar to Chen's study Chen et al. (2019). The released proportion of nutrients of twig are much lower than that of leaf, especially the C (**Figure 6**). The C, N, P, and K are not released at similar proportional rates in twig, leading to the inhibition of C release at the later stage of decomposition (Yin et al., 2019; Hou et al., 2021). High nitrogen concentration (Liu et al., 2021), high labile compounds content (Pei et al., 2019, 2020), and high surface area: volume ratio (Angst et al., 2018) of litter were all beneficial for releasing C and nutrients by improving microbial activity and contact area.

The effect of dry-season irrigation and fertilization on the proportions of released nutrients was mainly driven by the variation of initial stoichiometric characteristics (**Supplementary Table 6**). We find that fertilization increases the proportions of released N and P by increasing litter C/N and C/P, while dry-season irrigation affects the proportion of released K by increasing foliar C/K and decreasing C/K. This result is consistent with previous studies suggesting that initial stoichiometric characteristics (C/N, C/P, and C/K) were key determinants of nutrient release (Lanuza et al., 2018; Wang et al., 2021). Due to high N concentration suppressing the activity of ligninolytic enzymes, fertilization had little effect on C release of leaf (Frey et al., 2004). In previous studies, irrigation was shown to increase (Sanaullah et al., 2012; Santonja et al., 2017; Zhong et al., 2017), decrease (Walter et al., 2013), or have no effect on decomposition rate (Zhao et al., 2012), which would affect the proportions of released nutrients. However, our results show that dry-season irrigation influences the proportion of released K through C/K, but not the decomposition rate. The variation of initial C/K might be related to the change of K retranslocation under dry-season irrigation (Wan et al., 2021). Over the experimental period, fertilization and dry-season irrigation change the litter decomposition rate by affecting the stoichiometric characteristics of litter. But it is unclear how dry-season irrigation increases decomposition rate without affecting nutrient release. It is

necessary to further explore the effects of irrigation on nutrient cycling in *Eucalyptus* plantations under drier conditions.

Effect of Litterfall on Compensatory Growth

Previous studies on the effects of fertilization and irrigation on *Eucalyptus* growth have shown increased DBH, height, and biomass (Wright et al., 2011; Hua et al., 2021). In this study, fertilization and dry-season irrigation promoted the growth of DBH, height, and biomass, even though the effects of dry-season irrigation were not significant (**Supplementary Table 1**). This suggested that some compensatory responses occurred after nutrient and water restrictions were lifted. A high compensatory growth under fertilization may result from the up-regulation of photosynthesis capabilities and leaf biomass. Previous studies at this site have demonstrated that fertilization can increase photosynthesis (Hua et al., 2021) and promotes leaf growth (Yu et al., 2019a). By comparing the variations of biomass and litterfall production, it was found that the rise in biomass was much greater than that in litterfall production, promoting the growth of leaf biomass. Increased leaf biomass is especially beneficial for increasing photosynthetic products, which further enhances compensatory growth (Ma et al., 2020). Although the surface soil relative water content remained at a low level (**Supplementary Table 3**), dry-season irrigation had little effect on compensatory growth, which may be due to the utilization of deep soil water to alleviate water stress (Asensio et al., 2020). Another strategy that can be used to influence compensatory growth is altering the decomposition rate and release of nutrients in order to accelerate the nutrient cycle. The increase of decomposition rate and nutrient release under fertilization and dry-season irrigation can accelerate the nutrient cycle, and provide sufficient resources for compensatory growth (Van Staalduinen et al., 2010; Fischer et al., 2019).

CONCLUSION

Our results indicate that litterfall production of *E. urophylla* × *E. grandis* follows a seasonal pattern and its peak occurs in the rainy season. Fertilization significantly increases litterfall production (except leaf) while dry-season irrigation does not. Although temperature and rainfall are related to litterfall production, it is unclear whether this is caused by physical impacts (powerful wind or rain) or physiological characteristics. When litter enters topsoil, its decomposition is mainly affected by its traits (C/N, C/P, and C/K), followed by soil enzyme activity. Nutrients, rather than water, are the main factor limiting the litter decomposition in *E. urophylla* × *E. grandis* plantation. The positive effects of dry-season irrigation can be reflected only when nutrient limitation is alleviated. However, irrigation has little effect on litter nutrient release, which is contrary to previous studies. Therefore, more water supplement experiments in tropical/subtropical *Eucalyptus* plantations should be done to realize the effects of dry-season irrigation on the nutrient cycle under seasonal drought. Our finding shows that plantation management not only increased stand productivity, but also played an important role in the nutrient cycle.

DATA AVAILABILITY STATEMENT

The original contributions presented in the study are included in the article/**Supplementary Material**, further inquiries can be directed to the corresponding author.

AUTHOR CONTRIBUTIONS

JL and QQ: mainly contribute to the conceptualization of the work, funding acquisition, and investigation. JK, YL, and FH: methodology and analysis. YS, QH, and JK: project administration. WL, YS, JL, and QQ: resources. JK and WL: software. JK: visualization. QQ and QH: writing—original draft preparation. JK, QQ, and GW: writing—review, and editing. All authors have read and agreed to the version of manuscript to be published.

FUNDING

This research was supported by the National Natural Science Foundation of China (31800527), National Key Research and Development Program of China (2016YFD0600201 and 2016YFD060020102) and China Scholarship Council Grant (202008440171).

ACKNOWLEDGMENTS

We thank all members of Guangdong Key Laboratory for Innovative Development and Utilization of Forest Plant Germplasm for suggestions and support during the project.

SUPPLEMENTARY MATERIAL

The Supplementary Material for this article can be found online at: https://www.frontiersin.org/articles/10.3389/fevo.2022.919571/full#supplementary-material

REFERENCES

Adair, E. C., Parton, W. J., Del Grosso, S. J., Silver, W. L., Harmon, M. E., Hall, S. A., et al. (2008). Simple three-pool model accurately describes patterns of long-term litter decomposition in diverse climates. *Global Change Biol.* 14, 2636–2660. doi: 10.1111/j.1365-2486.2008.01674.x

Allison, S. D., Czimczik, C. I., and Treseder, K. K. (2008). Microbial activity and soil respiration under nitrogen addition in Alaskan boreal forest. *Global Change Biol.* 14, 1156–1168. doi: 10.1111/j.1365-2486.2008.01549.x

Almagro, M., Martínez-López, J., Maestre, F. T., and Rey, A. (2017). The contribution of photodegradation to litter decomposition in semiarid mediterranean grasslands depends on its interaction with local humidity conditions, litter quality and position. *Ecosystems* 20, 527–542. doi: 10.1007/s10021-016-0036-5

Angst, Š, Baldrian, P., Harantová, L., Cajthaml, T., and Frouz, J. (2018). Different twig litter (*Salix caprea*) diameter does affect microbial community activity and composition but not decay rate. *FEMS Microbiol. Ecol.* 94:y126. doi: 10.1093/femsec/fiy126

Antonious, G. F. (2009). Enzyme activities and heavy metals concentration in soil amended with sewage sludge. *J. Environ. Sci. Heal. A* 44, 1019–1024. doi: 10.1080/10934520902996971

Asensio, V., Domec, J., Nouvellon, Y., Laclau, J., Bouillet, J., Jordan-Meille, L., et al. (2020). Potassium fertilization increases hydraulic redistribution and water use efficiency for stemwood production in *Eucalyptus grandis* plantations. *Environ. Exp. Bot.* 176:104085. doi: 10.1016/j.envexpbot.2020.104085

Bai, K., Lv, S., Ning, S., Zeng, D., Guo, Y., and Wang, B. (2019). Leaf nutrient concentrations associated with phylogeny, leaf habit and soil chemistry in tropical karst seasonal rainforest tree species. *Plant Soil* 434, 305–326. doi: 10.1007/s11104-018-3858-4

Barlow, J., Gardner, T. A., Ferreira, L. V., Peres, and Carlos, A. (2007). Litter fall and decomposition in primary, secondary and plantation forests in the Brazilian Amazon. *Forest Ecol. Manag.* 247, 91–97. doi: 10.1016/j.foreco.2007.04.017

Blanco, J. A., Imbert, J. B., and Castillo, F. J. (2008). Nutrient return *via* litterfall in two contrasting *Pinus sylvestris* forests in the Pyrenees under different thinning intensities. *Forest Ecol. Manag.* 256, 1840–1852. doi: 10.1016/j.foreco.2008.07.011

Cajaiba, R. L., Périco, E., Caron, E., Dalzochio, M. S., Silva, W. B., and Santos, M. (2017). Are disturbance gradients in neotropical ecosystems detected using rove beetles? a case study in the Brazilian Amazon. *Forest Ecol. Manag.* 405, 319–327. doi: 10.1016/j.foreco.2017.09.058

Camargo, M., Giarrizzo, T., and Jesus, A. (2015). Effect of seasonal flooding cycle on litterfall production in alluvial rainforest on the middle Xingu River (Amazon basin. Brazil). *Braz. J. Biol.* 75, 250–256. doi: 10.1590/1519-6984.00514BM

Carter, M. R., and Gregorich, E. G. (2007). *Soil Sampling and Methods of Analysis. Canadian Society of Soil Science*. Boca Raton, FL: CRC Press, Taylor and Francis Group.

Chave, J., Navarrete, D., Almeida, S., Álvarez, E., Aragão, L. E. O. C., Bonal, D., et al. (2010). Regional and seasonal patterns of litterfall in tropical South America. *Biogeosciences* 7, 43–55. doi: 10.5194/bg-7-43-2010

Chen, Y., Zhang, Y., Cao, J., Fu, S., Hu, S., Wu, J., et al. (2019). Stand age and species traits alter the effects of understory removal on litter decomposition and nutrient dynamics in subtropical *Eucalyptus plantations*. *Glob. Ecol. Conserv.* 20:e693. doi: 10.1016/j.gecco.2019.e00693

Christina, C., and John, D. (2000). Litter quality influences on decomposition, ectomycorrhizal community structure and mycorrhizal root surface acid phosphatase activity. *Soil Biol. Biochem.* 32, 489–496. doi: 10.1016/s0038-0717(99)00178-9

Cizungu, L., Staelens, J., Huygens, D., Walangululu, J., Muhindo, D., Van Cleemput, O., et al. (2014). Litterfall and leaf litter decomposition in a central African tropical mountain forest and *Eucalyptus plantation*. *Forest Ecol. Manag.* 326, 109–116. doi: 10.1016/j.foreco.2014.04.015

Cotrufo, M. F., Soong, J. L., Horton, A. J., Campbell, E. E., Haddix, M. L., Wall, D. H., et al. (2015). Formation of soil organic matter *via* biochemical and physical pathways of litter mass loss. *Nat. Geosci.* 8, 776–779. doi: 10.1038/ngeo2520

Da Silva, W. B., Périco, E., Dalzochio, M. S., Santos, M., and Cajaiba, R. L. (2018). Are litterfall and litter decomposition processes indicators of forest regeneration in the neotropics? insights from a case study in the Brazilian Amazon. *Forest Ecol. Manag.* 429, 189–197. doi: 10.1016/j.foreco.2018.07.020

Dai, A. (2013). Increasing drought under global warming in observations and models. *Nat. Clim. Change* 3, 52–58. doi: 10.1038/nclimate1633

Dawoe, E. K., Isaac, M. E., and Quashie-Sam, J. (2010). Litterfall and litter nutrient dynamics under cocoa ecosystems in lowland humid Ghana. *Plant Soil* 330, 55–64. doi: 10.1007/s11104-009-0173-0

De Queiroz, M. G., Da Silva, T. G. F., Zolnier, S., De Souza, C. A. A., De Souza, L. S. B., Steidle Neto, A. J., et al. (2019). Seasonal patterns of deposition litterfall in a seasonal dry tropical forest. *Agr. Forest Meteorol.* 279:107712. doi: 10.1016/j.agrformet.2019.107712

Demessie, A., Singh, B. R., Lal, R., and Strand, L. T. (2012). Leaf litter fall and litter decomposition under Eucalyptus and coniferous plantations in Gambo District, southern Ethiopia. *Acta Agr. Scand. B-S P* 62, 467–476. doi: 10.1080/09064710.2011.645497

Dong, X., Gao, P., Zhou, R., Li, C., Dun, X., and Niu, X. (2021). Changing characteristics and influencing factors of the soil microbial community during litter decomposition in a mixed *Quercus acutissima Carruth*. and *Robinia pseudoacacia* L. forest in Northern China. *Catena* 196:104811. doi: 10.1016/j.catena.2020.104811

Dubreuil, V., Fante, K. P., Planchon, O., and Sant'Anna Neto, J. L. (2019). Climate change evidence in Brazil from Köppen's climate annual types frequency. *Int. J. Climatol.* 39, 1446–1456. doi: 10.1002/joc.5893

Fischer, R. A., Moreno Ramos, O. H., Ortiz Monasterio, I., and Sayre, K. D. (2019). Yield response to plant density, row spacing and raised beds in low latitude spring wheat with ample soil resources: an update. *Field Crop Res.* 232, 95–105. doi: 10.1016/j.fcr.2018.12.011

Frey, S. D., Knorr, M., Parrent, J. L., and Simpson, R. T. (2004). Chronic nitrogen enrichment affects the structure and function of the soil microbial community in temperate hardwood and pine forests. *Forest Ecol. Manag.* 196, 159–171. doi: 10.1016/j.foreco.2004.03.018

Ge, X., Zeng, L., Xiao, W., Huang, Z., Geng, X., and Tan, B. (2013). Effect of litter substrate quality and soil nutrients on forest litter decomposition: a review. *Acta Ecol. Sinica* 33, 102–108. doi: 10.1016/j.chnaes.2013.01.006

Gonzalez, I., Sixto, H., Rodriguez-Soalleiro, R., and Oliveira, N. (2020). Nutrient contribution of litterfall in a short rotation plantation of pure or mixed plots of *Populus alba* L. and *Robinia pseudoacacia* L. *Forests* 11:1133. doi: 10.3390/f11111133

Guan, S. (1986). *Soil Enzyme and its Research Approaches*. Beijing: China Agriculture Press.

Hou, S. L., Hättenschwiler, S., Yang, J. J., Sistla, S., Wei, H. W., Zhang, Z. W., et al. (2021). Increasing rates of long-term nitrogen deposition consistently increased litter decomposition in a semi-arid grassland. *New Phytol.* 229, 296–307. doi: 10.1111/nph.16854

Hu, Y. L., Wang, S. L., and Zeng, D. H. (2006). Effects of single chinese fir and mixed leaf litters on soil chemical, microbial properties and soil enzyme activities. *Plant Soil* 282, 379–386. doi: 10.1007/s11104-006-0004-5

Hua, L., Yu, F., Qiu, Q., He, Q., Su, Y., Liu, X., et al. (2021). Relationships between diurnal and seasonal variation of photosynthetic characteristics of *Eucalyptus plantation* and environmental factors under dry-season irrigation with fertilization. *Agr. Water Manage* 248:106737. doi: 10.1016/j.agwat.2021.106737

Kamruzzaman, M., Basak, K., Paul, S. K., Ahmed, S., and Osawa, A. (2019). Litterfall production, decomposition and nutrient accumulation in *Sundarbans mangrove* forests, Bangladesh. *Forest Sci. Technol.* 15, 24–32. doi: 10.1080/21580103.2018.1557566

Lanuza, O., Casanoves, F., Delgado, D., and Van den Meersche, K. (2018). Leaf litter stoichiometry affects decomposition rates and nutrient dynamics in tropical forests under restoration in Costa Rica. *Restor. Ecol.* 27, 549–558. doi: 10.1111/rec.12893

Li, C., Barclay, H., Roitberg, B., and Lalonde, R. (2020). Forest productivity enhancement and compensatory growth: a review and synthesis. *Front. Plant. Sci.* 11:575211. doi: 10.3389/fpls.2020.575211

Li, D. (2006). Review of fungal chitinases. *Mycopathologia* 161, 345–360. doi: 10.1007/s11046-006-0024-y

Liu, C., Westman, C. J., Berg, B., Kutsch, W., Wang, G. Z., Man, R., et al. (2004). Variation in litterfall-climate relationships between coniferous and broadleaf forests in Eurasia. *Global Ecol. Biogeogr.* 13, 105–114. doi: 10.1111/j.1466-882X.2004.00072.x

Liu, D., Ogaya, R., Barbeta, A., Yang, X., and Peñuelas, J. (2015). Contrasting impacts of continuous moderate drought and episodic severe droughts on the aboveground-biomass increment and litterfall of three coexisting

Mediterranean woody species. *Global Change Biol.* 21, 4196–4209. doi: 10.1111/gcb.13029

Liu, P., Huang, J., Han, X., Sun, O. J., and Zhou, Z. (2006). Differential responses of litter decomposition to increased soil nutrients and water between two contrasting grassland plant species of Inner Mongolia. China. *Appl. Soil Ecol.* 34, 266–275. doi: 10.1016/j.apsoil.2005.12.009

Liu, S., Behm, J. E., Wan, S., Yan, J., Ye, Q., Zhang, W., et al. (2021). Effects of canopy nitrogen addition on soil fauna and litter decomposition rate in a temperate forest and a subtropical forest. *Geoderma* 382:114703. doi: 10.1016/j.geoderma.2020.114703

Liu, W., Fan, H., Gao, C., Huang, R., and Su, B. (2009). Litter production and its nutrient fluxes in an age sequence of *Eucalyptus plantations*. *Chinese J. Ecol.* 28, 1928–1934.

Lu, H., Xu, J., Li, G., and Liu, W. (2020). Site classification of *Eucalyptus urophylla* × *Eucalyptus grandis* plantations in China. *Forests* 11:871. doi: 10.3390/f11080871

Lu, R. (2000). *Soil Agricultural Chemical Analysis Method. China Agricultural*. Beijing: Science Press.

Ma, H., Zheng, C., Gao, Y., Baskin, C. C., Sun, H., and Yang, H. (2020). Moderate clipping stimulates over-compensatory growth of *Leymus chinensis* under saline-alkali stress through high allocation of biomass and nitrogen to shoots. *Plant Growth Regul.* 92, 95–106. doi: 10.1007/s10725-020-00622-3

Malik, A. A., Swenson, T., Weihe, C., Morrison, E. W., Martiny, J. B. H., Brodie, E. L., et al. (2020). Drought and plant litter chemistry alter microbial gene expression and metabolite production. *ISME J.* 14, 2236–2247. doi: 10.1038/s41396-020-0683-6

McBride, S. G., Choudoir, M., Fierer, N., and Strickland, M. S. (2020). Volatile organic compounds from leaf litter decomposition alter soil microbial communities and carbon dynamics. *Ecology* 101:e3130. doi: 10.1002/ecy.3130

Menegale, M., Rocha, J., Harrison, R., Almeida, R., Piccolo, M., Hubner, A., et al. (2016). Effect of timber harvest intensities and fertilizer application on stocks of soil C. N, P, and S. *Forests* 7:319. doi: 10.3390/f7120319

Ministry of Agriculture of the People's Republic of China (2010). *Soil Testing – Cutting Ring Method for Determination of Field Water – Holding Capacity in Soil*. Beijing: Ministry of Agriculture of the People's Republic of China.

Ministry of Forestry of the People's Republic of China (2015). *Technical Regulation on Management of Eucalypt High-yielding Plantation*. Beijing: Ministry of Agriculture of the People's Republic of China.

Mora-Gómez, J., Boix, D., Duarte, S., Cássio, F., Pascoal, C., Elosegi, A., et al. (2020). Legacy of summer drought on autumnal leaf litter processing in a temporary Mediterranean stream. *Ecosystems* 23, 989–1003. doi: 10.1007/s10021-019-00451-0

Ni, X., Lin, C., Chen, G., Xie, J., Yang, Z., Liu, X., et al. (2021). Decline in nutrient inputs from litterfall following forest plantation in subtropical China. *Forest Ecol. Manag.* 496:119445. doi: 10.1016/j.foreco.2021.119445

Nouvellon, Y., Epron, D., Marsden, C., Kinana, A., Le Maire, G., Deleporte, P., et al. (2012). Age-related changes in litter inputs explain annual trends in soil CO2 effluxes over a full Eucalyptus rotation after afforestation of a tropical savannah. *Biogeochemistry* 111, 515–533. doi: 10.1007/s10533-011-9685-9

Paudel, E., Dossa, G. G. O., Xu, J., and Harrison, R. D. (2015). Litterfall and nutrient return along a disturbance gradient in a tropical montane forest. *Forest Ecol. Manag.* 353, 97–106. doi: 10.1016/j.foreco.2015.05.028

Pei, G., Liu, J., Peng, B., Gao, D., Wang, C., Dai, W., et al. (2019). Nitrogen, lignin, C/N as important regulators of gross nitrogen release and immobilization during litter decomposition in a temperate forest ecosystem. *Forest Ecol. Manag.* 440, 61–69. doi: 10.1016/j.foreco.2019.03.001

Pei, G., Liu, J., Peng, B., Wang, C., Jiang, P., and Bai, E. (2020). Nonlinear coupling of carbon and nitrogen release during litter decomposition and its responses to nitrogen dddition. *J. Geophys. Res-Biogeo* 125:e2019J. doi: 10.1029/2019JG005462

Petraglia, A., Cacciatori, C., Chelli, S., Fenu, G., Calderisi, G., Gargano, D., et al. (2019). Litter decomposition: effects of temperature driven by soil moisture and vegetation type. *Plant Soil* 435, 187–200. doi: 10.1007/s11104-018-3889-x

Prieto, I., Almagro, M., Bastida, F., and Querejeta, J. I. (2019). Altered leaf litter quality exacerbates the negative impact of climate change on decomposition. *J. Ecol.* 107, 2364–2382. doi: 10.1111/1365-2745.13168

Prosser, J., Speir, T., Stott, D. E., and Dick, R. (2011). *Soil Oxidoreductases and FDA Hydrolysis*. Madison, WI: Soil Science Society of America.

Rawat, M., Arunachalam, K., Arunachalam, A., Alatalo, J. M., and Pandey, R. (2020). Predicting litter decomposition rate for temperate forest tree species by the relative contribution of green leaf and litter traits in the Indian Himalayas region. *Ecol. Indic.* 119:106827. doi: 10.1016/j.ecolind.2020.106827

Ribeiro, C., Madeira, M., and Araújo, M. C. (2002). Decomposition and nutrient release from leaf litter of *Eucalyptus globulus* grown under different water and nutrient regimes. *Forest Ecol. Manag.* 171, 31–41. doi: 10.1016/s0378-1127(02)00459-0

Ribeiro, F., Gatto, A., Oliveira, A., Pulrolnik, K., and Neto, S. (2018). Litter dynamics in eucalyptus and native forest in the brazilian cerrado. *J. Agr. Sci-Cambridge* 10, 29–43. doi: 10.5539/jas.v10n11p29

Salazar, S., Sánchez, L. E., Alvarez, J., Valverde, A., Galindo, P., Igual, J. M., et al. (2011). Correlation among soil enzyme activities under different forest system management practices. *Ecol. Eng.* 37, 1123–1131.

Sanaullah, M., Rumpel, C., Charrier, X., and Chabbi, A. (2012). How does drought stress influence the decomposition of plant litter with contrasting quality in a grassland ecosystem? *Plant Soil* 352, 277–288. doi: 10.1007/s11104-011-0995-4

Santonja, M., Fernandez, C., Proffit, M., Gers, C., Gauquelin, T., Reiter, I. M., et al. (2017). Plant litter mixture partly mitigates the negative effects of extended drought on soil biota and litter decomposition in a Mediterranean oak forest. *J. Ecol.* 105, 801–815. doi: 10.1111/1365-2745.12711

Santos, F. M., Balieiro, F. D. C., Fontes, M. A., and Chaer, G. M. (2018). Understanding the enhanced litter decomposition of mixed-species plantations of *Eucalyptus* and *Acacia mangium*. *Plant Soil* 423, 141–155. doi: 10.1007/s11104-017-3491-7

Schreeg, L. A., Mack, M. C., and Turner, B. L. (2013). Nutrient-specific solubility patterns of leaf litter across 41 lowland tropical woody species. *Ecology* 94, 94–105. doi: 10.1890/11-1958.1

Staelens, J., Nachtergale, L., De Schrijver, A., Vanhellemont, M., Wuyts, K., and Verheyen, K. (2011). Spatio-temporal litterfall dynamics in a 60-year-old mixed deciduous forest. *Ann. Forest Sci.* 68, 89–98. doi: 10.1007/s13595-011-0010-5

Tang, J., Cao, M., Zhang, J., and Li, M. (2010). Litterfall production, decomposition and nutrient use efficiency varies with tropical forest types in Xishuangbanna. SW China: a 10-year study. *Plant Soil* 335, 271–288. doi: 10.1007/s11104-010-0414-2

Van Staalduinen, M. A., Dobarro, I., and Peco, B. (2010). Interactive effects of clipping and nutrient availability on the compensatory growth of a grass species. *Plant Ecol.* 208, 55–64. doi: 10.1007/s11258-009-9686-0

Walter, J., Hein, R., Beierkuhnlein, C., Hammerl, V., Jentsch, A., Schädler, M., et al. (2013). Combined effects of multifactor climate change and land-use on decomposition in temperate grassland. *Soil Biol. Biochem.* 60, 10–18. doi: 10.1016/j.soilbio.2013.01.018

Wan, F., Ross-Davis, A. L., Davis, A. S., Song, X., Chang, X., Zhang, J., et al. (2021). Nutrient retranslocation in Larix principis-rupprechtii Mayr relative to fertilization and irrigation. *New Forest* 52, 69–88. doi: 10.1007/s11056-020-09783-5

Wang, B., Xue, S., Liu, G. B., Zhang, G. H., Li, G., and Ren, Z. P. (2012). Changes in soil nutrient and enzyme activities under different vegetations in the Loess Plateau area, Northwest China. *Catena* 92, 186–195. doi: 10.1016/j.catena.2011.12.004

Wang, C., Han, G., Jia, Y., Feng, X., Guo, P., and Tian, X. (2011). Response of litter decomposition and related soil enzyme activities to different forms of nitrogen fertilization in a subtropical forest. *Ecol. Res.* 26, 505–513. doi: 10.1007/s11284-011-0805-8

Wang, L., Chen, Y., Zhou, Y., Xu, Z., Tan, B., You, C., et al. (2021). Environmental conditions and litter nutrients are key determinants of soluble C, N, and P release during litter mixture decomposition. *Soil Till Res.* 209:104928. doi: 10.1016/j.still.2020.104928

Wang, L., Zhang, G., Zhu, P., and Wang, X. (2020). Comparison of the effects of litter covering and incorporation on infiltration and soil erosion under simulated rainfall. *Hydrol. Process* 34, 2911–2922. doi: 10.1002/hyp.13779

Wright, S. J., Yavitt, J. B., Wurzburger, N., Turner, B. L., Tanner, E. V. J., Sayer, E. J., et al. (2011). Potassium, phosphorus, or nitrogen limit root allocation, tree growth, or litter production in a lowland tropical forest. *Ecology* 92, 1616–1625. doi: 10.1890/10-1558.1

Xie, Y., Arnold, R. J., Wu, Z., Chen, S., Du, A., and Luo, J. (2017). Advances in eucalypt research in China. *Front. Agr. Sci. Eng.* 4:380–390. doi: 10.15302/J-FASE-2017171

Xu, Y., Wang, Z., Zhu, W., and Du, A. (2019). Litterfall and nutrient cycling of *Eucalyptus plantation* with different ages on Leizhou Peninsula. *J. Trop. Subtropical Botany* 27, 359–366.

Yin, R., Eisenhauer, N., Auge, H., Purahong, W., Schmidt, A., and Schädler, M. (2019). Additive effects of experimental climate change and land use on faunal contribution to litter decomposition. *Soil Biol. Biochem.* 131, 141–148. doi: 10.1016/j.soilbio.2019.01.009

Yu, F., Truong, T. V., He, Q., Hua, L., Su, Y., and Li, J. (2019a). Dry season irrigation promotes leaf growth in *Eucalyptus urophylla* × *E. grandis* under fertilization. *Forests* 10:67. doi: 10.3390/f10010067

Yu, S., Mo, Q., Li, Y., Li, Y., Zou, B., Xia, H., et al. (2019b). Changes in seasonal precipitation distribution but not annual amount affect litter decomposition in a secondary tropical forest. *Ecol. Evol.* 9, 11344–11352. doi: 10.1002/ece3.5635

Zhang, H., Yuan, W., Dong, W., and Liu, S. (2014). Seasonal patterns of litterfall in forest ecosystem worldwide. *Ecol. Complex* 20, 240–247. doi: 10.1016/j.ecocom.2014.01.003

Zhang, M., Cheng, X., Geng, Q., Shi, Z., Luo, Y., and Xu, X. (2019). Leaf litter traits predominantly control litter decomposition in streams worldwide. *Global Ecol. Biogeogr.* 28, 1469–1486. doi: 10.1111/geb.12966

Zhao, H., Huang, G., Ma, J., Li, Y., and Zhou, L. (2012). Responses of surface litter decomposition to seasonal water addition in desert. *Chinese J. Plant Ecol.* 36, 471–482. doi: 10.3724/sp.j.1258.2012.00471

Zhen, Z., Wang, S., Luo, S., Ren, L., Liang, Y., Yang, R., et al. (2005). How different reforestation approaches affect red soil properties in southern China. *Land Degrad Dev.* 16, 387–396. doi: 10.1002/ldr.650

Zhen, Z., Wang, S., Luo, S., Ren, L., Liang, Y., Yang, R., et al. (2019). Significant impacts of both total amount and availability of heavy metals on the functions and assembly of soil microbial communities in different land use patterns. *Front. Microbiol.* 10:2293.

Zhong, Y., Yan, W., Wang, R., and Shangguan, Z. (2017). Differential responses of litter decomposition to nutrient addition and soil water availability with long-term vegetation recovery. *Biol. Fert. Soils* 53, 939–949.

Zhou, G., Wei, X., Wu, Y., Liu, S., Huang, Y., Yan, J., et al. (2011). Quantifying the hydrological responses to climate change in an intact forested small watershed in Southern China. *Global Change Biol.* 17, 3736–3746. doi: 10.1111/j.1365-2486.2011.02499.x

Zhu, X., Liu, W., Chen, H., Deng, Y., Chen, C., and Zeng, H. (2019). Effects of forest transition on litterfall, standing litter and related nutrient returns: implications for forest management in tropical China. *Geoderma* 333, 123–134. doi: 10.1016/j.geoderma.2018.07.023

Zhu, X., Zou, X., Lu, E., Deng, Y., Luo, Y., Chen, H., et al. (2021). Litterfall biomass and nutrient cycling in karst and nearby non-karst forests in tropical China: a 10-year comparison. *Sci. Total Environ.* 758:143619. doi: 10.1016/j.scitotenv.2020.143619

Conflict of Interest: The authors declare that the research was conducted in the absence of any commercial or financial relationships that could be construed as a potential conflict of interest.

Publisher's Note: All claims expressed in this article are solely those of the authors and do not necessarily represent those of their affiliated organizations, or those of the publisher, the editors and the reviewers. Any product that may be evaluated in this article, or claim that may be made by its manufacturer, is not guaranteed or endorsed by the publisher.

frontiers | Frontiers in Plant Science

TYPE Original Research
PUBLISHED 15 September 2022
DOI 10.3389/fpls.2022.947476

OPEN ACCESS

EDITED BY
Bernard Roitberg,
Simon Fraser University, Canada

REVIEWED BY
Jun Zhao,
University of Florida, United States
Zhiguang Liu,
Shandong Agricultural University, China

*CORRESPONDENCE
Xiao-Ling Wang
wangxl@haust.edu.cn

SPECIALTY SECTION
This article was submitted to Functional Plant Ecology, a section of the journal Frontiers in Plant Science

RECEIVED 18 May 2022
ACCEPTED 16 August 2022
PUBLISHED 15 September 2022

CITATION
Wang X-L, Ma K, Qi L, Liu Y-H, Shi J, Li X-L, Zhang L-X, Liu W and Song P (2022) Effect of ammonia-oxidizing bacterial strain that survives drought stress on corn compensatory growth upon post-drought rewatering. *Front. Plant Sci.* 13:947476. doi: 10.3389/fpls.2022.947476

Effect of ammonia-oxidizing bacterial strain that survives drought stress on corn compensatory growth upon post-drought rewatering

Xiao-Ling Wang[1]*, Ke Ma[2], Lin Qi[1], Yu-Hua Liu[1], Jiang Shi[1], Xue-Lin Li[1], Li-Xia Zhang[1], Wei Liu[1] and Peng Song[1]

[1]College of Agronomy, Henan University of Science and Technology, Luoyang, China, [2]Henan Agricultural Broadcasting and Television School, Zhengzhou, China

A pot experiment was performed under rain–shelter conditions to explore the effects of drought stress and post-drought rewatering on the abundance of an ammonia-oxidizing bacteria (AOB) strain in corn (*Zea mays* L.) rhizosphere soils and the relationship between the AOB strain and corn (*Zea mays* L.) compensatory growth after drought stress rewatering. Corn seedlings were used as test materials, and one AOB strain was isolated and screened from the soil. The experimental design included six treatments: (1) wet (WT), (2) wet with AOB strain inoculation during wetness (WI), (3) wet with AOB strain inoculation during rewatering (WR), (4) post-drought rewatering (DT), (5) post-drought rewatering with AOB strain inoculation during wetness (DI), and (6) post-drought rewatering with AOB strain inoculation during rewatering (DR). Wetness and drought stress were obtained by keeping the soil water content at 75–80% and 50–55% of the field capacities, respectively. The results showed that the isolated and screened AOB strain (S2_8_1) had 100% similarity to *Ensifer sesbaniae*. The inoculation of S2_8_1 during the wet period in the DI treatment caused it to colonize the rhizosphere soil. Drought stress decreased its abundance, but rewatering resulted in a great increase. The S2_8_1 in the DI treatment increased the total biomass, water use efficiencies, net photosynthetic rates, rhizosphere soil nitrification rates, leaf cytokinin concentrations, xylem sap cytokinin concentrations, copy number of S2_8_1 in rhizosphere soils, and organic carbon contents in rhizosphere soils by 23, 104, 35, 30, 18, 29, 104, and 23% on day 10 after rewatering compared with WT treatment. In the DI treatment, the increase in rhizosphere soil nitrification rates caused by S2_8_1 during wetness was closely related to the cytokinin delivery from roots to leaves and increased leaf cytokinin concentrations. The increase in leaf cytokinin concentrations improved rewatering corn growth, which caused compensatory growth and increased water use. Compensatory and over-compensatory growths occurred in DT and DR treatments, respectively. Therefore, the coexistence of the strain of AOB with corn in rhizosphere soil increased the corn compensatory growth by regulating soil nitrification and root-induced leaf cytokinin.

KEYWORDS

ammonia-oxidizing bacterial strain, coexistence, corn, compensatory growth, cytokinin, rewatering upon drought stress

Introduction

The lack of rainfall and irrigation water is a serious threat to crop production in Northern China (Yan et al., 2018; Liu et al., 2020). Crop water use should be improved to meet the challenge of water shortage. For this reason, water-saving agricultural technologies, namely, supplemental irrigation, regulated deficit irrigation, deficit irrigation, and rainwater harvesting irrigation have been widely used in the region (Ali et al., 2019; Zhang et al., 2019a,b; Liu et al., 2021; Shi et al., 2021). Essentially, these water-saving techniques were all based on growth inhibition under drought stress and growth acceleration during subsequent rewatering, namely compensatory growth upon post-drought rewatering. Plant under-compensation, compensation, and over-compensation growths refer to the compensatory biomasses during recovery growth below, equal to, and exceeding the lost biomass during environmental stress, respectively (Belsky, 1986; Grogan and Zamin, 2018). Thus, research efforts in crop post-drought rewatering compensatory growth should continuously focus on the development of water-saving strategies in agricultural production.

Crop post-drought rewatering compensatory growth is the fast growth caused by rewatering stimulation, and the root is the most direct organ that receives the stimulation; therefore, crop post-drought rewatering is very important for compensatory regrowth. Wang et al. (2016, 2018a) reported that leaf cytokinin induced by its synthesis in the roots promoted fast corn growth during post-drought rewatering, and nitrate (NO_3^-) in the soil is the key factor that promoted the synthesis of cytokinin in corn roots. Wang et al. (2020a,b) observed that NO_3^- released from the soil, which was caused by rhizosphere soil nitrification, directly induced corn root cytokinin synthesis and its delivery to the leaves, thereby increasing post-drought rewatering compensatory growth. Furthermore, soil ammonia-oxidizing bacteria (AOB) play a key role in the compensatory growth of crops. Wang et al. (2021) reported that a strain of the AOB *Acinetobacter pittii*, which was isolated and screened from the soil, promoted rhizosphere soil nitrification and the compensatory growth of corn. However, the reports on the relationship between soil AOB and crop are limited. The present study aimed to reveal the crop post-drought rewatering compensatory growth mechanism based on the coexistence of soil AOB with the crop.

The rhizosphere is an area where many bacteria colonize and play a role in host plant growth (Gagné-Bourque et al., 2016); it is a good place for soil AOB to coexist with crops. Crops during post-drought rewatering experience soil wetness, drought stress, and rewatering. The variable soil water environments of crops under post-drought rewatering growth influence the AOB abundance because drought stress restrains the bacterial number, but wetness can play a positive role in it (Monokrousos et al., 2020). However, several studies have reported the abundance of soil AOB in crop rhizosphere during post-drought rewatering. The study of the relationship between the abundance of rhizosphere soil AOB with crop post-drought compensatory growth will reveal its mechanism from a coexisting view.

In the present study, corn seedlings were selected as the test materials because their seedling growth is susceptible to drought stress and rewatering. Corn is the largest crop in China and the third largest crop in the world. Determining its compensatory mechanism during post-drought rewatering is beneficial for agricultural production and the development of water-saving strategies. We intended to reveal a rhizosphere soil AOB strain that would survive drought stress, show increased growth with rewatering, and improve corn compensatory growth during post-drought rewatering. To test this hypothesis, we isolated and screened one strain of AOB from the soil of the study site to test the effect of soil AOB on corn growth. Then, the isolated AOB strain was inoculated into the soil to detect its abundance by quantitative fluorescence polymerase chain reaction (PCR). Quantitative PCR is an accurate method for detecting bacterial numbers in soils (Bland et al., 2021). The effects of drought stress and post-drought rewatering on the abundance of the isolated AOB strain in rhizosphere soils and the relationship between the abundance of the isolated AOB strain and soil nitrification rates in rhizosphere soils, leaf cytokinin, and leaf photosynthesis were investigated to understand the compensatory growth mechanisms.

Materials and methods

Experimental design

Isolation and screening of soil AOB strain

AOB strain isolation from soil

In the present study, a liquid medium containing 0.5 g $(NH_4)_2SO_4$, 0.75 g KH_2PO_4, 0.25 g NaH_2PO_4, 0.01 g $MnSO_4{\cdot}4H_2O$, 0.03 g $MgSO_4{\cdot}7H_2O$, and 5.0 g $CaCO_3$ dissolved in 1 L of distilled water was obtained to isolate and screen soil AOB strain, and the solution pH was regulated to 7.2. The 1 L of the liquid medium was dissolved in 2.5 g of agar to form a solid medium. A mixture of 5 g of yeast extracts, 10 g of NaCl, and 10 g of tryptone was dissolved in 1 L of distilled water with pH being regulated to 7.0 and served as the LB medium.

Soil samples were collected from the corn rhizosphere soil, and they were added to the liquid medium to cultivate for 15–25 days at 28 °C in the dark. Then, the liquid medium was examined with Griess reagent to qualitatively test the presence of the AOB strain. Griess reagent is a qualitative test reagent for nitrite; nitrite may be used to verify whether ammonia has been oxidized. The liquid medium (0.5 ml) was dropped onto a white porcelain colorimetric plate, followed by the addition of 0.1 ml of Griess reagent for colorization. The occurrence of red, pink, or dark red colors meant the presence of nitrite ions and

the AOB strain due to the oxidation of ammonia into nitrite. Then, we obtain a small portion of the liquid medium and added it to the new liquid medium for another cultivation using the same method. We repeated this process two times to obtain the liquid medium with pure AOB. Several of these pure AOB liquid media was applied on the surface of a solid medium to perform a 5–8-day cultivation at 28°C under dark conditions. When tip-size bacterial colonies were observed, we selected a single colony and applied it to the surface of another solid medium. The pure bacterial colony was obtained after repeating this process 5–10 times. Finally, one strain (S2_8_1) of bacteria was selected as the experimental strain.

The pure bacterial colonies were subsequently inoculated into the liquid medium solution, which ultimately served as the AOB culture in the present study. In addition, a portion of the AOB culture was inoculated into the LB medium to detect the heterotrophic growth of the bacterial strain. The characteristics of individual AOB were observed under an optical microscope, and the isolated AOB strains were examined through Gram staining.

Nitrification rate detection

The purified AOB culture (1 ml) and its control consisting of 1 ml of liquid medium without AOB were applied to 50 g soil samples to test AOB effects on soil nitrification. The soil samples had an organic carbon content of 24.3 g·kg^{-1} and total nitrogen content of 2.2 g·kg^{-1}. Then, 20 g of each soil sample was cultivated for 7 days at 25°C under a moisture level equal to 60% field capacity. The differences in soil NO_3^- content between the inoculated soil samples and those not inoculated were divided by 7 (for the 7 days) to obtain the soil nitrification rate per day.

Identification of AOB strains

A bacterial genome extraction kit (Bioer Technology Co., Ltd.) was used to extract the total bacterial DNA, and 16Sr DNA was amplified. The forward and reverse primers were 27F (5′-AGAGTTGATCCTGGCTCAG-3′) and 1492R (5′-TACCTTGTTACGACTT-3′), respectively. The 25 μL of PCR reaction system components included 2.5 μL of 10× Buffer (with Mg^{2+}), 2 μL of dNTP (2.5 mmol L^{-1}), 0.4 μL of each forward and reverse primer (10 μmol L^{-1}), 30 ng DNA template, and 0.75 U Ex Taq DNA polymerase and the rest being double-distilled water (ddH_2O) to reach a certain volume. The reaction procedure was as follows: pre-degeneration at 94°C for 4 min, degeneration at 94°C for 1 min, renaturation at 55°C for 45 s, extension at 72°C for 2 min, 30 circulations, and extension at 72°C for 10 min. We analyzed the amplification products using 1.0% agarose gels. DNA Fragment Purification Kit was used to purify a 1.5 kb target fragment. The purified products were sequenced by TinyGene Bio-Tech (shanghai) Co., Ltd. The genes of close strains were obtained by the comparative analysis of the DNA sequencing results with GenBank. Phylogenetic trees were constructed using the neighbor-joining method in MEGA3.1.

Corn compensatory growth of drought stress rewatering

A pot experiment was performed under rain–shelter conditions at the Henan University of Science and Technology, Luoyang City, Henan Province, China, and the results showed an average annual rainfall of 601 mm, an average annual temperature of 14.2°C, and average annual sunshine of 2,204.9 h. The corn (*Zea mays* L.) variety "Zhengdan 958" was used in the present study because of its drought resistance and good adaptability. Figure 1 displays the trial time course, treatment setting, and related indicators measured. On 5 June 2021, 200 plastic pots, which had a mouth diameter of 21.5 cm and a pot height of 20.0 cm, were planted with 15 corn seeds each. Each pot contained about 5.8 kg of soil with an organic carbon content of 24.7 g/kg and total nitrogen content of 2.15 g/kg. Corn seedling emergence occurred after about 6 days.

On the 6th day after emergence, thinning was performed in each pot to leave five seedlings that were growing well. In addition, 90 pots with well-growing seedlings were selected for the study. The 90 pots were evenly divided into four groups with 15 pots each, corresponding to the six experimental treatments in the present study: (1) wet (WT), (2) wet with AOB strain inoculation during wetness (WI), (3) wet with AOB strain inoculation during rewatering (WR), (4) post-drought rewatering (DT), (5) post-drought rewatering with AOB strain inoculation during wetness (DI), and (6) post-drought rewatering with AOB strain inoculation during rewatering (DR). The 15 pots in each treatment were divided into five subgroups with three pots each. The three pots in each subgroup were the three replicates for each treatment during each measurement.

The 10-day growth period of wetness was from the 11th to the 22nd day after emergence. On the first day of the wet period, 200 ml of purified AOB culture (216090 cfu·ml^{-1}) was added to the soils of DI and WI treatments to inoculate AOB, and 200 ml of liquid medium without AOB was added to the soils of other treatments. On the 6th day of the wet period, the first subgroup in each treatment was picked out to sample the rhizosphere soils that were used for the measurements of AOB stain number. At the end of the wet period, the second subgroup of each treatment was selected to measure the corn biomass, which was used for the measurement of corn water use efficiency.

On the 22nd to 42nd day after emergence, the 10-day growth periods of drought stress and rewatering were established. During the 10-day drought stress period, the drought stress experiment was conducted in the third, fourth, and fifth subgroups in DT, DI, and DR treatments. In addition, the third, fourth, and fifth subgroups of WT, WI, and WR treatments remained wet. At the end of the drought period,

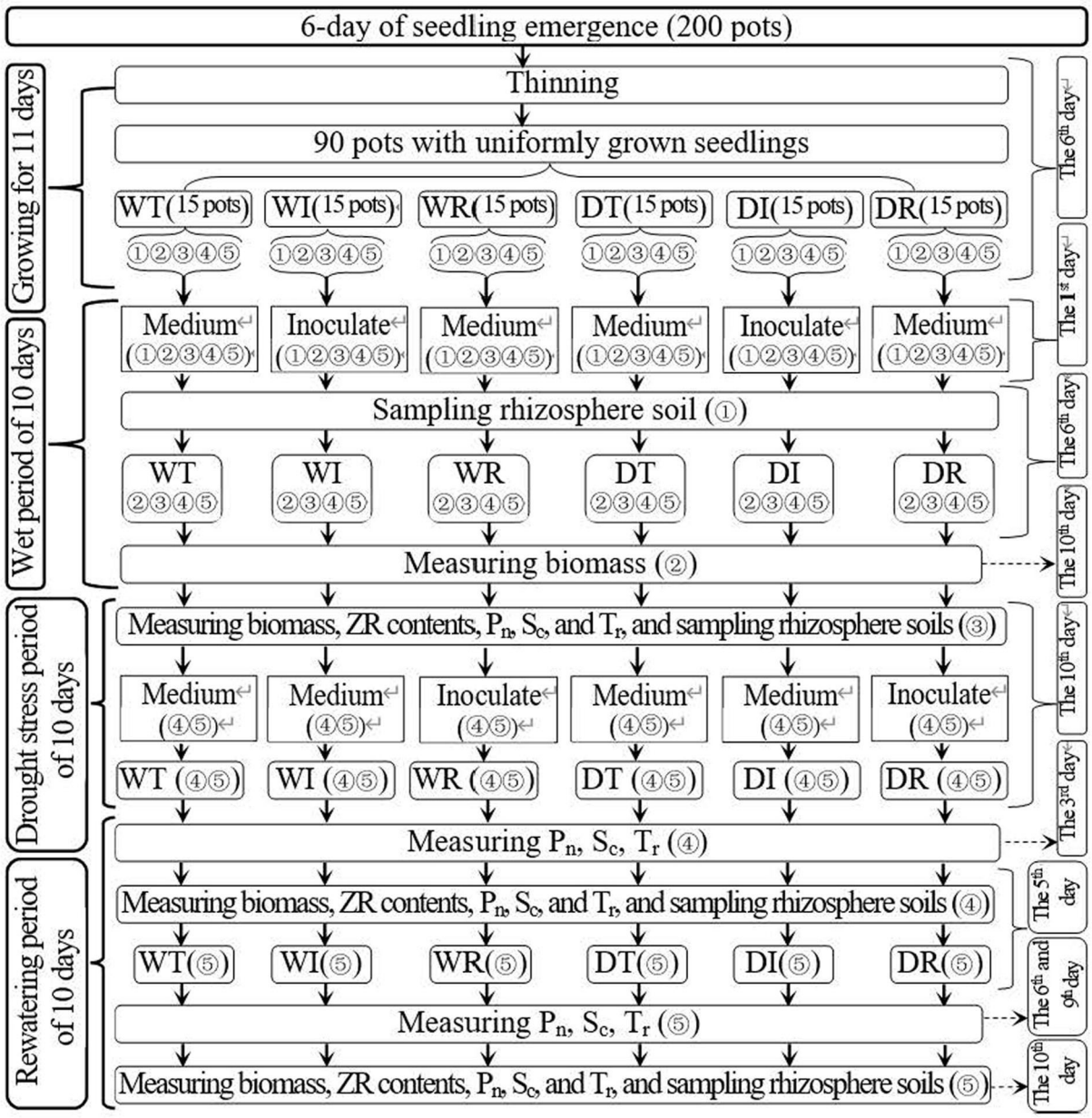

FIGURE 1
Schematic diagram for the experimental design. WT, WI, WR, DT, DI, and DR indicate treatments of wetness, wetness with AOB strain inoculation during wet period, wetness with AOB strain inoculation during rewatering period, post-drought rewatering, post-drought rewatering with AOB strain inoculation during wet period, post-drought rewatering with AOB strain inoculation during rewatering period, respectively. "①", "②", "③", "④", and "⑤" show the first, second, third, fourth, and fifth subgroups of each treatment, respectively. Pn, Sc, and Tr represent the net photosynthetic rate, stomatal conductance, and transpiration rate, respectively. "Inoculate" and "Medium" represent adding AOB stain solution and liquid medium without AOB, respectively.

corn biomass, zeatin riboside (ZR) content, net photosynthetic rate (P_n), transpiration rate (T_r), and stomatal conductance (S_c) were measured in the third subgroup of each treatment, and rhizosphere soils that were used for the measurement of soil nitrification rate, soil NH_4^+, and NO_3^- contents and AOB stain number were also sampled.

In the next 10 days of the rewatering period, all groups maintained wetness. At the beginning of the rewatering period, approximately 200 ml of purified AOB culture (216090 cfu·ml^{-1}) was added to the soils in the fourth and fifth subgroups of DR and WR treatments, and 200 ml of liquid medium without AOB was added to the soils in the fourth

and fifth subgroups of other treatment groups. At 5 and 10 days after rewatering, corn biomass and ZR content were measured in the fourth and fifth subgroups of each treatment group, and rhizosphere soils were sampled. At 3 days after rewatering, P_n, T_r, and S_c were measured in the fourth subgroup of each treatment. The same procedure was performed in the fifth subgroup of each treatment group on days 6 and 9 after rewatering.

Water was applied in pots with a soil water content below 50% of the field capacity to maintain 50–55% of the field capacity. Consequently, drought stress was obtained. Similarly, the soil water content was maintained at 75–80% of the field capacity by adding water. Then, wetness was obtained. In the study of Wang et al. (2018b), the soil water contents are calculated using Formula (1):

$$SWC = \frac{B_t - B_d - B_e - B_p}{B_d \times FWC} \times 100\% \quad (1)$$

where SWC, B_t, B_d, B_e, B_p, and FWC are the soil water content, temporary whole pot weight, net dried soil weight, empty pot weight, estimated fresh weight of all plants, and field water capacity in each pot, respectively. B_p was determined on extra pots early.

Measurements and data analysis

Biomass, photosynthesis, soil nitrification, and zeatin riboside

The roots were washed with water to remove soil. The roots, stems, and leaves were dried for 72 h at 65°C to obtain dry matter. The aboveground and total biomasses were the sums of dry matters of the stem and leaf, and root, stem, and leaf, respectively. Water used throughout the drought stress and rewatering periods was divided by the total biomass increase to calculate the water use efficiency. The difference in total biomass between the start of the drought stress period and the end of the rewatering period was used to calculate the total biomass increase. Water use was calculated by adding water throughout the drought stress and rewatering periods. LI-6400 photosynthesis equipment was used at 11:00 am to measure P_n, T_r, and G_s.

Soil NH_4^+ and NO_3^- contents were measured using the indophenol blue method and phenol disulfonic acid colorimetry, respectively (Lu, 1999). Soil samples that retained 60% water content of the field capacity were cultured for 7 days at 25°C to determine the soil net nitrification rate. The differences in soil NO_3^- content before and after culturing were divided by 7 days to obtain the daily soil net nitrification rate. Soil organic carbon (SOC) contents in rhizosphere soils were determined by the potassium dichromate outside heating method (Lu, 1999).

The corns were clipped at the stem base. Then, 1.0 g absorbent cotton was used to cover the wounds to absorb the xylem sap for 12 h. The xylem sap volume was obtained by dividing the cotton weight increase by 1 g/cm^3. The cotton was compacted, and the saps were squeezed out. The saps were collected for the measurement of the ZR concentration. Enzyme-linked immunosorbent assay was used for the measurement of the ZR content in the leaf and xylem saps (C_{ZR}) in accordance with the method of Qin and Wang (2020). The ZR content in the xylem saps that were collected per hour was used to express the ZR delivery rate from the roots to the leaves (R_{ZR}).

Quantitative real-time PCR and analysis

The total DNA of the soil genome was extracted from rhizosphere soil samples using the MO-BIO PowerSoil DNA Isolation Kit and used as a template for PCR amplification. The specific primers F (5′-ATGTACTGCGCTCAAATCCGA-3′), R (5′-ATGATGAAGGCAAAACCACGAT-3′), and probe P (5′-FAM-ACAACGCAGAAGTCGCACGGAAG-BHQ1-3′) of S2_8_1 were used for the PCR amplification of genomic DNA targeting the gene of S2_8_1, which was obtained by 16Sr DNA amplification in "2.1.1.3 Identification of AOB strains." The 25 μL of reaction system contained the following: 12.5 μL of Premix Ex Taq (qPCR probe) (2×), 0.5 μL of forward primer F (10 μM), 0.5 μL of reverse primer R (10 μM), 0.5 μL of probe (10 μM), 5 μL of DNA template, and 6 μL of ddH_2O. The reaction conditions were pre-denaturation at 95 °C for 30 s, denaturation at 95 °C for 10 s, annealing at 60 °C for 45 s, and recycling for 45 times. Each soil sample was tested three times. The extracted total DNA of the soil genome was amplified, and the Ct value of the sample obtained by quantitative fluorescence PCR was introduced into the standard curve equation to calculate the copy number of S2_8_1 (copies/g) in the rhizosphere soil of maize. The copy number was used to indicate the bacterial number.

The specific primers of S2_8_1 were amplified using PCR to construct the standard curve. The amplified products were purified, and the plasmids were constructed and transformed into *Escherichia coli* competent cells. The *E. coli* containing the target gene plasmid in the clone library was cultured in a shake flask at 37°C. The plasmid was extracted by Axygen Plasmid Miniprep Kit (Axygen) kit. The plasmid concentration was determined by Qubit 3.0 (Life Biotech), and the copy number of the plasmid was calculated. The gradient dilution results of the standard plasmid were as follows (5–7 points were generally diluted, and the points with good qPCR were selected as the standard curves): 5.86×10^5, 5.86×10^4, 5.86×10^3, 5.86×10^2, and 5.86 copies/μL. Five standard samples with different concentrations were subjected to quantitative fluorescence detection to establish a linear relationship between the Ct value and the concentration of S2_8_1 strain in corn rhizosphere soil. The abbreviations used in the text are summarized in Table 1. All values given in the figure are average values. The general linear

TABLE 1 Symbol definition.

Symbol	Definition	Symbol	Definition
AOB	Ammonia oxidizing bacteria	B_t	Temporary whole pot weight
S2_8_1	The AOB strains	B_d	Net dried soil weight
NO_3^-	Soil nitrate nitrogen	B_e	Empty pot weight
NH_4^+	Soil ammonium nitrogen	B_p	Estimated fresh weight of all plants
WT	Wetness	ZR	Zeatin riboside
WI	Wetness with AOB strain inoculation during wet period	R_{ZR}	Delivery rate of ZR from roots to leaves
WR	Wetness with AOB strain inoculation during rewatering period	C_{ZR}	ZR concentration in xylem sap
DT	Post-drought rewatering	P_n	Photosynthetic rate
DI	Post-drought rewatering with AOB strain inoculation during wet period	S_c	Stomatal conductance
DR	Post-drought rewatering with AOB strain inoculation during rewatering period	T_r	Transpiration rate
SWC	Soil water content	SOC	Soil organic carbon
FWC	Field water capacity	PCR	Polymerase chain reaction

model in SPSS 23 was used to conduct a one-way analysis of variance followed by Dunnett's test at the 0.05 probability level.

Results

Isolation and screening of soil AOB strain

The AOB strain S2_8_1 was isolated and screened in the present study. As shown in Figure 2, it belongs to *Ensifer* and has 100% similarity to *Ensifer sesbaniae*. Colonies appeared at 4–6 and 1–2 days after the inoculation of S2_8_1 into the separation and LB media, respectively (Figures 3A,B). The growth potential of S2_8_1 was higher in the LB medium than in the separation medium, which showed that the S2_8_1 had mixed nutritional characteristics and was inclined to be heterotrophic. On the AOB separation medium, the colonies of S2_8_1 appeared milky white and round with an irregular edge and smooth surface (Figure 3A). The S2_8_1 bacterium was 1.09-μm long and 0.54 μm wide and had a shape similar like a short bar under the microscope (Figure 3C). The soil nitrification rate was 10.89 and 5.89 mg/kg•d in soils with and without S2_8_1 added, respectively; and it was 1.85 times higher in soil with S2_8_1 added than that without S2_8_1 added. Therefore, S2_8_1 greatly increased the soil nitrification rate.

Biomass

The aboveground and total biomasses were significantly higher in WI and DI than in other treatments at the end of the wet period, and were significantly higher in WT than in DT, in WI than in DI, and in WR than in DR on day 0 after rewatering (Figure 4). These results showed that drought stress inhibited corn growth, whereas the inoculation of S2_8_1 during wet and drought stress periods increased corn growth. On the 10th day post-rewatering, similar aboveground and total biomasses were observed between WT and DT, and between WI and DI, and significantly higher total biomasses were observed in DR compared with WR. Therefore, rewatering increased corn growth. The total biomasses in DR on the 10th-day post-rewatering were 1.75, 1.79, and 1.43 times higher than those in WT, DT, and DI, respectively. Similarly, the total biomass in DI was 1.22 and 1.25 times higher than those in WT and DT, respectively. Thus, the inoculation of S2_8_1 during rewatering or wetness enhanced the growth of rewatering corn, but the inoculation during rewatering had a larger promotional effect than that during wetness.

The water use efficiencies in DR were 3.16, 2.82, 1.75, 2.09, and 1.72 times higher than those in WT, WI, WR, DT, and DI, respectively. The values were 1.84, 1.65, and 1.22 times higher in DI than those in WT, WI, and DT, respectively. In addition, water use efficiency was 1.51 times higher in DT than that in WT. Therefore, the inoculation of S2_8_1 during rewatering had the largest promotional effect on promoting water use, followed by the inoculation of S2_8_1 during wetness. Simple rewatering had the smallest effect.

Photosynthetic characteristics

Before rewatering, significantly higher values of P_n, T_r, and S_c were observed in WT than in DT, in WI than in DI, and in WR than in DR, which showed that drought stress restrained the photosynthesis of corn (Figure 5). The value of P_n was significantly higher in DI and DR than in WT on the third, sixth, and 9th days after rewatering, in DT than in WT on the third and 6th days after rewatering, and in DI and DR than in DT on the 6 and 9th days after rewatering. S_c was significantly higher in DR than in DT and in WR than in WT on the third and 6th days after rewatering; it was significantly

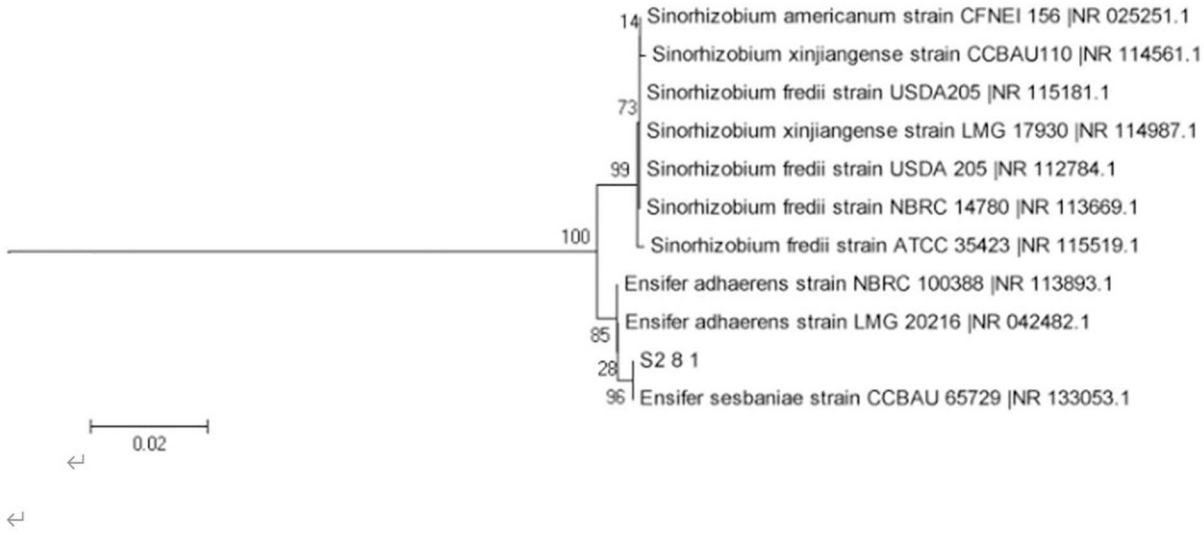

FIGURE 2
Phylogenetic tree based on the 16S rDNA sequence of 1 AOB strain. The S2_8_1 in the figure is the strain that has been isolated and screened in the present study.

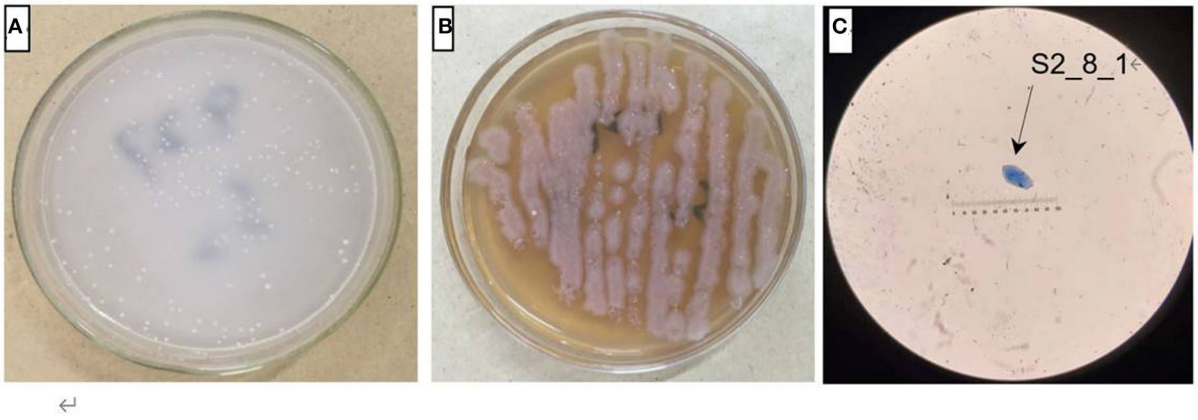

FIGURE 3
Cell and colonial morphology of strain S2_8_1. The S2_8_1 was the strain that has been isolated and screened in the present study. **(A,B)** showed the morphology characteristics of cell and colony of strain S2_8_1 in separation and LB mediums, respectively. **(C)** showed the size and sharp of strain S2_8_1, respectively.

higher in DR than in DT and in WR than in WT on the third and 6th days after rewatering. T_r was significantly higher in DT than in WT on the 6th day after rewatering, in DI and DR than in DT on the 9th day after rewatering, and in WI and WR than in WT on the 6th and 9th days after rewatering. These results showed that rewatering and inoculation of S2_8_1 improved photosynthesis.

The inoculation of S2_8_1 during rewatering had a larger promotional effect on photosynthesis than that before drought stress because significantly higher P_n was observed in DR than in DI on the 6th and 9th days after rewatering, and significantly higher T_r and S_c were noticed in DR than in DI on the 6th day after rewatering.

ZR, soil nitrification rate, soil NO_3^-, and NH_4^+ contents

Before rewatering, the leaf ZR content, R_{ZR}, and C_{ZR} of WT, WI, and WR significantly increased compared with those in DT, DI, and DR, respectively (Figure 6). Thus, drought stress

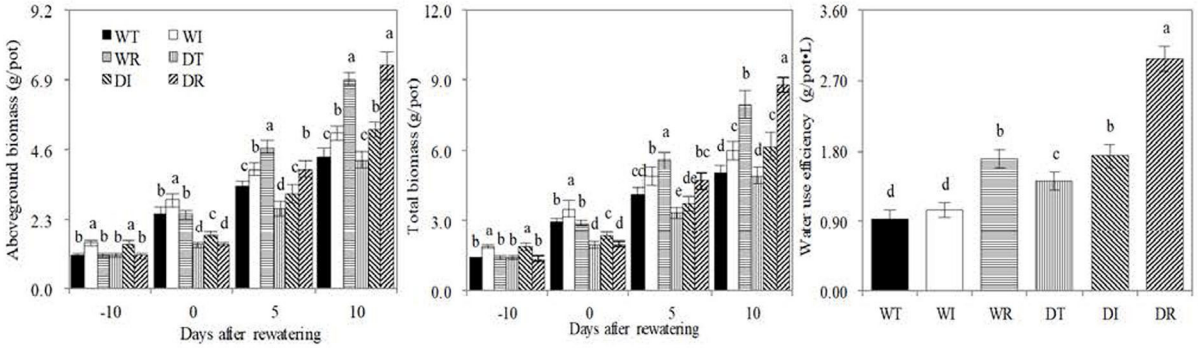

FIGURE 4
Biomass, water use efficiency in the different treatments in the study. WT, WI, WR, DT, DI, and DR indicate treatments of wetness, wetness with AOB strain inoculation during wet period, wetness with AOB strain inoculation during rewatering period, post-drought rewatering, post-drought rewatering with AOB strain inoculation during wet period, post-drought rewatering with AOB strain inoculation during rewatering period, respectively. In "−10" means the 10th day before the beginning of rewatering, namely the end of the wet period. In "0", "5", and "10" respectively stand for the beginning, 5th, 10th days of the 10-day rewatering period. The values are the mean ± standard error ($n = 3$). The different letters in each row indicate significant differences ($P < 0.05$).

decreased leaf cytokinin contents and delivery rates from the roots to the leaves. ZR is one of the major cytokinin forms. On the contrary, rewatering reversed this trend, with significant increases in the leaf ZR content found in DI compared with WI on the 5th day after rewatering and in DT and DR compared with WT and WR on the 10th day after rewatering, respectively. Non-significant lower R_{ZR} and C_{ZR} values were found in DT, DI, and DR than in WT, WI, and WR, respectively. In addition, the leaf ZR content and R_{ZR} were significantly higher in DR and DI than in WT and DT on the 5th or 10th days, which showed that S2_8_1 caused an increase in these indices of rewatering corn. The leaf ZR content was significantly higher in DR than in DI on the 10th day after rewatering. Therefore, the inoculation of S2_8_1 during rewatering had a larger promotional effect on leaf ZR content compared with inoculation during wetness.

As shown in Figure 7, significant increases in rhizosphere soil nitrification rates were observed in the WT compared with DT and in WR compared with DR before rewatering, which indicated that drought stress inhibited rhizosphere soil nitrification. On days 5 and 10 after rewatering, significantly higher rhizosphere soil nitrification rates were found in DT than in WT, in DR and DI than in DT, and in WI and WR than in WT. Therefore, rewatering and S2_8_1 inoculation promoted rhizosphere soil nitrification. Significantly higher soil nitrification rates in the rhizosphere environments were detected in DR than in DI on the 10th after rewatering, which indicated that the larger promotional effect on the nitrification rate occurred when inoculating during rewatering than during wetness. During the rewatering period, irregular results, that is, by chance, were observed in rhizosphere soil NO_3^- and NH_4^+ contents. Thus, the inoculation of S2_8_1 could not increase their contents.

Strain number and SOC content in rhizosphere soil

The copy number of S2_8_1 in rhizosphere soil was significantly higher in DI and WI than in WT, WR, DT, and DR during the wet period (Figure 8). Similarly, the copy number of S2_8_1 in DR and WR increased significantly compared with those in WT and DT during the rewatering period. Therefore, the inoculation of S2_8_1 increased its number in rhizosphere soil. The copy number of S2_8_1 was significantly higher in DR than in DI on day 10 after rewatering, which showed that inoculation during rewatering was more apt to increase the S2_8_1 amount in rhizosphere soil than inoculation during wetness. The copy number in WI was similar to that in DI during the wet period but was 1.5 times higher than that in DI at the end of the drought period. Thus, drought stress decreased the abundance of S2_8_1 in the rhizosphere soil. On the contrary, copy numbers of DI and DR were 1.4 and 2.7 times higher than that of WI and WR on day 10 after rewatering, respectively, which showed that rewatering increased the abundance of S2_8_1 in the rhizosphere soil.

Rhizosphere SOC contents were significantly higher in DT, DI, and DR than in WT, in DI than in WI, and in DR than in WR on days 0 and 5 after rewatering. Therefore, drought stress increased the rhizosphere SOC contents, and their lag effect continued until the rewatering period. On day 10 after rewatering, the rhizosphere SOC contents were significantly higher in DI and DR than in WT, WI, and WR, but similar SOC contents were observed between DT and WT. These results showed that rewatering corn used rhizosphere SOC. However, rewatering corn with S2_8_1 inoculation relatively maintained SOC stability.

10.3389/fpls.2022.947476

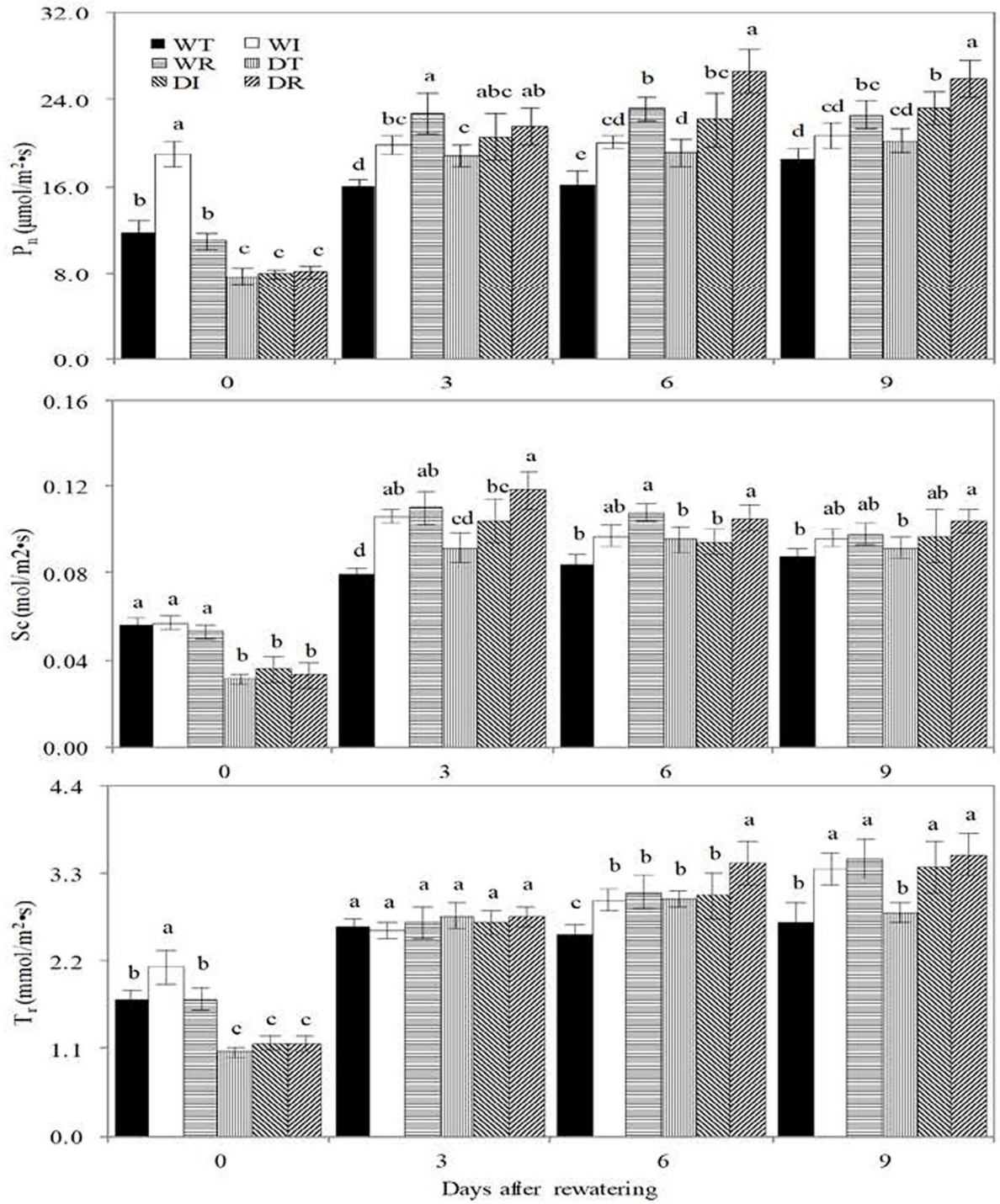

FIGURE 5
Biomass, water use efficiency in the different treatments in the study. WT, WI, WR, DT, DI, and DR indicate treatments of wetness, wetness with AOB strain inoculation during wet period, wetness with AOB strain inoculation during rewatering period, post-drought rewatering, post-drought rewatering with AOB strain inoculation during wet period, post-drought rewatering with AOB strain inoculation during rewatering period, respectively. In "0", "3", "6" and "9" respectively stand for the beginning, 3rd day, 6th day, 9th day of the 9-day rewatering period. Pn, Sc, and Tr represent the net photosynthetic rate, conductance, and transpiration rate, respectively. The values are the mean ± standard error ($n = 3$). The different letters in each row indicate significant differences ($P < 0.05$).

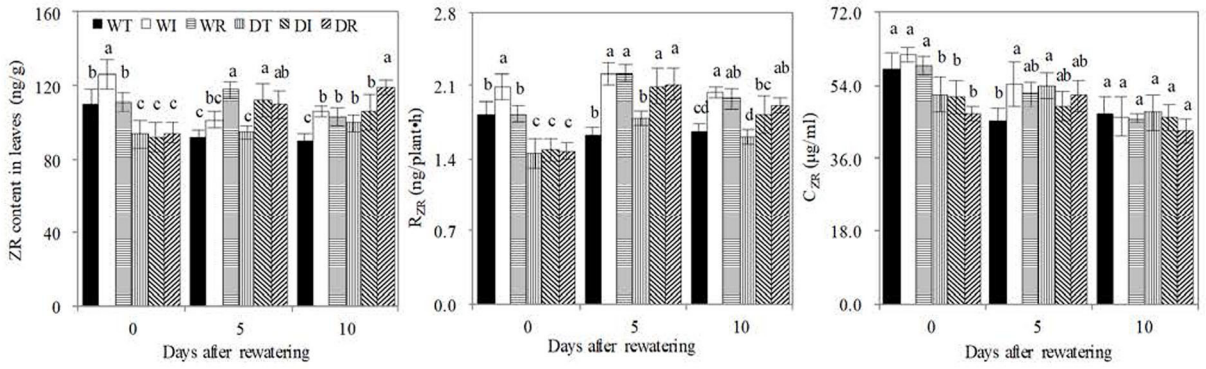

FIGURE 6
ZR, RZR, and CZR concentrations in the newly grown leaves. WT, WI, WR, DT, DI, and DR indicate treatments of wetness, wetness with AOB strain inoculation during wet period, wetness with AOB strain inoculation during rewatering period, post-drought rewatering, post-drought rewatering with AOB strain inoculation during wet period, post-drought rewatering with AOB strain inoculation during rewatering period, respectively. In "0", "5", and "10" respectively stand for the beginning, 5th day, 10th day of the 10-day rewatering period. CZR mean ZR concentrations in xylem sap. RZR mean delivery rates of ZR from roots to leaves, respectively. The values are the mean ± standard error ($n = 3$). The different letters in each row indicate significant differences ($P < 0.05$).

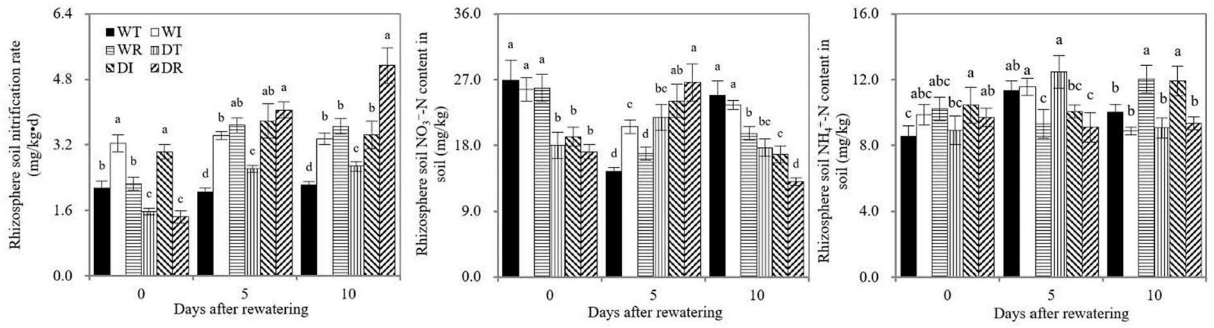

FIGURE 7
Soil nitrification rate, soil ammonium and nitrate nitrogen contents in the study. WT, WI, WR, DT, DI, and DR indicate treatments of wetness, wetness with AOB strain inoculation during wet period, wetness with AOB strain inoculation during rewatering period, post-drought rewatering, post-drought rewatering with AOB strain inoculation during wet period, post-drought rewatering with AOB strain inoculation during rewatering period, respectively. In "0", "5", and "10" respectively stand for the beginning, 5th day, 10th day of the rewatering period of 10 days. The values are the mean ± standard error ($n = 3$). The different letters in each row indicate significant differences ($P < 0.05$).

Discussion

Coexistence of S2_8_1 and corn

In the present study, a stable coexisting relationship was found between corn and S2_8_1 in DI. Based on the copy number of S2_8_1 in rhizosphere soil, the inoculation of S2_8_1 in DI during wetness caused some of it to colonize in rhizosphere soil. Then drought stress decreased the abundance of S2_8_1 in rhizosphere soil, but rewatering greatly increased its abundance. In addition, S2_8_1 increased corn growth during the continued growth periods of wetness, drought stress, and rewatering.

Soil AOB comprise autotrophic, heterotrophic, and mixotrophic AOB (Taylor et al., 2009; Kouki et al., 2011; Matsuno et al., 2013). The present study isolated and screened the AOB strain S2_8_1, which belongs to *Ensifer* and has mixotrophic characteristics, but is inclined to be heterotrophic. Preece et al. (2018) and Gargallo-Garriga et al. (2018) reported that growing heterotrophic AOB use organic substances as the substrate. Carbon is the chief element of organic compounds, and SOC may represent the amount of organic compounds in the soil (Zhao et al., 2021). High rhizosphere SOC in DI and DR caused the increase in S2_8_1 abundance compared with WI and WR during the rewatering period, respectively. On day 10 after rewatering, more S2_8_1 were observed in DR compared with those in DI. The explanation for this was that given its S2_8_1 content being 216090 cfu·ml^{-1}, the 200 ml of inoculation solution had a large number of S2_8_1. Therefore, under the condition of considerable rhizosphere organic substances caused by drought stress, more S2_8_1 easily colonized the

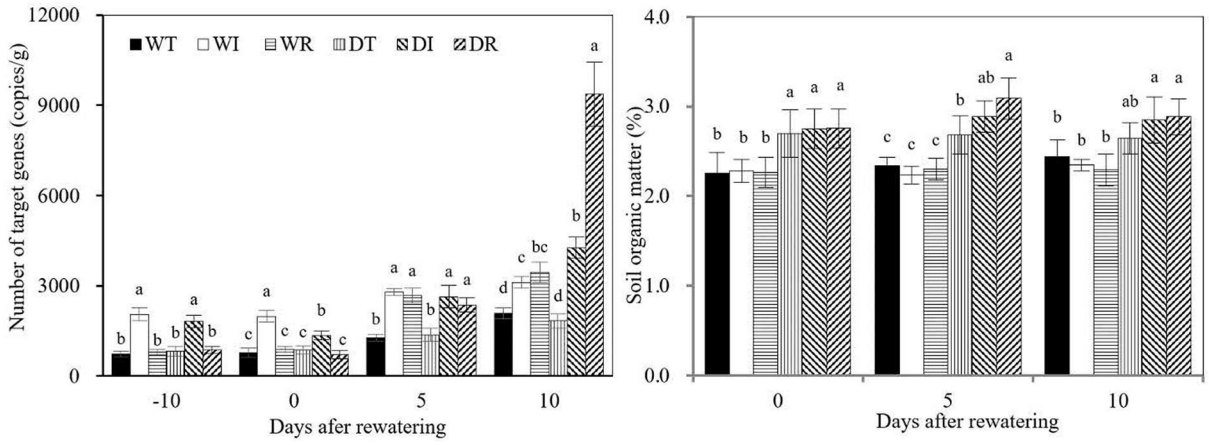

FIGURE 8
S2_8_1 number in rhizosphere soil and soil organic matter in the study. WT, WI, WR, DT, DI, and DR indicate treatments of wetness, wetness with AOB strain inoculation during wet period, wetness with AOB strain inoculation during rewatering period, post-drought rewatering, post-drought rewatering with AOB strain inoculation during wet period, post-drought rewatering with AOB strain inoculation during rewatering period, respectively. In "−10" means the 10th day before the beginning of rewatering, namely the end of the wet period. In "0", "5", and "10" respectively stand for the beginning, 5th day, 10th day of the rewatering period of 10 days. The values are the mean ± standard error ($n = 3$). The different letters in each row indicate significant differences ($P < 0.05$).

rhizosphere micro-environment in DR compared with DI during the rewatering period. This finding further shows that rhizosphere soil organic matter was the key factor promoting S2_8_1 to colonize in the rhizosphere micro-environment.

Carbon compounds, namely, carbohydrates, organic acids, and alcohol, are secreted by plant roots into the rhizosphere soil under drought stress (Karlowsky et al., 2018; Calvo et al., 2019; De Vries et al., 2020). In the present study, the high SOC content in rhizosphere soil in DI, DR, and DT during the rewatering period was mainly because drought stress stimulated the release of a number of carbon compounds into rhizosphere soil and exerted a lag effect. As a result, rewatering increased the abundance of S2_8_1 in the rhizosphere soil in DI and DR. On the contrary, during the wet period, the relatively low rhizosphere SOC caused less colonization by the S2_8_1 strains compared with the rewatering period. Because the copy number of S2_8_1 of rhizosphere soil in DI was 2.3 times higher at the end of the rewatering period than that at the end of the wet period. During the drought stress period, although a high rhizosphere SOC was observed in the treatments of DI, the lack of water decreased the abundance of S2_8_1 compared with the rewatering period.

The S2_8_1 in the DI and DR during the rewatering period increased corn growth because on day 10 after rewatering, the total biomass of DI equaled that of WI, and it increased by 11% than in DR than in WR. As a result, compensatory and over-compensatory growths occurred in DI and DR, respectively. Compensatory and over-compensatory growths in DI and DR caused water use to increase greatly, as shown by the water use efficiencies which were 2.04 and 3.16 times higher in DI and DR than in WT, respectively, throughout the drought stress and rewatering periods. The high number of S2_8_1 in the rhizosphere soil increased the total biomass and water use efficiency in the DR by 1.43 and 1.56 times compared with those in DI on day 10 after rewatering, respectively, which further demonstrated the role of S2_8_1 in corn rewatering growth and water use. High total biomass in DI compared with DT during wet and drought stress periods showed that the presence of S2_8_1 increased corn growth in these periods.

Root–shoot signaling of cytokinins

The present results revealed that the coexistence of S2_8_1 with corn in DI continuously increased the amount of root cytokinin delivered to leaves, thus improving corn rewatering growth and water use.

S2_8_1 caused the high rhizosphere soil nitrification rates in DI compared with DT or WT during rewatering because AOB are the main bacteria involved in soil nitrification. High rhizosphere soil nitrification rate caused the continuous release of more NO_3^- from the soil during the rewatering period, increasing the stimulation by NO_3^- in the roots. Soil NO_3^- can stimulate roots to synthesize cytokinins in various plants (Landrein et al., 2018; Poitout et al., 2018). As a result, more root cytokinins are synthesized and continuously delivered to increase the leaf cytokinin content in the DI. Cytokinins synthesized in the roots can be transmitted to the leaves by means of the xylem sap (Zaicovski et al., 2008; Wang et al., 2016). R_{ZR} indicates the delivery speed of cytokinins from roots to leaves in the darkness. The high R_{ZR} in DI compared with DT and WT during the rewatering period demonstrated the

additional cytokinins being synthesized and delivered to the leaves in darkness. The cytokinin delivery rate to the leaves in the presence of sunlight was the product of T_r and C_{ZR}, and transpiration drove the sap to transmit from roots to leaves under this condition. More cytokinins were synthesized and delivered to the leaves in DI compared with DT and WT in sunlight during the rewatering period. Similar C_{ZR} but high T_r were present in DI compared with DT and WT during the rewatering period.

Similarly, the higher number of S2_8_1 in DI compared with WI and in DR compared with WR, WT, and DT all caused the high rhizosphere soil nitrification rate, increased synthesis of root cytokinin and delivery to leaves, and rapid corn growth during the rewatering period. Wang et al. (2020a) reported a higher rhizosphere soil nitrification rate in corns after post-drought rewatering compared with wet corns. It was likewise that rewatering increased the rhizosphere soil nitrification rates of DT compared with WT in the present study. This condition caused more cytokinins to be delivered in DT compared with WT during the rewatering period, increasing the leaf cytokinin content and corn growth. Thus, compensatory growth and high water use efficiency occurred in DT compared with WT.

The similar copy numbers of S2_8_1 in WT and DT contributed less to the result of high rhizosphere soil nitrification rate in DT compared with WT during the rewatering period. Because no inoculation caused the low number of S2_8_1 in the rhizosphere soil of WT and DT; thus, it was hard to detect accurately. The potential role of heterotrophic AOB on the rhizosphere soil of post-drought rewatering crops required further investigation in the future.

The high leaf cytokinin content in DI during rewatering was beneficial for the increase in leaf P_n compared with DT, WI, and WT. Cytokinin plays a promotional role in photosynthesis (Kobayashi et al., 2012; De Moura et al., 2017). The occurrence of high P_n in DI compared with DT during rewatering led to compensatory growth as corn growth after rewatering was mainly involved in the fast photosynthetic organic matter accumulation. Similarly, given the high leaf P_n caused by cytokinin, compensatory and over-compensatory growths occurred in DT and DR, respectively.

In the study of Takei et al. (2001) on maize seedlings, cytokinins played essential roles in the plant response to nitrate, where they acted as secondary messengers in plants. Wang et al. (2020b) observed that root-originated cytokinins induced by the continued addition of NO_3^- caused the compensatory growth of post-drought rewatering due to its short duration in soil. The continuous delivery of cytokinins from roots to leaves is significant in corn compensatory growth, and the repeated addition of NO_3^- is an effective method to achieve this goal. However, the present study revealed that the coexistence of S2_8_1 with corn increased its compensatory growth in post-drought rewatering by inducing root cytokinin delivery to the leaves continuously.

The low increase effect of S2_8_1 on corn growth was observed in DI compared with DR. However, S2_8_1 coexistence with corn in DI showed significance for the feasibility of the technique when using soil heterotrophic AOB strains, which were isolated from soil similar to the present study in crop water use. Rainwater is the water source of crops in dry farming; most rainfall entering into soils is a process of post-drought rewatering (Barker, 2017; Preethi et al., 2020). However, the uncertainty of rainfall causes the difficult inoculation of soil heterotrophic AOB strains with crops of drying farms before raining. Similar to S2_8_1, the inoculation of soil heterotrophic AOB after emergence would cause coexistence with the crop, which would increase rainfall use in a timely manner. Similarly, most crop irrigation is also a process of post-drought rewatering. The irrigation is usually accompanied by nitrogen fertilizer application to increase the crop water use efficiency (Tao et al., 2021; Zain et al., 2021). The coexistence of soil heterotrophic AOB with crops can increase the timely irrigation water use, which plays a potential role in replacing nitrogen fertilizer. For the application of our findings in the present study, field experiments should further be carried out based on our experimental results.

Conclusion

The inoculation of S2_8_1 during wetness caused it to colonize the rhizosphere soil. Drought stress decreased its abundance, but rewatering greatly increased its abundance in rhizosphere soil. The S2_8_1 in rhizosphere soil during rewatering increased the soil nitrification rates, which played an important role in cytokinin synthesis in the roots and its delivery to the leaves. As a result, the cytokinin concentration in the leaves increased. The increase in corn leaf cytokinin caused by rewatering increased the photosynthetic rate, resulting in over-compensatory growth after post-drought rewatering and high water use efficiency. Thus, the coexistence of AOB strains with corn in rhizosphere soil increased corn compensatory growth by regulating soil nitrification and root-induced leaf cytokinin. Our findings are beneficial for developing strategies to increase crop water use.

Data availability statement

The original contributions presented in the study are publicly available. This data can be found here: NCBI, ON667919.

Author contributions

X-LW devised the project and supervised it. KM, Y-HL, LQ, and L-XZ conducted the experiments. PS, JS, and X-LL

performed the isolation and screening of soil ammonia-oxidizing bacteria strains. WL analyzed the data. KM and LQ prepared the figures and wrote the manuscript.

Funding

This work was funded by the National Natural Science Foundation of China (U1304326) and the Excellent Youth Foundation of Henan Scientific Committee (174100510004).

Acknowledgments

We would like to thank You-Fu Zhang and Wei Zhao for their technical assistance during this study.

Conflict of interest

The authors declare that the research was conducted in the absence of any commercial or financial relationships that could be construed as a potential conflict of interest.

Publisher's note

References

Ali, S., Xu, Y. Y., Ahmad, I., Jia, Q. M., Ma, X. C., Sohail, A., et al. (2019). The ridge-furrow system combined with supplemental irrigation strategies to improves radiation use efficiency and winter wheat productivity in semi-arid regions of China. *Agric. Water Manage.* 213, 76–86. doi: 10.1016/j.agwat.2018.10.006

Barker, G. (2017). Traditional arid lands agriculture: understanding the past for the future. *Environ. Archaeol.* 25, 445–446. doi: 10.1080/14614103.2017.1319530

Belsky, A. J. (1986). Does herbivory benefit plants—a review of the evidence. *Am. Nat.* 127, 870–892. doi: 10.1086/284531

Bland, A., Maider, A., and Clark, I. M. (2021). Quantification of ammonia oxidizing bacterial abundances in environmental samples by quantitative-PCR. *Methods Mol. Biol.* 2232, 135–146. doi: 10.1007/978-1-0716-1040-4_12

Calvo, O. C., Franzaring, J., Schmid, I., and Fangmeier, A. (2019). Root exudation of carbohydrates and cations from barley in response to drought and elevated CO_2. *Plant Soil.* 438, 127–142. doi: 10.1007/s11104-019-03998-y

De Moura, F. B., Da, S., Vieira, M. R., Simões, A. D. N., F., da Silva, S. L., et al. (2017). Participation of cytokinin on gas exchange and antioxidant enzymes activities. *Ind. J. Plant Physiol.* 22, 16–29. doi: 10.1007/s40502-017-0283-2

De Vries, F. T., Griffiths, R. I., Knight, C. G., Nicolitch, O., and Williams, A. (2020). Harnessing rhizosphere microbiomes for drought-resilient crop production. *Science* 368, 270–274. doi: 10.1126/science.aaz5192

Gagné-Bourque, F., Bertrand, A., Claessens, A., Aliferis, K. A., and Jabaji, S. (2016). Alleviation of drought stress and metabolic changes in Timothy (Phleum pratense L.) colonized with Bacillus subtilis B26. *Front. Plant Sci.* 7, 584. doi: 10.3389/fpls.2016.00584

Gargallo-Garriga, A., Preece, C., Sardans, J., Oravec, M., Urban, O., and Peñuelas, J. (2018). Root exudate metabolomes change under drought and show limited capacity for recovery. *Sci. Rep-Uk.* 8, 12696. doi: 10.1038/s41598-018-30150-0

Grogan, P., and Zamin, T. J. (2018). Growth responses of the common arctic graminoid Eriophorum vaginatum to simulated grazing are independent of soil nitrogen availability. *Oecologia* 186, 151–162. doi: 10.1007/s00442-017-3990-5

Karlowsky, S., Augusti, A., Ingrisch, J., Akanda, M. K. U., Bahn, M., and Gleixner, G. (2018). Drought-induced accumulation of root exudates supports post-drought recovery of microbes in mountain grassland. *Front. Plant Sci.* 9, 1593. doi: 10.3389/fpls.2018.01593

Kobayashi, H., Inoue, S., and Gyokusen, K. (2012). Photosynthesis-nitrogen relationship in a Hinoki cypress (Chamaecyparis obtusa) canopy: a comparison with Japanese cedar (Cryptomeria japonica). *Photosynthetica* 50, 317–320. doi: 10.1007/s11099-012-0030-x

Kouki, S., Saidi, N., Mhiri, F., Nasr, H., Cherif, H., Quzari, H., et al. (2011). Isolation and characterization of facultative mixotrophic ammonia-oxidizing bacteria from constructed wetlands. *J. Environ. Sci.* 23, 1699–1708. doi: 10.1016/S1001-0742(10)60596-7

Landrein, B., Formosa-Jordan, P., Malivert, A., Schuster, C., Melnyk, C. W., Yang, W. B., et al. (2018). Nitrate modulates stem cell dynamics in Arabidopsis shoot meristems through cytokinins. *P. Natl. Acad. Sci. USA* 115, 1382–1387. doi: 10.1073/pnas.1718670115

Liu, M., Wang, Z., Mu, L., Xu, R., and Yang, H. (2021). Effect of regulated deficit irrigation on alfalfa performance under two irrigation systems in the inland arid area of midwestern China. *Agric. Water Manage.* 248, 106764. doi: 10.1016/j.agwat.2021.106764

Liu, S. L., Wu, W. B., Yang, X. G., Yang, P., and Sun, J. (2020). Exploring drought dynamics and its impacts on maize yield in the Huang-Huai-Hai farming region of China. *Clim. Change* 163, 415–430. doi: 10.1007/s10584-020-02880-6

Lu, R. K. (1999). *Analysis Method of the Soil Agricultural Chemistry*. Beijing: China Agricultural Science and Technology Press.

Matsuno, T., Horil, S., Sato, T., Matsumiya, Y., and Kubo, M. (2013). Analysis of nitrification in agricultural soil and improvement of nitrogen circulation with autotrophic ammonia-oxidizing bacteria. *Appl. Biochem. Biotech.* 169, 795–809. doi: 10.1007/s12010-012-0029-6

Monokrousos, N., Papatheodorou, E. M., Orfanoudakis, M., Jones, D. G., Scullion, J., and Stamou, G. P. (2020). The effects of plant type, AMF inoculation and water regime on rhizosphere microbial communities. *Eur. J. Soil Sci.* 71, 265–278. doi: 10.1111/ejss.12882

Poitout, A., Crabos, A., Petrík, I., Novak, O., Krouk, G., Lacombe, B., et al. (2018). Responses to systemic nitrogen signaling in Arabidopsis roots involve trans-zeatin in shoots. *Plant Cell* 30, 1243–1257. doi: 10.1105/tpc.18.00011

Preece, C., Farré-Armengol, G., Llusià, J., and Peñuelas, J. (2018). Thirsty tree roots exude more carbon. *Tree Physiol.* 38, 690–695. doi: 10.1093/treephys/tpx163

Preethi, V., Yin, X. Y., Paul, C. S., and Sheshshayee, S. (2020). Responses of lowland, upland and aerobic rice genotypes to water limitation during different phases. *Rice Sci.* 27, 345–354. doi: 10.1016/j.rsci.2020.05.009

Qin, R. R., and Wang, X. L. (2020). Effects of crown height on the compensatory growth of Italian ryegrass based on combined effects of stored organic matter and cytokinin. *Grassl Sci.* 66, 29–39. doi: 10.1111/grs.12243

Shi, J. C., Wu, X., Zhang, M., Wang, X. Y., Zuo, Q., Wu, X. G., et al. (2021). Numerically scheduling plant water deficit index-based smart irrigation to optimize crop yield and water use efficiency. *Agric. Water Manage.* 248, 106774. doi: 10.1016/j.agwat.2021.106774

Takei, K., Sakakibara, H., Taniguchi, M., and Sugiyama, T. (2001). Nitrogen-dependent accumulation of cytokinins in root and thetranslocation to leaf: implication of cytokinin species that induces geneexpression of maize response regulator. *Plant Cell Physiol.* 42, 85–93. doi: 10.1093/pcp/pce009

Tao, Q. B., Bai, M. J., Jia, C. Z., Han, Y. H., and Wang, Y. R. (2021). Effects of irrigation and nitrogen fertilization on seed yield, yield components, and water use efficiency of cleistogenes songorica. *Agronomy-Basel* 11, 466. doi: 10.3390/agronomy11030466

Taylor, S. M., He, Y. L., Zhao, B., and Huang, J. (2009). Heterotrophic ammonium removal characteristics of an aerobic heterotrophic nitrifying denitrifying bacterium, Providencia rettgeri YL. *J. Environ Sci.* 21, 1336–1341. doi: 10.1016/S1001-0742(08)62423-7

Wang, X. L., Duan, P. L., Sun, R. H., Qi, L., Shi, J., Li, X. L., et al. (2020a). Effects of soil nitrification on compensatory growth upon post-drought rewatering of corns based on cytokinin. *Int. J. Agric. Biol.* 23, 882–888. doi: 10.17957/IJAB/15.1365

Wang, X. L., Duan, P. L., Yang, S. J., Liu, Y. H., Qi, L., Shi, J., et al. (2020b). Corn compensatory growth upon post-drought rewatering based on the effects of rhizosphere soil nitrification on cytokinin. *Agric. Water Manage.* 241, 106436. doi: 10.1016/j.agwat.2020.106436

Wang, X. L., Qin, R. R., Sun, R. H., Hou, X. G., Qi, L., and Shi, J. (2018b). Effects of plant population density and root induced cytokinin on the corn compensatory growth during post-drought rewatering. *PLoS ONE* 13, e0198878. doi: 10.1371/journal.pone.0198878

Wang, X. L., Qin, R. R., Sun, R. H., Wang, J. J., Hou, X. G., Qi, L., et al. (2018a). No post-drought compensatory growth of corns with root cutting based on cytokinin induced by roots. *Agric. Water Manage.* 205, 9–20. doi: 10.1016/j.agwat.2018.04.035

Wang, X. L., Sun, R. H., Wu, D., Liu, Y. H., Shi, J., Li, X. L., et al. (2021). Increasing corn compensatory growth upon post-drought rewatering using ammonia-oxidising bacterial strain inoculation. *Agric. Water Manage.* 256, 107066. doi: 10.1016/j.agwat.2021.107066

Wang, X. L., Wang, J. J., Sun, R. H., Hou, X. G., Zhao, W., Shi, J., et al. (2016). Correlation of the corn compensatory growth mechanism after post-drought rewatering with cytokinin induced by root nitrate absorption. *Agr. Water Manage.* 166, 77–85. doi: 10.1016/j.agwat.2015.12.007

Yan, Q. Y., Yang, F., Dong, F., Lu, J. X., Li, F., Duan, Z. Q., et al. (2018). Yield loss compensation effect and water use efficiency of winter wheat under double-blank row mulching and limited irrigation in northern China. *Field Crop Res.* 216, 63–74. doi: 10.1016/j.fcr.2017.11.009

Zaicovski, C. B., Zimmerman, T., Nora, L., Nora, F. R., Silva, J. A., and Rombaldi, C. V. (2008). Water stress increases cytokinin biosynthesis and delays postharvest yellowing of broccoli florets. *Postharvest Biol. Tec.* 49, 436–439. doi: 10.1016/j.postharvbio.2008.02.001

Zain, M., Si, Z. Y., Li, S., Gao, Y., Mehmood, F., Rahman, S. U., et al. (2021). The coupled effects of irrigation scheduling and nitrogen fertilization mode on growth, yield and water use efficiency in drip-irrigated winter wheat. *Sustainability* 13, 2742. doi: 10.3390/su13052742

Zhang, H. B., Han, K., Gu, S. B., and Wang, D. (2019a). Effects of supplemental irrigation on the accumulation, distribution and transportation of ^{13}C-photosynthate, yield and water use efficiency of winter wheat. *Agric. Water Manage.* 214, 1–8. doi: 10.1016/j.agwat.2018.12.028

Zhang, P., Wei, T., Li, Y. L., Zhang, Y., Cai, T., Ren, X. L., et al. (2019b). Effects of deficit irrigation combined with rainwater harvesting planting system on the water use efficiency and maize (Zea mays L.) yield in a semiarid area. *Irri. Sci.* 37, 611–625. doi: 10.1007/s00271-019-00628-4

Zhao, M. S., Qiu, S. Q., Wang, S. H., Li, D. C., and Zhang, G. L. (2021). Spatial-temporal change of soil organic carbon in Anhui Province of East China. *Geoderma Reg.* 26, e00415. doi: 10.1016/j.geodrs.2021.e00415

frontiers | Frontiers in Plant Science

TYPE Original Research
PUBLISHED 29 November 2022
DOI 10.3389/fpls.2022.1037047

OPEN ACCESS

EDITED BY
Bernard Roitberg,
Simon Fraser University, Canada

REVIEWED BY
Monica Kersch-Becker,
The Pennsylvania State University (PSU), United States
Ikkei Shikano,
University of Hawaii at Manoa, United States
Paul J. Ode,
Colorado State University, United States
Christopher J. Frost,
University of Arizona, United States

*CORRESPONDENCE
Carlos Bustos-Segura
bustossc@gmail.com

SPECIALTY SECTION
This article was submitted to Functional Plant Ecology, a section of the journal Frontiers in Plant Science

RECEIVED 05 September 2022
ACCEPTED 17 November 2022
PUBLISHED 29 November 2022

CITATION
Bustos-Segura C, González-Salas R and Benrey B (2022) Early damage enhances compensatory responses to herbivory in wild lima bean. *Front. Plant Sci.* 13:1037047. doi: 10.3389/fpls.2022.1037047

Early damage enhances compensatory responses to herbivory in wild lima bean

Carlos Bustos-Segura*, Raúl González-Salas and Betty Benrey

Laboratory of Evolutionary Entomology, Institute of Biology, University of Neuchâtel, Neuchâtel, Switzerland

Damage by herbivores can induce various defensive responses. Induced resistance comprises traits that can reduced the damage, while compensatory responses reduce the negative effects of damage on plant fitness. Timing of damage may be essential in determining the patterns of induced defenses. Here, we tested how timing and frequency of leaf damage affect compensatory responses in wild lima bean plants in terms of growth and seed output, as well as their effects on induced resistance to seed beetles. To this end, we applied mechanical damage to plants at different ontogenetical stages, at one time point (juvenile stage only) or two time points (seedling and juvenile stage or juvenile and reproductive stage). We found that plants damaged at the seedling/juvenile stage showed higher compensatory growth, and seed output compared to plants damaged only at the juvenile stage or juvenile/reproductive stage. Seeds from plants damaged at the juvenile and juvenile/reproductive stages had fewer beetles than seeds from undamaged plants, however this was driven by a density dependent effect of seed abundance rather than a direct effect of damage treatments. We did not find differences in parasitism rate by parasitoid wasps on seed beetles among plant treatments. Our results show that damage at the seedling stage triggers compensatory responses which implies that tolerance to herbivory is enhanced or primed by early damage. Herbivory often occurs at several time points throughout plant development and this study illustrates that, for a full understanding of the factors associated with plant induced responses in a dynamic biotic environment, it is important to determine the multitrophic consequences of damage at more than one ontogenetical stage.

KEYWORDS

multitrophic interactions, ontogeny, tolerance, defense induction, defense priming, timing of herbivory, seed interactions

Introduction

The nature and magnitude of plant induced responses depend on several factors, such as the type, frequency and timing of damage and herbivore identity (Karban, 2011; Schuman and Baldwin, 2016). Herbivore damage can occur at several times throughout a plant's life, during the same ontogenetical stage or at different stages. However, it is still not fully understood how the timing and frequency of herbivore damage affect the plant's induced defense responses. Induced plant responses to damage comprise plastic traits that help plants increasing their fitness in the presence of natural enemies (Karban and Baldwin, 1997; Baldwin and Preston, 1999). Such responses can be classified as two different strategies, induced resistance and tolerance. Induced resistance includes inducible traits that protect plants from future attacks (Karban, 2011), such as direct defenses, both chemical (e.g. secondary metabolites) and physical (trichomes) defenses, and indirect defenses (volatile compounds and extrafloral nectar), that aid in the recruitment of natural enemies of herbivores (Gatehouse, 2002; Heil and Baldwin, 2002; Turlings and Erb, 2018).

Tolerance to herbivory refers to the plant's response after herbivory to reduce the negative effects of damage on fitness (Strauss and Agrawal, 1999; Núñez-Farfán et al., 2007) and it is the result of compensatory responses which can often be measured as compensatory growth and/or seed production (the ability of a plant to increase its biomass or reproduction after suffering damage). As tolerance involves changes in resource allocation that occur as a response to damage, it is also considered an induced defense (Karban and Myers, 1989). Because resistance and tolerance can be induced by herbivore damage, the time at which damage occurs determines the expression of both strategies. Yet it is still unclear the extent to which the timing of multiple damage events influences the expression of each strategy.

Plants present ontogenetic trajectories consisting of changes in the production and investment of defenses that occur across the developmental stages of the plant (Boege and Marquis, 2005; Barton and Boege, 2017). They are influenced by abiotic factors, type of defense, and/or amount and timing of herbivory. For example, in *Casearia nitida* it was shown that plants damaged at the sapling or reproductive stage compensate for defoliation by growing more new leaves than undamaged plants (Boege, 2005). However, this response varied with the amount of defoliation, since saplings compensated better than reproductive plants at high defoliation levels. The interactions between plants and a dynamic community of antagonists (herbivores) and mutualists (pollinators and natural enemies of herbivores) will be fundamental in shaping the ontogenetical patterns of defensive strategies. In this context, plants can use different strategies depending on the stage at which they interact with other species (Barton and Boege, 2017). For example, plants that suffer a single damage event would favor investment in compensatory responses, while plants that experience repeated damage could favor a higher investment in induced resistance (Karban et al., 1999). Ontogenetic trajectories for tolerance can also be species-specific. Barton (2013) found that tolerance mechanisms were different between two *Plantago* species depending on their ontogeny. While tolerance in *P. lanceolata* was associated with flowering and shoot biomass in plants damaged at a mature stage, in *P. major* it was associated more with biomass and photosynthetic parameters when damaged at seedling and juveniles stages, respectively. Finally, plant resistance and tolerance may have different trajectories. This could also indicate trade-offs between both strategies if the expression of one strategy over the other switches according to the ontogenetical stage. For example, it has been shown that in *Raphanus sativus* juvenile plants show higher resistance but less tolerance than reproductive plants (Boege et al., 2007), but in *Arabidopsis thaliana* the cost of tolerance at different stages was not associated with a trade-off with resistance (Kornelsen and Avila-Sakar, 2015).

Plant resistance and tolerance responses to herbivore damage can cascade to other interactions that occur later during the plant's life. Rusman et al. (2020) studied the interaction between the timing of herbivore damage on flower traits and the pollinator community in *Brasica nigra*. They found that plants attacked at vegetative stages by some herbivore species had lower number of flowers, fewer flower visitations by pollinators and lower seed output than control undamaged plants, while damage at the budding stage had positive effects on flower visitation. Similarly, previous work with wild lima bean, showed that damage by leaf beetles reduced subsequent attack by seed beetles at a later stage of the plant's life (Abdala-Roberts et al., 2016; Hernández-Cumplido et al., 2016; Bustos-Segura et al., 2020). However, this type of induction depends on herbivore species and on the plant's stage when the first damage occurs (in leaves or bean pods) (Hernández-Cumplido et al., 2016). In another study, Cuny et al. (2018) found that when lima bean plants were exposed to a single herbivory event by leaf caterpillars, plants produced more leaves compared to undamaged plants, indicating leaf overcompensation. The results from the studies above provide strong evidence that induced responses in wild lima bean are dependent on several biotic factors, however the extent to which the frequency and time of damage influence these responses has not been tested. Particularly, it remains unknown whether early leaf damage events can modify or even improve tolerance to herbivory or affect seed quality and preferences of seed feeders and their predators or parasitoids. Analyses of ontogenetic interactions, could provide insights into how ontogenetical trajectories influence defense induction for future interactions in a multitrophic context.

Here we used wild lima bean to test the effects of frequency of damage and damage at different ontogenetic stages on compensatory responses and subsequent interactions with seed insects. To represent better the frequency and timing of herbivory

as it occurs in the wild, we applied mechanical damage at two time points representing early damage (at seedling + juvenile stages) or late damage (at the juvenile + reproductive stages). In addition, to analyze the influence of one vs. two damage events at different ontogenetical stages on tolerance and induced resistance, another group of plants was damaged only at the juvenile stage. This design allowed us to test differences in timing (seedling vs. reproductive) and the synergistic effects of different events of damage (one vs two events of damage) that comprise the span of the plant's development. Once seeds were matured, we examined the effects of leaf damage on seed infestation by exposing seeds to natural populations of seed beetles and their parasitoids. We addressed the following questions: 1) How does the timing and frequency of leaf damage influence plant growth and reproductive output? 2) How does timing and frequency of leaf damage alter the subsequent interactions between seeds and their associated insects? In addition, because we expected that a damage event early in the plant's life could determine the investment in tolerance to damage at future stages, we tested the hypothesis that damage at the seedling stage will enhance plant tolerance, compared to damage at the juvenile stage or repeated damage at the juvenile and adult stages.

Material and methods

Study system

Wild lima bean (*Phaseolus lunatus*) is distributed along the Pacific coast from Mexico to South America (Freytag and Debouck, 2002). In the south pacific Mexican coast this annual legume germinates in June–July, produces flowers in October–November and seeds in December–January (Heil and Silva Bueno, 2007; Moreira et al., 2015; Hernández-Cumplido et al., 2016). During the growing stage, lima bean plants are attacked by a number of leaf-chewing insects, including the velvet armyworm *Spodoptera latifascia*, Lepidoptera: Noctuidae (Cuny et al., 2018). This polyphagous caterpillar attacks several crops including maize, beans, tomato and chili pepper (Habib et al., 1982; Chabaane et al., 2022). During seed production, which lasts around two months, seed beetle species such as *Zabrotes subfasciatus* (Coleoptera: Chrysomelidae) and *Acanthoscelides obtectus* (Coleoptera: Chrysomelidae) enter dry pods and lay eggs on lima bean seeds, the larvae develop and pupate inside the seed (Benrey et al., 1998; Alvarez et al., 2005; Šešlija et al., 2009). They are both considered insect pests that also attack other species of stored cultivated beans (Birch et al., 1985; Paul et al., 2009). Both species are parasitized by several solitary parasitoid species, among them, the ectoparasitoid *Stenocorse bruchivora* (Aebi et al., 2008; Moreira et al., 2015; Hernández-Cumplido et al., 2016).

Plants

To explore the effects of timing of herbivory on plant responses, we conducted an experiment at the field station of the Universidad del Mar, Campus Puerto Escondido during the field season 2019-2020. We planted three seeds of wild lima bean in each of 80 pots (5 l volume) by November 15th, 2019. Seeds were collected in the same site the year before. After germination, we thinned the seedlings to leave only one per pot. Pots were kept in a large tent (Lumite® 3.66 m × 1.83 m × 1.83 m, Bioquip, CA, USA) to avoid unwanted insects attacking the plants. After two weeks of germination, we selected 64 seedlings (with only one trifolia developed) and distributed them randomly in 16 mesh tents (four plants per tent; Lumite® 1.83 m × 1.83 m × 1.83 m, Bioquip, CA, USA). Then, we applied damage treatments on these plants with the objective of studying induced plant responses to damage produced at different times throughout plant development, at seedling, juvenile or reproductive stage.

Experimental procedure

Four treatments were randomly assigned to the four plants in each of the 16 tents. The treatments to one plant per tent were as follows: C: control plants with no artificial damage. S-J: Plants damaged at the seedling and juvenile stages (at two and six weeks after germination). J: Plants damaged only at the juvenile stage (at six weeks after germination). J-R: plants damaged at the juvenile and reproductive stages (at six and ten weeks after germination; see Figure 1). So that all tents contained one plant of each treatment. For each damaged plant, we cut half of each leaflet with scissors. In addition, we also removed the apical meristem of growing tendrils. This was based on the damage that common herbivores, such as *Spodoptera latifascia*, produce on wild plants, as they would readily eat both the meristems and leaves (Bustos-Segura, personal observation).

Plant measurements and collection of seed insects

We counted the number of leaves and branches per plant three times throughout plant development (5, 9 and 14 weeks after germination). As the mesh tent was not 100% effective at keeping out naturally occurring insect, we observed some damage on the plants (mainly by *Spodoptera* spp. and *Diabrotica baleata*). Thus, throughout the experiment we recorded the proportion of damaged leaves. We also recorded the date when each plant produced the first flower to calculate the time to flowering (days from germination to the production of the first flower).

When pods were mature, they were removed from the experimental plants and placed inside a single green mesh bag

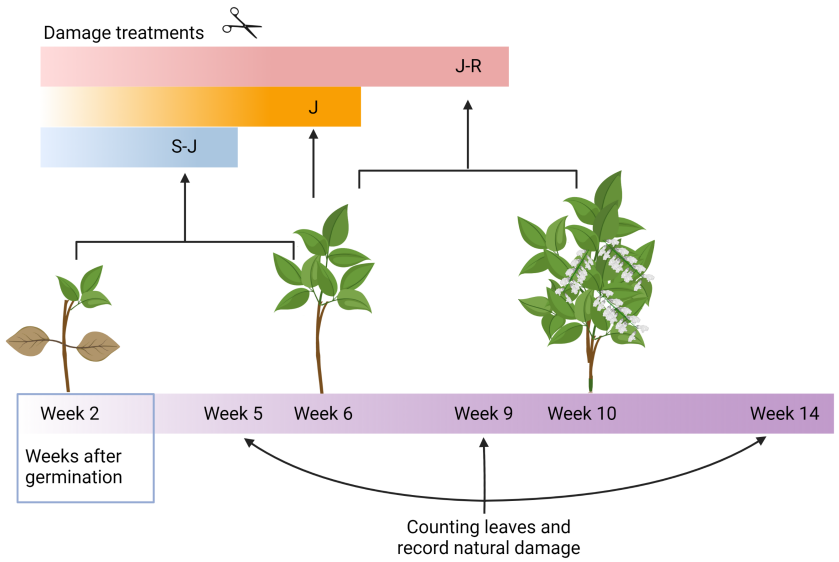

FIGURE 1
Schematic representation of the experimental design. Damage treatments on lima bean plants consisted of artificial damage on leaves at two different ontogenetical stages (S-J and J-R) or at one (J).

per plant, next to each plant following the methods from Bustos-Segura et al. (2020). This mesh was wide enough to allow the entrance of seed beetles and their parasitoids, but small enough to hold seeds inside the bags. Twelve weeks after germination, when most of the seeds were collected in mesh bags, the tent was removed to allow natural infestation by seed insects (including seed beetles and their parasitoids). After two weeks of exposure, the seeds were placed in plastic bags for two weeks to allow the emergence of insects developing inside the seeds. Then seeds were placed in a freezer at -20°C for one day. Insects found in each bag were counted and identified. We also counted the number of seeds and weighed 10 healthy seeds per plant.

Statistical methods

All analyses were performed with R system (version 4.2.0; R Core Team, 2022). We used generalized linear mixed models (GLMM) to analyze differences among damage treatments on plant and insect variables using package *lme4* (Bates et al., 2015). For all models we included damage treatment as a fixed effect and tent as a random effect. For the number of leaves and natural damage we included time point of measurement and the interaction with treatment as another fixed effect, and plant ID as a random effect. For analyzing number of leaves, number of branches, number of seeds, and number of insects, a Poisson error distribution was used. For analyzing the number of seed insects we included the number of seeds (log-transformed) as a covariate to account for the density-dependent relationship between insects and seeds. As seed beetles are attacked by solitary parasitoids, the number of total seed insects (beetles plus parasitoids) indicates the initial infestation by seed beetles. Whenever the dispersion ration of Poisson models was higher than 2, we included an observation level factor as a random factor to control for overdispersion. For comparing natural damage among treatments we used a binomial error distribution (as the proportion of damage leaflets). Time to first flowering was analyzed with a Cox proportional hazards mixed model, with package *coxme*. Seed mass in seeds was analyzed with a normal error distribution. Differences in parasitism rate among treatments were analyzed with a GLMM and a binomial distribution. We performed a structural equation model (SEM) for testing the causal pathway among Treatment groups, number of trifolia (at the last measurement), number of seeds and number of insects. Parasitism rate was not included in the SEM, given it could only be estimated for 30 plants. We used the piecewiseSEM package in R system that allows to include GLMs and mixed models in a SEM (Lefcheck, 2016).

Results

Overall, there was a significant effect of damage treatment on the number of trifolia across the season ($\chi^2_{(3)}$=10.63; P=0.014, Figure 2A), with only plants from the J treatment having significantly fewer leaves than control plants (Table S1). The effect sizes of the different contrasts ranged in the lower values (Cohen's d from -0.04 to 0.11, Table S1). Time significantly explained the change in number of trifolia ($\chi^2_{(2)}$=2452; P<0.0001), meanwhile, the interaction between treatment and time was not

statistically significant ($\chi^2_{(6)}$=3.15; P=0.79).The number of branches increased with time ($\chi^2_{(2)}$=170; P<0.0001; Figure S1A), but damage treatment and its interaction with time had a non-significant effect ($\chi^2_{(3)}$=6.26; P=0.1; $\chi^2_{(6)}$ =1.72; P=0.94, respectively). Despite the plants being inside tents, some insects entered and caused damage. For this minor but uncontrolled damage, there were differences across time ($\chi^2_{(2)}$=1115; P<0.0001), with higher damage at the beginning of the season (Figure 2B), but treatment as a main factor did not explain much of the variation ($\chi^2_{(3)}$=5.72; P=0.13). There was however, an effect of the interaction between treatment and time ($\chi^2_{(6)}$=29.38; P<0.0001), where in the middle of the season undamaged control plants received more natural damage than mechanically damaged plants (regardless of the timing of damage).This effect was small compared to the treatment damage and was not detected at the beginning, nor at the end of the season (Figure 2B).

The time from germination to first flowering was affected by the damage treatment ($\chi^2_{(3)}$=7.81; P=0.05). Plants from damage treatments S-J showed the longest time to production of the first flower and control plants the shortest time (Figure S1B). However, a multiple comparison posthoc test did not reveal specific differences between treatment pairs.

Fifty-two plants out of 64 produced seeds, but this was not influenced by the damage treatment ($\chi^2_{(3)}$=1.17; P=0.76). There was a significant effect of damage treatment on seed production ($\chi^2_{(3)}$=217; P<0.0001; Figure 3A). Control plants produced the most seeds, followed by plants damaged at the seedling stage (S-J), and then J and J-R plants. J and J-R plants produced similar number of seeds (Table S1). The effect sizes for comparisons between controls and damage treatments were relatively high (Table S1), while the effect sizes among damage treatments were lower (Table S1). Seed mass was not significantly different among treatments ($\chi^2_{(3)}$=5.55; P=0.14).

The total number of beetles and parasitoids collected was 87 and 21, respectively. Beetles emerging from the seeds were mostly of the species *Acanthoscelides obtectus*, with *Zabrotes subfasciatus* only present in two plants, so both species were pooled for analyses. We found that damage treatment had an effect on the abundance of seed beetles ($\chi^2_{(3)}$=22.83; P<0.0001; Figure 3B). The number of seed insects in seeds from control plants was not significantly different from plants from the S-J treatment (Tukey's *post-hoc* test: P=0.27), but was higher than in J and J-R treatment (Tukey's *post-hoc* test: P=0.003 and P<0.001, respectively). When the number of seeds per plant was used as a covariate to explain insect abundance, its effect was highly significant ($\chi^2_{(1)}$=25.41; P<0.0001), but the effect of damage treatment was no longer important ($\chi^2_{(3)}$=0.79; P=0.85), with more insects emerging from plants that produced more seeds. The parasitism rate on beetles was in average 0.122 ± 0.038 and was not different among damage treatments ($\chi^2_{(3)}$=0.62; P=0.89). The structural equation model confirmed the association among variables and showed an association between number of leaves and number of seeds (Figure 4). Damage treatment affected the number of trifolia, however this path does not show an influence on number of seeds. Thus, the effect of treatment on number of seeds was independent from the number of trifolia. There is an indirect effect of treatment on number of seed beetles, mediated by number of seeds, with no direct effect of treatment on number of beetles.

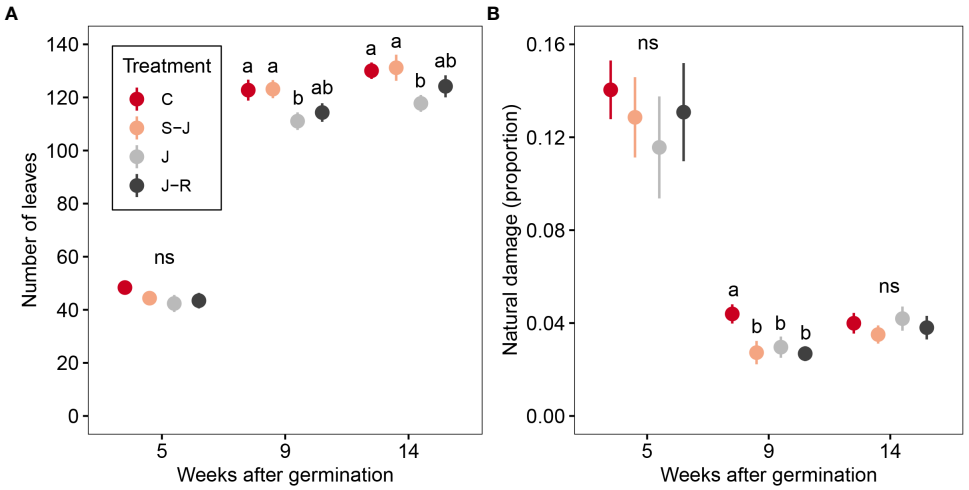

FIGURE 2
Effects of timing and frequency of damage on lima bean leaves. **(A)** number of leaves, **(B)** proportion of leaflets with uncontrolled natural herbivory. Treatment groups were: mechanically undamaged control plants (C); plants damaged at the seedling and juvenile stage (S-J), only at the juvenile stage or at the juvenile stage and reproductive stage (J-R). Different letters indicate significant differences among damage treatments within the same time point. ns indicate non-significant difference among damage treatments.

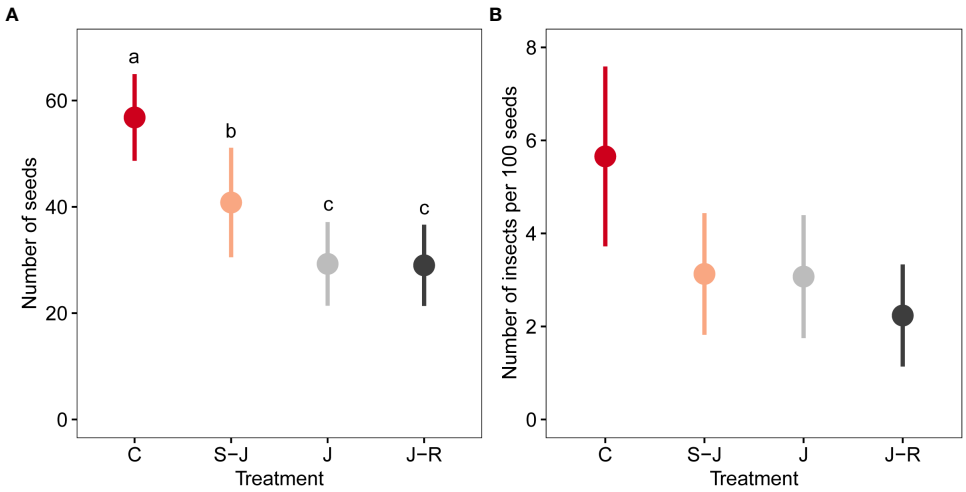

FIGURE 3
Effects of timing and frequency of damage on seed production and interactions with seed insects. **(A)** number of seeds as a measure of reproductive output and **(B)** number of seed insects per 100 seeds per plant. The number of insects includes seed beetles and parasitoids, thus indicating the initial infestation by seed beetles. Treatment groups were: mechanically undamaged control plants (C); plants damaged at the seedling and juvenile stage (S-J), only at the juvenile stage or at the juvenile stage and reproductive stage (J-R). Different letters indicate significant differences among damage treatments.

Discussion

The ability of a plant to recover from herbivore damage is crucial for its success in a natural environment. Plant ontogeny is known to play an important role in determining the compensation and defense responses against herbivory. While most studies on the effects of plant ontogeny on induced responses focus on isolated developmental stages, in nature, herbivores can attack throughout plant development at different points in time. Here we aimed to study the consequences of herbivory occurring at more than one ontogenetic stage with repeated or single damage events, on plant compensatory responses. This approach can give us information about the influence of early damage on the responses to subsequent damage events. We found that early damage (at the seedling and

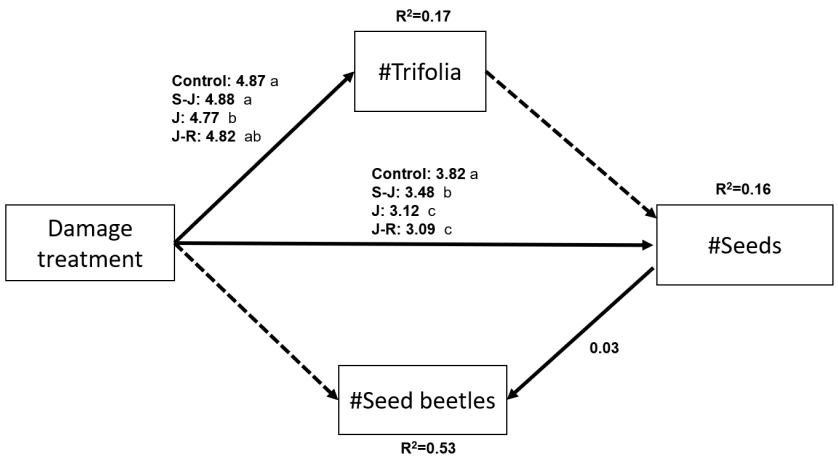

FIGURE 4
Diagram of the structural equation model including pathways between measured variables. Solid arrows indicate statistically significant positive pathways and dashed arrows indicate no significant pathways. The differences between treatments are given next to pathways from the Damage treatment variable and different letters indicate significant differences between groups according to a Tukey's post-hoc test. R square values given for each individual endogenous variables are conditional r squares (excluding random effects). All pathways were analyzed with GLMs and a Poisson error distribution. The estimates are given in the log scale. Model goodness-of-fit: Fisher's C=0.25, P=0.88.

juvenile stages) results in better compensatory growth and seed output than late damage (at the juvenile stage alone, or together with damage at the reproductive stage). But early and repeated damage is still positive in terms of leaf and seed production when compared to a single damage event occurring at the juvenile stage. This indicates that damage at the seedling stage can enhance plant tolerance to future damage. Conversely, we did not find evidence that leaf damage induced defenses on seeds against attack by seed beetles. Infestation by beetles in seeds of damaged plants was not so different from infestation in seeds from undamaged control plants, regardless of the timing and number of damage events.

Plants damaged at the seedling stage compensated by producing more leaves than plants from the other damage treatments, while maintaining a similar leaf production compared to control plants. This suggests that early damage stimulated growth to compensate for the loss of photosynthetic area, as compared to plants damaged at later stages. A larger photosynthetic area as compared to plants damaged later in their development could provide enough resources to produce more seeds (Tiffin, 2000; Wise and Abrahamson, 2005). However, the SEM in the present study showed no association between number of trifolia and seed set, but a direct effect of damage treatment on the number of leaves, which indicates a change in resource allocation. A plausible explanation may be that when the apical meristem of seedlings was cut, it stimulated branching and this increased leaf and flower production (Tiffin, 2000). Interestingly, the number of branches was not affected by early damage, so that compensation was only for leaf production with no evidence of change in plant morphology in response to early herbivory. A meta-analysis on defense ontogeny (Barton and Koricheva, 2010) showed that tolerance does not generally change with ontogenetic stage. This could be an indicator that the ontogenetic patterns in tolerance are not consistent and depend on the plant system. If tolerance is an adaptation to the specific community and its interactions, then it could be expected that each plant species evolves compensatory responses well suited for their biotic environment (Pearse et al., 2017). However, this meta-analysis did not include studies that analyze tolerance to seedling damage. As seedlings have limited resources available from photosynthetic area or root reserves, they are expected to invest more in growth than in resistance strategies (Barton and Boege, 2017). Damage at the seedling stage can be particularly relevant, given the lack of resources in this early developmental stage (Barton and Hanley, 2013; Quintero and Bowers, 2013), any stressor could drastically alter resource allocation with consequences for the whole plant development. Thus, interactions at the seedling stage deserve more attention in studies of tolerance ontogeny.

Induced responses to damage can also be influenced by the plant's exposure to previous events. For example, plants can be primed with stimuli such as egg oviposition, early herbivore damage or volatiles from damaged neighbors that prepare them for future attacks and increase the induction of defenses (Conrath et al., 2006; Heil and Kost, 2006; Hilker et al., 2016; Martinez-Medina et al., 2016). However, priming effects are not commonly linked to the responses in different ontogenetical stages. It is possible that when a stimulus occurs in an early ontogenetic stage of the plant, it could prime it to induce responses for later damage events. Thus, priming and ontogenetic trajectories can be linked by these early damage events. Yet, very few studies have examined the effect of an initial herbivory event at early ontogenetic stages on future plant compensatory responses. In wild radish, mechanical damage at the juvenile stage reduced seed output, while damage at a reproductive stage did not (Boege et al., 2007). However, when both types of damage were applied, seed output was similar to that in plants with only juvenile damage. As the specific physiological changes that take place to induce compensation need an external stimulus, it is possible that an early stimulus such as seedling damage, could prime the plant's compensatory responses to future herbivory. While priming for future attacks is a phenomenon expected to occur in most plant species, it has been mainly tested for resistance and not for tolerance traits (Conrath et al., 2006; Hilker et al., 2016). In our study we show that seed output was higher for plants damaged as seedlings after repeated damage at the juvenile stage compared to plants damaged at only the juvenile stage or at the juvenile and reproductive stage, indicating that plants damaged at the seedling stage tolerated damage better than plants damaged at later stages. This, supports the existence of priming for tolerance in lima bean. Importantly, this is not an effect of only repeated damage, since plants damaged at the juvenile and reproductive stage did not compensate better than plants with one damage event at the juvenile stage. Alternatively, it is possible that damage at the seedling stage alters the plant's resource allocation with an increased investment on growth and seed output, regardless of future damage.

Other types of priming stimuli for tolerance that are independent of damage such as application of oral secretion from herbivores or exposure to plant volatiles, can be tested. Induction of enhanced growth by volatiles has been shown for some plant species, including *Arabidopsis thaliana* (Shimola and Bidart, 2019), *Brassica* sp. (Pashalidou et al., 2020), lima bean (Freundlich et al., 2021) and *Medicago trunculata* (Maurya et al., 2022). In *Brassica*, volatiles emitted by plants infested with eggs of *Pieris brassicae* induce a higher reproductive output in undamaged exposed plants than in plants not exposed to volatiles. But when exposed plants were damaged by *P. brassicae* caterpillars, the reproductive output was similar to that of damaged plants not exposed to plant volatiles (Pashalidou et al., 2020). Thus, in this case tolerance to herbivory was not affected by exposure to eggs-infested plant volatiles. Tolerance can increase plant fitness in environments where herbivory is intense (Fornoni, 2011). Since it allows plants to reproduce despite herbivore damage, it is especially useful when herbivores are adapted to resistance traits (Best et al., 2008; Fornoni, 2011). Thus, compensatory responses associated with tolerance to herbivory play an important role in the establishment and maintenance of plant individuals and populations in communities with intense antagonistic interactions. Future studies should

examine with more detail different tolerance priming stimuli and their outcome at varying herbivore pressure.

Induced resistance to herbivory at different ontogenetic stages is also an important component of plant defense. Here, our results show that plants damaged at the juvenile and reproductive stages had fewer seed insects than control plants, while plants damaged at the seedling stage had intermediate numbers of seed insects. However, this was driven by a density dependent effect of the number of seeds, with more seed insects present in plants with more seeds. Therefore, we did not detect an induction of seed defenses, which may suggest that this mechanism can vary with environmental conditions and the type of damage. This result could be also influenced by the nature of the damage (herbivores vs. mechanical damage). Induction of plant defenses have been shown to be influenced by direct cues from herbivores such as elicitors or microbes (Shikano et al., 2017), but also the type and amount of damage may play a role. For example, a single mechanical damage event did not induce herbivore associated plant volatiles in lima bean plants, but continuous mechanical damage can replicate the whole spectrum of volatiles as compared to plants damaged by herbivores (Mithöfer et al., 2005). Thus, it seems likely that the mechanical damage used in our study was not enough to induce defenses in the seeds as has been shown in studies using damage by herbivores in lima bean (Hernández-Cumplido et al., 2016; Bustos-Segura et al., 2020). Mechanical damage allowed us to control for the amount of damage among plants and between different time points which would not have been possible with herbivores in field conditions. Moreover, the amount of damage is particularly important for analyzing tolerance to herbivory (Muola et al., 2010). Previous studies on indirect defenses, plant volatiles (Heil and Silva Bueno, 2007) and extrafloral nectar (Blue et al., 2015), and on plant-plant communication (Moreira et al., 2016) have shown that mechanical damage induces plant responses in lima bean. However, the difference between the effects of mechanical and natural damage on lima bean seed defenses and tolerance has not been examined.

In synthesis, we provide evidence for the role of ontogeny in plant resource allocation which results in differential growth compensation and tolerance. We also show that frequency together with timing of damage will affect these responses, as early damage influenced the plant's tolerance to future damage. Given that in nature, interactions with herbivores occur throughout the plant's life, we emphasize the importance of analyzing the consequences of plant herbivory at multiple ontogenetic stages. Such an approach will increase our understanding of the factors associated with plant adaptations to a dynamic biotic environment.

Data availability statement

The raw data supporting the conclusions of this article will be made available by the authors, without undue reservation.

Author contributions

CB-S and BB: Conceptualization. CB-S and RG-S: Investigation. CB-S: Data curation and formal analysis. CB-S: Methodology. BB: Funding acquisition. CB-S: original draft preparation. CB-S and BB: review and editing. All authors contributed to the article and approved the submitted version.

Funding

This research was financially supported by the Swiss National Science Foundation (Project No. 31003A_162860) awarded to BB.

Acknowledgments

We thank the Universidad del Mar, campus Puerto Escondido for logistical support, particularly Dr. Jose Arcos and Alfredo Lopez-Rojas. We also thank Lucas Malacari and Yosra Chabaane for help in the field and Philippine Surer for her assistance with the seed analyses. The authors declare no conflict of interest.

Conflict of interest

The authors declare that the research was conducted in the absence of any commercial or financial relationships that could be construed as a potential conflict of interest.

Publisher's note

Supplementary material

The Supplementary Material for this article can be found online at: https://www.frontiersin.org/articles/10.3389/fpls.2022.1037047/full#supplementary-material

References

Abdala-Roberts, L., Hernández-Cumplido, J., Chel-Guerrero, L., Betancur-Ancona, D., Benrey, B., and Moreira, X. (2016). Effects of plant intraspecific diversity across three trophic levels: Underlying mechanisms and plant traits. *Am. J. Bot.* 103, 1–9. doi: 10.3732/ajb.1600234

Aebi, A., Shani, T., Hansson, C., Contreras-Garduno, J., Mansion, G., and Benrey, B. (2008). The potential of native parasitoids for the control of Mexican bean beetles: A genetic and ecological approach. *Biol. Control* 47, 289–297. doi: 10.1016/j.biocontrol.2008.07.019

Alvarez, N., Hossaert-McKey, M., Rasplus, J. Y., McKey, D., Mercier, L., Soldati, L., et al. (2005). Sibling species of bean bruchids: A morphological and phylogenetic study of acanthoscelides obtectus say and acanthoscelides obvelatus bridwell. *J. Zool. Syst. Evol. Res.* 43, 29–37. doi: 10.1111/j.1439-0469.2004.00286.x

Baldwin, I. T., and Preston, C. A. (1999). The eco-physiological complexity of plant responses to insect herbivores. *Planta* 208, 137–145. doi: 10.1007/s004250050543

Barton, K. E. (2013). Ontogenetic patterns in the mechanisms of tolerance to herbivory in *Plantago*. *Ann. Bot.* 112, 711–720. doi: 10.1093/aob/mct083

Barton, K. E., and Boege, K. (2017). Future directions in the ontogeny of plant defence: understanding the evolutionary causes and consequences. *Ecol. Lett.* 20, 403–411. doi: 10.1111/ele.12744

Barton, K. E., and Hanley, M. E. (2013). Seedling–herbivore interactions: Insights into plant defence and regeneration patterns. *Ann. Bot.* 112, 643–650. doi: 10.1093/aob/mct139

Barton, K. E., and Koricheva, J. (2010). The ontogeny of plant defense and herbivory: Characterizing general patterns using meta-analysis. *Am. Nat.* 175, 481–493. doi: 10.1086/650722

Bates, D., Mächler, M., Bolker, B., and Walker, S. (2015). Fitting linear mixed-effects models using lme4. *J. Stat. Software* 67, 1. doi: 10.18637/jss.v067.i01

Benrey, B., Callejas, A., Rios, L., Oyama, K., and Denno, R. F. (1998). The effects of domestication of *Brassica* and *Phaseolus* on the interaction between phytophagous insects and parasitoids. *Biol. Control* 11, 130–140. doi: 10.1006/bcon.1997.0590

Best, A., White, A., and Boots, M. (2008). Maintenance of host variation in tolerance to pathogens and parasites. *Proc. Natl. Acad. Sci. U. S. A.* 105, 20786–20791. doi: 10.1073/pnas.0809558105

Birch, N., Southgate, B. J., and Fellows, L. E. (1985). "Wild and semi-cultivated legumes as potential sources of resistance to bruchid beetles for crop breeder: a study of Vigna/Phaseolus," in *Plants for arid lands* (Dordrecht: Springer), 303–320.

Blue, E., Kay, J., Younginger, B. S., and Ballhorn, D. J. (2015). Differential effects of type and quantity of leaf damage on growth, reproduction and defence of lima bean (*Phaseolus lunatus* l.). *Plant Biol.* 17, 712–719. doi: 10.1111/plb.12285

Boege, K. (2005). Influence of plant ontogeny on compensation to leaf damage. *Am. J. Bot.* 92, 1632–1640. doi: 10.3732/ajb.92.10.1632

Boege, K., Dirzo, R., Siemens, D., and Brown, P. (2007). Ontogenetic switches from plant resistance to tolerance: Minimizing costs with age? *Ecol. Lett.* 10, 177–187. doi: 10.1111/j.1461-0248.2006.01012.x

Boege, K., and Marquis, R. J. (2005). Facing herbivory as you grow up: the ontogeny of resistance in plants. *Trends Ecol. Evol.* 20, 441–448. doi: 10.1016/j.tree.2005.05.001

Bustos-Segura, C., Cuny, M. A. C., and Benrey, B. (2020). Parasitoids of leaf herbivores enhance plant fitness and do not alter caterpillar-induced resistance against seed beetles. *Funct. Ecol.* 34, 586–596. doi: 10.1111/1365-2435.13478

Chabaane, Y., Marques-Arce, C., Glauser, G., and Benrey, B. (2022). Altered capsaicin levels in domesticated chili pepper varieties affect the interaction between a generalist herbivore and its ectoparasitoid. *J. Pest. Sci.* 95, 735–747. doi: 10.1007/s10340-021-01399-8

Conrath, U., Beckers, G. J. M., Flors, V., García-Agustín, P., Jakab, G., Mauch, F., et al. (2006). Priming: Getting ready for battle. *Mol. Plant-Microbe Interact.* 19, 1062–1071. doi: 10.1094/MPMI-19-1062

Cuny, M. A. C., Gendry, J., Hernández-Cumplido, J., and Benrey, B. (2018). Changes in plant growth and seed production in wild lima bean in response to herbivory are attenuated by parasitoids. *Oecologia* 187, 447–457. doi: 10.1007/s00442-018-4119-1

Fornoni, J. (2011). Ecological and evolutionary implications of plant tolerance to herbivory. *Funct. Ecol.* 25, 399–407. doi: 10.1111/j.1365-2435.2010.01805.x

Freundlich, G. E., Shields, M., and Frost, C. J. (2021). Dispensing a synthetic green leaf volatile to two plant species in a common garden differentially alters physiological responses and herbivory. *Agronomy* 11, 958. doi: 10.3390/agronomy11050958

Freytag, G. F., and Debouck, D. G. (2002). *Taxonomy, distribution and ecology of the genus phaseolus (Leguminosae-papilionoideae) in north America, Mexico and central America* (Texas, USA: BRIT Press).

Gatehouse, J. A. (2002). Plant resistance towards insect herbivores: A dynamic interaction. *New Phytol.* 156, 145–169. doi: 10.1046/j.1469-8137.2002.00519.x

Habib, M. E. M., Paleari, L. M., and Amaral, M. E. C. (1982). Effect of three larval diets on the development of the armyworm, *Spodoptera latifascia* walke (Noctuidae, Lepidoptera). *Rev. Bras. Zool.* 1, 177–182. doi: 10.1590/S0101-81751982000300007

Heil, M., and Baldwin, I. T. (2002). Fitness costs of induced resistance: emerging experimental support for a slippery concept. *Trends Plant Sci.* 7, 61–67. doi: 10.1016/S1360-1385(01)02186-0

Heil, M., and Kost, C. (2006). Priming of indirect defences. *Ecol. Lett.* 9, 813–817. doi: 10.1111/j.1461-0248.2006.00932.x

Heil, M., and Silva Bueno, J. C. (2007). Within-plant signaling by volatiles leads to induction and priming of an indirect plant defense in nature. *Proc. Natl. Acad. Sci.* 104, 5467–5472. doi: 10.1073/pnas.0610266104

Hernández-Cumplido, J., Glauser, G., and Benrey, B. (2016). Cascading effects of early-season herbivory on late-season herbivores and their parasitoids. *Ecology* 97, 1283–1297. doi: 10.1890/15-1293.1

Hilker, M., Schwachtje, J., Baier, M., Balazadeh, S., Bäurle, I., Geiselhardt, S., et al. (2016). Priming and memory of stress responses in organisms lacking a nervous system. *Biol. Rev.* 91, 1118–1133. doi: 10.1111/brv.12215

Karban, R. (2011). The ecology and evolution of induced resistance against herbivores. *Funct. Ecol.* 25, 339–347. doi: 10.1111/j.1365-2435.2010.01789.x

Karban, R., Agrawal, A. A., Thaler, J. S., and Adler, L. S. (1999). Induced plant responses and information content about risk of herbivory. *Trends Ecol. Evol.* 14, 443–447. doi: 10.1016/S0169-5347(99)01678-X

Karban, R., and Baldwin, I. T. (1997). *Induced responses to herbivory* (United States: University of Chicago Press).

Karban, R., and Myers, J. H. (1989). Induced plant responses to herbivory. *Annu. Rev. Ecol. Syst.* 20, 331–348. doi: 10.1146/annurev.es.20.110189.001555

Kornelsen, J., and Avila-Sakar, G. (2015). Ontogenetic changes in defence against a generalist herbivore in arabidopsis thaliana. *Plant Ecol.* 216, 847–857. doi: 10.1007/s11258-015-0472-x

Lefcheck, J. S. (2016). piecewiseSEM: Piecewise structural equation modelling in r for ecology, evolution, and systematics. *Methods Ecol. Evol.* 7, 573–579. doi: 10.1111/2041-210X.12512

Martinez-Medina, A., Flors, V., Heil, M., Mauch-Mani, B., Pieterse, C. M. J., Pozo, M. J., et al. (2016). Recognizing plant defense priming. *Trends Plant Sci.* 21, 818–822. doi: 10.1016/j.tplants.2016.07.009

Maurya, A. K., Pazouki, L., and Frost, C. J. (2022). Priming seeds with indole and (Z)-3-hexenyl acetate enhances resistance against herbivores and stimulates growth. *J. Chem. Ecol.* 48, 441–454. doi: 10.1007/s10886-022-01359-1

Mithöfer, A., Wanner, G., and Boland, W. (2005). Effects of feeding spodoptera littoralis on lima bean leaves. II. continuous mechanical wounding resembling insect feeding is sufficient to elicit herbivory-related volatile emission. *Plant Physiol.* 137, 1160–1168. doi: 10.1104/pp.104.054460

Moreira, X., Abdala-Roberts, L., Hernández-Cumplido, J., Rasmann, S., Kenyon, S. G., and Benrey, B. (2015). Plant species variation in bottom-up effects across three trophic levels: A test of traits and mechanisms. *Ecol. Entomol.* 40, 676–686. doi: 10.1111/een.12238

Moreira, X., Petry, W. K., Hernández-Cumplido, J., Morelon, S., and Benrey, B. (2016). Plant defence responses to volatile alert signals are population-specific. *Oikos* 125, 950–956. doi: 10.1111/oik.02891

Muola, A., Mutikainen, P., Laukkanen, L., Lilley, M., and Leimu, R. (2010). Genetic variation in herbivore resistance and tolerance: the role of plant life-history stage and type of damage. *J. Evol. Biol.* 23, 2185–2196. doi: 10.1111/j.1420-9101.2010.02077.x

Núñez-Farfán, J., Fornoni, J., and Valverde, P. L. (2007). The evolution of resistance and tolerance to herbivores. *Annu. Rev. Ecol. Evol. Syst.* 38, 541–566. doi: 10.1146/annurev.ecolsys.38.091206.095822

Pashalidou, F. G., Eyman, L., Sims, J., Buckley, J., Fatouros, N. E., De Moraes, C. M., et al. (2020). Plant volatiles induced by herbivore eggs prime defences and mediate shifts in the reproductive strategy of receiving plants. *Ecol. Lett.* 23, 1097–1106. doi: 10.1111/ele.13509

Paul, U. V., Lossini, J. S., Edwards, P. J., and Hilbeck, A. (2009). Effectiveness of products from four locally grown plants for the management of *Acanthoscelides obtectus* (Say) and *Zabrotes subfasciatus* (Boheman) (both coleoptera: Bruchidae)

in stored beans under laboratory and farm conditions in northern T. *J. Stored Prod. Res.* 45, 97–107. doi: 10.1016/j.jspr.2008.09.006

Pearse, I. S., Aguilar, J., Schroder, J., and Strauss, S. Y. (2017). Macroevolutionary constraints to tolerance: trade-offs with drought tolerance and phenology, but not resistance. *Ecology* 98, 2758–2772. doi: 10.1002/ecy.1995

Quintero, C., and Bowers, M. D. (2013). Effects of insect herbivory on induced chemical defences and compensation during early plant development in *Penstemon virgatus*. *Ann. Bot.* 112, 661–669. doi: 10.1093/aob/mct011

R Core Team (2022). *R: A language and environment for statistical computing. R Foundation for Statistical Computing* Vienna, Austria: R Foundation for Statistical Computing. Available at: https://www.R-project.org/

Rusman, Q., Lucas-Barbosa, D., Hassaan, K., and Poelman, E. H. (2020). Plant ontogeny determines strength and associated plant fitness consequences of plant-mediated interactions between herbivores and flower visitors. *J. Ecol.* 108, 1046–1060. doi: 10.1111/1365-2745.13370

Schuman, M. C., and Baldwin, I. T. (2016). The layers of plant responses to insect herbivores. *Annu. Rev. Entomol.* 61, 373–394. doi: 10.1146/annurev-ento-010715-023851

Šešlija, D., Stojković, B., Tucić, B., and Tucić, N. (2009). Egg-dumping behaviour in the seed beetle *Acanthoscelides obtectus* (Coleoptera: Chrysomelidae: Bruchinae) selected for early and late reproduction. *Eur. J. Entomol.* 106, 557–563. doi: 10.14411/eje.2009.070

Shikano, I., Rosa, C., Tan, C. W., and Felton, G. W. (2017). Tritrophic interactions: Microbe-mediated plant effects on insect herbivores. *Annu. Rev. Phytopathol.* 55, 313–331. doi: 10.1146/annurev-phyto-080516-035319

Shimola, J., and Bidart, M. G. (2019). Herbivory and plant genotype influence fitness-related responses of *Arabidopsis thaliana* to indirect plant-plant interactions. *Am. J. Plant Sci.* 10, 1287–1299. doi: 10.4236/ajps.2019.108093

Strauss, S. Y., and Agrawal, A. A. (1999). The ecology and evolution of plant tolerance to herbivory. *Trends Ecol. Evol.* 14, 179–185. doi: 10.1016/S0169-5347(98)01576-6

Tiffin, P. (2000). Mechanisms of tolerance to herbivore damage: What do we know? *Evol. Ecol.* 14, 523–536. doi: 10.1023/A:1010881317261

Turlings, T. C. J., and Erb, M. (2018). Tritrophic interactions mediated by herbivore-induced plant volatiles: Mechanisms, ecological relevance, and application potential. *Annu. Rev. Entomol.* 63, 433–452. doi: 10.1146/annurev-ento-020117-043507

Wise, M. J., and Abrahamson, W. G. G. (2005). Beyond the compensatory continuum : Environmental resource levels and plant tolerance of herbivory. *Oikos* 109, 417–428. doi: 10.1111/j.0030-1299.2005.13878.x

frontiers | Frontiers in Plant Science

TYPE Review
PUBLISHED 01 December 2022
DOI 10.3389/fpls.2022.1004553

OPEN ACCESS

EDITED BY
Bernard Roitberg,
Simon Fraser University, Canada

REVIEWED BY
E. Tobias Krause,
Friedrich-Loeffler-Institute, Germany
Yong Zhang,
Southwest Forestry University, China
Wenping Yuan,
Sun Yat-sen University, China

*CORRESPONDENCE
Yuhui Wang
yhwang@ibcas.ac.cn
Guang Yang
5475@cnu.edu.cn
Xu Wang
wangxu01@caas.cn

SPECIALTY SECTION
This article was submitted to Functional Plant Ecology, a section of the journal Frontiers in Plant Science

RECEIVED 27 July 2022
ACCEPTED 21 November 2022
PUBLISHED 01 December 2022

CITATION
Zhou H, Hou L, Lv X, Yang G, Wang Y and Wang X (2022) Compensatory growth as a response to post-drought in grassland. *Front. Plant Sci.* 13:1004553. doi: 10.3389/fpls.2022.1004553

Compensatory growth as a response to post-drought in grassland

Huailin Zhou[1], Lulu Hou[2], Xiaomin Lv[1], Guang Yang[3]*, Yuhui Wang[4]* and Xu Wang[2]*

[1]State Key Laboratory of Severe Weather, Chinese Academy of Meteorological Sciences, China Meteorological Administration, Beijing, China, [2]Institute of Agricultural Resources and Regional Planning, Chinese Academy of Agricultural Sciences, Beijing, China, [3]College of Teacher Education, Capital Normal University, Beijing, China, [4]State Key Laboratory of Vegetation and Environmental Change, Institute of Botany, Chinese Academy of Sciences, Beijing, China

Grasslands are structurally and functionally controlled by water availability. Ongoing global change is threatening the sustainability of grassland ecosystems through chronic alterations in climate patterns and resource availability, as well as by the increasing frequency and intensity of anthropogenic perturbations. Compared with many studies on how grassland ecosystems respond during drought, there are far fewer studies focused on grassland dynamics after drought. Compensatory growth, as the ability of plants to offset the adverse effects of environmental or anthropogenic perturbations, is a common phenomenon in grassland. However, compensatory growth induced by drought and its underlying mechanism across grasslands remains not clear. In this review, we provide examples of analogous compensatory growth from different grassland types across drought characteristics (intensity, timing, and duration) and explain the effect of resource availability on compensatory growth and their underlying mechanisms. Based on our review of the literature, a hypothetic framework for integrating plant, root, and microbial responses is also proposed to increase our understanding of compensatory growth after drought. This research will advance our understanding of the mechanisms of grassland ecosystem functioning in response to climate change.

KEYWORDS

compensatory growth, grassland ecosystem, drought, resilience, recovery, mechanism

Introduction

Grasslands, as one of the world's most widespread vegetation types, cover approximately 30% of the Earth's land surface (Parton et al., 2012) and 69% of agricultural land area (Dixon et al., 2014), respectively. Grasslands not only serve as an important global reservoir of food production (Schirpke et al., 2019), but also play a

critical role in the global carbon and water cycle, as well as plant-soil feedback to climate change (Bowman et al., 2015; Putten et al., 2016; Pugnaire et al., 2019). Grassland growth and productivity are largely regulated by temperature and soil water content, particularly the amount and timing of precipitation events (Knapp and Smith, 2001; Knapp et al., 2002; Huxman et al., 2004; Hufkens et al., 2016). In recent decades, ongoing global changes in temperature and precipitation have significantly increased the frequency, severity, and duration of drought events (Dai, 2012; IPCC, 2013; Trenberth et al., 2014; Cook et al., 2015), which also projected to continue to increase in the near future (Vicente-Serrano et al., 2020). The alterations in water availability before or during the growing season are weakening the stability and functionality of grassland ecosystems around the world, particularly in arid and semi-arid regions (Macdougall et al., 2013; Song and Yu, 2015). Because drought events could directly or indirectly affect plant community structure (Knapp et al., 2008; Cherwin and Knapp, 2012; Carlyle et al., 2014; Tielborger et al., 2014), threaten grassland productivity (Knapp and Smith, 2001; Volaire et al., 2014; Frank et al., 2015) and even cause grassland degradation (Breshears et al., 2005), and then alter carbon and nitrogen dynamics (Mackie et al., 2019). Naturally, to deal with the negative impacts of drought on grasslands functions and services, it is urgent to understand how grasslands respond to drought.

Many studies on grassland responses during drought have been well synthesized in both reviews (Grman et al., 2010; Niu et al., 2014; Hoover et al., 2018) and meta-analyses (Matos et al., 2019; Deng et al., 2021), which have considerably improved our understandings of the impacts of drought on grassland biotic and abiotic processes. For example, the mean effect of drought on aboveground net primary production (ANPP) is demonstrated to be negative (Hoover et al., 2014; Niboyet et al., 2017; Li et al., 2022). Droughts have legacy effects on bacterial and fungal community composition, which could, in turn, influence plant growth and ecosystem through plant-soil feedback (De Vries et al., 2012b; Kaisermann et al., 2017; Griffin-Nolan et al., 2018). Except for the ability of grasslands to resist drought (e.g., resistance), the recovery ability of grasslands after drought (e.g., resilience) is another important entry point for clarifying the responses of grasslands to drought (Vogel et al., 2012; Mori et al., 2013; Hoover et al., 2014; Oliver et al., 2015; Xu et al., 2021). However, the recovery ability of grasslands to different drought characteristics (e.g., timing, intensity, and duration) and climate contexts were rarely studied (Vilonen et al., 2022). Besides, our knowledge of grassland drought response is incomplete without understanding the responses after drought and to what extent grasslands can recover. Therefore, understanding the change patterns in the structure and function of grassland ecosystems during the period of after drought and exploring their underlying mechanisms, are crucial for forecasting grassland ecosystem function and dynamics under climate change.

Compensatory growth (CG), defined as the accelerated growth response of plants to damage (Belsky, 1986), which is implied the ability of plants to offset the adverse effects of tissue damage, restore organic functionality, and maintain their original growth state after perturbations (Mcnaughton, 1983). CG has received wide acceptance as a survival strategy of organisms under stressful conditions and a fundamental mechanism for ecosystem stability (Mangel and Munch, 2005; Gonzalez and Loreau, 2009). In fact, it sometimes takes different names, like resilience, recovery, and compensatory dynamic; they all share the essential meaning that accelerated growth organism when recovering from a period of unfavorable conditions (Li et al., 2021). According to the relative strength of growth rate after disturbance compared to the undisturbed group, CG can be classified into three types: under-compensation, exact-compensation, and over-compensation (Figure 1) (Belsky, 1986; Li et al., 2021). Although the existence of CG is widely acknowledged in ecological systems but has received little attention in stress-ecological studies (Metcalfe and Monaghan, 2001; Gessler et al., 2020). In general, it is conventionally to constrain the period of CG assessment through a pre-defined post-drought period or to

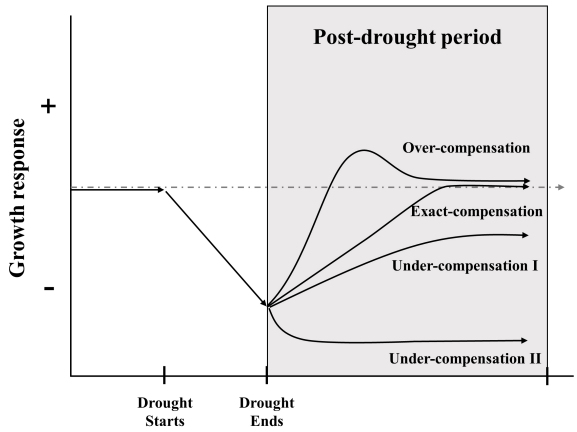

FIGURE 1
Framework for describing the growth response of grassland ecosystem after drought ends. The grey and dashed line represents growth response in condition without drought, the solid line indicated possible compensatory patterns under drought. Over-compensation means the growth rate increase rapidly after the end of a drought, then exceed the response level of control treatment to some extent, and finally reach the same response level of control treatment; exact-compensation represents the growth rate return to be comparable with control treatment after drought; under-compensation I indicates that the growth rate cannot reach the same level of control treatment with slow growth rate; under-compensation II denotes the collapse of grassland ecosystem with much slower growth rate (Frank et al., 2015; Li et al., 2021; Vilonen et al., 2022).

the status where growth returns to a historic norm (Ovenden et al., 2021). The capacities of grassland CG are different among species (Knapp et al., 2015), community components (Carlsson et al., 2017; Stampfli et al., 2018; Wilcox et al., 2020), life forms (Volaire, 2003; Nippert and Knapp, 2007), nutrient stress tolerances (Macgillivray et al., 1995; Bharath et al., 2020), interactions among soil microbes (De Vries et al., 2012a; Fry et al., 2018) and disturbance's properties (Chen et al., 2020; Saeidnia et al., 2020; Li et al., 2022). Besides, CG could be evaluated by a variety of quantitative indicators, such as productivity, biomass, species number, coverage, and so on (Yuan et al., 2020). Recent research on the prevalence and detection of CG leaves a large gap in the knowledge of the mechanisms that affect the temporal and scale of CG (Kahl et al., 2019; Li et al., 2020; Saeidnia et al., 2020; Hossain and Li, 2021; Jiao et al., 2021; Li et al., 2021; Ovenden et al., 2021; Vilonen et al., 2022). Thus, a deeper understanding of the pattern of grassland CG and its variation is a major challenge for the emerging extreme climate events and human disturbance.

Here we reviewed current knowledge on the CG of grasslands to drought stress. We firstly discuss differences in CG response to drought imposed by manipulated experiments or natural precipitation variations. Then, CG patterns under different drought timing, intensity, and duration were compared and discussed. Meanwhile, as plant-soil feedback plays a key role in the CG response to drought, resource availability was also addressed in the text. In the following section, we concluded the underlying mechanisms of CG in response to drought across biotic and abiotic reasons. Finally, suggestions for future research were also given to deepen our understanding of the responses during the period after drought and benefit for forecasting grassland ecosystem function and dynamics under climate change.

Compensatory growth among different grassland ecosystems

Numerous rainfall manipulation experiments have been conducted to investigate the growth responses of different grassland ecosystems after drought (Hoover et al., 2018; Matos et al., 2019). In the mesic grasslands of North America and Switzerland, ANPP can fully recover (the same as exact-compensation) within a single year after a short-term extreme drought with grass species compensating for the decreased forb productivity (Hoover et al., 2014; Stampfli et al., 2018; Mackie et al., 2019; Wilcox et al., 2020). Besides, a study focused on belowground net primary productivity (BNPP) also suggested that drought-induced reductions in root production can recover rapidly in a coming wet year even though the drought legacy effects may persist for years after drought (Slette et al., 2022). By contrast, the CG of burned sites was mostly contributed to annual forb ANPP compensating for reduced grass ANPP, while the CG of unburned sites was promoted by subdominant annual and perennial grass species in a savanna grassland in South Africa (Wilcox et al., 2020). The opposite roles played by forbs and grass species mentioned above might be mainly due to the difference in community composition in these sites. As forbs are often less resistant to drought than grasses, if the plant community was dominated by forbs, then the CG of the total ANPP may decrease (Xu et al., 2021). Additionally, annual forbs are more resilient than perennial forbs, which are characterized by limited seedling recruitment and slow regrowth from surviving belowground organs after drought (Wilcox et al., 2020; Xu et al., 2021).

Meanwhile, semi-arid grassland seems to require more time for the ANPP to achieve exact-compensation from drought. Xu et al. (2021) explored the recovery potential of ANPP by inducing two years of extreme drought (66% reduction in ambient growing season precipitation) followed by two years of recovery (ambient precipitation) in a semi-arid grassland ecosystem in Inner Mongolia, China. The results show that ANPP decreased by approximately 33% during the two years of extreme drought. However, one year after the extreme droughts, the ANPP of the drought plots returned to 83% of the ambient plots and fully recovered to ambient ANPP by the second year. The authors attributed these differences to three points: (a) the lower precipitation efficiently limits CG in the semi-arid regions; (b) the reduction of ANPP in the semiarid grassland is much higher than that in the mesic grassland (Ma et al., 2020), which increase the recovery time; (c) a large proportion of high resistance and low resilience of perennial forb species may delay the recovery time of the semiarid grassland (Tello-García et al., 2020).

As for arid grasslands, the CG rate may more slowly due to greater resource limitations and more severe impacts (Stuart-Haentjens et al., 2018). A study in Inner Mongolia suggested that the net primary productivity was less affected by light to moderate drought than moderate to severe drought (Liu et al., 2021). At the same time, another study conducted in the Chihuahuan Desert found that drought consistently and strongly decreased the cover of a dominant C4 grass (*Bouteloua eriopoda*), whereas water addition slightly increased the cover, even with little variation between years (Báez et al., 2013). The limited CG of *Bouteloua eriopoda* responding to increased water availability may reflect morphological constraints on this rhizomatous grass (Báez et al., 2013).

In general, grasslands are composed of two dominant herbaceous functional groups: grass and forb, which show great differences in their vulnerability to extreme drought (Taylor et al., 2011; Wilcox et al., 2020). Grass species are generally better able to tolerate drought, especially C4 grasses, whereas forb species may avoid drought *via* deeper rooting profiles (Nippert and Knapp, 2007). Besides, the growth responses of annual and perennial species may be different during and after drought (Volaire, 2003). Therefore, CG in

grasslands may depend on function diversity in predrought communities (Stampfli et al., 2018; Wilcox et al., 2020). However, a study conducted in 13 extreme natural-drought experiments spreading over two biogeographic regions (five sites in annual-dominated grasslands in California and eight sites in perennial-dominated grasslands in the Great Plains) suggested there was no correlation between pre-drought plant diversity and post-drought resilience (Bharath et al., 2020). More importantly, the productivity of grassland ecosystems is simultaneously co-limited by nutrients and water across a wide range of precipitation (Bharath et al., 2020). For example, species-rich semi-natural grasslands exhibited a lower CG compared with intensively managed agricultural grasslands (De Keersmaecker et al., 2016).

Compensatory growth response to drought intensity, timing, and duration

Drought intensity, timing, and duration are fundamental characteristics of experimental or natural drought events. Drought stress can cause a series of reductions in morphological and physiological functional traits (e.g., plant height, specific leaf area, length of roots, leaf water potential, and photosynthetic capacity), which may finally lead to a reduction in productivity (Cenzano et al., 2013; Wellstein et al., 2017). Response diversity, describing the variation of responses to environmental change among species in a particular community, maybe a key determinant of ecosystem stability and functionality (Elmqvist et al., 2003; Mori et al., 2013). For instance, perennial caespitose grasses and rhizomatous grasses showed different growth response strategies to drought, as the CG of rhizomatous grasses declined with increasing water stress intensity while caespitose grasses displayed little CG with strong drought resistance (Zhang et al., 2018). Besides, defoliation could stimulate the CG of rhizomatous grasses under wet conditions, but the positive effects of defoliation can be weakened by drought intensity (Zhang et al., 2018). Even though, the CG of grassland dominated by perennial species almost remains constant with increasing drought intensity (Ruppert et al., 2015). The main reason may be contributed to the degree of drought intensity being below the upper limit that could cause ecosystem collapse (Dechant and Moradkhani, 2015).

The responses of grassland ecosystems to drought may vary with different seasonal drought timing. When droughts occur in the early season, the reductions in current-year biomass appear to be large enough due to the limitation length of a peak growth period for biomass accumulation (Meng et al., 2019). On contrary, when droughts happen in the late season, the decreased biomass will be reflected in the following year because of large negative legacy effects (Jiao et al., 2021). For example, the timing of drought significantly decreased ANPP (18%~26% reduction compared to the control treatments) during the growing season in a mesic grassland, with later droughts (early summer drought and late summer drought, respectively) having a larger effect than earlier drought (late spring drought), while BNPP was not significantly affected by any manipulated drought timing (Denton et al., 2016). Similar findings were also confirmed in a meadow steppe where spring and summer droughts decreased ANPP but did not affect BNPP (Meng et al., 2019). Furthermore, grasslands subjected to mid-summer drought tend to be primed for greater CG in the following year than grasslands experiencing earlier drought in the season (De Vries et al., 2012b; Denton et al., 2016).

The duration of drought is important to explain the variability of CG, with longer droughts resulting in slower grassland CG, through causing the depletion of seedbank and stored resources needed for re-establishment and resprouting of the drought-sensitive species (Ruppert et al., 2015; Estiarte et al., 2016; Matos et al., 2019). In the North American semi-arid grassland biome, reductions in ANPP appeared to be greater when the rainfall patterns of the growing season were dominated by many small events (that is, chronic drought), while it turned out to be not when rainfall patterns were characterized by large rain events (Cherwin and Knapp, 2012). Compared with wood biomes, grasslands exhibited a stronger CG when exposed to chronic drought, by contrast, displayed a weaker CG when exposed to intense drought (Jiao et al., 2021). Furthermore, the adverse effects of intense drought on ANPP were found to be more significant than chronic drought, additionally, drought duration appeared to hardly alter this pattern (Carroll et al., 2021). Therefore, the compensation of grassland ANPP in response to future droughts may be reduced when the rainfall regimes of the growing season being more extreme.

Compensatory growth under different resource availability

The amount of CG can be also affected by resource availability through the plant-soil feedback (Van Staalduinen et al., 2009). Due to changes in the soil water availability during and after drought, the turnover of C and N in soils is also altered. Increased duration and intensity of drought are usually associated with decreasing C and N mineralization and inorganic N fluxes (Borken and Matzner, 2009; Deng et al., 2021). Even though, a pulse in net C and N mineralization following the wetting of dry soil is generally observed (Wu and Brookes, 2005). Previous grassland studies indicate that drought stresses alleviate N limitation and have a positive effect on forage quality (Dumont et al., 2015). Additionally, increasing N deposition resulting from anthropogenic N emissions can improve grassland CG after a drought even in arid environments (Kinugasa et al., 2012). Besides, the wetting pulses have a greater impact on C and N

mineralization or flux rates in arid and semiarid grasslands than that in humid and subhumid grassland (Borken and Matzner, 2009). Whereas, it is worth noting that the cumulative C and N mineralization are most likely less compared with soil under optimum moisture even with wetting pulses, which implies that wetting pulse cannot compensate for small mineralization rates during periods (Borken and Matzner, 2009). In another word, the grassland CG pulsed by the short-term C and N mineralization may be not sustainable if the droughts become frequent.

The dynamics of soil C and N are affected not only by plant organic matter input but also by microbial activities (Deng et al., 2021). Soil microorganisms participate in all aspects of C and N dynamics, regulate the formation of soil organic matter and release extracellular enzymes through C and N turnover (Ren et al., 2017). Meanwhile, microbial decomposition of soil organic matter can cause CO_2 efflux and gaseous N emissions by producing C and N-degrading extracellular enzymes (Ren et al., 2017). Interestingly, both microbial and extracellular enzyme activities appear to be more sensitive to soil water content and temperature than to their nutritional resources (Nielsen and Ball, 2015). Therefore, drought can alter soil microbial composition and enzyme activities, then affect the soil C and N balance (Ren et al., 2017), and finally influence both the belowground and aboveground performances of plants in response to drought.

However, previous studies have no consistent results on the relationship between CG and resource availability. Some studies suggested that plants tend to overcompensate more frequently under unfavorable growth conditions (Coughenour et al., 1990; Hawkes and Sullivan, 2001). In contrast, some researcher insisted that CG only occur under abundant even optimal conditions (Belsky et al., 1993), known as the compensatory continuum hypothesis (CCH). Furthermore, even for the same functional type, CG varies among different resource levels (Hawkes and Sullivan, 2001). For instance, *Leymus chinensis* had less CG under dry conditions compared with wet conditions, while it is opposite for *Stipa krylovii* (Van Staalduinen and Anten, 2005). Besides, the chronic nutrient addition in the Great Plains reduced grassland drought resistance and increased drought resilience regardless of annual-dominated or perennial-dominated grassland (Bharath et al., 2020). Based on CCH, a limited resource model (LRM) was once introduced to explain the range of observed effects of resource levels on and prediction for compensation for herbivory (Wise and Abrahamson, 2005), which suggested that CG depends on the type of resource and disturbance intensity (e.g., drought, heat stress, herbivore) under consideration (Metcalfe and Monaghan, 2001; Michael and Warren, 2007). The LRM model introduced the roles of limiting and non-limiting resources, and analyzed which resource was affected by the disturbance. If the disturbance mainly affects the first limiting resource, then higher CG is expected to occur at high resource availability. The application of the LRM model needs to take certain experimental requirements into account, including full factorial experimental design, consistent levels of disturbance across environments, determining whether a focal resource is liming plant fitness, and identifying the resource affected by disturbance (Wise and Abrahamson, 2005). Even though, the application of LRM to predict CG in response to drought still remain with many uncertainties and need to be tested in future study, with the complex backgrounds of climate region, grassland type, and species diversity (Monaghan, 2008).

Underlying mechanisms of compensatory growth in response to drought

The CG response of grassland to drought is a synthesis result of plant, root, and soil feedback (Figure 2). With respect to aboveground plant responses, CG under drought conditions may be triggered by the recovery of existing individuals within a grassland ecosystem, or by compensatory dynamics where particular individuals or species increase in abundance to counterbalance reductions in other individuals or species (Tilman and Downing, 1994). Compensatory effects, arising from various responses of different plants or functional groups to perturbations, are an important mechanism for sustaining ecosystem stability (Gonzalez and Loreau, 2009; Song and Yu, 2015). Besides, compensatory changes in species population in response to environmental fluctuations can maintain an appreciated steady state between the rate of resource supply and its consumption (Morgan Ernest and Brown, 2001). The difference in performance between functional traits is a good indicator of plant growth strategy in response to post-drought. For example, *Leymus chinensis* exhibited a greater capacity for CG than *Stipa krylovii*, because it has a stronger ability in storing carbohydrates and reallocating them after leaf losses, and a more positive effect of defoliation on light penetration through the canopy (Van Staalduinen and Anten, 2005). The CG of the different grassland ecosystems responding to drought may occur through two fundamentally different biotic mechanisms (Wilcox et al., 2020): (1) drought-tolerant plants increase in abundance and functionally compensate for declines in drought-intolerant species, which is called compensatory dynamics (Gonzalez and Loreau, 2009; Hoover et al., 2014); (2) all individuals within the community recover fully after drought, which is defined as physiological compensatory (Connell and Ghedini, 2015). Physiological compensation often happens with short-term and (or) moderate drought, while compensatory dynamics are more likely to occur under long-term and (or) extreme drought by rearranging species abundances (Smith, 2011).

Nevertheless, plant roots and microbial community also play a key role in mediating the post-drought responses (Figure 2). Root traits, like specific root length, root dry matter content, and toot

10.3389/fpls.2022.1004553

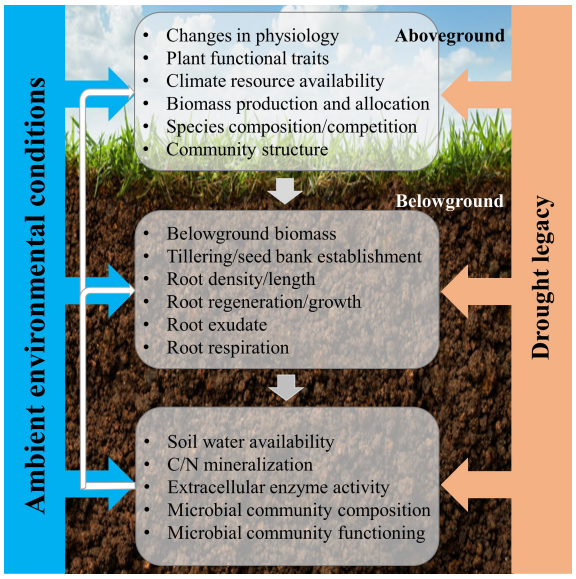

FIGURE 2
Conceptual framework of the responses of aboveground and belowground processes to post-drought for compensatory growth. The three main three components include aboveground plant, root, and soil microorganism, which are determined by plant community trait, soil type and climate (ambient environmental conditions). The effects of drought on the three components are achieved individually, but we hypothesize that the responses of the aboveground plant determine the responses of root after drought, thereby, the microbial community responses, which react on aboveground plant growth, community composition, ultimately, ecosystem stability and function (Williams and De Vries, 2020).

tissue density, are important for shaping post-drought responses and vary across a range of grassland species with different growth strategies (De Vries et al., 2016; Williams and De Vries, 2020). In addition, root exudates form a pathway for plant-microbial communication and have the potential to influence plant tolerance and recovery during and/or after drought (Williams and De Vries, 2020). The drought-induced changes in the quality of root exudates might have implications for the recovery of plants and microbes (De Vries et al., 2019). Besides, the structure of the microbial community can determine the functional responses of the grassland ecosystems, through the expression of functional genes. Furthermore, CG was almost certainly promoted by a drought-induced increase in soil N availability as a higher mineral N supply rate appeared in the month after rewetting, and then increased plant nitrogen content two months after rewetting (Mackie et al., 2019). Due to an increase in plant-available N, the plant photosynthetic activities are upregulated during post-drought, and then drive a short-term increase in forage quality (Bloor and Bardgett, 2012; Niboyet et al., 2017). Therefore, this field of research will need to be driven forward by studying general mechanisms, focusing on mechanisms that link below- and aboveground processes and responses (Figure 2).

Limitations and suggestions for future research

With growing concerns about grassland vulerability, a comprehensive understanding of grassland response to drought is becoming increasingly important. Previous studies have mainly focused on the plant or ecosystem responses during drought, however, there is still limited understanding of the period after drought. Here, we reviewed compensatory growth across grassland types, drought characteristics, and resource availabilities. Besides, the underlying mechanisms of CG were also summed up. However, there is still a lot of work to achieve the ultimate target on how to accurately quantify CG and predict its direction and strength under changing ambient environmental conditions. The followings are some suggestions for further research on CG.

Firstly, the assessment method of CG mentioned above implicitly assumes that the reference growth level (the pre-defined post-drought period or the historic norm status) is where the drought legacy ends. However, the legacy of drought might be extending far beyond a return to reference growth level under some conditions (Ingrisch and Bahn, 2018; Ovenden et al., 2021). Thus, when CG is activated and then how long it will take are still debatable, which need to be finely defined in future study. Besides, as plant functional traits play an important role in determining net carbon assimilation and allocation, therefore, a better understanding of the post-drought recovery performance of plant functional traits could improve our ability to predict grassland ecosystem production in a rapidly changing climate (Yin and Bauerle, 2017). In order to improve the evaluation accuracy of CG, filtering out suitable plant-soil functional traits may be a good pathway (Figure 2).

Secondly, the adverse impacts of a single drought might be reflected in plant water and nutrient acquisition than in ecosystem carbon cycling, while both sides could be emphasized by a second drought or repeated droughts (Slette et al., 2022). The potential consequences of repeated drought on CG may range from increased adaptation to increased sensitivity, which remains unclear (Slette et al., 2022). Some studies have suggested that the adaptation of soil microbial communities to a previous drought can increase the drought tolerance of plants in facing a subsequent drought event (Lau and Lennon, 2012; Meisner et al., 2013). Besides, drought-exposure history could increase complementarity between plant species in response to future droughts (Chen et al., 2022). Due to more frequent droughts are expected in many parts of the world in the future, studies on the CG response to repeated droughts are needed to improve our knowledge of grassland stability.

Thirdly, even though extensive studies have been focusing on the effects of drought on grasslands, there is limited understanding of the period after drought due to a lack of studies on belowground responses and an undue emphasis on

aboveground ecosystem responses (Vilonen et al., 2022). ANPP is the most common indicator or function for evaluating the aboveground ecosystem responses to drought (Hoover et al., 2014; Knapp et al., 2015), because aboveground biomass is easier to obtain than belowground biomass. In fact, grasslands allocate a substantial portion of total net primary production to roots and then store most of their carbon belowground (Hui and Jackson, 2006; Silver et al., 2010). Belowground responses, such as BNPP and soil CO_2 flux, are of particular importance in determining the size of the soil carbon pool (Post et al., 1982; Slette et al., 2021). Previous studies have demonstrated that the CG of ANPP and BNPP is different over time, like average precipitation amounts are sufficient for CG in ANPP after extreme drought, while CG in BNPP might be more resource-demanding (Slette et al., 2022). Due to the different patterns of ANPP and BNPP response to changes in water availability, belowground processes and their underlying mechanisms should be addressed in future work modeling ecosystem responses to climate change (Denton et al., 2016).

Conclusion

Overall, in light of the persistence and intensification of climate change, the responses of ecosystems to drought need to be paid more attention. In past decades, a series of analogous compensatory growth of net primary productivity and community stability to drought disturbance in different grassland ecosystems were discussed based on effective indicators, like recovery and resilience. In this review, we discussed compensatory growth across different grassland ecosystems and drought characteristics, explained the effect of resource availability on compensatory growth, and summed up the mechanism by which compensatory growth may occur. The review suggests that the CG is likely to be primarily due to the different responses of plant functional groups and their interactions with soil microbes to water availability. We propose identifying the starting time and duration of compensatory growth; better describing the symbol of CG with plant-soil functional traits; conducting more research on the plant-soil feedback and the decoupling of above- and belowground processes. These proposed researches would expand our understanding of compensatory growth, and increase our ability to evaluate the stability and sustainability of grassland ecosystems in the face of climate change.

Author contributions

HZ, LH, XL, GY, YW and XW jointly conceived and wrote the paper. All authors contributed to the article and approved the submitted version.

Funding

This work was financially supported by the Second Tibetan Plateau Scientific Expedition and Research (STEP) program (2019QZKK0106) and the National Natural Science Foundation of China (42205126, 41975145, 41775108).

Acknowledgments

The authors thank the reviewers for the constructive comments on an earlier version of this manuscript.

Conflict of interest

The authors declare that the research was conducted in the absence of any commercial or financial relationships that could be construed as a potential conflict of interest.

Publisher's note

References

Báez, S., Collins, S. L., Pockman, W. T., Johnson, J. E., and Small, E. E. (2013). Effects of experimental rainfall manipulations on chihuahuan desert grassland and shrubland plant communities. *Oecologia* 172, 1117–1127. doi: 10.1007/s00442-012-2552-0

Belsky, A. J. (1986). Does herbivory benefit plants? a review of the evidence. *Am. Nat.* 127, 870–892. doi: 10.1086/284531

Belsky, A. J., Carson, W. P., Jensen, C. L., and Fox, G. A. (1993). Overcompensation by plants: Herbivore optimization or red herring? *Evol. Ecol.* 7, 109–121. doi: 10.1007/BF01237737

Bharath, S., Borer, E. T., Biederman, L. A., Blumenthal, D. M., Fay, P. A., Gherardi, L. A., et al. (2020). Nutrient addition increases grassland sensitivity to droughts. *Ecology* 101, e02981. doi: 10.1002/ecy.2981

Bloor, J. M. G., and Bardgett, R. D. (2012). Stability of above-ground and below-ground processes to extreme drought in model grassland ecosystems: Interactions with plant species diversity and soil nitrogen availability. *Perspect. Plant Ecol. Evol. Syst.* 14, 193–204. doi: 10.1016/j.ppees.2011.12.001

Borken, W., and Matzner, E. (2009). Reappraisal of drying and wetting effects on c and n mineralization and fluxes in soils. *Glob Chang Biol.* 15, 808–824. doi: 10.1111/j.1365-2486.2008.01681.x

Bowman, D. M., Perry, G. L., and Marston, J. B. (2015). Feedbacks and landscape-level vegetation dynamics. *Trends Ecol. Evol.* 30, 255–260. doi: 10.1016/j.tree.2015.03.005

Breshears, D. D., Cobb, N. S., Rich, P. M., Price, K. P., Allen, C. D., Balice, R. G., et al. (2005). Regional vegetation die-off in response to global-change-type drought. *Proc. Natl. Acad. Sci. U.S.A.* 102, 15144–15148. doi: 10.1073/pnas.0505734102

Carlsson, M., Merten, M., Kayser, M., Isselstein, J., and Wrage-Mönnig, N. (2017). Drought stress resistance and resilience of permanent grasslands are shaped by functional group composition and n fertilization. *Agric. Ecosyst. Environ.* 236, 52–60. doi: 10.1016/j.agee.2016.11.009

Carlyle, C. N., Fraser, L. H., and Turkington, R. (2014). Response of grassland biomass production to simulated climate change and clipping along an elevation gradient. *Oecologia* 174, 1065–1073. doi: 10.1007/s00442-013-2833-2

Carroll, C. J. W., Slette, I. J., Griffin-Nolan, R. J., Baur, L. E., Hoffman, A. M., Denton, E. M., et al. (2021). Is a drought a drought in grasslands? productivity responses to different types of drought. *Oecologia* 197, 1017–1026. doi: 10.1007/s00442-020-04793-8

Cenzano, A. M., Varela, M. C., Bertiller, M. B., and Luna, M. V. (2013). Effect of drought on morphological and functional traits of poa ligularis and pappostipa speciosa, native perennial grasses with wide distribution in Patagonian rangelands, Argentina. *Aust. J. Bot.* 61, 383. doi: 10.1071/bt12298

Chen, Y., Vogel, A., Wagg, C., Xu, T., Iturrate-Garcia, M., Scherer-Lorenzen, M., et al. (2022). Drought-exposure history increases complementarity between plant species in response to a subsequent drought. *Nat. Commun.* 13, 3217. doi: 10.1038/s41467-022-30954-9

Chen, N., Zhang, Y., Zu, J., Zhu, J., Zhang, T., Huang, K., et al. (2020). The compensation effects of post-drought regrowth on earlier drought loss across the tibetan plateau grasslands. *Agric. For. Meteorol.* 281, 107822. doi: 10.1016/j.agrformet.2019.107822

Cherwin, K., and Knapp, A. (2012). Unexpected patterns of sensitivity to drought in three semi-arid grasslands. *Oecologia* 169, 845–852. doi: 10.1007/s00442-011-2235-2

Connell, S. D., and Ghedini, G. (2015). Resisting regime-shifts: the stabilising effect of compensatory processes. *Trends Ecol. Evol.* 30, 513–515. doi: 10.1016/j.tree.2015.06.014

Cook, B. I., Ault, T. R., and Smerdon, J. E. (2015). Unprecedented 21st century drought risk in the American southwest and central plains. *Sci. Adv.* 1, e1400082. doi: 10.1126/sciadv.1400082

Coughenour, M. B., Detling, J. K., Bamberg, I. E., and Mugambi, M. M. (1990). Production and nitrogen responses of the African dwarf shrub indigofera spinosa to defoliation and water limitation. *Oecologia* 83, 546–552. doi: 10.1007/BF00317208

Dai, A. (2012). Increasing drought under global warming in observations and models. *Nat. Clim. Change* 3, 52–58. doi: 10.1038/nclimate1633

Dechant, C. M., and Moradkhani, H. (2015). Analyzing the sensitivity of drought recovery forecasts to land surface initial conditions. *J. Hydrol.* 526, 89–100. doi: 10.1016/j.jhydrol.2014.10.021

De Keersmaecker, W., Van Rooijen, N., Lhermitte, S., Tits, L., Schaminée, J., Coppin, P., et al. (2016). Species-rich semi-natural grasslands have a higher resistance but a lower resilience than intensively managed agricultural grasslands in response to climate anomalies. *J. Appl. Ecol.* 53, 430–439. doi: 10.1111/1365-2664.12595

Deng, L., Peng, C., Kim, D.-G., Li, J., Liu, Y., Hai, X., et al. (2021). Drought effects on soil carbon and nitrogen dynamics in global natural ecosystems. *Earth Sci. Rev.* 214, 103501. doi: 10.1016/j.earscirev.2020.103501

Denton, E. M., Dietrich, J. D., Smith, M. D., and Knapp, A. K. (2016). Drought timing differentially affects above- and belowground productivity in a mesic grassland. *Plant Ecol.* 218, 317–328. doi: 10.1007/s11258-016-0690-x

De Vries, F. T., Brown, C., and Stevens, C. J. (2016). Grassland species root response to drought: consequences for soil carbon and nitrogen availability. *Plant Soil* 409, 297–312. doi: 10.1007/s11104-016-2964-4

De Vries, F. T., Liiri, M. E., Bjørnlund, L., Bowker, M. A., Christensen, S., Setälä, H. M., et al. (2012a). Land use alters the resistance and resilience of soil food webs to drought. *Nat. Clim. Change* 2, 276–280. doi: 10.1038/nclimate1368

De Vries, F. T., Liiri, M. E., Bjørnlund, L., Setälä, H. M., Christensen, S., and Bardgett, R. D. (2012b). Legacy effects of drought on plant growth and the soil food web. *Oecologia* 170, 821–833. doi: 10.1007/s00442-012-2331-y

De Vries, F. T., Williams, A., Stringer, F., Willcocks, R., Mcewing, R., Langridge, H., et al. (2019). Changes in root-exudate-induced respiration reveal a novel mechanism through which drought affects ecosystem carbon cycling. *New Phytol.* 224, 132–145. doi: 10.1111/nph.16001

Dixon, A. P., Faber-Langendoen, D., Josse, C., Morrison, J., Loucks, C. J., and Ebach, M. (2014). Distribution mapping of world grassland types. *J. Biogeogr.* 41, 2003–2019. doi: 10.1111/jbi.12381

Dumont, B., Andueza, D., Niderkorn, V., Lüscher, A., Porqueddu, C., and Picon-Cochard, C. (2015). A meta-analysis of climate change effects on forage quality in grasslands: specificities of mountain and Mediterranean areas. *Grass Forage Sci.* 70, 239–254. doi: 10.1111/gfs.12169

Elmqvist, T., Folke, C., Nyström, M., Peterson, G., Bengtsson, J., Walker, B., et al. (2003). Response diversity, ecosystem change, and resilience. *Front. Ecol. Environ.* 1, 488–494. doi: 10.1890/1540-9295(2003)001[0488:RDECAR]2.0.CO;2

Estiarte, M., Vicca, S., Peñuelas, J., Bahn, M., Beier, C., Emmett, B. A., et al. (2016). Few multiyear precipitation–reduction experiments find a shift in the productivity–precipitation relationship. *Glob Chang Biol.* 22, 2570–2581. doi: 10.1111/gcb.13269

Frank, D., Reichstein, M., Bahn, M., Thonicke, K., Frank, D., Mahecha, M. D., et al. (2015). Effects of climate extremes on the terrestrial carbon cycle: concepts, processes and potential future impacts. *Glob Chang Biol.* 21, 2861–2880. doi: 10.1111/gcb.12916

Fry, E. L., Johnson, G. N., Hall, A. L., Pritchard, W. J., Bullock, J. M., and Bardgett, R. D. (2018). Drought neutralises plant-soil feedback of two mesic grassland forbs. *Oecologia* 186, 1113–1125. doi: 10.1007/s00442-018-4082-x

Gessler, A., Bottero, A., Marshall, J., and Arend, M. (2020). The way back: recovery of trees from drought and its implication for acclimation. *New Phytol.* 228, 1704–1709. doi: 10.1111/nph.16703

Gonzalez, A., and Loreau, M. (2009). The causes and consequences of compensatory dynamics in ecological communities. *Annu. Rev. Ecol. Evol. Syst.* 40, 393–414. doi: 10.1146/annurev.ecolsys.39.110707.173349

Griffin-Nolan, R. J., Carroll, C. J. W., Denton, E. M., Johnston, M. K., Collins, S. L., Smith, M. D., et al. (2018). Legacy effects of a regional drought on aboveground net primary production in six central US grasslands. *Plant Ecol.* 219, 505–515. doi: 10.1007/s11258-018-0813-7

Grman, E., Lau, J. A., Schoolmaster, D. R.Jr., and Gross, K. L. (2010). Mechanisms contributing to stability in ecosystem function depend on the environmental context. *Ecol. Lett.* 13, 1400–1410. doi: 10.1111/j.1461-0248.2010.01533.x

Hawkes, C. V., and Sullivan, J. J. (2001). The impact of herbivory on plants in different resource conditions: A meta-analysis. *Ecology* 82, 2045–2058. doi: 10.1890/0012-9658(2001)082[2045:TIOHOP]2.0.CO;2

Hoover, D. L., Knapp, A. K., and Smith, M. D. (2014). Resistance and resilience of a grassland ecosystem to climate extremes. *Ecology* 95, 2646–2656. doi: 10.1890/13-2186.1

Hoover, D. L., Wilcox, K. R., and Young, K. E. (2018). Experimental droughts with rainout shelters: a methodological review. *Ecosphere* 9, e02088. doi: 10.1002/ecs2.2088

Hossain, M. L., and Li, J. (2021). NDVI-based vegetation dynamics and its resistance and resilience to different intensities of climatic events. *Glob. Ecol. Conserv.* 30, e01768. doi: 10.1016/j.gecco.2021.e01768

Hufkens, K., Keenan, T. F., Flanagan, L. B., Scott, R. L., Bernacchi, C. J., Joo, E., et al. (2016). Productivity of north American grasslands is increased under future climate scenarios despite rising aridity. *Nat. Clim. Change* 6, 710–714. doi: 10.1038/nclimate2942

Hui, D., and Jackson, R. B. (2006). Geographical and interannual variability in biomass partitioning in grassland ecosystems: a synthesis of field data. *New Phytol.* 169, 85–93. doi: 10.1111/j.1469-8137.2005.01569.x

Huxman, T. E., Snyder, K. A., Tissue, D., Leffler, A. J., Ogle, K., Pockman, W. T., et al. (2004). Precipitation pulses and carbon fluxes in semiarid and arid ecosystems. *Oecologia* 141, 254–268. doi: 10.1007/s00442-004-1682-4

Ingrisch, J., and Bahn, M. (2018). Towards a comparable quantification of resilience. *Trends Ecol. Evol.* 33, 251–259. doi: 10.1016/j.tree.2018.01.013

IPCC (2013). "Climate change 2013," in *The physical science basis: Working group I contribution to the fifth assessment report of the intergovernmental panel on climate change* (Cambridge: Cambridge University Press).

Jiao, T., Williams, C. A., De Kauwe, M. G., Schwalm, C. R., and Medlyn, B. E. (2021). Patterns of post-drought recovery are strongly influenced by drought duration, frequency, post-drought wetness, and bioclimatic setting. *Glob Chang Biol.* 27, 4630–4643. doi: 10.1111/gcb.15788

Kahl, S. M., Lenhard, M., Joshi, J., and Teller, B. (2019). Compensatory mechanisms to climate change in the widely distributed species silene vulgaris. *J. Ecol.* 107, 1918–1930. doi: 10.1111/1365-2745.13133

Kaisermann, A., De Vries, F. T., Griffiths, R. I., and Bardgett, R. D. (2017). Legacy effects of drought on plant-soil feedbacks and plant-plant interactions. *New Phytol.* 215, 1413–1424. doi: 10.1111/nph.14661

Kinugasa, T., Tsunekawa, A., and Shinoda, M. (2012). Increasing nitrogen deposition enhances post-drought recovery of grassland productivity in the Mongolian steppe. *Oecologia* 170, 857–865. doi: 10.1007/s00442-012-2354-4

Knapp, A. K., Beier, C., Briske, D. D., Classen, A. T., Luo, Y., Reichstein, M., et al. (2008). Consequences of more extreme precipitation regimes for terrestrial ecosystems. *Bioscience* 58, 811–821. doi: 10.1641/b580908

Knapp, A. K., Carroll, C. J. W., Denton, E. M., La Pierre, K. J., Collins, S. L., and Smith, M. D. (2015). Differential sensitivity to regional-scale drought in six central US grasslands. *Oecologia* 177, 949–957. doi: 10.1007/s00442-015-3233-6

Knapp, A. K., Fay, P. A., Blair, J. M., Collins, S. L., Smith, M. D., Carlisle, J. D., et al. (2002). Rainfall variability, carbon cycling, and plant species diversity in a mesic grassland. *Science* 298, 2202–2205. doi: 10.1126/science.1076347

Knapp, A. K., and Smith, M. D. (2001). Variation among biomes in temporal dynamics of aboveground primary production. *Science* 291, 481–484. doi: 10.1126/science.291.5503.481

Lau, J. A., and Lennon, J. T. (2012). Rapid responses of soil microorganisms improve plant fitness in novel environments. *Proc. Natl. Acad. Sci. U. S. A.* 109, 14058–14062. doi: 10.1073/pnas.1202319109

Li, C., Barclay, H., Roitberg, B., and Lalonde, R. (2020). Forest productivity enhancement and compensatory growth: A review and synthesis. *Front. Plant Sci.* 11. doi: 10.3389/fpls.2020.575211

Li, C., Barclay, H., Roitberg, B., and Lalonde, R. (2021). Ecology and prediction of compensatory growth: From theory to application in forestry. *Front. Plant Sci.* 12. doi: 10.3389/fpls.2021.655417

Li, L., Qian, R., Liu, W., Wang, W., Biederman, J. A., Zhang, B., et al. (2022). Drought timing influences the sensitivity of a semiarid grassland to drought. *Geoderma* 412, 115714. doi: 10.1016/j.geoderma.2022.115714

Liu, X., Zhu, Z., Yu, M., and Liu, X. (2021). Drought-induced productivity and economic losses in grasslands from inner Mongolia vary across vegetation types. *Reg. Environ. Change* 21, 1–12. doi: 10.1007/s10113-021-01789-9

Macdougall, A. S., Mccann, K. S., Gellner, G., and Turkington, R. (2013). Diversity loss with persistent human disturbance increases vulnerability to ecosystem collapse. *Nature* 494, 86–89. doi: 10.1038/nature11869

Macgillivray, C. W., Grime, J. P., and The Integrated Screening Programme, T. (1995). Testing predictions of the resistance and resilience of vegetation subjected to extreme events. *Funct. Ecol.* 9, 640–649. doi: 10.2307/2390156

Mackie, K. A., Zeiter, M., Bloor, J. M. G., Stampfli, A., and De Vries, F. (2019). Plant functional groups mediate drought resistance and recovery in a multisite grassland experiment. *J. Ecol.* 107, 937–949. doi: 10.1111/1365-2745.13102

Ma, W., Liang, X., Wang, Z., Luo, W., Yu, Q., and Han, X. (2020). Resistance of steppe communities to extreme drought in northeast China. *Plant Soil*, 473, 181–194. doi: 10.1007/s11104-020-04767-y

Mangel, M., and Munch, S. B. (2005). A life-history perspective on short- and long-term consequences of compensatory growth. *Am. Nat.* 166, E155–E176. doi: 10.1086/444439

Matos, I. S., Menor, I. O., Rifai, S. W., Rosado, B. H. P., and Grytnes, J. A. (2019). Deciphering the stability of grassland productivity in response to rainfall manipulation experiments. *Glob. Ecol. Biogeogr.* 29, 558–572. doi: 10.1111/geb.13039

Mcnaughton, S. J. (1983). Compensatory plant growth as a response to herbivory. *Oikos* 40, 329–336. doi: 10.2307/3544305

Meisner, A., De Deyn, G. B., De Boer, W., and van der Putten, W. H. (2013). Soil biotic legacy effects of extreme weather events influence plant invasiveness. *Proc. Natl. Acad. Sci. U. S. A.* 110, 9835–9838. doi: 10.1073/pnas.1300922110

Meng, B., Shi, B., Zhong, S., Chai, H., Li, S., Wang, Y., et al. (2019). Drought sensitivity of aboveground productivity in leymus chinensis meadow steppe depends on drought timing. *Oecologia* 191, 685–696. doi: 10.1007/s00442-019-04506-w

Metcalfe, N. B., and Monaghan, P. (2001). Compensation for a bad start: grow now, pay later? *Trends Ecol. Evol.* 16, 254–260. doi: 10.1016/S0169-5347(01)02124-3

Michael, J. W., and Warren, G. A. (2007). Effects of resource availability on tolerance of herbivory: A review and assessment of three opposing models. *Am. Nat.* 169, 443–454. doi: 10.1086/512044

Monaghan, P. (2008). Early growth conditions, phenotypic development and environmental change. *Philos. Trans. R. Soc Lond. B Biol. Sci.* 363, 1635–1645. doi: 10.1098/rstb.2007.0011

Morgan Ernest, S. K., and Brown, J. H. (2001). Homeostasis and compensation: The role of species and resources in ecosystem stability. *Ecology* 82, 2118–2132. doi: 10.1890/0012-9658(2001)082[2118:HACTRO]2.0.CO;2

Mori, A. S., Furukawa, T., and Sasaki, T. (2013). Response diversity determines the resilience of ecosystems to environmental change. *Biol. Rev. Camb. Philos. Soc* 88, 349–364. doi: 10.1111/brv.12004

Niboyet, A., Bardoux, G., Barot, S., and Bloor, J. M. G. (2017). Elevated CO_2 mediates the short-term drought recovery of ecosystem function in low-diversity grassland systems. *Plant Soil* 420, 289–302. doi: 10.1007/s11104-017-3377-8

Nielsen, U. N., and Ball, B. A. (2015). Impacts of altered precipitation regimes on soil communities and biogeochemistry in arid and semi-arid ecosystems. *Glob Chang Biol.* 21, 1407–1421. doi: 10.1111/gcb.12789

Nippert, J. B., and Knapp, A. K. (2007). Soil water partitioning contributes to species coexistence in tallgrass prairie. *Oikos* 116, 1017–1029. doi: 10.1111/j.0030-1299.2007.15630.x

Niu, S., Luo, Y., Li, D., Cao, S., Xia, J., Li, J., et al. (2014). Plant growth and mortality under climatic extremes: An overview. *Environ. Exp. Bot.* 98, 13–19. doi: 10.1016/j.envexpbot.2013.10.004

Oliver, T. H., Heard, M. S., Isaac, N. J. B., Roy, D. B., Procter, D., Eigenbrod, F., et al. (2015). Biodiversity and resilience of ecosystem functions. *Trends Ecol. Evol.* 30, 673–684. doi: 10.1016/j.tree.2015.08.009

Ovenden, T. S., Perks, M. P., Clarke, T. K., Mencuccini, M., and Jump, A. S. (2021). Life after recovery: Increased resolution of forest resilience assessment sheds new light on post-drought compensatory growth and recovery dynamics. *J. Ecol.* 109, 3157–3170. doi: 10.1111/1365-2745.13576

Parton, W., Morgan, J., Smith, D., Del Grosso, S., Prihodko, L., Lecain, D., et al. (2012). Impact of precipitation dynamics on net ecosystem productivity. *Glob Chang Biol.* 18, 915–927. doi: 10.1111/j.1365-2486.2011.02611.x

Post, W. M., Emanuel, W. R., Zinke, P. J., and Stangenberger, A. G. (1982). Soil carbon pools and world life zones. *Nature* 298, 156–159. doi: 10.1038/298156a0

Pugnaire, F. I., Morillo, J. A., Peñuelas, J., Reich, P. B., Bardgett, R. D., Gaxiola, A., et al. (2019). Climate change effects on plant-soil feedbacks and consequences for biodiversity and functioning of terrestrial ecosystems. *Sci. Adv.* 5, eaaz1834. doi: 10.1126/sciadv.aaz1834

Putten, W. H., Bradford, M. A., Pernilla Brinkman, E., Voorde, T. F. J., Veen, G. F., and Bailey, J. K. (2016). Where, when and how plant–soil feedback matters in a changing world. *Funct. Ecol.* 30, 1109–1121. doi: 10.1111/1365-2435.12657

Ren, C., Zhao, F., Shi, Z., Chen, J., Han, X., Yang, G., et al. (2017). Differential responses of soil microbial biomass and carbon-degrading enzyme activities to altered precipitation. *Soil Biol. Biochem.* 115, 1–10. doi: 10.1016/j.soilbio.2017.08.002

Ruppert, J. C., Harmoney, K., Henkin, Z., Snyman, H. A., Sternberg, M., Willms, W., et al. (2015). Quantifying drylands' drought resistance and recovery: the importance of drought intensity, dominant life history and grazing regime. *Glob Chang Biol.* 21, 1258–1270. doi: 10.1111/gcb.12777

Saeidnia, F., Majidi, M. M., Mirlohi, A., Spanani, S., Karami, Z., and Abdollahi Bakhtiari, M. (2020). A genetic view on the role of prolonged drought stress and mating systems on post-drought recovery, persistence and drought memory of orchardgrass (*Dactylis glomerata l.*). *Euphytica* 216. doi: 10.1007/s10681-020-02624-8

Schirpke, U., Kohler, M., Leitinger, G., Fontana, V., Tasser, E., and Tappeiner, U. (2019). Future impacts of changing land-use and climate on ecosystem services of mountain grassland and their resilience. *Ecosyst. Serv.* 26, 79–94. doi: 10.1016/j.ecoser.2017.06.008

Silver, W. L., Ryals, R., and Eviner, V. (2010). Soil carbon pools in california's annual grassland ecosystems. *Rangel Ecol. Manag* 63, 128–136. doi: 10.2111/REM-D-09-00106.1

Slette, I. J., Blair, J. M., Fay, P. A., Smith, M. D., and Knapp, A. K. (2021). Effects of compounded precipitation pattern intensification and drought occur belowground in a mesic grassland. *Ecosystems* 25, 1265–1278. doi: 10.1007/s10021-021-00714-9

Slette, I. J., Hoover, D. L., Smith, M. D., and Knapp, A. K. (2022). Repeated extreme droughts decrease root production, but not the potential for post-drought recovery of root production, in a mesic grassland. *Oikos*. doi: 10.1111/oik.08899

Smith, M. D. (2011). An ecological perspective on extreme climatic events: a synthetic definition and framework to guide future research. *J. Ecol.* 99, 656–663. doi: 10.1111/j.1365-2745.2011.01798.x

Song, M. H., and Yu, F. H. (2015). Reduced compensatory effects explain the nitrogen-mediated reduction in stability of an alpine meadow on the Tibetan plateau. *New Phytol.* 207, 70–77. doi: 10.1111/nph.13329

Stampfli, A., Bloor, J. M. G., Fischer, M., and Zeiter, M. (2018). High land-use intensity exacerbates shifts in grassland vegetation composition after severe experimental drought. *Glob Chang Biol.* 24, 2021–2034. doi: 10.1111/gcb.14046

Stuart-Haentjens, E., De Boeck, H. J., Lemoine, N. P., Mand, P., Kroel-Dulay, G., Schmidt, I. K., et al. (2018). Mean annual precipitation predicts primary production resistance and resilience to extreme drought. *Sci. Total Environ.* 636, 360–366. doi: 10.1016/j.scitotenv.2018.04.290

Taylor, S. H., Ripley, B. S., Woodward, F. I., and Osborne, C. P. (2011). Drought limitation of photosynthesis differs between C(3) and C(4) grass species in a comparative experiment. *Plant Cell Environ.* 34, 65–75. doi: 10.1111/j.1365-3040.2010.02226.x

Tello-García, E., Huber, L., Leitinger, G., Peters, A., Newesely, C., Ringler, M.-E., et al. (2020). Drought- and heat-induced shifts in vegetation composition impact biomass production and water use of alpine grasslands. *Environ. Exp. Bot.* 169, 103921. doi: 10.1016/j.envexpbot.2019.103921

Tielborger, K., Bilton, M. C., Metz, J., Kigel, J., Holzapfel, C., Lebrija-Trejos, E., et al. (2014). Middle-Eastern plant communities tolerate 9 years of drought in a multi-site climate manipulation experiment. *Nat. Commun.* 5, 5102. doi: 10.1038/ncomms6102

Tilman, D., and Downing, J. A. (1994). Biodiversity and stability in grasslands. *Nature* 367, 363–365. doi: 10.1038/367363a0

Trenberth, K. E., Dai, A., van der Schrier, G., Jones, P. D., Barichivich, J., Briffa, K. R., et al. (2014). Global warming and changes in drought. *Nat. Clim. Change* 4, 17–22. doi: 10.1038/nclimate2067

Van Staalduinen, M. A., and Anten, N. P. (2005). Differences in the compensatory growth of two co-occurring grass species in relation to water availability. *Oecologia* 146, 190–199. doi: 10.1007/s00442-005-0225-y

Van Staalduinen, M. A., Dobarro, I., and Peco, B. (2009). Interactive effects of clipping and nutrient availability on the compensatory growth of a grass species. *Plant Ecol.* 208, 55–64. doi: 10.1007/s11258-009-9686-0

Vicente-Serrano, S. M., Quiring, S. M., Peña-Gallardo, M., Yuan, S., and Domínguez-Castro, F. (2020). A review of environmental droughts: Increased risk under global warming? *Earth Sci. Rev.* 201, 102953. doi: 10.1016/j.earscirev.2019.102953

Vilonen, L., Ross, M., and Smith, M. D. (2022). What happens after drought ends: synthesizing terms and definitions. *New Phytol.* 235, 420–431. doi: 10.1111/nph.18137

Vogel, A., Scherer-Lorenzen, M., and Weigelt, A. (2012). Grassland resistance and resilience after drought depends on management intensity and species richness. *PLoS One* 7, e36992. doi: 10.1371/journal.pone.0036992

Volaire, F. (2003). Seedling survival under drought differs between an annual (*Hordeum vulgare*) and a perennial grass (*Dactylis glomerata*). *New Phytol.* 160, 501–510. doi: 10.1046/j.1469-8137.2003.00906.x

Volaire, F., Barkaoui, K., and Norton, M. (2014). Designing resilient and sustainable grasslands for a drier future: Adaptive strategies, functional traits and biotic interactions. *Eur. J. Agron.* 52, 81–89. doi: 10.1016/j.eja.2013.10.002

Wellstein, C., Poschlod, P., Gohlke, A., Chelli, S., Campetella, G., Rosbakh, S., et al. (2017). Effects of extreme drought on specific leaf area of grassland species: A meta-analysis of experimental studies in temperate and sub-Mediterranean systems. *Glob Chang Biol.* 23, 2473–2481. doi: 10.1111/gcb.13662

Wilcox, K. R., Koerner, S. E., Hoover, D. L., Borkenhagen, A. K., Burkepile, D. E., Collins, S. L., et al. (2020). Rapid recovery of ecosystem function following extreme drought in a south African savanna grassland. *Ecology* 101, e02983. doi: 10.1002/ecy.2983

Williams, A., and De Vries, F. T. (2020). Plant root exudation under drought: implications for ecosystem functioning. *New Phytol.* 225, 1899–1905. doi: 10.1111/nph.16223

Wise, M. J., and Abrahamson, W. G. (2005). Beyond the compensatory continuum: environmental resource levels and plant tolerance of herbivory. *Oikos* 109, 417–428. doi: 10.1111/j.0030-1299.2005.13878.x

Wu, J., and Brookes, P. C. (2005). The proportional mineralisation of microbial biomass and organic matter caused by air-drying and rewetting of a grassland soil. *Soil Biol. Biochem.* 37, 507–515. doi: 10.1016/j.soilbio.2004.07.043

Xu, C., Ke, Y., Zhou, W., Luo, W., Ma, W., Song, L., et al. (2021). Resistance and resilience of a semi-arid grassland to multi-year extreme drought. *Ecol. Indic.* 131, 108139. doi: 10.1016/j.ecolind.2021.108139

Yin, J., and Bauerle, T. L. (2017). A global analysis of plant recovery performance from water stress. *Oikos* 126, 1377–1388. doi: 10.1111/oik.04534

Yuan, J., Li, H., and Yang, Y. (2020). The compensatory tillering in the forage grass hordeum brevisubulatum after simulated grazing of different severity. *Front. Plant Sci.* 11. doi: 10.3389/fpls.2020.00792

Zhang, R., Schellenberg, M. P., Han, G., Wang, H., and Li, J. (2018). Drought weakens the positive effects of defoliation on native rhizomatous grasses but enhances the drought-tolerance traits of native caespitose grasses. *Ecol. Evol.* 8, 12126–12139. doi: 10.1002/ece3.4671

frontiers | Frontiers in Plant Science

TYPE Original Research
PUBLISHED 07 December 2022
DOI 10.3389/fpls.2022.1044637

OPEN ACCESS

EDITED BY
Runguo Zang,
Chinese Academy of Forestry, China

REVIEWED BY
Rongzhou Man,
Ontario Ministry of Northern Development, Mines, Natural Resources and Forestry, Canada
Miguel Montoro Girona,
Université du Québec en Abitibi Témiscamingue, Canada

*CORRESPONDENCE
Chao Li
chao.li@NRCan-RNCan.gc.ca

†Retired

‡Deceased

SPECIALTY SECTION
This article was submitted to Functional Plant Ecology, a section of the journal Frontiers in Plant Science

RECEIVED 14 September 2022
ACCEPTED 22 November 2022
PUBLISHED 07 December 2022

CITATION
Li C, Barclay H, Huang S, Roitberg B, Lalonde R, Xu W and Chen Y (2022) Modelling the stand dynamics after a thinning induced partial mortality: A compensatory growth perspective. *Front. Plant Sci.* 13:1044637. doi: 10.3389/fpls.2022.1044637

Modelling the stand dynamics after a thinning induced partial mortality: A compensatory growth perspective

Chao Li[1*], Hugh Barclay[2†‡], Shongming Huang[3], Bernard Roitberg[1,4†], Robert Lalonde[5], Wenli Xu[6] and Yingbing Chen[6]

[1]Canadian Wood Fibre Centre, Canadian Forest Service, Edmonton, AB, Canada, [2]Pacific Forestry Centre, Canadian Forest Service, Victoria, BC, Canada, [3]Alberta Agriculture, Forestry and Rural Economic Development, Edmonton, AB, Canada, [4]Department of Biological Sciences, Simon Fraser University, Burnaby, BC, Canada, [5]Department of Biology, University of British Columbia, Okanagan, Canada, [6]Ministry of Forests, Lands, Natural Resource Operations and Rural Development, Victoria, BC, Canada

Introduction: With increasing forest areas under management, dynamics of managed stands have gained more attention by forest managers and practitioners. Improved understanding on how trees and forest stands would respond to different disturbances is required to predict the dynamics of managed stand.s. Partial mortality commonly occurs in stand development, and different response patterns of trees and stands to partial mortality would govern stand dynamics.

Methods: To investigate the possible response patterns using existing knowledge of growth and yield relationships, we developed TreeCG model, standing for Tree's Compensatory Growth, a state-dependent individual tree-based forest growth model that simulates the compensatory growth of trees after experiencing a partial mortality. The mechanism behind the simulation is the redistribution of resources, including nutrients and space, freed from died trees to surviving trees. The developed new algorithm simplified the simulations of annual growth increments of individual trees over a long period of stand development.

Results: The model was able to reproduce the forest growth patterns displayed in long-term precommercial thinning experiments. The simulated forest growth displayed the process of compensatory growth from under compensation, to compensation-induced-equality, and to overcompensation over time.

Discussion: Our model can simulate stand growth trajectories after different partial harvest regimes at different times and intensities, thus support decisions in best partial harvest strategies. This generic model can be refined with given tree species and specific site conditions to predict stand dynamics after given

partial mortality for any jurisdictions under management. The simulation reassembles growth trajectories of natural stands when no thinning is conducted.

KEYWORDS

over-compensation, partial harvest, productivity evaluation, stand growth trajectory, tree-based state-dependent model, TreeCG, Wood Fibre Value Simulation Model

Introduction

Forest productivity, defined as the accumulated standing forest volume since stand initiation, and often referred to as yield in studies of growth and yield (Avery and Burkhart, 1994; Weetman and Mitchell, 2013), can be influenced by many factors including changes in environmental conditions such as disturbances and climate change (e.g., Shugart et al., 2003; Shell and Bongers, 2020). To improve forest productivity forecasting, it is crucial to understand the response patterns of trees and forest stands to changing environmental conditions to determine the adaptation strategy in sustainable forest management. Climate change, as one particular change in environmental conditions, can influence forest dynamics either directly or indirectly (Crookston et al., 2010). The direct influence could occur *via* altered growth rates of trees due to changing environmental pressure or by altering the suitability of ecological niche for the species (e.g., Hiura et al., 2019). Such indirect influence could be through changing natural disturbance regimes, which could in turn modify the mortality of trees and thus the stage structure of forest stands (e.g., Dale et al., 2001; IPCC, 2014). The current study focuses on how forest stands might respond to partial mortality, using controllable thinning operations as an example, to reduce stochastic uncertainties in partial mortality caused by natural disturbances.

Partial mortality may be common in forest stand development caused by many different factors including various types of disturbances, such as thinning. Thinning is a partial-cut treatment where a portion of the trees in the stand are harvested, which modifies the subsequent growth process of that stand. It is a silvicultural intervention tool that is used to modify the process of natural stand development for achieving desirable forest conditions, serving as a form of anthropogenic disturbances (e.g., Nyland, 1996; Ares et al., 2009; Kitagawa et al., 2018). When performed before the trees are ready for harvest for commodity products, it is called precommercial thinning (PCT), which reduces stand density and generally results in faster growth of remaining trees in diameter than that of untreated sites (Weetman and Mitchell, 2013). As a result, trees with bigger diameters are expected to favor lumber industries and increase the stand value dramatically when trees grow into the sawlog class.

Although short-term observations seldom demonstrated that stand gross volumes in thinned sites exceed those in unthinned sites (e.g., Bose et al., 2018), several long-term observations confirm that stand gross volumes in many treated sites can exceed that in untreated sites as surveyed by Li et al. (2020). For example, 42 years following initial PCT treatments, balsam fir (*Abies balsamea* (L.) Mill.) stand volumes in treated sites were about 15% higher than those from untreated sites in the Green River watershed of northwestern New Brunswick, Canada (Pitt and Lanteigne, 2008). Harvest analyses raised questions on whether this apparent productivity enhancement might be a common expectation from PCT, and how this could influence the forecast of long-term stand productivity, which is the foundation of sustainable forest management planning (e.g., Manitoba Conservation and Water Stewardship, 2013). To answer these questions, understanding of the mechanism(s) behind the observations becomes a necessity.

Compensatory growth (CG) is a common cross-taxa phenomenon in biology (Li et al., 2021). The earliest report of CG can be traced back to Osborne and Mendel (1915; 1916) in their famous study on nutrition and growth. Though CG has been termed differently in different biological fields, the essential

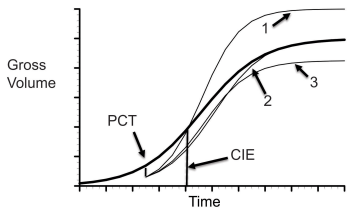

FIGURE 1
Illustration of CG. The solid line represents gross volume in natural stands. The dished lines indicate possible compensatory outcomes to a PCT operation at 12 years after planting: 1 - over-compensation; 1 - exact compensation, and 3 - under-comensation.

meaning is consistent. For example, Mangel and Munch (2005) referred to CG as the ability of an organism to grow at an accelerated rate following a period of resource deprivation. Diverse CG patterns have been found, and they can be grouped into three main statuses (Belsky, 1986; Maschinski and Whitham, 1989; Whitham et al., 1991; Li et al., 2020; Li et al., 2021):

1. under-compensation, in which biomass or body mass of treated group is lower than that of untreated group;
2. compensation-induced-equality (CIE) or exact compensation, in which biomass or body mass of treated group equals to that of untreated group; and
3. over-compensation, in which biomass or body mass of treated group exceeds that of untreated group.

Each of these hypothetical patterns for CG following a PCT are showed in Figure 1.

CG has been observed in plants, invertebrates, and vertebrates, both in the laboratory and in the wild and in both juveniles and adults as reviewed in Li et al. (2021). Mangel and Munch (2005) summarized that the diverse CG patterns are dependent on species, social environment, seasonal development, temperature, food availability, and physiological factors such as internal state and age. Therefore, there is no single "fixed" pattern of CG, but there may be general principles that allow deepening understanding and predicting the patterns, given the context.

In forestry, CG can be defined as a change in growth rate, usually positive, in a forest stand following a disturbance that reduces biomass and/or individuals from the population (Li et al., 2021). For example, the lens of CG was able to explain the over-compensation displayed in the coastal Douglas-fir (*Pseudotsuga menziesii* [Mirb.] Franco) stands near the Shawnigan Lake, British Columbia, Canada, 40 years after PCT and fertilization treatments (Li et al., 2018). Li et al. (2022) further demonstrated that CG may also be common in forest stands, using three published long-term silviculture datasets for major tree species across Canada, including lodgepole pine (*Pinus contorta* Douglas) in the MacKey thinning experiment, foothills Alberta, red pine (*Pinus resinosa* Aiton) in commercial thinning experiment of the Petawawa Research Forest, Ontario, and the costal Douglas-fir in the Shawnigan Lake trial. Nevertheless, systematic studies of CG in forestry are still rare, thus limiting the benefit of such exploration for the forest sector, despite significant benefits obtained from CG research results by other industries including livestock, crops, and aquaculture (Li et al., 2021). With the CG as a conceptual framework, however, it is possible to explain and thus predict stand dynamics after a partial mortality. This study is an example of how this framework could provide a mechanistic tool that could benefit forest sector in achieving sustainable forest management.

Methodologically, an experimental approach has been commonly employed to determine whether CG occurred in the experimental systems, and if existed, the type or status of CG. These results can help different industries to benefit from the CG through altering the management regimes (Li et al., 2021). For trees with a long lifespan, however, the experimental approach might not be widely applicable (see a summary in Li et al., 2020). In silvicultural experiments, the normal guidelines defined 10 years after-initial-treatments as appropriate period of observation (e.g., Reukema, 1975 for coastal Douglas fir PCT). However, the results from such a short-term observation might not provide a full picture of how forests might respond to such treatments as demonstrated in Pitt and Lanteigne (2008) and (Li et al. 2018; 2021). Since very few silvicultural experiments last 40 years or beyond, long-term observation results are rarely reported in the literature, simply because they require efforts from at least two continuous generations of professional careers. Therefore, to design and implement field CG experiments and then wait for results might be impractical due to the time and costs restraints. Nevertheless, Li et al. (2022) was able to demonstrate that CG might also be common in forest stands using legacy datasets (30-60 years) at the stand and tree levels of three major tree species across Canada, though these experiments were originally designed for other purposes. Considering that operational decisions in forest management are usually urgent and cannot wait for suitable data to become available, ecological modeling approach can play an important role in assisting decision support (Mangel et al., 2001).

Conceivably, if the CG phenomena commonly occurred in trees and forest stands as demonstrated in Li et al. (2022), one should be able to develop a simulation model, using existing growth-and-yield relationships, to corroborate the CG process within a lifespan of trees and forest stands triggered by thinning. Such a model could help elucidate the mechanism(s) underlying diverse CG patterns and facilitate design of the best strategy to take advantage of the CG phenomena by the forest sector. As plenty of growth and yield relationships are readily available for natural stands across North America and Europe, the first step would be to investigate whether this body of knowledge could be used for forecasting CG consequences. Such an attempt would have at least two meaningful consequences: one would be to produce a tool for predicting CG effect on stand dynamics, and the other would be to confirm that CG is probably an understandable natural process in stand dynamics, rather than a suspicious or out-of-the-ordinary phenomenon. In the current study, we show this attempt is possible through proper utilization of available growth and yield relationships.

The objectives of the current study are two-fold: first, to describe a state-dependent individual tree-based forest growth model called TreeCG, standing for Tree's Compensatory Growth, representing an alternative modeling approach to predict dynamics of stands after thinning operations; and second, to show how this modeling approach can successfully

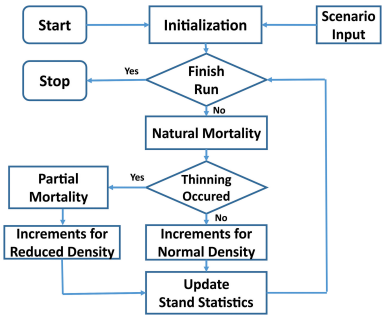

FIGURE 2
Data flow of the TreeCG simulation model.

reproduce the CG patterns observed in long-term silviculture (thinning) experiments. The possible applications of this modeling approach are also briefly discussed.

Materials and methods

Simulation model structure and major components

The TreeCG forest growth simulation model was used in the current study. Different from age-dependent growth and yield models that aimed at predicting mean stand volume over time under given site index for specific tree species or stand type, the state-dependent TreeCG model simulates the annual increments of diameter at breast height (*DBH*) and height (*H*) of individual trees within a stand, in which the annual increments are determined by the internal state of tree age and external state of resource availability. Therefore, the TreeCG model can capture the detailed responses of trees to changing environment conditions at any given tree age. Results from such a model structure allow estimation of different volume- and value-based assessment of stand productivity. Figure 2 shows the data flow of our model.

The major components of the model are as follows:

Initialization: This component sets up the initial conditions defined in the ***Scenario Input*** including stand density, the years of thinning operation, thinning intensity and method, and the distributions of diameter and height that assigned to each individual tree, thus allowing the program to keep track of the fate of each individual tree over time.

Natural mortality: $M_{Natural}$, is estimated using the following equation (Botkin et al., 1972; Keane et al., 2011):

$$M_{Natural} = 1 - \exp(-4/Age_{Max}) \quad (1)$$

where Age_{Max} is the longevity of tree. Lodgepole pine is a pioneer species that is distributed in western Canada and Rocky Mountain area. Kaufmann (1996) reported that the old-growth lodgepole pine trees varied in age from 250 and 296 years with about 31 cm in diameter in the Fraser Experimental Forest near Fraser, Colorado. In current study, 250 was used as the longevity of lodgepole pine.

Tree growth without thinning: the variable-density yield tables for natural stands of lodgepole pine in Alberta (Johnstone, 1976) were used to account for the effect of stand density on the relationship between *H* and age, *Age*:

$$\log_{10} H = 1.0688 - 0.00276672 \times Age + 0.717927 \log_{10} Age - 0.0000371084 \times Stems - 0.132622 \log_{10} Stems \quad (2)$$

where *H* is height in m, *Stems* is the number of stems no less than 0.6 inch (i.e., 1.524 cm) of *DBH* outside bark per acre and Age was based on years. We converted the units in the formula from British system into metric system, thus enabling the calculation of *H* of each tree at a given stand density.

Tree *DBH* is expressed as a function of *H*, estimated using the softwood equation of Huang (2016):

$$DBH = \{b_1/b_2 \times [1 - \exp(-b_1 \times b_2 \times (H - 1.3)]\}^{1/b_3} \quad (3)$$

For lodgepole pine in Alberta, $b_1 = 2.0584$, $b_2 = -0.0407$, and $b_3 = 1.5310$. The annual increment of *DBH*, DBH_{Inc}, was then calculated as:

$$DBH_{Inc,t} = DBH_{t+1} - DBH_t \quad (4)$$

where the subscripts *t* and *t+1* indicate the measured variables at year *t* and *t+1*, respectively. Figure 3 shows surface plot generated by equation (4), in which the DBH_{Inc} decreases with increasing tree age and stand density, reflecting the dynamics of tree vigor or vitality. This is consistent with the common observations of faster growth of trees in young stands.

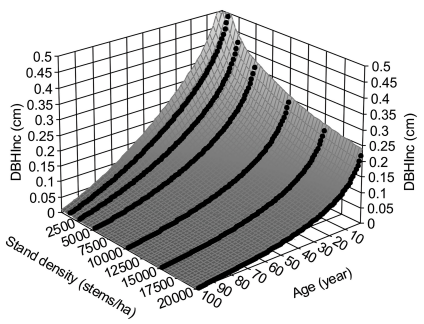

FIGURE 3
Annual increments of *DBH*, DBH_{Inc}, for lodgepole pine, at different stand age and stand density based on the variable density yield table of Johnstone (1976).

Applying the surface smoothing techniques using the software TableCurve3D (SYSTAT Software Inc., 2002) DBH_{Inc} at any given age and density could be estimated as:

$$z = a + b\ln(x) + c\ln(y) + d(\ln(x))^2 + e(\ln(y))^2 + f\ln(x)\ln(y) + g(\ln(x))^3 + h(\ln(y))^3 + i\ln(x)(\ln(y))^2 + j(\ln(x))^2\ln(y) \quad (5)$$

where x is tree age, y is stand density, and z is DBH_{Inc}. Parameter a = -0.47912889, b = -0.09398818, c = 0.585319033, d = -0.08405214, e = -0.09621235, f = 0.04071322, g = -0.000857125, h = 0.004492331, i = -0.00377608, and j = 0.008262739. The surface fitting has R^2 = 0.9942 and F = 8652.8217 and p< 0.0001.

Tree growth with thinning: at the year of thinning, the altered tree $DBH_{Inc,new}$ can be decomposed as the DBH_{Inc} of stand density before thinning, $DBH_{Inc,natural}$, plus the released growth, $DBH_{Inc,natural-new}$, of stand density after thinning:

$$DBH_{Inc,new}(cm) = DBH_{Inc,natural}(cm) + DBH_{Inc,natural-new}(cm) \quad (6)$$

where the subscripts of *natural* and *new* indicate the stand density before and after the thinning operation. To calculate $DBH_{Inc,new}(cm)$, we need to have both $DBH_{Inc,natural}(cm)$ and $DBH_{Inc,natural-new}(cm)$, where $DBH_{Inc,natural-new}(cm)$ is the extra (released) growth of *DBH* induced by the thinning operation. To simplify the $DBH_{Inc,natural-new}(cm)$ calculation, $DBH_{Inc,natural}(cm)$ and $DBH_{Inc,new}(cm)$ are presented in a relative sense (with regarding to an assumed maximal stand density of 20,000 stems/ha for lodgepole pine, and in this case as $RDBH_{Inc,natural}(\%)$ and $RDBH_{Inc,new}(\%)$, respectively:

$$RDBH_{Inc,natural}(\%) = DBH_{Inc,natural}(cm)/DBH_{Inc,20,000}(cm) \times 100 \quad (7a)$$

$$RDBH_{Inc,new}(\%) = DBH_{Incm,new}(cm)/DBH_{Inc,20,000}(cm) \times 100 \quad (7b)$$

We then calculated $DBH_{Inc,new}(cm)$ as

$$DBH_{Inc,new}(cm) = DBH_{Inc,natural}(cm) \times [1 + RDBH_{Inc,natural-new}(\%)] \quad (8)$$

where $RDBH_{Inc,natural-new}(\%)$ is calculated as:

$$RDBH_{Inc,natural-new}(\%) = \frac{RDBH_{Inc,new}(\%) - RDBH_{Inc,natural}(\%)}{RDBH_{Inc,natural}(\%)} \times 100 \quad (9)$$

With above treatments, the $DBH_{Inc,new}(cm)$ can be directly estimated from the stand densities before and after thinning. The parameters were estimated using the surface smoothing for equation (5), where x is tree age, y is stand density, and z is $DBH_{Inc,new}(cm)$. Results for the numerical simulation results are a = 9214.78559, b = 2726.639714, c = 2258.136021, d = -325.333346, e = -229.149066, f = -259.997371, g = 14.89819094, h = 8.856809336, i = 4.586019568, and j = 16.20041778. The surface fitting has R^2 = 0.9994 and F = 85893.681 with p< 0.0001. In other words, $RDBH_{Inc,natural-new}(\%)$ can be obtained by calculating two stand densities, before and after thinning, using the same equation as shown in Figure 4.

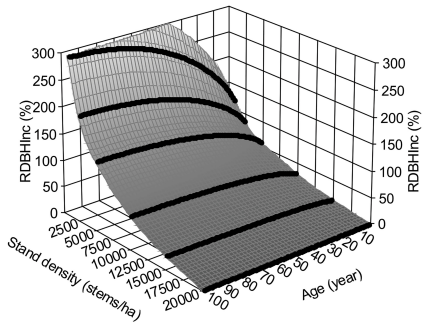

FIGURE 4
Relative annual *DBH* increment, $RDBH_{Inc}(\%)$, regarding an assumed maximal stand density of 20,000 stems/ha.

The surface of H after the released growth, corresponding to $DBH_{Inc,new}(cm)$, can then be obtained using the provincial equation for lodgepole pine (Huang et al., 2013):

$$H = 1.3 + 35.7547/\{1 + \exp[3.8234 - 1.2824\ln(DBH)]\} \quad (10)$$

For clarity, we summarized the set of variables in our model along with their definitions in Table 1.

Model validation

Since the current version of the TreeCG is generic, our model validation is performed qualitatively in terms of examining whether the model structure and assumptions are reasonable. If the answer was positive, the simulation results should be able to reproduce the diverse patterns of CG in stands after different thinning operations. As an example, we compared the simulated CG patterns qualitatively to what displayed in the Shawnigan Lake long-term silviculture experiments using the relative growth (RG):

$$RG = (Vol_{Thinned}/Vol_{Control}) \times 100\,\% \quad (11)$$

where $Vol_{Thinned}$ and $Vol_{Control}$ are the gross volumes for thinned and control stands, respectively. If the model structure and assumptions are reasonable, the simulated RG over time should be able to show the temporal transition from under-

TABLE 1 List of variable definitions.

Variable	Definition
$M_{Natural}$	Natural mortality in %
Age_{max}	Tree longevity in years
H	Tree height in m
Stem	Number of stems ≥ 0.6 inch (i.e., 1.524 cm) of *DBH* per acre
DBH	Diameter at breast height outside bark, in cm
DBH_t	*DBH* measured at year *t*
DBH_{t+1}	*DBH* measured at year *t+1*
$DBH_{Inc,natural}(cm)$	Annual *DBH* increment, before thinning, in cm
$DBH_{Inc,20,000}(cm)$	Annual *DBH* increment at an assumed maximal stand density of 20,000 stems/ha
$DBH_{Inc,new}(cm)$	Annual *DBH* increment, after thinning, in cm
$RDBH_{Inc,natural}(\%)$	Annual *DBH* increment, before thinning, in % relative to assumed maximal stand density of 20,000 stems/ha
$RDBH_{Inc,new}(\%)$	Annual *DBH* increment, after thinning, in % relative to assumed maximal stand density of 20,000 stems/ha
$RDBH_{Inc,natural-new}(\%)$	Relative *DBH* annual increment of released growth in %

compensation to CIE and over-compensation in thinned stands compared to unthinned stands (Li et al., 2018).

Model simulation experiment

Our model simulations were designed to test the premise that the CG capacity of a tree is a function of internal (age) and external (intensity of thinning, i.e., the level of stimulus/mortality) states. The premise came from the diverse CG patterns observed in different PCT experiments. If this premise were true, the simulation results should show the different responses of a forest stand to different thinning operations. As such, one could expect that existing growth and yield relationships from natural stands could be used to predict the growth trajectories of stands under different thinning operations. Furthermore, one could also expect that an optimal thinning regime or strategy could be identified, in terms of optimal timing and intensity of a thinning operation, for achieving a maximized stand productivity.

The initial stand density was set as 7,500 stems/ha, and the simulation results were evaluated for the total gain over a planning horizon of 100 years, which accounted for the sum of the immediate gain from thinning operation and the gain from the remaining trees at the year 100. Thinning operations were implemented at two different stand ages of 30 (representing an early partial mortality) and 60 (representing a late partial mortality) years old. A control without thinning was also implemented. The partial mortality was represented by the intensity of thinning, which was set as removal of 33% (as a light mortality) and 66% (as a heavy mortality) of total number of trees. If this premise were true, the simulated CG capacity could differ under early and late partial mortality, as well as light and heavy mortality.

The model output includes the stand conditions (*DBH* and *H* of each living tree) at initialization and every 5-year interval until 100 years, and harvested wood at the year of thinning.

Evaluation of stand productivity

The stand productivity evaluation for the simulated stand dynamics was conducted using the Wood Fibre Value Simulation Model (WFVSM) (Li et al., 2017; Li et al., 2022). As a unified valuation tool, the WFVSM simulates both volume- and value-based indicators of a given tree-based forest inventory, represented by harvested logs segregated into different types of treatment centres for different products, including sawmills, pulp mills, veneer mills, plywood mills, and bio-refineries, as well as used as a source of biomass for heat and electricity, and carbon capture. The calculations of these indicators were primarily based on knowledge from the field of forest engineering such as Briggs (1994), except sawmill recovery, which is based on the simulation results of the Optitek, an industrial sawmill operation software package (FPInnovations, 2014), at possible combinations of *DBH* (at the interval of 1 cm) and *H* (at the interval of 1 m).

Gross volume, merchantable volume, lumber volume recovery, lumber value recovery, and net sawmill value are used in current analysis. The gross volume, *Vol*, was calculated using the lodgepole pine tree volume equation for Alberta (Penner et al., 1997):

$$Vol = 4.421585 \times 10^{-5} DBH^{1.926909} H^{1.00304} \quad (12)$$

The merchantable volume is the log volume transported to the mill gate. The lumber recovery and all by-products are obtained from the look-up-table tallied from multiple simulations using the Optitek. The total value recovery from sawmill, $Val_{Sawmill}$, can be calculated as

$$Val_{Sawmill} = Val_{Lumber} + Val_{Chips} + Val_{Sawdust} + Val_{Shaving} + Val_{Bark} \quad (13)$$

where Val_{Lumber}, Val_{Chips}, $Val_{Sawdust}$, $Val_{Shaving}$, and Val_{Bark} are the

value recoveries from lumber, chips, sawdust, shavings, and bark, respectively. The lumber sale price was defined as $400 per thousand board feet (MBF), chips sale of $140 per Metric Tons (MT), sawdust price of $25/MT, shaving price of $15/MT, bark price of $10/MT, and the average wood density was set to 400kg/m^3. The costs in sawmill operations are also included in the Optitek simulations, which are the fixed costs of $15/$m^3$ lumber recovery, planing costs of $25/MBF, drying cost of $15/MBF, and sawing cost of $60/MBF. These values employed were taken from the default set in the Optitek software package reflecting the mean market situation of early 2000s in North America, and the mean operational costs from a large number of Canadian sawmills at the time. The values used in this investigation serve as a standard of comparing simulation results under different thinning operations. The Optitek provides a flexibility of allowing users to define their own values based on their specific mill machine configuration and fluctuating commodity market.

Results

Simulated forest growth pattern

A direct method of exploring the outcome of a stand dynamics model is to examine the long-term stand growth trajectories under different thinning scenarios. When no thinning operation is applied, the modeled stand growth trajectory will constitute a forest growth pattern under the control scenario, equivalent to natural stand condition. This trajectory can serve as a baseline case to compare with each of simulated growth trajectories under different partial mortalities caused by prescribed thinning operations. An over-compensation can be indicated when the stand growth trajectory is higher than the baseline case. An under-compensation will be denoted when the stand growth trajectory is lower than the baseline case. An exact compensation, or CIE can be called when the stand growth trajectory ends up at some point being equal to the baseline case (see illustration in Figure 1).

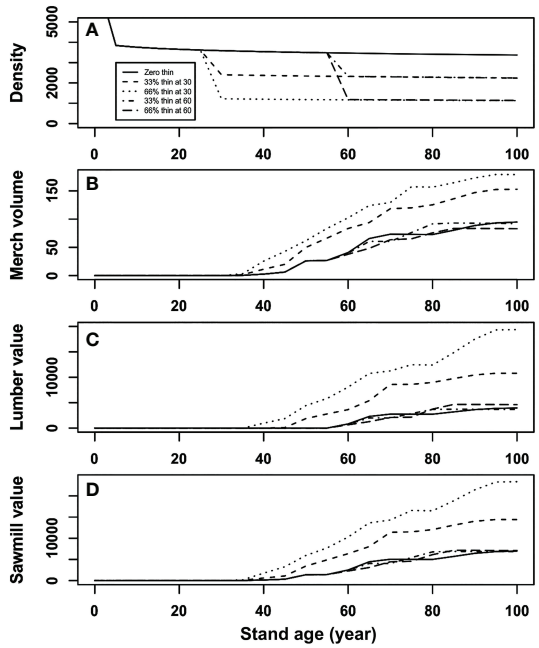

FIGURE 5
Simulation results of **(A)** stand density (stems/ha), **(B)** merchantable volume (m^3/ha), **(C)** value recovery of lumber ($/ha), and **(D)** total value recovery of sawmill ($/ha) of initial stand density of 7,500 stems/ha under different thinning intensities for a hypothetical stand of lodgepole pine at age 30 and 60 years.

The results of our simulation were expressed throughout a graphical representation that covered a planning period of 100 years (Figure 5). Stand density decreased exponentially at the early stand development that is determined by the natural mortality function (equation (1)), and then decreased proportionally at the year of thinning operation according to the intensity of partial mortality (Figure 5A). Moreover, our results also show that final merchantable volume after early partial mortality can exceed that from control, i.e., overcompensation, and a heavier mortality could result in a higher merchantable volume than that from a lighter mortality (Figure 5B). However, such a trend may not always be the case when a late partial mortality is experienced, which resulted in either under-compensation or CIE. In other words, both thinning intensity and timing can result in different stand productivity at the end of simulation. In addition, the evolution of the lumber and sawmill value (Figs. 5c and 5d) could suggest an increase when value recovery occurred from the merchantable volume, which is probably because of the increased percentage of large dimension lumber products.

The results suggest that the stand's capability for compensation could be higher at a younger age than that at an elder age, and heavier thinning could result in a higher compensation capability than that from a lighter thinning. The simulation results also suggest that a partial harvest performed at age 60 might be too late with very little or no benefit to be expected from the CG phenomenon. This is probably true because age 60 is usually the minimal stand age of conventional harvest in many jurisdictions based upon decelerating growth.

Simulated total gains

Forest managers usually take a certain planning horizon for evaluating the consequences of a given management operation. The planning horizon could vary depending on the purpose of planning. For example, a typical forest harvest planning process could have multiple 20-year planning periods with a total of 200 years as the strategic planning horizon for the province of Manitoba, Canada (Li et al., 2011). In the current study, we explored the consequences of a

TABLE 2 Simulated gains from different timings and intensities of thinning over 100 years.

Treatment	Items	From thinning	From final harvest	Total
Control	**Merchantable volume (m^3/ha)**		94.841	94.841
	Lumber vale recovery ($/ha)		3,958.86	3,958.86
	Sawmill value recovery ($/ha)		6,981.77	6,981.77
1/3 mortality at 30 years	**Merchantable volume (m^3/ha)**		152.8	152.8
	Lumber vale recovery ($/ha)		10,792.20	10,792.20
	Sawmill value recovery ($/ha)		14,408.52	14,408.52
1/3 mortality at 60 years	**Merchantable volume (m^3/ha)**	11.308	80.687	91.995
	Lumber vale recovery ($/ha)	144.13	3,521.51	3,665.64
	Sawmill value recovery ($/ha)	658.497	6,150.306	6,808.803
2/3 mortality at 30 years	**Merchantable volume (m^3/ha)**		178.869	178.869
	Lumber vale recovery ($/ha)		19,383.74	19,383.74
	Sawmill value recovery ($/ha)		23,350.73	23,350.73
2/3 mortality at 60 years	**Merchantable volume (m^3/ha)**	23.242	59.722	82.964
	Lumber vale recovery ($/ha)	326.5	4,282.64	4,609.14
	Sawmill value recovery ($/ha)	1,367.36	5,729.17	7,096.53

thinning operation during a planning horizon of 100 years, with every 5-year as an output period. This enables evaluation of changing stand value over the planning horizon.

To evaluate the consequences of different thinning operations, we compared several indicators of total gain at the end of a planning horizon of 100 years for the operations as showed in Table 2. In the case of early thinning, there is no immediate benefit from the operations, but the final harvest could be significantly higher than that from the unthinned stand. Late thinning can have some immediate benefit from operations (11.308 and 23.242 m^3/ha merchantable volumes from 33% and 66% removal of surviving trees, respectively); however, they could not make up the lost in final harvest at the end of planning horizon for the total merchantable volume, although the value recoveries could still be higher than that from unthinned stands probably due to the large dimension of sawlogs. Simulation results showed that under a late thinning regime, thinned stands would eventually (> 15 years) outperform unthinned ones after an initial underperformance.

These results suggest that at the earlier stage of stand development, trees might have a higher capacity of CG due to increased vigor of surviving trees. The capacity of CG could reduce with aging trees. Therefore, to take full advantage of CG capacity in enhancing long-term stand productivity, the thinning should not be performed too late (e.g., before 60 years of stand age in current planning scenario) in the process of stand development.

Model validation

A qualitative model validation was conducted through comparing the simulated forest growth patterns to a long-term silvicultural experiment, which was a 40-year trial of PCT and fertilization on the coastal Douglas-fir near the Shawnigan Lake, British Columbia (Crown and Brett, 1975). The focus of the comparison is not *via* matching of absolute values, because the relationships employed in our simulation model were not specifically from the coastal Douglas-fir forests. The dataset from the Shawnigan Lake trial contains multiple repeated measurements for a combination of three levels of PCT and three levels of fertilization treatments. As reported in Li et al. (2018), the diverse stand growth patterns can be expressed by growth relative to the control in percentage. In the current

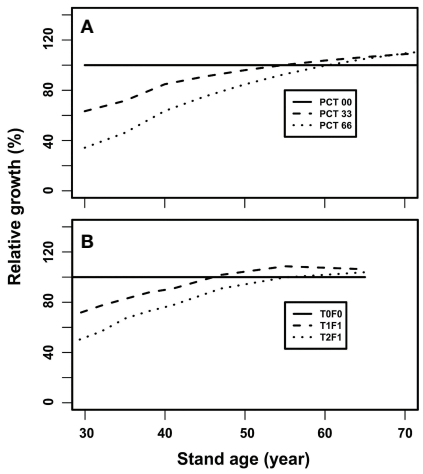

FIGURE 6
The stand growth trajectories after experiencing a thinning operation: **(A)** simulated growth trajectories after experiencing a PCT at age 30, and **(B)** observed growth trajectories after PCT at age 24 based on the PCT and fertilization (224 kg N/ha) treatments at the Shawnigan Lake trial, BC Canada.

model validation, the relative growth is used to compare the CG growth patterns as shown in Figure 6.

As a longitudinal process, one can follow stand gross volume after experiencing an early thinning at year 30 under three levels of intensity (i.e., 0, 33%, and 66% removal for the initial stand density of 3,950 stems/ha). Here, partial mortality first reduced gross stand volume but then the stand gross volume gradually catches-up with that of the control stand, and eventually exceeds the control and generates over-compensation (Figure 6A). The heavier thinning (66% mortality) resulted in higher over-compensation than that of the lighter thinning (33% mortality) (Figure 6A). The trends displayed in this series of simulations appeared consistent with observed by the 40-year's measurements from the Shawnigan Lake trial (Figure 6B). This indicates that our simulation results are validated qualitatively by the observations from this long-term PCT and fertilization experiment.

Note that only the simulation results between age 30 (the year the thinning operations are conducted) and 70 are plotted, because the observations from the Shawnigan Lake trial cover 40 years only as the treatments were started at age 24 and measured for 40 years.

Our results suggested that short-term (10-year) observations defined by Reukema (1975) after PCT, will generate under-compensation (Figure 6). The over-compensation can only be observed in long-term observations such as 40-year after the PCT treatments. This is because slow growing trees need sufficient time for the treated stands to compensate the lost volume at the treatments. This confirmed that the sufficient condition for over-compensation to occur is having enough time (Li et al., 2018).

Discussion

Our results confirmed the premise that a simulation model based on existing growth and yield relationships, can reproduce diverse CG patterns observed in long-term thinning experiments. In this section, we discuss our CG research approach in general, examine the logical consequences of thinning, and briefly go over the potential management applications of our model TreeCG.

CG research approach

Management of forest growth is one of the major components in modern forest management. It aims at promoting productive forestry, in terms of proactively seeking ways of enhancing forest productivity (Li et al., 2020). In other words, a major concern is how management operations might enhance forest productivity. To reach this goal, improved understanding on the dynamics of managed stands appears essential. Existing forest growth and yield models characterize the growth responses of forest stands under natural conditions including some fluctuations caused by some random events (e.g., Martin, 1991; Huang et al., 2001). However, it has not been thoroughly examined as to whether these relationships also apply to managed stands, probably due to insufficient data sources. Nevertheless, some studies revealed that they are probably not the same. This was evidenced in Huuskonen and Hynynen (2006), who found that the diameter increment of trees after PCT can be characterized by a function of dominant height, initial stand density and the actual stem number of the PCT treated growing stock, and the regeneration method. Recently, Burkhart and Yang (2022) found that the carrying capacity, an indicator of productivity, in intensively managed plantation plots of loblolly pine (*Pinus taeda*) was significantly higher than that of non-intensively managed plantation plots, which suggested that stand growth trajectories in the two types of plantations were different.

Existing growth and yield relationships generally assume that the observed productivity of a forest stand results from the

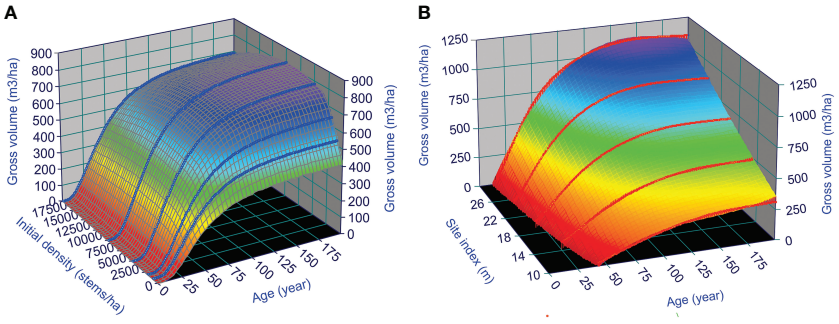

FIGURE 7
GYPSY model predicted surfaces of lodgepole pine yield in AB, Canada: under different **(A)** initial stand densities when site index is 30 m, and **(B)** site index when initial stand density is 7,500 stems/ha.

optimal utilization of space and nutrients of the trees living in the stand (Li et al., 2020). Thus, the growth and yield models of natural stands should represent the optimal stand productivity. This can serve as a starting point for understanding the dynamics of managed stands, such as the CG phenomenon after thinning. As an example, such yield surfaces of lodgepole pine can be illustrated in Figure 7, by using GYPSY model (Huang et al., 2001; Huang et al., 2009) in Alberta (AB), Canada: the stand yield surface under different initial stand densities over stand age when site index is 30 m (Figure 7A), and under different site indices over stand age when initial stand density is fixed as 7,500 stems/ha (Figure 7B). These surfaces should allow practitioners to estimate the stand productivity of the species at any given stand age, site index, and initial stand density.

When a thinning operation is conducted at a specific stand age, one could assume that the stand productivity would switch from the stand growth trajectory from the initial stand density to the stand growth trajectory indicated by the stand density after the thinning operation at the specific stand age. Though this assumption could be too rough possibly due to delay for the stand to detect the new level of space and nutrients availability under the new stand density, it provides a possible way of predicting stand productivity after the thinning operation, using the information contained in growth and yield curves for natural stands.

A challenge in implementing this switch is to determine the corresponding initial stand density for the trajectory with stand density after the thinning operation at the specific stand age. Such a challenge was also appeared in studying population dynamics of mountain pine beetle (*Dendroctonus ponderosae* Hopkins) (MPB) after a management operation, in which the challenge is the estimation of population density after the operation. Safranyik et al. (1999) developed a MPB population dynamics model at a spatial scale of one hectare, to forecast the population dynamics with a flexible initial population density. However, the population reduction from a management operation will require the trajectory of the population dynamics to be adjusted due to the reduced population density at the time of the operation. Therefore, researchers had to perform two separate runs of the model: one for population dynamics before the operation under the initial population density, and the other for population dynamics after the operation under the reduced population density. Due to the stochastic nature of the model, it appeared difficult to estimate the initial population density under which the population density after the operation could be exactly harmonized, and multiple runs of guessed initial population densities might be needed to match accurately the population density after the operation.

This guessing of initial population density is similar to the challenge of modelling the stand growth trajectory after a thinning operation. Despite the fact that stand density after the thinning can be relatively easy to estimate, the new trajectory at different timings could still present a challenge in identifying the corresponding initial stand density under which the stand density will be the same as the reduced stand density right after the operation. This means multiple runs might be needed to "guess" the right growth trajectory for after the thinning operation. TreeCG model resolved this issue by developing a new algorithm described in the methods section.

Most existing forest growth and yield models are analytical, with a premise that once the specific tree species or stand type and site index are known, stand yield curve of the natural stand can be determined (e.g., King, 1966). This fixed shape of stand yield curve for natural stands facilitates straightforward applications by practitioners but compromises the flexibility of capturing changes between years. For managed stands, such a fixed shape of stand yield curve might not always apply because significant disturbances such as both catastrophic fire events and thinning operations could reduce biomass or stand density and thus alter the stand yield curve dramatically. To capture such changes between years, a simulation approach would likely perform better than an analytical approach, because it usually handles better the complicated system dynamics that are difficult to represent by a single analytical model. In the state-dependent forest growth model TreeCG, the dynamics of stand volume consist of before and after thinning stages, and the stand volume at any given year is the sum of volumes of individual trees within the stand, calculated yearly using its annual increments of *DBH* and *H*. Since the simulation results will reassemble the dynamics of natural stands under different stand density and site index conditions, the TreeCG model can simulate the dynamics of both natural and managed stands.

The CG phenomenon has been well-known to animal and annual plant researchers, but less familiar to foresters. Application of the CG concept to tree and forest biology is an example of how forestry can benefit from the principles and results of general biology and ecology. The modeling approach presented in current study could also be applied to different industries or fields to take advantages of CG. Theoretically, the modeling approach could be complementary to the experimental approach commonly employed in functional trials (Zirbel et al., 2017; Hanisch et al., 2020). It speeds up our understanding about functional plant ecology.

Logical consequences from thinning operations

Research results from thinning and stand density management are the primary driver for our understanding CG phenomenon in forests. Combined with initial spacing, thinning is widely used for stand density management (e.g., Long, 1985). It results in a partial mortality to the stand (Bose et al., 2014), and also altered stand structure (Pamerleau-Couture et al., 2015), radial growth response (Montoro Girona et al., 2016),

wood quality (Lemay et al., 2018), and mortality (Montoro Girona et al., 2019) and windstorm after partial harvest (Lavoie et al., 2012). Conceptually, if the stand does not respond to the partial mortality, the surviving trees will continue their normal growth trajectories and thus no compensation would occur, which result in the freed nutrients and space from dead trees left unused. However, this is unlikely owing to the inter-tree competition. If partial mortality could be seen as a stimulus to the normal growth of the stand, it could trigger a CG for the remaining trees in the stand. Obviously, compensation will not occur in dead trees, however, CG could happen at the stand level such that the surviving trees grow faster than normal. This is achieved by utilizing the extra nutrients and space freed from the dead trees, as indicated by widely observations from PCT experiments (e.g., Bose et al., 2018). As we know, each thinning regime is a combination of the timing and intensity of a thinning operation. If the response of a stand to partial mortality would differ under different thinning regimes, one could expect diverse response curves or growth trajectories of the stand after thinning operations. Thus, the challenge is to identify the best combination of timing and intensity of a thinning operation that can lead to the maximized stand productivity (Li et al., 2020). This appears consistent with the goal of silviculture experiments (e.g., Zeide, 2008).

Redistribution of resources (including space and nutrients) from dead trees to surviving trees has been implemented in some process-based models. For example, the Tree And Stand Simulator (TASS) model (Mitchell, 1975) demonstrated that PCT and fertilization could lead to overcompensation in terms of basal area as a result of the redistribution of space and light. Unfortunately, this potential had been largely ignored until very recently a PCT experiment conducted using the Table Interpolation Program for Stand Yields (TIPSY, a "meta-model" software program giving electronic access to a vast database of yield tables produced by TASS) showed that PCT could result in a full CG process in stand growth trajectory including overcompensation (Figure 8), in which a CG process is triggered by a PCT at year 10, and over time experiencing under compensation up to year 75, exact compensation at year 76, and overcompensation after year 77. Though 65 years are needed for the catch-up in stand gross volume in the PCTed site, that is about a quater of lodgepole pine's lifespan, which might not be too slow compared with most short lifespan species proportionally. Considering the importance of nutrients in tree growth, a reasonable inference is that the real CG could probably be even more significant and clear than simulated by TASS-TIPSY model.

The TreeCG model provides a possible way of speeding-up the understanding of CG mechanism through the exploration of the model behaviour, or logical consequences from different thinning operations. This exploration can be performed through carefully designed multiple simulations, or model experiments.

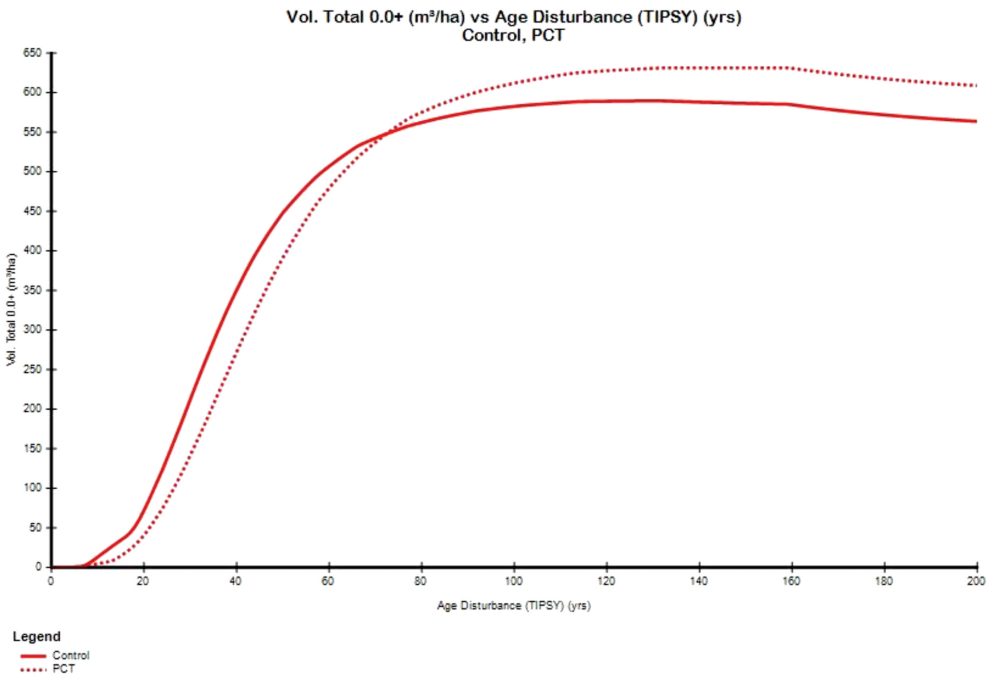

FIGURE 8
A CG process simulated by using the TIPSY 4.4 through comparing the stand growth curves (PCTed vs. control) in a planted lodgepole pine stand with a site index of 24 m.

For example, effect of different thinning regimes on the stand productivity could be conducted by different timing and intensity of thinning, and the simulation results could be evaluated by a unified procedure of volume and value-based inventory assessment, i.e., by running the WFVSM in our case. The WFVSM can provide fast assessment to measured silviculture results of an experiment with the unified procedure, despite its absolute values of indicators could vary slightly in different settings of product treatment centres. In other words, the logical consequences of different thinning prescriptions on stand productivity can be investigated through combination of using a simulation tool of TreeCG and a valuation tool like WFVSM.

Management applications

Our generic TreeCG model can be refined using local growth and yield relationships for addressing specific regional issues. For example, the most recent lodgepole pine stand growth projection (Figure 9) using the GYPSY model (Huang et al., 2001; Huang et al., 2009) with more specific on-site index could replace the surface presented in Figure 3, for the calibration to address specific issues under investigation in Alberta. Similar approaches can be applied to other jurisdictions such as British Columbia using the relationships built-in the Variable Density Yield Projection (VDYP) model for natural stands (British Columbia Ministry of Forests, Lands, Natural Resource Operations and Rural Development, 2019).

Calibrated growth and yield models can help addressing practical issues such as:

- Estimation of released growth for crop trees;
- Identification of optimal prescriptions of thinning operations for maximized stand productivity;
- Exploration of optimal spacing for plantation programs;
- Determination of possible elevation of regional annual allowable cut (AAC) through enhanced stand productivity for mitigating the wood supply shortfall;
- Enhancement of carbon capture through forest management for improving regional carbon budget;
- Reduction of fuel accumulation through partial harvest for decreasing fire risk;
- Improvement of biofuel and bioeconomy through increased feedstock for producing heat and electricity.

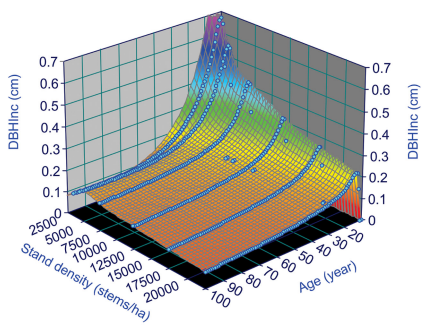

FIGURE 9
Annual increments of *DBH*, *DBHInc*, of lodgepole pine predicted by GYPSY model in Alberta, Canada, at the site index of 20 m and different stand age and stand density.

Since there has been no reported evidence showing that trees are capable of distinguishing the causes of partial mortality, the TreeCG can be expanded to include partial mortality induced by other disturbances such as fire, insect outbreaks, and windstorm, etc. to capture the corresponding responses of forests.

The TreeCG model can help when estimating the growth trajectories influenced by the disturbance regimes altered by climate change. Like most existing growth and yield models, however, the TreeCG model might be technically unsuitable to address potential climate change impact on the growth trajectories of trees and stands directly, simply because it does not respond to changes in climate variables. It would be better to have a climate sensitive growth and yield model through an alternative approach, such as from a life-history perspective that might be more suitable because it takes adaptation of trees to changes in the probability distributions of climate variables and disturbances into account, with hybrids of existing growth and yield relationships. We will describe this approach in a separate manuscript.

Conclusions and research recommendations

A state-dependent TreeCG model based on the CG conceptual framework was able to reproduce the CG patterns observed in the Shawnigan Lake long-term PCT and fertilization experiment. The new algorithm of simulating CG process reduced the computing demand and simplified the calculation of annual growth increments for individual trees over time. Our results suggested that stand growth trajectories could be altered considerably by different timing and intensity of thinning operations. They explained the diverse CG patterns observed in different PCT experiments. Our model TreeCG can contribute to the understanding of growth trajectories of stands after a partial mortality and could be utilized to address many questions in theory and applications.

Data availability statement

Permission to use the Shawnigan Lake dataset in this study was obtained from the data provider. Requests to access this

dataset should be directed to Cosmin Filipescu of the Canadian Forest Service.

Author contributions

CL, HB, and SH: model design, implementation, model experiment, data analysis, and draft writing. CL, HB, SH, BR, RL, WX, and YC: review, revision, and editing. All authors contributed to the article and approved the submitted version.

Funding

This work was financially supported by Natural Resources Canada-Canadian Forest Service's Developing Sustainable Fibre Solutions Research Program.

Acknowledgments

The authors thank Cindy Chen of the University of British Columbia and Sirak Ghebremusse of the Northern Alberta Institute of Technology for assisting the initial implementation of the simulation model. We also thank Sharad Baral of the Canadian Forest Service for helpful discussions, providing Figure 8, and feedback on an earlier version of this manuscript, and Yuqing Yang and Cam Brown of the Forsite for helping with GYPSY model simulations. We also thank Harold Burkhart of the Virginia Tech for his kindly providing related literature, and two reviewers for their constructive comments that improved the quality of this manuscript. This work was financially supported by Natural Resources Canada-Canadian Forest Service's Developing Sustainable Fibre Solutions Research Program.

Conflict of interest

The authors declare that the research was conducted in the absence of any commercial or financial relationships that could be construed as a potential conflict of interest.

Publisher's note

All claims expressed in this article are solely those of the authors and do not necessarily represent those of their affiliated organizations, or those of the publisher, the editors and the reviewers. Any product that may be evaluated in this article, or claim that may be made by its manufacturer, is not guaranteed or endorsed by the publisher.

References

Ares, A., Berryman, S. D., and Puettann, K. J. (2009). Understory vegetation response to thinning disturbance of varying complexity in coniferous stands. *Appl. Vegetation Sci.* 12, 472–487. doi: 10.1111/j.1654-109X.2009.01042.x

Avery, T. E., and Burkhart, H. E. (1994). *Forest measurements. 4th Ed* (Boston, MA: McGraw-Hill, Inc).

Belsky, A. J. (1986). Does herbivory benefit plants? *A Rev. Evid. Am. Nat.* 127, 870–892. doi: 10.1086/284531

Bose, A. K., Harvey, D. H., and Brais, S. (2014). Sapling recruitment and mortality dynamics following partial harvesting in aspen-dominated mixedwoods in eastern Canada. *For. Ecol. Manage.* 329, 37–48. doi: 10.1016/j.foreco.2014.06.004

Bose, A. K., Weiskittel, A., Kuehne, C., Wagner, R. G., Turnblom, E., and Burkhart, H. E. (2018). Tree-level growth and survival following commercial thinning of four major softwood species in north America. *For. Ecol. Manage.* 427, 355–364. doi: 10.1016/j.foreco.2018.06.019

Botkin, D. B., Janak, J., and F. and Wallis, J. R. (1972). Some ecological consequences of a computer model of forest growth. *J. Ecol.* 60, 849–872. doi: 10.2307/2258570

Briggs, D. G. (1994). "Forest products measurement and conversion factors: With special emphasis on the U.S," in *Pacific Northwest* (Seattle, WA, USA: College of Forest Resources, University of Washington).

British Columbia Ministry of Forests, Lands, Natural Resource Operations and Rural Development (2019) *Variable density yield projection.* Available at: https://www2.gov.bc.ca/assets/gov/farming-natural-resources-and-industry/forestry/stewardship/forest-analysis-inventory/growth-yield/volume_1_vdyp_overview_2019.pdf.

Burkhart, H. E., and Yang, S.-I. (2022). A retrospective comparison of carrying capacity of two generations of loblolly pine plantations. *For. Ecol. Manage.* 504, 119834. doi: 10.1016/j.foreco.2021.119834

Crookston, N. L., Rehfeldt, G. E., Dixon, G. E., and Weiskittel, A. R. (2010). Addressing climate change in the forest vegetation simulator to assess impacts on landscape forest dynamics. *For. Ecol. Manage.* 260, 1198–1211. doi: 10.1016/j.foreco.2010.07.013

Crown, M., and Brett, C. P. (1975). "Fertilization and thinning effect on a Douglas fir ecosystem at shawnigan lake: An establishment report," in *Information report BC-X-110* (Canada: Pacific Forestry Centre, Canadian Forest Service, Environment Canada, Victoria, British Columbia).

Dale, V. H., Joyce, L. A., McNulty, S., Neilson, R. P., Ayres, M. P., Flannigan, M. D., et al. (2001). Climate change and forest disturbances : Climate change can affect forests by altering the frequency, intensity, duration, and timing of fire, drought, introduced species, insect and pathogen outbreaks, hurricanes, windstorms, ice storms, or landslides. *Bioscience* 51, 723–734. doi: 10.1641/0006-3568(2001)051[0723:CCAFD]2.0.CO;2

FPInnovations (2014). *Optitek 10: User's manual* (Pointe-Claire, QC, Canada).

Hanisch, M., Schweiger, O., Cord, A. F., Volk, M., and Knapp, S. (2020). Plant functional traits shape multiple ecosystem services, their trade-offs and synergies in grasslands. *J. Appl. Ecol.* 57, 1535–1550. doi: 10.1111/1365-2664.13644

Hiura, T., Go, S., and Iijima, H. (2019). Long-term forest dynamics in response to climate change in northern mixed forests in Japan: A 38-year individual-based approach. *For. Ecol. Manage.* 449, 117469. doi: 10.1016/j.foreco.2019.117469

Huang, S. (2016). *Individual tree diameter prediction models from tree height* (Edmonton, Alberta: Forest Management Branch, Alberta Agriculture and Forestry), 59 p. Technical Report Publication No. T/606.

Huang, S., Meng, S. X., and Yang, Y. (2009). *A growth and yield projection system (GYPSY) for natural and post-harvest stands in Alberta* (Edmonton, Alberta, Canada: Alberta Sustainable Resource Development).

Huang, S., Morgan, D., Klappstein, G., Heidt, J., Yang, Y., and Greidanus, G. (2001). *GYPSY: A growth and yield projection system for natural and regenerated stands within an ecologically based, enhanced forest management framework* (Edmonton, Alberta, Canada: Alberta Sustainable Resource Development).

Huang, S., Yang, Y., and Aitkin, D. (2013). *Population and plot-specific individual tree height-diameter models for major Alberta tree species* (Edmonton, Alberta: Forestry and Emergency Response Division, Alberta Ministry of Environment and Sustainable Resource Development), 81 p. Technical Report, Publication No. T/600.

Huuskonen, S., and Hynynen, J. (2006). Timing and intensity of precommercial thinning and their effects on the first commercial thinning in scots pine stands. *Silva Fennica* 40, 645–662. doi: 10.14214/sf.320

IPCC (2014). "Climate change 2014: synthesis report," in *Contribution of working groups I, II and III to the fifth assessment report of the intergovernmental panel on climate change*. Eds. R. K. Pachauri and L. A. Meyer (Geneva, Switzerland: IPCC), 151 p.

Johnstone, W. D. (1976). *Variable-density yield tables for natural stands of lodgepole pine in Alberta* (Ottawa, ON: Canadian Forest Service, Department of Fisheries and Environment, Forest Technical Report 20).

Kaufmann, M. R. (1996). To live fast or not: growth, vigor and longevity of old-growth ponderosa pine and lodgepole pine trees. *Tree Physiol.* 16, 139–144. doi: 10.1093/treephys/16.1-2.139

Keane, R. E., Loehman, R. A., and Holsinger, L. M. (2011). "The FireBGCv2 landscape fire and succession model: a research simulation platform for exploring fire and vegetation dynamics," in *General technical report. RMRS-GTR-255* (Fort Collins, CO: U.S. Department of Agriculture, Forest Service, Rocky Mountain Research Station), 137 p.

King, J. E. (1966). *Site index curves for Douglas-fir in the pacific Northwest* (Centralia, Washington: Weyerhaeuser Forestry Paper No. 8), 49 p.

Kitagawa, R., Ueno, M., and Masaki, T. (2018). Initial effects of thinning and concomitant disturbance on the understory woody community in Japanese cedar plantation. *J. For. Res.* 23, 120–128. doi: 10.1080/13416979.2018.1430653

Lavoie, S., Ruel, J. C., Bergeron, Y., and Harvey, B. D. (2012). Windthrow after group and dispersed tree retention in eastern Canada. *For. Ecol. Manage.* 269, 158–167. doi: 10.1016/j.foreco.2011.12.018

Lemay, A., Krause, C., Achim, A., and Bégin, J. (2018). Growth and wood quality of black spruce and balsam fir following careful logging around small merchantable stems (CLASS) in the boreal forest of Quebec, Canada. *Forest.: Int. J. For. Res.* 91, 271–282. doi: 10.1093/forestry/cpw060

Li, C., Barclay, H., Huang, S., Roitberg, B., Lalonde, R., and Thiffault, N. (2022). Detecting compensatory growth in silviculture trials: empirical evidence from three case studies across Canada. *Front. Plant Sci.* 13. doi: 10.3389/fpls.2022.907598

Li, C., Barclay, H., Huang, S., and Sidders, D. (2017). Wood fibre value simulation model: a new tool to assist measuring changes in forest landscapes by evaluating forest inventory. *Landscape Ecol.* 32, 1517–1530. doi: 10.1007/s10980-016-0406-6

Li, C., Barclay, H., Roitberg, B., and Lalonde, R. (2020). Forest productivity enhancement and compensatory growth: a review and synthesis. *Front. Plant Sci.* 11. doi: 10.3389/fpls.2020.575211

Li, C., Barclay, H., Roitberg, B., and Lalonde, R. (2021). Ecology and prediction of compensatory growth: from theory to application in forestry. *Front. Plant Sci.* 12. doi: 10.3389/fpls.2021.655417

Li, C., Huang, S., Barclay, H., and Filipescu, C. N. (2018). Estimation of compensatory growth of coastal Douglas-fir following pre-commercial thinning across a site quality gradient. *For. Ecol. Manage.* 429, 308–316. doi: 10.1016/j.foreco.2018.07.028

Li, C., Liu, J., Lafortezza, R., and Chen, J. (2011). "Managing forest landscapes under global change scenarios," in *Landscape ecology in forest management and conservation: Challenges and solutions for global change*. Eds. C. Li, R. Lafortezza and J. Chen (Beijing: Higher Education Press – Springer-Verlag. Beijing – Berlin Heidelberg), Pages 3–21.

Long, J. N. (1985). A practical approach to density management. *Forest. Chronicle*, 23–27. doi: 10.5558/tfc61023-1

Mangel, M., Fiksen, O., and Giske, J. (2001). "Theoretical and statistical models in natural resource management and research," in *Modelling in natural resource management: Development, interpretation, and application*. Eds. T. M. Shenk and A. B. Franklin (Washington, USA: Island Press), Pp. 57–Pp. 72.

Mangel, M., and Munch, S. B. (2005). A life-history perspective on short- and long-term consequences of compensatory growth. *Am. Nat.* 166 (6), E155–E176. doi: 10.1086/444439

Manitoba Conservation and Water Stewardship (2013) *Wood supply analysis report: forest management unit 24*. Available at: http://digitalcollection.gov.mb.ca/awweb/pdfopener?smd=1&did=22926&md=1 (Accessed March 1, 2021).

Martin, P. (1991). *Growth and yield prediction systems* (British Columbia Ministry of Forests), 31 p.

Maschinski, J., and Whitham, T. G. (1989). The continuum of plant responses to herbivory: the influence of plant association, nutrient availability and timing. *Am. Nat.* 134, 1–9. doi: 10.1086/284962

Mitchell, K. J. (1975). Dynamics and simulated yield of Douglas-fir. *For. Sci. Monograph* 17, 39 pp.

Montoro Girona, M., Morin, H., Lussier, J. M., and Ruel, J. C. (2019). Post-cutting mortality following experimental silvicultural treatments in unmanaged boreal forest stands. *Front. Forests Global Change* 2. doi: 10.3389/ffgc.2019.00004

Montoro Girona, M., Morin, H., Lussier, J. M., and Walsh, D. (2016). Radial growth response of black spruce stands ten years after experimental shelterwoods and seed-tree cuttings in boreal forest. *Forests* 7, 240. doi: 10.3390/f7100240

Nyland, R. D. (1996). *Silviculture: Concepts and applications* (New York. NY: The McGraw-Hill Companies, Inc), 633 p.

Osborne, T. B., and Mendel, L. B. (1915). The resumption of growth after long continued failure to grow. *J. Biol. Chem.* 23, 439–454. doi: 10.1016/S0021-9258(18)87585-8

Osborne, T. B., and Mendel, L. B. (1916). Acceleration of growth after retardation. *Am. J. Physiol.* 40, 16–20. doi: 10.1152/ajplegacy.1916.40.1.16

Pamerleau-Couture, E., Krause, C., Pothier, D., and Weiskittel, A. (2015). Effect of three partial cutting practices on stand structure and growth of residual black spruce trees in north-eastern Quebec. *Forest.: Int. J. For. Res.* 88, 471–483. doi: 10.1093/forestry/cpv017

Penner, M., Power, K., Muhairwe, C., Tellier, R., and Wang, Y. (1997). "Canada's forest biomass resources: deriving estimates from canada's forest inventory," in *Information report BC-X-370* (Canada: Pacific Forestry Centre, Canadian Forest Service, Natural Resources Canada, Victoria, British Columbia).

Pitt, D., and Lanteigne, L. (2008). Long-term outcome of precommercial thinning in northwestern new Brunswick: growth and yield of balsam fir and red spruce. *Can. J. For. Res.* 38, 592–610. doi: 10.1139/X07-132

Reukema, D. L. (1975). "Guidelines for precommercial thinning of Douglas-fir," in *General technical report PNW-GTR-030* (Portland, OR: U.S. Department of Agriculture, Forest Service, Pacific Northwest Research Station), 10 p.

Safranyik, L., Barclay, H. J., Thomson, A., and Riel, W. G. (1999). "A population dynamics model for the mountain pine beetle, dendroctonus ponderosae hopk. (Coleoptera : Scolytidae)," in *Information report BC-X-386* (Canada: Pacific Forestry Centre, Canadian Forest Service, Victoria, British Columbia), 35 pages.

Shell, D., and Bongers, F. (2020). Interpreting forest diversity-productivity relationships: volume values, disturbance histories and alternative inferences. *For. Ecosyst.* 7, 6. doi: 10.1186/s40663-020-0215-x

Shugart, H., Sedjo, R., and Sohngen, B. (2003) *Forests & global climate change: potential impacts on U.S. forest resources. prepared for the pew center on global climate change*. Available at: https://www.c2es.org/wp-content/uploads/2003/03/forests-global-climate-change.pdf.

SYSTAT Software Inc. (2002). *TableCurve 3D user's manual. version 4.0 for windows* (Chicago, IL).

Weetman, G. F., and Mitchell, S. J. (2013). "Silviculture," in *Forestry handbook for British Columbia, 5th edition*. Eds. S. B. Watts and L. Tolland (Vancouver, BC: The Forestry Undergraduate Society, Faculty of Forestry, UBC), 394–431.

Whitham, T. G., Maschinski, J., Larson, K. C., and Paige, K. N. (1991). "Plant responses to herbivory: the continuum from negative to positive and underlying physiological mechanism," in *Plant-animal interactions: Evolutionary ecology in tropical and temperate regions*. Eds. P. W. Price, T. M. Lewinsohn, G. W. Fernandes and W. W. Benson (New York: John Wiley & Sons), 227–256.

Zeide, B. (2008). The science of forestry. *J. Sustain. Forest.* 27, 345–473. doi: 10.1080/10549810802339225

Zirbel, C. R., Bassett, T., Grman, E., and Brudvig, L. A. (2017). Plant functional traits and environmental conditions shape community assembly and ecosystem functioning during restoration. *J. Appl. Ecol.* 54, 1070–1079. doi: 10.1111/1365-2664.12885

frontiers | Frontiers in Plant Science

TYPE Original Research
PUBLISHED 21 November 2023
DOI 10.3389/fpls.2023.1260707

OPEN ACCESS

EDITED BY
Bernard Roitberg,
Simon Fraser University, Canada

REVIEWED BY
Qaiser Javed,
Jiangsu University, China
Babar Iqbal,
Jiangsu University, China

*CORRESPONDENCE
Xin Xiong
xiongx@scbg.ac.cn

RECEIVED 18 July 2023
ACCEPTED 18 October 2023
PUBLISHED 21 November 2023

CITATION
Wu A, Xiong X, González-M R, Li R, Li A, Liu J, Tang X and Zhang Q (2023) Climate change reshapes plant trait spectrum to explain biomass dynamics in an old-growth subtropical forest.
Front. Plant Sci. 14:1260707.
doi: 10.3389/fpls.2023.1260707

Climate change reshapes plant trait spectrum to explain biomass dynamics in an old-growth subtropical forest

Anchi Wu[1,2], Xin Xiong[2,3]*, Roy González-M[4,5], Ronghua Li[6], Andi Li[2], Juxiu Liu[2], Xuli Tang[2] and Qianmei Zhang[2]

[1]Hubei Key Laboratory of Biologic Resources Protection and Utilization, Hubei Minzu University, Enshi, China, [2]Key Laboratory of Vegetation Restoration and Management of Degraded Ecosystem, South China Botanical Garden, Chinese Academy of Sciences, Guangzhou, China, [3]Lushan Botanical Garden, Chinese Academy of Sciences, Jiujiang, China, [4]Programa Ciencias Básicas de la Biodiversidad, Instituto de Investigación de Recursos Biol ógicos Alexander von Humboldt, Bogotá, Colombia, [5]Department of Biology, Faculty of Natural Sciences, Universidad del Rosario, Bogotá, Colombia, [6]College of Natural Resources and Environment, South China Agricultural University, Guangzhou, China

Climate change leads to novel species interactions and continues to reshuffle ecological communities, which significantly declines carbon accumulation rates in mature forests. Still, little is known about the potential influence of multiple global change factors on long-term biomass dynamics and functional trait combinations. We used temporal demographic records spanning 26 years and extensive databases of functional traits to assess how old-growth subtropical forest biomass dynamics respond to various climatic change scenarios (extreme drought, subsequent drought, warming, elevated CO_2 concentrations, and windstorm). We found that the initial severe drought, subsequent drought and windstorm events increased biomass loss due to tree mortality, which exceeded the biomass gain produced by survivors and recruits, ultimately resulting in more negative net biomass balances. These drought and windstorm events caused massive biomass loss due to tree mortality that tended towards acquisition species with high hydraulic efficiency, whereas biomass growth from survivors and recruits tended to consist of acquisition species with high hydraulic safety. Compensatory growth in this natural forest provided good explanation for the increase in biomass growth after drought and windstorm events. Notably, these dominant-species transitions reduced carbon storage and residence time, forming a positive carbon-climate feedback loop. Our findings suggest that climate changes could alter functional strategies and cause shifts in new dominant species, which could greatly reduce ecological functions and carbon gains of old-growth subtropical forests.

KEYWORDS

carbon sequestration, compensatory growth, demographic rates, trait probability density, extreme drought, subtropical forest

Introduction

Climate change has potentially large consequence for ecosystem composition and structure (Allen et al., 2010; Aleixo et al., 2019; Zhao et al., 2022; Liu et al., 2023), thereby affecting local and global net carbon balances (Reichstein et al., 2013; Yang et al., 2022). However, demographic changes are critical for understanding forest carbon balance and its response to interannual climatic variations (Lewis et al., 2009; Pan et al., 2013; Chen et al., 2016; Luo et al., 2019). Net changes in aboveground forest biomass are modulated by a combination of three demographic processes, including biomass growth of surviving trees, biomass increase from recruitment of new stems, and biomass loss due to mortality (Brienen et al., 2015; Hisano et al., 2019; González-M et al., 2020). Changes in net biomass can be attributed to either a faster temporal increase in tree mortality than growth, or increased mortality accompanied by decreased growth due to temporal decreases in water availability, persistent increases in air temperature and CO_2 concentrations, and the occurrence of climatic extremes (Breshears et al., 2005; van Mantgem et al., 2009; Ma et al., 2012; Brienen et al., 2015; Greenwood et al., 2017; O'Brien et al., 2017; Anderegg et al., 2020). Species-rich subtropical forest ecosystem, as a particularly important biome in the forest regions of East Asia, is pivotal for regulating the global carbon and water cycles (Yu et al., 2014; Wu et al., 2022). However, few studies have reported the long-term responses of net biomass changes and their three components to climatic perturbations in species-rich subtropical communities.

Systematic variations in demographic processes that underpin community assembly and dynamics over time have not provided underlying mechanistic explanations to generalize interspecific variations in response to both biotic and abiotic stresses (McGill et al., 2006; Meiners et al., 2015; Li et al., 2023). Plant functional traits that reflect life-history strategies and respond to environmental change could address this knowledge gap (McGill et al., 2006; Westoby and Wright, 2006; Adler et al., 2014; Swenson et al., 2020). Plant traits impact fitness indirectly via influencing survival, growth, and reproduction (Lavorel and Garnier, 2002; Violle et al., 2007), and can effectively predict various ecosystem processes and services (Wright et al., 2004; Wright et al., 2005; Shipley et al., 2006; Laughlin, 2014; Reich, 2014; González-M et al., 2020; Chacón-Labella et al., 2022). Environmental conditions alter ecological trade-offs and adaptive strategies associated with interspecific trait combinations, and the fitness and amount of trait variability are contingent on the nature and magnitude of environmental drivers (McGill et al., 2006; Díaz et al., 2007; Haddad et al., 2008; Mouillot et al., 2013; Adler et al., 2014; Bruelheide et al., 2018; Yang et al., 2018; Sarker et al., 2021; Iqbal et al., 2023). Herein, applying trait-based approaches to study the functional responses of most coexisting tree species to ongoing climate change and how these responses translate into changes in biomass carbon sinks could improve our ability to predict forest changes under future climate change scenarios (McDowell et al., 2008; González-M et al., 2020; Caleño-Ruiz et al., 2023).

Ecophysiological trait trade-offs that define fundamental niche differences and fitness among species in response to environmental conditions can be used to understand species coexistence mechanisms and ecosystem processes (Sterck et al., 2011; Craven et al., 2015; Aguirre-Gutierrez et al., 2019; Ge et al., 2019; Poorter et al., 2019; González-M et al., 2020; van der Plas et al., 2020). In species-rich forests, variations in multiple traits are organized along two main dimensions corresponding to trade-offs in resource acquisition-conservation and hydraulic safety-efficiency (Wright et al., 2004; González-M et al., 2020). Conservative species with high wood density exhibit high levels of hydraulically safe tissues and mechanical stability, plant survival, shade and drought tolerance, as well as better defense against herbivores, fungi, and pathogens (Van Gelder et al., 2006; Chave et al., 2009; Méndez-Alonzo et al., 2012). Consequently, they are also less vulnerable to hydraulic failure, have a lower mortality risk, may keep their stomata open and maintain a positive carbon-gaining capacity even under dry conditions (McDowell et al., 2008; Poorter, 2008; Quero et al., 2011). In contrast, acquisitive species with low wood density are related to larger xylem vessels, higher hydraulic conductivity, and higher photosynthetic rates and carbon gains (Coley, 1983; Santiago et al., 2004; Markesteijn et al., 2011; Méndez-Alonzo et al., 2012; Yin et al., 2023). Under drought conditions, it is expected that acquisitive species close their stomata and reduce transpiration to avoid hydraulic failure and cavitation of the xylem water column, thereby limiting the ability of plants to supply water to leaves for photosynthetic gas exchange (Hetherington and Woodward, 2003; McDowell et al., 2008; Quero et al., 2011). However, it is still not entirely clear how environmental factors determine the two-dimensional spectrum of plant form and function (Wright et al., 2010; Joswig et al., 2022).

Understanding the change patterns in the structure and function of forest ecosystem during and after multiple climate events such as droughts, storms, floods, fire, and lightning strikes, as well as exploring their underlying mechanisms, are crucial for forecasting forest ecosystem function and dynamics under global climate change. Therefore, there is a need for a general theory that can be applied to specific cases. Compensatory growth refers to the accelerated growth response of plants to damage, thereby offsetting adverse effects, restoring functionality, and maintaining their original growth state after perturbations (Mcnaughton, 1983; Belsky, 1986). It also appears as a common phenomenon in biology, and can provide a unique perspective to explain diverse forest growth patterns after partial mortality, including three forms: under-compensation, exact-compensation, and over-compensation (Li et al., 2021). The form of compensatory growth can be applied to explain changes in various forest growth indicators such as leaves, productivity, biomass, density, fecundity and recruitment (Jutila and Grace, 2002; Rea and Massicotte, 2010; Ascoli et al., 2019; Li et al., 2021). In nature forests, various factors could influence the pattern of forest growth over time. The responses and growth rates of certain tree species may vary significantly when site conditions change (light, soil nutrients, water and space, etc). However, detecting compensatory growth patterns and status after experiencing a period of unfavorable conditions in forests is important for the forest sector in designing future research strategies (Li et al., 2020; Li et al., 2021; Li et al., 2022).

The response trajectories and mechanistic explanations of subtropical forests to climate change remains poorly understood, partly due to the scarcity of highly replicated chronosequence data

for numerous tree species during and following extreme climatic events. Over the past three decades, subtropical forest ecosystems have been threatened by various environmental fluctuations, such as severe droughts, storms, ongoing warming, and elevated CO_2 concentrations (Pan et al., 2013; Zhou et al., 2011; Fauset et al., 2012; Zhou et al., 2014; Li et al., 2015). Of them, old forest trees with various ages, sizes and ontogenies cannot stably coexist over time, yet any large and persistent changes to the demographic processes over a short period could be the consequence of exogenous environmental changes (van Mantgem and Stephenson, 2007; van Mantgem et al., 2009). Old forests are irreplaceable, which has important implications for predicting forest vegetation dynamics. In a subtropical monsoon evergreen broad-leaved forest that is over 400 years old, we utilized repeat census data for a 1-ha permanent plot spanning 26 years and a dataset of 11 functional traits from 69 coexisting tree species (> 4,330 stems) to evaluate the long-term biomass dynamics and biomass-related plant trait spectrum space in response to multiple climatic scenarios. Specifically, we aimed to address two questions: (1) How have multiple climate stresses alter community biomass assembly and dynamics in an old-growth subtropical forest over the past two decades? (2) In the presence of multiple climatic stresses, can shifts in the plant functional trait spectrum space elucidate biomass assembly dynamics and the underlying mechanisms within this forest? We hypothesize that compared to favorable environmental conditions, higher climatic stresses have a greater impact on biomass dynamics and functional trait combinations.

Materials and methods

Study site and tree censuses

This study site was located in the Dinghushan Biosphere Reserve (20°09′21″–23°11′30″N, 112°32′39″–112°35′41″E) approximately 84 kilometers west of Guangzhou, in Guangdong Province, southern China. The reserve was established in 1950 to protect the natural monsoon evergreen broad-leaved forests in the southern subtropics and was accredited as China's first national natural reserve in 1956. This region belongs to a typical southern subtropical monsoon climate with distinct dry and wet seasons. Annual average precipitation oscillates between 1,099 and 2,221 mm with a mean of 1,653 mm (based on data from 1960–2020), of which nearly 80% falls during the wet season (April–September) and the rest 20% falls during the dry season (October–March). The mean temperature is 9.6 °C in January and 30.7 °C in August with an annual mean of 22.4 °C. The site has red and yellow soils developed from the bedrock that consists of sandstone and shale. Soil clay, silt, and sand contents are 18.5%, 66.0%, and 15.6%, respectively, with a soil pH of 4.1 and an Fe content of 5.4 g kg^{-1} (Yu et al., 2019).

A 1-ha long-term permanent plot was established in the center of the reserve at an altitude of 200–300 m with a south-facing slope of 25–30° for long-term forest monitoring. The forest community is a species-rich old-growth subtropical lowland evergreen forest that has remained undisturbed for at least 400 years (Zhou et al., 2006). Since the establishment of the permanent sample plot, tree censuses have typically been carried out every ~5 years. All freestanding woody stems ≥1 cm diameter at breast height (DBH, measured at 1.3 m height) were identified, tagged, measured, and mapped using standardized census protocols. This study utilized six census data for this permanent sample plot (1994, 1999, 2004, 2010, 2015 and 2020).

Climate change drivers

Based on 26-year records, we used the mean annual temperature (MAT), annual precipitation (AP), standardized precipitation and evapotranspiration index (SPEI), atmospheric CO_2 concentration, and two extreme climatic events to assess the long-term changes in multiple biomass dimensions and their related plant trait spectrum space. MAT and AP data were obtained from the local weather station. The CO_2 concentrations were derived from the Mouna Loa System Research Laboratory in Hawaii (http://www.esrl.noaa.gov/gmd/ccgg/trends/co2_data_mlo.html). The monthly-scale SPEI used in this study was extracted from the global drought monitor dataset at a 1° resolution from 1960–2020 to calculate the SPEI (Beguería et al., 2010; Vicente-Serrano et al., 2010). Both AP and SPEI values reached their lowest points in 2003 during the study period. Ciais et al. (2005) reported that an extreme global drought occurred in 2003. In addition, this permanent plot was observed to be affected by the windstorm "Super Typhoon Mangkhut" on August 16, 2018, by combining drone aerial images before, during, and after the windstorm.

Functional traits

We selected five individual trees per species and measured 11 functional traits from 345 populations of 69 tree species belonging to 36 families. We selected sun-exposed branches and mature leaves from the designated trees to measure various traits. The 69 species accounted for more than 98% of the individuals and standing biomass in this plot from 1994 to 2020. The following multiple traits were used to describe the adaptation strategies of multiple species to environmental changes: specific leaf area (SLA, $cm^2\ g^{-1}$), leaf nitrogen concentration (N_L, mg g^{-1}), leaf phosphorous concentration (P_L, mg g^{-1}), leaf N:P ratio ($N:P_L$, mg g^{-1}), photosynthetic capacity at maximum CO_2 assimilation rates (A_{sat}, μmol $m^{-2}\ s^{-1}$), stomatal conductance (g_s, mol $m^{-2}\ s^{-1}$), sapwood-specific hydraulic conductivity (*Ks*, kg $m^{-1}\ s^{-1}\ MPa^{-1}$), leaf-to-sapwood area ratio (A_L/A_S, $m^2\ mm^{-2}$), water potential turgor loss point (TLP, MPa), predawn leaf water potential (ψ_{PD}, MPa), and wood density (WD, g cm^{-3}).

Aboveground biomass and biomass changes

In any point in time, we estimated aboveground biomass (AGB, t ha^{-1}) for each species of this permanent plot by using DBH-based

allometric biomass equations for the stems, branches, and leaves, respectively (Wen et al., 1997). Between two successive censuses, biomass growth of survivors (BGS, t ha^{-1} yr^{-1}) for each species was calculated as the annual biomass increment resulting from the growth of all surviving trees from the first census (T_0) to the last census (T_1). Biomass growth of recruits (BGR, t ha^{-1} yr^{-1}) for each species was estimated as the annual biomass increment of trees that reached at least 1 cm DBH in T_1 and were not sampled in T_0. Biomass mortality (BM, t ha^{-1} yr^{-1}) for each species was estimated as the biomass of all died trees between T_0 and T_1. Net biomass change (NBC, t ha^{-1} yr^{-1}) for each species was calculated as the difference between biomass gain (BGS + BGR) and biomass loss (BM) in both censuses. Positive changes in net biomass (NBC^+) indicated net biomass gain, while negative changes in net biomass (NBC^-) indicated net biomass loss.

Data analyses

Firstly, to describe changes in the functional trait space, we performed principal component analysis (PCA) with multiple traits at the individual level using the 'princomp' function in R. We selected the first two PC axes to create a two-dimensional trait space. The ordination of species across this surface presents a two-dimensional continuum, integrating ecological strategies in eleven trait combinations. To effectively visualize the functional spectra as density areas of species with 'peak-valleys', we used trait probability density (TPD) approach to calculate the occurrence probability of given combinations of trait values and employed two-dimensional kernel density estimation to construct color gradients and contour lines. For each scenario, we extracted contours at the 0.5 and 0.99 quantile thresholds of the probability distribution, thus highlighting the regions of the highest and lowest trait occurrence probability. The color gradient illustrates regions where the relative density of trait combinations is expected to increase (red) or decrease (yellow) as a result of functional transitions. These analyses were performed using the 'TPD' and 'ks' R packages (Chacón and Duong, 2018; Carmona et al., 2019).

Secondly, to quantify the amount of plant trait spectrum spaces (functional richness, FR) occupied by biomass dimension (i.e. aboveground biomass, demographic biomass and net biomass changes) in response to the TPD, we estimated the functional space using the sum of each biomass dimension's hypervolumes and considering their probability distributions for values above 0 (Carmona et al., 2016; Carmona et al., 2019). In parallel, similarly to the use of β-diversity to determine the pairwise dissimilarity of species composition (Baselga, 2010). We used an overlap-based functional dissimilarity (β_O) index to quantify the dissimilarities on the trait spectrum space occupancy between biomass dimensions. The β_O index ranges from 0, when two units are functionally identical (overlap = 1), to 1, when there was no functional overlap between them (Carmona et al., 2019). To verify the reliability of the results for the variations in trait spectrum space, we randomly selected 35 species (close to half) during each census period and performed 999 iterations to estimate the functional trait space and functional dissimilarity differences in biomass dimensions. All statistical analyses were performed in R version 3.5.3 (R Core Team, 2019).

Results

Long-term variability of atmospheric CO_2, temperature, precipitation, and SPEI

Atmospheric CO_2 increased constantly from 1960 to 2020 (R^2 = 0.99, $P < 0.001$), and increased persistently by 2.13 ppm yr^{-1} from 1995 to 2020 (ranging from 358.96 to 414.24 ppm, Figure 1A). MAT increased significantly from 1960 to 2020 ($R^2 = 0.42$, $P < 0.001$). More specifically, MAT increased significantly from 1960 to 1994 (R^2 = 0.21, $P < 0.01$), with an average rise of 0.20 °C per decade. MAT showed a non-significant upward trend from 1995 to 2020 ($R^2 = 0.01$, $P = 0.66$), with an approximate increase of 0.5 °C compared to the period from 1960 to 1994 (Figure 1B). During the period from 1960 to 2020, there were no significant trends observed for AP ($R^2 = 0.00$, $P = 0.86$) and SPEI ($R^2 = 0.00$, $P = 0.95$). The study plot experienced frequent and severe droughts from 1999 to 2011, with the AP falling below 1,500 mm in 9 out of 13 years (Figure 1C). The period from 2000 to 2004 was characterized as the driest, with the lowest average AP and SPEI values. Among these dry years, the lowest AP and SPEI values occurred in 2003, with values of 1,251.80 mm and –0.66 (a monthly SPEI < –0.5 indicates extreme drought), respectively (Figures 1C, D). Furthermore, the windstorm in 2018 also posed a threat to the forest community (Figures 1E–G).

Aboveground biomass dynamics and its trait space in response to climate change

During the period of high rainfall (1995–1999), the total AGB in the permanent study plot increased by 8.57 t ha^{-1}. During the period of initial severe drought (2000–2004), especially the impact of the extreme drought in 2003, AGB decreased by 34.46 t ha^{-1}. During the subsequent drought period with low rainfall (2005–2010), AGB continued to decline by 5.1 t ha^{-1}. During the recovery period with high rainfall following two drought events (2011–2015), AGB increased by 9.47 t ha^{-1}. However, during the windstorm disturbance period in 2018 (2016–2020), AGB decreased significantly by 8.6 t ha^{-1} (Figure 2A). Simultaneously, the proportion of accumulating biomass in dominant species persistently declined since the first census, while that of other subordinate and rare species significantly increased (Figure 2B; Supplementary Table S1).

Eleven functional traits based on 345 populations of 69 species were summarized in the first two PC axes (its associated eigenvalues > 1), which together captured 47.03% of variation. The first PC axis associated with all traits explained 29.35% of variation, reflecting the resource acquisitive-conservative trade-off axis. Acquisitive species were linked to lower values of WD and $N:P_L$, and higher values of other traits, whereas conservative species exhibited the opposite trait values. The second PC axis explained 17.68% of variation, reflecting the hydraulic safety-efficiency trade-off axis.

10.3389/fpls.2023.1260707

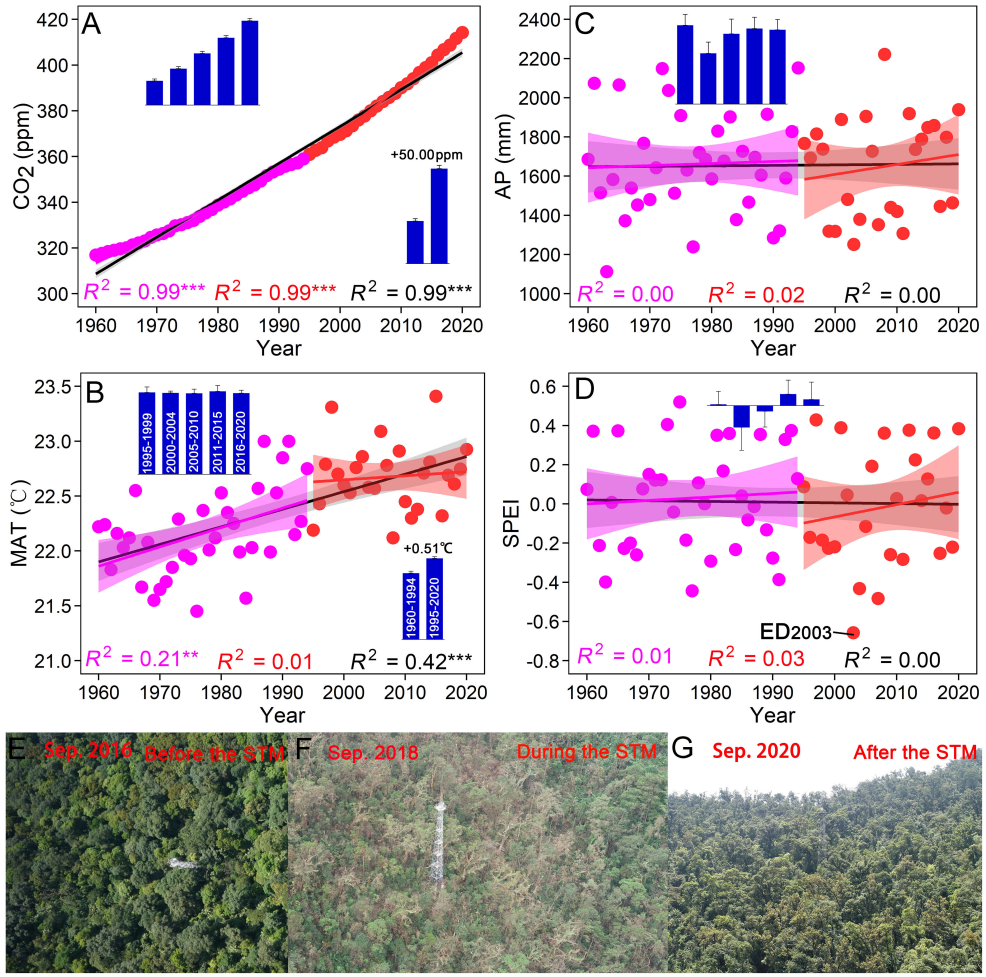

FIGURE 1
Long-term climatic changes from 1960 to 2020. **(A)** Atmospheric CO_2 concentration. **(B)** Mean annual temperature (MAT). **(C)** Annual precipitation (AP). **(D)** Standardized precipitation and evapotranspiration index (SPEI). **(E–G)** Forest landscape before, during and after the windstorm in 2018. Bar graphs show changes in climatic indices during different census periods (mean ± SE). ED_{2003} and STM_{2018} are respectively the extreme drought in 2003 and the windstorm "Super Typhoon Mangkhut" in 2018.

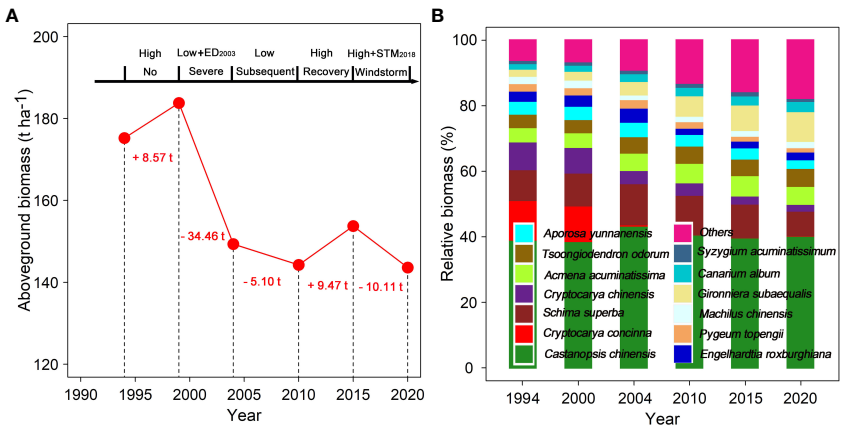

FIGURE 2
Long-term changes in aboveground biomass **(A)** and species biomass proportion **(B)** in a 1-ha forest plot from 1994 to 2020. The figure font indicates the difference in aboveground biomass between the next census and the last census. ED_{2003} and STM_{2018} indicate respectively extreme drought in 2003 and the windstorm "Super Typhoon Mangkhut" in 2018. Low and high indicate low and high rainfall in each census period.

The negative values indicated species with high hydraulic efficiency, which were strongly related to high photosynthetic capacity (A_{sat} and g_s) and weakly related to high *Ks*, WD, and N:P_L. The positive values were related to high hydraulic safety (A_L/A_S, TLP and ψ_{PD}) and leaf indicators (N_L, P_L and SLA) (Figure 3A; Supplementary Tables S2, S3).

When the trait probability threshold of equivalent weight was rescaled by the AGB per species over the study period, it was observed that 50% functional space was related to biomass-dominant species with high hydraulic efficiency, and only a small space was associated with species with high hydraulic safety. The 50–99% trait space exhibited a broad distribution (Figure 3B). The 50% and 99% trait space occupation in 1994, 2004 and 2015 was higher than other years. Notably, the initial severe drought resulted in the highest functional dissimilarities (βo) within all probability thresholds (low overlap trait space), followed by the effects of subsequent drought and windstorm (Figures 3C, D).

Demographic biomass and its trait space in response to climate change

During the period of high rainfall, BGS (2.76 t ha^{-1} yr^{-1}) was significantly higher than BGR (1.11 t ha^{-1} yr^{-1}) and BM (0.08 t ha^{-1} yr^{-1}) (Figures 4A, G, M). Compared to the period of high rainfall, during the initial severe and subsequent drought, BGS significantly decreased by 2.45 and 2.52 t ha^{-1} yr^{-1}, while BGR significantly increased by 0.23 and 0.31 t ha^{-1} yr^{-1}, and BM significantly increased by 9.58 and 3.68 t ha^{-1} yr^{-1}, respectively (Figures 4D, C, H, I, N, O). During the recovery period, BGS (3.39 t ha^{-1} yr^{-1}) increased significantly, while BGR (1.59 t ha^{-1} yr^{-1}) and BM (0.10 t ha^{-1} yr^{-1}) decreased significantly (Figures 4D, J, P). After the windstorm disturbance, BM, BGS, and BGR reached 5.47, 3.31 and 0.34 t ha^{-1} yr^{-1} respectively (Figures 4E, K, Q). From 1995 to 2020, BM, BGS, and BGR were 3.55, 1.81 and 0.52 t ha^{-1} yr^{-1} respectively (Figures 4F, L, R).

Compared to the period of high rainfall, BGS covered a narrower trait spectrum space within all probability thresholds during the period of severe drought and windstorm disturbance, but covered a broader trait space during the period of subsequent drought and recovery (Figures 4A–E). In contrast, BGR and BM covered a broader trait space within all probability thresholds during the initial severe drought, subsequent drought, and windstorm disturbance, while they covered a narrower trait space during the recovery period (Figures 4G–K, M–Q). Long-term BM and BGR covered a broader trait space than BGS (Figures 4F, L, R). Yet, BGS and BM were located alongside the hydraulic efficient-safety trade-off axis but only at the high acquisitive side. BGR was located along resource acquisitive-conservative trade-off axis but only on the side associated with high hydraulic safety (Figure 4).

In 50% threshold trait spectrum space, compared to the period of high rainfall, the initial severe drought, subsequent drought and windstorm events resulted in the trait space occupation of BGS to transform from high hydraulic-efficiency species to higher hydraulic-safety species, whereas that of BM shifted from high hydraulic-safety species towards high hydraulic-efficiency species. The trait space of BGR shifted from conservative to acquisitive species during the drought and windstorm events (Figure 4). The βo values among three biomass demographic dimensions declined significantly over time (Figures 5A–C). The results of 999 randomizations were consistent with the relative trait space occupancy described above (Supplementary Table S4).

Net positive and negative biomass changes and its trait space in response to climate change

Compared to the period of high rainfall (NBC^+ = 2.13 t ha^{-1} yr^{-1}) and recovery (NBC^+ = 2.78 t ha^{-1} yr^{-1}), NBC^+ significantly decreased during the initial severe drought (0.88 t ha^{-1} yr^{-1}), subsequent drought (1.62 t ha^{-1} yr^{-1}) and windstorm (1.10 t ha^{-1} yr^{-1}).

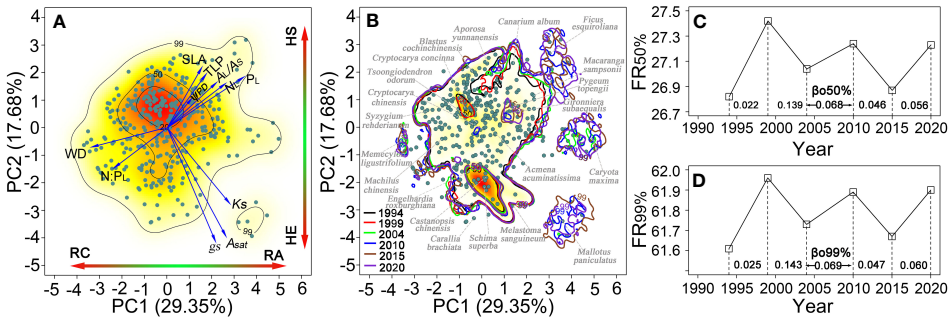

FIGURE 3
Trait probability densities (TPD) show the functional trait combinations of species populations along an axis of resource acquisition-conservation (PC1, 29.35% explained variance) and an axis of hydraulic safety-efficiency (PC2, 17.68% explained variance). **(A)** TPD where 69 tree species in this plot has an equivalent weight. **(B)** TPD where each species population is rescaled by its equivalent aboveground biomass in this plot from 1994 to 2020. **(C, D)** Functional richness (FR) of 50% and 99% probability threshold changes over time. The fonts indicate overlap-based functional dissimilarity (β_O) in different consecutive census periods. The relevant indicators defined as: N_L, leaf nitrogen concentration; P_L, leaf phosphorous concentration; N:P_L, leaf N:P ratio; SLA, specific leaf area; A_{sat}, photosynthetic capacity at maximum CO_2 assimilation rates; g_s, stomatal conductance; *Ks*, sapwood-specific hydraulic conductivity; A_L/A_S, leaf area to sapwood area ratio; TLP, water potential turgor loss point; ψ_{PD}, predawn leaf water potential; WD, wood density; RC, resource conservation; RA, resource acquisition; HE, hydraulic efficiency; HS, hydraulic safety.

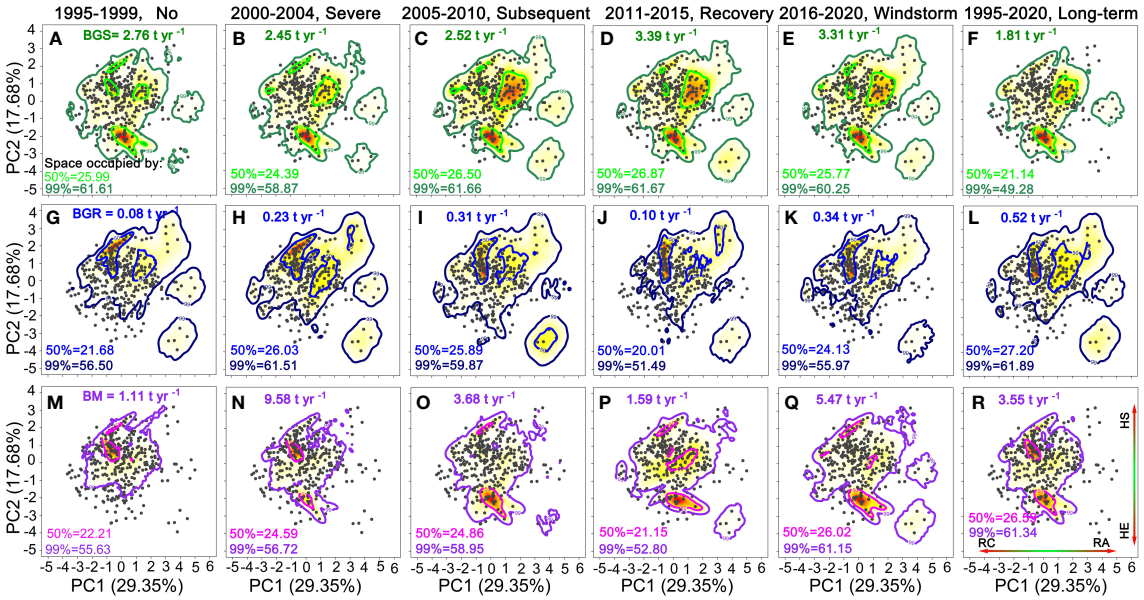

FIGURE 4
Trait probability densities (TPD) showing the functional trait combinations of each species populations is rescaled by its equivalent biomass growth of survivors (BGS in green colours, **A–F**), biomass growth of recruits (BGR in blue colours, **G–L**) and biomass mortality (BM in purple colours, **M–R**). Functional richness (FR) of 50% and 99% probability threshold in the TPD. RC, resource conservation; RA, resource acquisition; HE, hydraulic efficiency; HS, hydraulic safety.

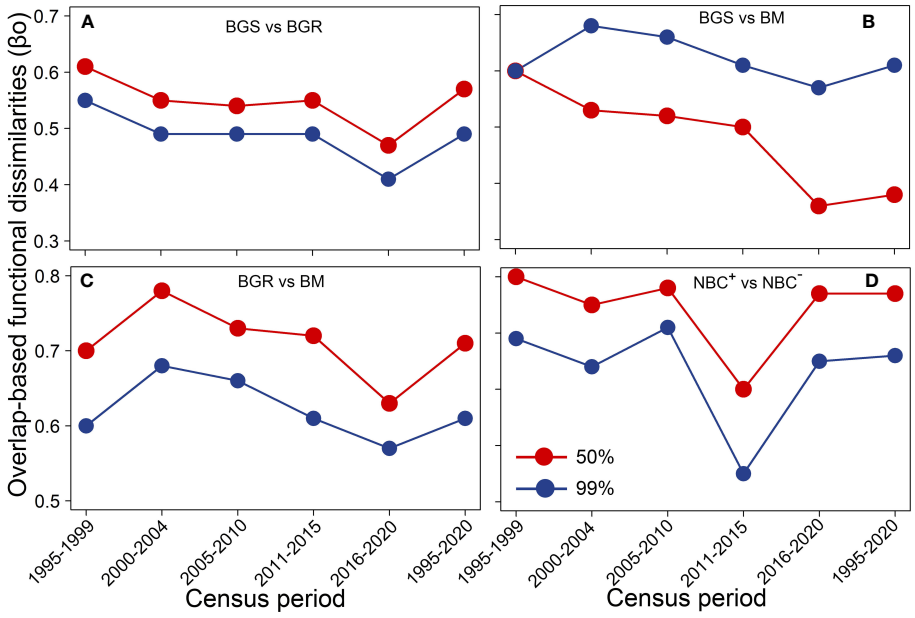

FIGURE 5
Overlap-based functional dissimilarities (βo) among biomass dimensions **(A–D)** within 50% and 99% probability thresholds during different census periods. BGS, biomass growth of survivors; BGR, biomass growth of recruits; BM, biomass mortality; NBC^+, positive net biomass changes; NBC^-, negative net biomass changes.

10.3389/fpls.2023.1260707

However, compared to the period of high rainfall (NBC^- = 0.42 t ha^{-1} yr^{-1}) and recovery (NBC^- = 0.89 t ha^{-1} yr^{-1}), NBC^- increased significantly during the initial severe drought (7.78 t ha^{-1} yr^{-1}), subsequent drought (2.47 t ha^{-1} yr^{-1}) and windstorm disturbance (3.32 t ha^{-1} yr^{-1}). Long-term NBC^- (2.31 t ha^{-1} yr^{-1}) was higher than NBC^+ (1.10 t ha^{-1} yr^{-1}) (Figure 6).

Compared to the period of high rainfall and recovery, NBC^+ covered a narrower proportion of trait spectrum space during the period of initial severe drought, subsequent drought and windstorm disturbance, while NBC^-covered a broader proportion within all probability thresholds. Long-term NBC^+ covered a broader proportion of trait space than NBC^- (Figure 6). In particular, NBC^- trait space induced by subsequent drought increased continuously compared to the initial severe drought period. Notably, the windstorm-induced NBC^+ trait space was narrower, while the windstorm-induced NBC^- trait space was broader compared to the two drought periods. During the period of initial severe drought, subsequent drought, and windstorm disturbance, the differences in trait space between NBC^+ and NBC^-(Diff.FR = | NBC^+–NBC^-|) greatly narrowed for all probability thresholds. The windstorm-induced trait space for NBC^-covered a broader proportion than those for NBC^+ at 99% probability thresholds. The trait space occupation for NBC^+ tended to consist of acquisitive species, while that of NBC^-tended to consist of conservative species with high hydraulic efficiency at 50% probability thresholds (Figure 6). Notably, the βo values between NBC^+ and NBC^-decreased significantly over time and reached their lowest point during the recovery period (Figure 5D).

Discussion

The impacts of old forests on the global carbon cycle will not be replaceable if they are lost due to global climate change. Here, we used long-term demographic records spanning 26 years and multiple functional traits of 69 coexisting subtropical forest tree species to assess the responses of community biomass dynamics and plant trait spectrum space to climate change. We observed that the occurrence of drought and windstorm events interacting with air warming and elevated CO_2 reduces biomass gains and increases biomass losses, resulting in more net negative biomass balances. The shifts in functional trait combinations resulting from various climate stresses show new dominant acquisition species with high hydraulic safety gradually emerged and established dominance in the old-growth community. Although compensatory growth was observed during and after drought and storm events, massive biomass loss reduced carbon storage and residence time, ultimately forming a positive carbon-climate feedback loop. Together, in addition to analyzing and expanding demographic biomass dynamics of an old-growth subtropical forest, applying trait-based approaches examines and predicts directional variation of current and future vegetation composition under global climate

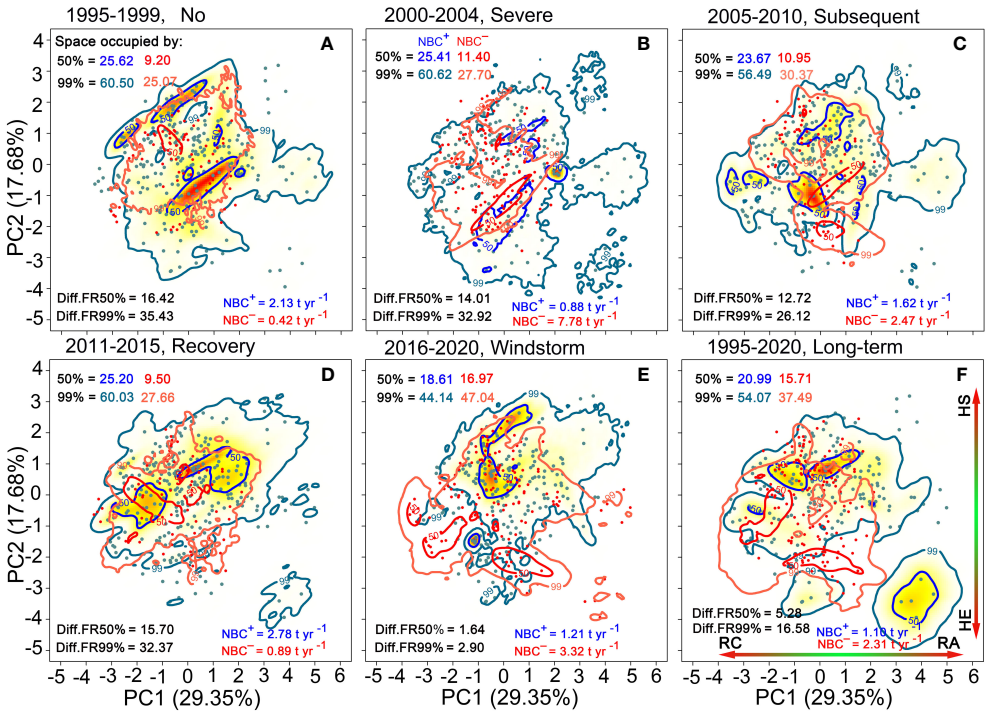

FIGURE 6
Trait probability densities (TPD) showing the functional trait combinations for species populations is rescaled by positive net biomass changes (NBC^+ in blue colors) and by negative net biomass changes (NBC^- in red colors) **(A–F)**. Functional richness (FR) of 50% and 99% probability threshold in the TPD. Diff.FR refers to differences in FR between NBC^+ and NBC^-. RC, resource conservation; RA, resource acquisition; HE, hydraulic efficiency; HS, hydraulic safety.

change. This study makes a substantial contribution to our understanding of community composition dynamics and the drivers of subtropical old-growth forests.

Climate change increases net negative biomass change

Growing evidence suggests that severe drought is one of the most consequential climatic extremes, exerting a significant impact on the terrestrial carbon cycle (Ciais et al., 2005; Reichstein et al., 2013; Zscheischler et al., 2014). Severe drought may lead to tree mortality directly through hydraulic failure, carbon starvation, or a combination of both (McDowell et al., 2008; Sevanto et al., 2014; Adams et al., 2017), or indirectly through increased vulnerability to forest pests (McDowell et al., 2008; Anderegg et al., 2012; Anderegg et al., 2015a). Severe drought significantly increases tree mortality and biomass loss through limited water availability across species and biomes (Allen et al., 2010; Peng et al., 2011; Anderegg et al., 2015a; Adams et al., 2017; McDowell et al., 2018; van Mantgem et al., 2009; González-M et al., 2020), and it also impacts overall forest structure, biodiversity, and ecosystem function (Anderegg et al., 2012; Anderegg et al., 2015b; Anderegg et al., 2020). Our results demonstrate that the initial severe drought triggers immediate and chronic biomass loss due to tree mortality (Figures 2A, 4N), constrains the biomass growth of survivors (Figure 4B), and ultimately increases net negative biomass changes in an old-growth subtropical forest (Figure 6B). Furthermore, forest biomass loss remains elevated during subsequent drought and recovery periods because the initial severe drought resulted in numerous cascading indirect effects (Figures 4O, P). This indicates that drought-induced mortality can occur immediately or may be delayed, and that biomass loss attributable to tree mortality remains elevated even after drought episode ends, congruent with studies of drought events in the Amazonian rainforest (Aleixo et al., 2019). Severe drought caused by reduced rainfall and warmer air temperatures increases mortality rates for up to two years after the climatic event, synergistically interacting with pathogens, insects, wind throw, and storm damage (Phillips et al., 2010). In particular, large trees are more sensitive to drought stress than smaller trees (Nepstad et al., 2007; Allen et al., 2010; Phillips et al., 2010; Zhou et al., 2013; Zhou et al., 2014; Bennett et al., 2015). Our results highlight that the relative proportions of biomass-dominant species in the old forest under dry conditions have continuously declined since the first census (Figure 2B).

Also, strong winds would cause leaf loss, tree collapse, and tree mortality, especially for trees that are less vigorous or have already suffered from droughts, pathogens, and pests (Aleixo et al., 2019; Yee et al., 2019). Our findings suggest that biomass loss caused by windstorm-induced tree mortality exceeds biomass gain produced by survivors and recruits (Figures 4E, K, Q), resulting in greater net negative biomass changes in subsequent years (Figure 6E). Climatic events cause tree mortality, cumulative physiological and mechanical damage, and the substantial accumulation of leaf litter and woody debris, thereby increasing nutrients available in the soil and potentially benefiting the biomass gained by survivors and recruits (Lodge et al., 1991; Steudler et al., 1991; Suarez and Kitzberger, 2010; Aleixo et al., 2019; Yee et al., 2019). Drought and windstorm events increase the biomass gained by survivors' growth and facilitate the establishment of recruiting stems for the subsequent recovery period (Figures 4C–E, I–K). Increased water availability, climatic warming, and elevated CO_2 concentrations are expected to enhance plant biomass gain and carbon sequestration in forest ecosystems (Ciais et al., 2005; Brienen et al., 2015; Luo and Chen, 2015; Chen et al., 2016; Hisano et al., 2019). Possibly, the increased growth of surviving trees resulted from the resources released as a result of increased mortality (Brienen et al., 2015; Luo and Chen, 2015). In fact, our results have demonstrated compensatory growth, that is, an increase in biomass growth from survivors and recruits both during and soon after drought and storm events. These mechanisms adequately explain the biomass losses and gains of this old forest in response to various climate change scenarios. Our findings demonstrate that drought and windstorm events increase biomass loss due to tree mortality, decrease biomass gain and even cause significant disruptions to the net carbon balance. These extreme climatic events substantially alter the forest structure and composition, erode the health quality of forest ecosystems, reverse carbon sinks to carbon sources and create positive carbon-climate feedback. That answers the first question we want to solve.

Climate change reshapes functional trait spectrum space across species

Plant traits associated with the whole-plant economic spectrum suggest that essential patterns of form and function across species can be captured by the two-dimensional spectra of multiple trait combinations (Lavorel and Garnier, 2002; McGill et al., 2006; Westoby and Wright, 2006; Diaz et al., 2015; Laughlin and Messier, 2015; Joswig et al., 2022). As such, quantifying plant trait spectrum space can better capture the breadth and adaptability of tree form and function (Maynard et al., 2022). This old-growth forest across species demonstrates that multiple trait combinations are fundamentally shaped by two main trade-off axes: resource acquisition-conservation and hydraulic safety-efficiency (Figure 3A). The widely distributed trait spectrum space across species reveals that greater plant phenotype diversity exhibits multiple alternative combinations and fitness levels under the same environmental conditions. Notably, acquisitive species inherently possess high leaf photosynthetic capacity, stomatal conductance, resource compensation points, capabilities for water and nutrient uptake, and relative growth rates compared to conservative species (Lambers and Poorter, 1992; Sterck et al., 2011). Dominant trees located in the canopy display high hydraulic efficiency, whereas shade- and drought-tolerant smaller trees exhibit high hydraulic safety (Poorter and Bongers, 2006; Prior

and Bowman, 2014; Rüger et al., 2018). Likewise, we note that the plant trait spectrum space associated with high-biomass trees tends to include more acquisitive species with high hydraulic efficiency, whereas that related to low-biomass trees contains more conservative species with high hydraulic safety (Figure 3B).

The composition and variation of functional traits are shaped by climate variations, resource availability, and disturbance (Feeley et al., 2011; van der Sande et al., 2016; González-M et al., 2020; Lai et al., 2020; Laughlin et al., 2020). Over a 26-year period, climatic perturbations have a pronounced influence on functional trait space occupation in an old-growth subtropical forest. Both during and soon after extreme drought, the trait spectrum space for mortality biomass and recruitment biomass covers a broader range, whereas that for biomass growth covers a narrower range (Figures 4B, C, H, I, N, O). Additionally, a broader range of trait space is associated with negative than with positive net biomass changes (Figures 6B, C). Similar results have also been observed in tropical dry forests (González-M et al., 2020). During the initial severe and subsequent droughts, biomass loss caused by mortality is strongly negatively associated with net biomass changes (Supplementary Figures S1B, C). Prior studies have identified that drought-induced tree mortality is ubiquitous across multiple tree taxa, with less adapted species generating more net negative biomass balances (Allen et al., 2010; Anderegg et al., 2012; Anderegg et al., 2020; González-M et al., 2020). Plant functional traits related to hydraulic damage and stomatal control are useful predictors for the physiological causes of drought-induced mortality (McDowell et al., 2008; Mencuccini et al., 2015; Skelton et al., 2015; Anderegg et al., 2016; Adams et al., 2017). Additionally, the trait spectrum space for windstorm-induced mortality biomass is significantly broader than that for growth and recruitment (Figures 4E, K, Q), and even the space of negative net biomass changes is significantly broader than that of positive net biomass changes (Figure 6E). Moreover, tall trees with deep crowns and heavy weight are more susceptible to xylem hydraulic failure under water deficits and warming conditions. These trees are also more prone to being affected by windstorms. In this study, high-biomass species with high hydraulic efficiency caused by both drought and windstorm occupy more trait space for tree mortality (Figures 4N–Q). While two consecutive drought events increase biomass loss due to selective tree mortality, windstorms cause mortality biomass to cover a wider trait space and threaten more species. The dominant trait space of mortality biomass undergoes a transition from high hydraulic-safety species to high hydraulic-efficiency species, particularly in the presence of drought and windstorm events. This shift signifies the loss of fast-growing pioneer species within this diverse old-growth forest.Selective mortality of specific tree species drives long-term transitions in the dominant species and alters new plant-community assemblages, which can reset or shift successional trajectories (Kreyling et al., 2011; Anderegg et al., 2012). Specifically, biomass growth of surviving trees has a stronger positive correlation with biomass loss due to tree mortality during the initial severe and subsequent droughts, as well as after the windstorm (Supplementary Figure S2). It is important to note that widespread rapid mortality events and subsequent alterations could strongly impact tree species and functional composition of survivors and recruits under current climate change, altering the forest composition trajectory of existing communities. Our findings show that drought and windstorm events release stand resource space by removing overstorey trees with high hydraulic efficiency, which could potentially compensate for biomass growth of species with high hydraulic safety. The dominant trait space of biomass growth of survivors undergoes a transition from species with high hydraulic efficiency towards more species with high hydraulic safety (Figures 4D, G, M). Eventually, these transitions result in slow-growing tree species being dominant, thereby causing lower carbon sequestration.

Additionally, the dynamic process of tree establishment and growth is highly dependent on recruitment in species-rich communities. Small new recruits suppressed in the understory have a higher tolerance to shade and drought and a lower risk of hydraulic failure under dry conditions. To escape being shaded by competing or neighboring trees, newly established saplings or adult trees tend to grow more rapidly under increased understory light availability (King et al., 2005; Hérault et al., 2011; Iida et al., 2012; Rüger et al., 2018). Tree mortality caused by drought and windstorm events opens up the canopy, creating opportunities for new establishment and growth of understory components. These newly recruited trees with rapid resource acquisition ultimately have greater biomass gains (Figures 4B, C, E). We indeed found that biomass recruitment affected by drought and storm disturbance has exceeded that of the undisturbed, indicating a clear case of over-compensation. In combination, positive net biomass changes, consisting of both survivors and recruits, cover less functional trait space and include more acquisitive species with high hydraulic safety, both during and soon after climatic extremes (Figures 6B, C, E). Acquisition species with hydraulic safety often have shorter lifespans and higher turnover rates, resulting in faster carbon-water cycling and less carbon storage at the beginning of an extreme event and later in the year. Besides, the functional dissimilarities of multiple demographic dimensions are correlated with the increased availability of resources, such as increased rainfall, warming, and elevated CO_2 (Figure 5E). Climatic extremes interact with subsequent drought, warming, and elevated CO_2 to reshape function trait space in the forest ecosystem, which reduces carbon storage and residence time. Together, our study has offered a reasonable explanation for biomass composition and dynamics through trait-based approaches, addressing the second scientific question.

Conclusions

In a species-rich old-growth subtropical forest, the responses of multiple biomass dimensions and their functional trait combinations to multiple climatic scenarios are closely matched to the overall temporal period. Functional trait combinations are associated with the trade-offs between resource acquisition-conservation and hydraulic safety-efficiency. Climatic extreme events synergize with subsequent drought, warming, and elevated CO_2 to alter long-term biomass dynamics and reshape new dominant trait space. In particular, acquisitive species with hydraulic safety increase biomass gain, whereas acquisitive species with hydraulic efficiency experience greater biomass loss due to increased mortality. In parallel, changing

plant trait spectrum space suggests that ongoing climatic changes leads to a shift from being carbon sinks to carbon sources in the old-growth forest, with significant consequences for forest carbon cycle. Based on trait ecology, this study provides a framework to understand the responses of long-term carbon dynamics and vegetation composition changes to various climate change scenarios and underlying mechanism, filling in our knowledge of the forest degradation trajectories and future trends of subtropical forest communities under global climate change.

Data availability statement

The original contributions presented in the study are included in the article/Supplementary Material, further inquiries can be directed to the corresponding author.

Ethics statement

The manuscript presents research on animals that do not require ethical approval for their study.

Author contributions

AW: Conceptualization, Investigation, Formal analysis, Methodology, Visualization, Writing – original draft. XX: Conceptualization, Funding acquisition, Project administration, Supervision, Writing – review & editing. RG: Investigation, Formal analysis, Methodology, Visualization, Writing – review & editing. RL, AL, JL, XT and QZ: Investigation, Visualization, Writing – review & editing. All authors contributed to the article and approved the submitted version.

Funding

The author(s) declare financial support was received for the research, authorship, and/or publication of this article. This research was supported by the Natural Science Foundation of Guangdong Province (Grant Nos. 2022A1515110403), the National Natural Science Foundation of China (Grant Nos. 42130506 and 42071031), the Key Research and Development Program of Guangdong Province (Grant Nos. 2020B1111530004) and the Archives of Chinese Academy of Sciences (Grant Nos. Y821341001).

Conflict of interest

The authors declare that the research was conducted in the absence of any commercial or financial relationships that could be construed as a potential conflict of interest.

Publisher's note

Supplementary material

The Supplementary Material for this article can be found online at: https://www.frontiersin.org/articles/10.3389/fpls.2023.1260707/full#supplementary-material

References

Adams, H. D., Zeppel, M. J. B., Anderegg, W. R. L., Hartmann, H., Landhausser, S. M., Tissue, D. T., et al. (2017). A multi-species synthesis of physiological mechanisms in drought-induced tree mortality. *Nat. Ecol. Evol.* 1, 1285–1291. doi: 10.1038/s41559-017-0248-x

Adler, P. B., Salguero-Gómez, R., Compagnoni, A., Hsu, J. S., Ray-Mukherjee, J., Mbeau-Ache, C., et al. (2014). Functional traits explain variation in plant life history strategies. *Proc. Natl. Acad. Sci. U.S.A.* 111, 740–745. doi: 10.1073/pnas.1315179111

Aguirre-Gutierrez, J., Oliveras, I., Rifai, S., Fauset, S., Adu-Bredu, S., Affum-Baffoe, K., et al. (2019). Drier tropical forests are susceptible to functional changes in response to a long-term drought. *Ecol. Lett.* 22, 855–865. doi: 10.1111/ele.13243

Aleixo, I., Norris, D., Hemerik, L., Barbosa, A., Prata, E., Costa, F., et al. (2019). Amazonian rainforest tree mortality driven by climate and functional traits. *Nat. Clim. Change* 9, 384–388. doi: 10.1038/s41558-019-0458-0

Allen, C. D., Macalady, A. K., Chenchouni, H., Bachelet, D., McDowell, N., Vennetier, M., et al. (2010). A global overview of drought and heat-induced tree mortality reveals emerging climate change risks for forests. *For. Ecol. Manage.* 259, 660–684. doi: 10.1016/j.foreco.2009.09.001

Anderegg, W. R., Hicke, J. A., Fisher, R. A., Allen, C. D., Aukema, J., Bentz, B., et al. (2015a). Tree mortality from drought, insects, and their interactions in a changing climate. *New Phytol.* 208, 674–683. doi: 10.1111/nph.13477

Anderegg, W. R. L., Kane, J., and Anderegg, L. D. L. (2012). Consequences of widespread tree mortality triggered by drought and temperature stress. *Nat. Clim. Change* 3, 30–36. doi: 10.1038/nclimate1635

Anderegg, W. R. L., Klein, T., Bartlett, M. K., Sack, L., Pellegrini, A. F. A., Choat, B., et al. (2016). Meta-analysis reveals that hydraulic traits explain cross-species patterns of drought-induced tree mortality across the globe. *Proc. Natl. Acad. Sci. U.S.A.* 113, 5024–5029. doi: 10.1073/pnas.1525678113

Anderegg, W. R. L., Schwalm, C., Biondi, F., Camarero, J. J., Koch, G., Litvak, M., et al. (2015b). Pervasive drought legacies in forest ecosystems and their implications for carbon cycle models. *Science* 349, 528–532. doi: 10.1126/science.aab1833

Anderegg, W. R. L., Trugman, A. T., Badgley, G., Konings, A. G., and Shaw, J. (2020). Divergent forest sensitivity to repeated extreme droughts. *Nat. Clim. Change* 10, 1091–1095. doi: 10.1038/s41558-020-00919-1

Ascoli, D., Hacket-Pain, A., Hacket-Pain, A., LaMontagne, J. M., Cardil, A., Conedera, M., et al. (2019). Climate teleconnections synchronize Picea glauca masting and fire disturbance: evidence for a fire-related form of environmental prediction. *J. Ecol.* 108, 1186–1198. doi: 10.1111/1365-2745.13308

Baselga, A. (2010). Partitioning the turnover and nestedness components of beta diversity. *Global Ecol. Biogeogr.* 19, 134–143. doi: 10.1111/j.1466-8238.2009.00490.x

Beguería, S., Vicente-Serrano, S. M., and Angulo-Martínez, M. (2010). A multiscalar global drought dataset: the SPEIbase: a new gridded product for the analysis of drought variability and impacts. *B. Am. Meteorol. Soc* 91, 1351–1356. doi: 10.1175/2010BAMS2988.1

Belsky, A. J. (1986). Does herbivory benefit plants? a review of the evidence. *Am. Nat.* 127, 870–892. doi: 10.1086/284531

Bennett, A. C., McDowell, N. G., Allen, C. D., and Anderson-Teixeira, K. J. (2015). Larger trees suffer most during drought in forests worldwide. *Nat. Plants* 1, 1–5. doi: 10.1038/nplants.2015.139

Breshears, D. D., Cobb, N., Rich, P. M., Price, K., Allen, A. D., Balice, R. G., et al. (2005). Regional vegetation die-off in response to global-change-type drought. *Proc. Natl. Acad. Sci. U.S.A.* 102, 15144–15148. doi: 10.1073/pnas.0505734102

Brienen, R. J. W., Phillips, O. L., Feldpausch, T. R., Gloor, E., Baker, T. R., Lloyd, J., et al. (2015). Long-term decline of the Amazon carbon sink. *Nature* 519, 344–348. doi: 10.1038/nature14283

Bruelheide, H., Dengler, J., Purschke, O., Lenoir, J., Jimenez-Alfaro, B., Hennekens, S. M., et al. (2018). Global trait–environment relationships of plant communities. *Nat. Ecol. Evol.* 2, 1906–1917. doi: 10.1038/s41559-018-0699-8

Caleño-Ruiz, B. L., Garzón, F., López-Camacho, R., Pizano, C., Salinas, V., and González-M, R. (2023). Soil resources and functional trait trade-offs determine species biomass stocks and productivity in a tropical dry forest. *Front. For. Glob. Change* 6, 1028359. doi: 10.3389/ffgc.2023.1028359

Carmona, C. P., de Bello, F., Mason, N. W. H., and Leps, J. (2016). Traits without borders: integrating functional diversity across scales. *Trends Ecol. Evol.* 31, 382–394. doi: 10.1016/j.tree.2016.02.003

Carmona, C. P., de Bello, F. D., Mason, N. W. H., and Lepš, J. (2019). Trait probability density TPD.: measuring functional diversity across scales based on TPD with R. *Ecology* 100, e02876. doi: 10.1002/ecy.2876

Chacón, J. E., and Duong, T. (2018). *Multivariate kernel smoothing and its applications. 1st edn* (New York: Chapman and Hall/CRC).

Chacón-Labella, J., Hinojo-Hinojo, C., Bohner, T., Castorena, M., Violle, C., Vandvik, V., et al. (2022). How to improve scaling from traits to ecosystem processes. *Trends Ecol. Evol.* 38, 228–237. doi: 10.1016/j.tree.2022.10.007

Chave, J., Coomes, D., Jansen, S., Lewis, S. L., Swenson, N. G., and Zanne, A. E. (2009). Towards a worldwide wood economics spectrum. *Ecol. Lett.* 12, 351–366. doi: 10.1111/j.1461-0248.2009.01285.x

Chen, H. Y. H., Luo, Y., Reich, P. B., Searke, E. B., and Biswas, S. R. (2016). Climate change-associated trends in net biomass change are age dependent in western boreal forests of Canada. *Ecol. Lett.* 19, 1150–1158. doi: 10.1111/ele.12653

Ciais, P., Reichstein, M., Viovy, N., Granier, A., Ogee, J., Allard, V., et al. (2005). Europe-wide reduction in primary productivity caused by the heat and drought in 2003. *Nature* 437, 529–533. doi: 10.1038/nature03972

Coley, P. D. (1983). Herbivory and defensive characteristics of tree species in a lowland tropical forest. *Ecol. Monogr.* 53, 209–233. doi: 10.2307/1942495

Craven, D., Hall, J. S., Berlyn, G. P., Ashton, M. S., and van Breugel, M. (2015). Changing gears during succession: shifting functional strategies in young tropical secondary forests. *Oecologia* 179, 293–305. doi: 10.1007/s00442-015-3339-x

Diaz, S., Kattge, J., Cornelissen, J. H. C., Wright, I. J., Lavorel, S., Dray, S., et al. (2015). The global spectrum of plant form and function. *Nature* 529, 167–171. doi: 10.1038/nature16489

Díaz, S., Lavorel, S., de Bello, F., Quétier, F., Grigulis, K., and Robson, T. M. (2007). Incorporating plant functional diversity effects in ecosystem service assessments. *Proc. Natl. Acad. Sci. U.S.A.* 104, 20684–20689. doi: 10.1073/pnas.0704716104

Fauset, S., Baker, T. R., Lewis, S. L., Feldpausch, T. R., Affum-Baffoe, K., Foli, E. G., et al. (2012). Drought-induced shifts in the floristic and functional composition of tropical forests in Ghana. *Ecol. Lett.* 15, 1120–1129. doi: 10.1111/j.1461-0248.2012.01834.x

Feeley, K. J., Davies, S. J., Perez, R., Hubbell, S. P., and Foster, R. (2011). Directional changes in the species composition of a tropical forest. *Ecology* 92, 871–882. doi: 10.1890/10-0724.1

Ge, X. Y. M., Scholl, J. P., Basinger, U., Huxman, T. E., and Venable, D. L. (2019). Functional trait trade-off and species abundance: insights from a multi-decadal study. *Ecol. Lett.* 22, 583–592. doi: 10.1111/ele.13217

González-M, R., Posada, J. M., Carmona, C. P., Garzón, F., Salinas, V., Idárraga-Piedrahita, Á., et al. (2020). Diverging functional strategies but high sensitivity to an extreme drought in tropical dry forests. *Ecol. Lett.* 24, 451–463. doi: 10.1111/ele.13659

Greenwood, S., Ruiz-Benito, P., Martínez-Vilalta, J., Lloret, F., Kitzberger, T., Allen, C. D., et al. (2017). Tree mortality across biomes is promoted by drought intensity, lower wood density and higher specific leaf area. *Ecol. Lett.* 20, 539–553. doi: 10.1111/ele.12748

Haddad, N. M., Holyoak, M., Mata, T. M., Davies, K. F., Melbourne, B. A., and Preston, K. (2008). Species' traits predict the effects of disturbance and productivity on diversity. *Ecol. Lett.* 11, 348–356. doi: 10.1111/j.1461-0248.2007.01149.x

Hérault, B., Bachelot, B., Poorter, L., Rossi, V., Bongers, F., Chave, J., et al. (2011). Functional traits shape ontogenetic growth trajectories of rain forest tree species. *J. Ecol.* 99, 1431–1440. doi: 10.1111/j.1365-2745.2011.01883.x

Hetherington, A. M., and Woodward, F. I. (2003). The role of stomata in sensing and driving environmental change. *Nature* 424, 901–908. doi: 10.1038/nature01843

Hisano, M., Chen, H. Y. H., Searle, E. B., and Reich., P. B. (2019). Species-rich boreal forests grew more and suffered less mortality than species-poor forests under the environmental change of the past half-century. *Ecol. Lett.* 22, 999–1008. doi: 10.1111/ele.13259

Iida, Y., Poorter, L., Sterck, F. J., Kassim, A. R., Kubo, T., Potts, M. D., et al. (2012). Wood density explains architectural differentiation across 145 co-occurring tropical tree species. *Funct. Ecol.* 26, 274–282. doi: 10.1111/j.1365-2435.2011.01921.x

Iqbal, B., Javed, Q., Khan, I., Tariq, M., Ahmad, N., Elansary, H. O., et al. (2023). Influence of soil microplastic contamination and cadmium toxicity on the growth, physiology, and root growth traits of *Triticum aestivum L. S. Afr. J. Bot.* 160, 369–375. doi: 10.1016/j.sajb.2023.07.025

Joswig, J. S., Wirth, C., Schuman, M. C., Kattge, J., Reu, B., Wright, I. J., et al. (2022). Climatic and soil factors explain the two-dimensional spectrum of global plant trait variation. *Nat. Ecol. Evol.* 6, 36–50. doi: 10.1038/s41559-021-01616-8

Jutila, H., and Grace, J. B. (2002). Effects of disturbance on germination and seedling establishment in a coastal prairie grassland: a test of the competitive release hypothesis. *J. Ecol.* 90, 291–302. doi: 10.1046/j.1365-2745.2001.00665.x

King, D. A., Davies, S. J., Nur Supardi, M. N., and Tan, S. (2005). Tree growth is related to light interception and wood density in two mixed dipterocarp forests of Malaysia. *Funct. Ecol.* 19, 445–453. doi: 10.1111/j.1365-2435.2005.00982.x

Kreyling, J., Jentsch, A., and Beierkuhnlein, C. (2011). Stochastic trajectories of succession initiated by extreme climatic events. *Ecol. Lett.* 14, 758–764. doi: 10.1111/j.1461-0248.2011.01637.x

Lai, H. R., Chong, K. Y., Yee, A. T. K., Tan, H. T. W., and van Breugel, M. (2020). Functional traits that moderate tropical tree recruitment during post-windstorm secondary succession. *J. Ecol.* 108, 1322–1333. doi: 10.1111/1365-2745.13347

Lambers, H., and Poorter, H. (1992). Inherent variation in growth-rate between higher-plants – a search for physiological causes and ecological consequences. *Adv. Ecol. Res.* 23, 187–261. doi: 10.1016/S0065-2504(08)60148-8

Laughlin, D. C. (2014). Applying trait-based models to achieve functional targets for theory-driven ecological restoration. *Ecol. Lett.* 17, 771–784. doi: 10.1111/ele.12288

Laughlin, D. C., Gremer., J. R., Adler, P. B., Mitchell, R. M., and Moore, M. M. (2020). The net effect of functional traits on fitness. *Trends Ecol. Evol.* 35, 1037–1047. doi: 10.1016/j.tree.2020.07.010

Laughlin, D. C., and Messier, J. (2015). Fitness of multidimensional phenotypes in dynamic adaptive landscapes. *Trends Ecol. Evol.* 30, 487–496. doi: 10.1016/j.tree.2015.06.003

Lavorel, S., and Garnier, E. (2002). Predicting changes in community composition and ecosystem functioning from plant traits: revisiting the Holy Grail. *Funct. Ecol.* 16, 545–556. doi: 10.1046/j.1365-2435.2002.00664.x

Lewis, S. L., Lopez-Gonzalez, G., Sonké, B., Affum-Baffoe, K., Baker, T. R., Ojo, L. O., et al. (2009). Increasing carbon storage in intact African tropical forests. *Nature* 457, 1003–1006. doi: 10.1038/nature07771

Li, C., Barclay, H., Huang, S., Roitberg, B., Lalonde, R., and Thiffault, N. (2022). Detecting compensatory growth in silviculture trials: empirical evidence from three case studies across Canada. *Front. Plant Sci.* 13, 907598. doi: 10.3389/fpls.2022.907598

Li, C., Barclay, H., Roitberg, B., and Lalonde, R. (2020). Forest productivity enhancement and compensatory growth: a review and synthesis. *Front. Plant Sci.* 11, 575211. doi: 10.3389/fpls.2020.575211

Li, C., Barclay, H., Roitberg, B., and Lalonde, R. (2021). Ecology and prediction of compensatory growth: from theory to application in forestry. *Front. Plant Sci.* 12, 655417. doi: 10.3389/fpls.2021.655417

Li, G., Zhao, X., Iqbal, B., Zhao, X., Liu, J., Javed, Q., et al. (2023). The effect of soil microplastics on *Oryza sativa L.* root growth traits under alien plant invasion. *Front. Ecol. Evol.* 11, 1172093. doi: 10.3389/fevo.2023.1172093

Li, R., Zhu, S., Chen, H. Y. H., John, R., Zhou, G., Zhang, D., et al. (2015). Are functional traits a good predictor of global change impacts on tree species abundance dynamics in a subtropical forest? *Ecol. Lett.* 18, 1181–1189. doi: 10.1111/ele.12497

Liu, Q., Peng, C., Schneider, R., Cyr, D., Liu, Z., Zhou, X., et al. (2023). Vegetation browning: global drivers, impacts, and feedbacks. *Trends Plant Sci.* 28, 1014–1032. doi: 10.1016/j.tplants.2023.03.024

Lodge, D. J., Scatena, F. N., Asbury, C. E., and Sanchez, M. J. (1991). Fine litterfall and related nutrient inputs resulting from Hurricane Hugo in subtropical wet and lower montane rain forests of Puerto Rico. *Biotropica* 23, 336–342. doi: 10.2307/2388249

Luo, Y., and Chen, H. Y. H. (2015). Climate change-associated tree mortality increases without decreasing water availability. *Ecol. Lett.* 18, 1207–1215. doi: 10.1111/ele.12500

Luo, Y., Chen, H. Y. H., McIntire, E. J. B., and Andison, D. W. (2019). Divergent temporal trends of net biomass change in western Canadian boreal forests. *J. Ecol.* 107, 69–78. doi: 10.1111/1365-2745.13033

Ma, Z., Peng, C., Zhu, Q., Chen, H., Yu, G., Li, W., et al. (2012). Regional drought-induced reduction in the biomass carbon sink of Canada's boreal forests. *Proc. Natl. Acad. Sci. U.S.A.* 109, 2423–2427. doi: 10.1073/pnas.1111576109

Markesteijn, L., Poorter, L., Bongers, F., Paz, H., and Sack, L. (2011). Hydraulics and life history of tropical dry forest tree species, Coordination of species' drought and shade tolerance. *New Phytol.* 191, 480–495. doi: 10.1111/j.1469-8137.2011.03708.x

Maynard, D. S., Bialic-Murphy, L., Zohner, C. M., Averill, C., van den Hoogen, J., Ma, H. Z., et al. (2022). Global relationships in tree functional traits. *Nat. Commun.* 13, 3185. doi: 10.1038/s41467-022-30888-2

McDowell, N., Allen, C. D., Anderson-Teixeira, K., Brando, P., Brienen, R., Chambers, J., et al. (2018). Drivers and mechanisms of tree mortality in moist tropical forests. *New Phytol.* 219, 851–869. doi: 10.1111/nph.15027

McDowell, N., Pockman, W. T., Allen, C. D., Breshears, D. D., Cobb, N., Kolb, T., et al. (2008). Mechanisms of plant survival and mortality during drought: Why do some plants survive while others succumb to drought? *New Phytol.* 178, 719–739. doi: 10.1111/j.1469-8137.2008.02436.x

McGill, B. J., Enquist, B. J., Weiher, E., and Westoby, M. (2006). Rebuilding community ecology from functional traits. *Trends Ecol. Evol.* 21, 178–185. doi: 10.1016/j.tree.2006.02.002

Mcnaughton, S. J. (1983). Compensatory plant growth as a response to herbivory. *Oikos* 40, 329–336. doi: 10.2307/3544305

Meiners, S. J., Cadotte, M. W., Fridley, J. D., Pickett, S. T. A., and Walker, L. R. (2015). Is successional research nearing its climax? New approaches for understanding dynamic communities. *Funct. Ecol.* 29, 154–164. doi: 10.1111/1365-2435.12391

Mencuccini, M., Minunno, F., Salmon, Y., Martinez-Vilalta, J., and Holtta, T. (2015). Coordination of physiological traits involved in drought-induced mortality of woody plants. *New Phytol.* 208, 396–409. doi: 10.1111/nph.13461

Méndez-Alonzo, R., Paz, H., Zuluaga, R. C., Rosell, J. A., and Olson, M. E. (2012). Coordinated evolution of leaf and stem economics in tropical dry forest trees. *Ecology* 93, 2397–2406. doi: 10.1890/11-1213.1

Mouillot, D., Graham, N. A. J., Villéger, S., Mason, N. W. H., and Bellwood, D. R. (2013). A functional approach reveals community responses to disturbances. *Trends Ecol. Evol.* 28, 167–177. doi: 10.1016/j.tree.2012.10.004

Nepstad, D. C., Tohver, I. M., Ray, D., Moutinho, P., and Cardinot, G. (2007). Mortality of large trees and lianas following experimental drought in an Amazon forest. *Ecology* 88, 2259–2269. doi: 10.1890/06-1046.1

O'Brien, M. J., Engelbrecht, B. M. J., Joswig, J., Pereyra, G., Schuldt, B., Jansen, S., et al. (2017). A synthesis of tree functional traits related to drought-induced mortality in forests across climatic zones. *J. Appl. Ecol.* 54, 1669–1686. doi: 10.1111/1365-2664.12874

Pan, Y., Birdsey, R. A., Phillips, O. L., and Jackson, R. B. (2013). The structure, distribution, and biomass of the world's forests. *Ann. Rev. Ecol. Evol.* S. 44, 593–622. doi: 10.1146/annurev-ecolsys-110512-135914

Peng, C. H., Ma, Z. H., Lei, X. D., Zhu, Q., Chen, H., Wang, W. F., et al. (2011). A drought-induced pervasive increase in tree mortality across Canada's boreal forests. *Nat. Clim. Change* 1, 467–471. doi: 10.1038/nclimate1293

Phillips, O. L., van der Heijden, G., Lewis, S. L., López-González, G., Aragão, L. E. O. C., and Lloyd, J. (2010). Drought-mortality relationships for tropical forests. *New Phytol.* 187, 631–646. doi: 10.1111/j.1469-8137.2010.03359.x

Poorter, L. (2008). The relationships of wood-, gas-, and water fractions of tree stems to performance and life history variation in tropical trees. *Ann. Bot.* 102, 367–375. doi: 10.1093/aob/mcn103

Poorter, L., and Bongers, F. (2006). Leaf traits are good predictors of plant performance across 53 rain forest species. *Ecology* 87, 1733–1743. doi: 10.1890/0012-9658(2006)87[1733:LTAGPO]2.0.CO;2

Poorter, L., Rozendaal, D. M. A., Bongers, F., de Almeida-Cortez, J. S., Zambrano, A. M. A., Alvarez, F. S., et al. (2019). Wet and dry tropical forests show opposite successional pathways in wood density but converge over time. *Nat. Ecol. Evol.* 3, 928–934. doi: 10.1038/s41559-019-0882-6

Prior, L. D., and Bowman, D. M. J. S. (2014). Big eucalypts grow more slowly in a warm climate: evidence of an interaction between tree size and temperature. *Global Change Biol.* 20, 2793–2799. doi: 10.1111/gcb.12540

Quero, J. L., Sterck, F. J., Martínez-Vilalta, J., and Villar, R. (2011). Water-use strategies of six coexisting Mediterranean woody species during a summer drought. *Oecologia* 166, 45–57. doi: 10.1007/s00442-011-1922-3

R Core Team. (2019). *R: A language and environment for statistical computing (v. 3.5.3)* (Vienna, Austria: R Foundation for Statistical Computing). Available at: https://www.R-project.org/.

Rea, R. V., and Massicotte, H. B. (2010). Viewing plant systematics through a lens of plant compensatory growth. *Am. Biol. Teach.* 72, 541–544. doi: 10.1525/abt.2010.72.9.4

Reich, P. B. (2014). The world-wide 'fast–slow' plant economics spectrum: A traits manifesto. *J. Ecol.* 102, 275–301. doi: 10.1111/1365-2745.12211

Reichstein, M., Bahn, M., Ciais, P., Frank, D., Mahecha, M. D., and Seneviratne, S. I. (2013). Climate extremes and the carbon cycle. *Nature* 500, 287–295. doi: 10.1038/nature12350

Rüger, N., Comita, L. S., Condit, R., Purves, D., Rosenbaum, B., Visser, M. D., et al. (2018). Beyond the fast–slow continuum: demographic dimensions structuring a tropical tree community. *Ecol. Lett.* 21, 1075–1084. doi: 10.1111/ele.12974

Santiago, L. G., Goldstein, G., Meinzer, F. C., Fisher, J. B., MaChado, K., Woodruff, D., et al. (2004). Leaf photosynthetic traits scale with hydraulic conductivity and wood density in Panamanian forest canopy trees. *Oecologia* 140, 543–550. doi: 10.1007/s00442-004-1624-1

Sarker, S. K., Reeve, R., and Matthiopoulos, J. (2021). Solving the fourth-corner problem: forecasting ecosystem primary production from spatial multispecies trait-based models. *Ecol. Monogr.* 91, e01454. doi: 10.1002/ecm.1454

Sevanto, S., Mcdowell, N. G., Dickman, L. T., Pangle, R., and Pockman, W. T. (2014). How do trees die? A test of the hydraulic failure and carbon starvation hypotheses. *Plant Cell Environ.* 37, 153–161. doi: 10.1111/pce.12141

Shipley, B., Lechowicz, M. J., Wright, I., and Reich, P. B. (2006). Fundamental trade-offs generating the worldwide leaf economics spectrum. *Ecology* 87, 535–541. doi: 10.1890/05-1051

Skelton, R. P., West, A. G., and Dawson, T. E. (2015). Predicting plant vulnerability to drought in biodiverse regions using functional traits. *Proc. Natl. Acad. Sci. U.S.A.* 112, 5744–5749. doi: 10.1073/pnas.1503376112

Sterck, F., Markesteijn, L., Schieving, F., and Poorter, L. (2011). Functional traits determine trade-offs and niches in a tropical forest community. *Proc. Natl. Acad. Sci. U.S.A.* 108, 20627–20632. doi: 10.1073/pnas.1106950108

Steudler, P. A., Melillo, J. M., Bowden, R. D., and Castro, M. S. (1991). The effects of natural and human disturbances on soil nitrogen dynamics and trace gas fluxes in a Puerto Rican wet forest. *Biotropica* 23, 356–363. doi: 10.2307/2388252

Suarez, M. L., and Kitzberger, T. (2010). Differential effects of climate variability on forest dynamics along a precipitation gradient in northern Patagonia. *J. Ecol.* 98, 1023–1034. doi: 10.1111/j.1365-2745.2010.01698.x

Swenson, N. G., Hulshof, C. M., Katabuchi, M., and Enquist, B. J. (2020). Long-term shifts in the functional composition and diversity of a tropical dry forest: a 30-yr study. *Ecol. Monogr.* 90, e01408. doi: 10.1002/ecm.1408

van der Plas, F., Schroder-Georgi, T., Weigelt, A., Barry, K., Meyer, S., Alzate, A., et al. (2020). Plant traits alone are poor predictors of ecosystem properties and long-term ecosystem functioning. *Nat. Ecol. Evol.* 4, 1602–1611. doi: 10.1038/s41559-020-01316-9

van der Sande, M. T., Arets, E. J. M. M., Peña-Claros, M., de Avila, A. L., Roopsind, A., Mazzei, L., et al. (2016). Old-growth Neotropical forests are shifting in species and trait composition. *Ecol. Monogr.* 86, 228–243. doi: 10.1890/15-1815.1

Van Gelder, H. A., Poorter, L., and Sterck, F. J. (2006). Wood mechanics, allometry, and life-history variation in a tropical rain forest tree community. *New Phytol.* 171, 367–378. doi: 10.1111/j.1469-8137.2006.01757.x

van Mantgem, P. J., and Stephenson, N. L. (2007). Apparent climatically induced increase of tree mortality rates in a temperate forest. *Ecol. Lette.* 10, 909–916. doi: 10.1111/j.1461-0248.2007.01080.x

van Mantgem, P. J., Stephenson, N. L., Byrne, J. C., Daniels, L. D., Franklin, J. F., Fule, P. Z., et al. (2009). Widespread increase of tree mortality rates in the western United States. *Science* 323, 521–524. doi: 10.1126/science.1165000

Vicente-Serrano, S. M., Beguería, S., López-Moreno, J. I., Angulo, M., and El Kenawy., A. (2010). A new global 0.5° gridded dataset, (1901–2006) of a multiscalar drought index: comparison with current drought index datasets based on the Palmer Drought Severity Index. *J. Hydrometeorol.* 11, 1033–1043. doi: 10.1175/2010JHM1224.1

Violle, C., Navas, M. L., Vile, D., Kazakou, E., Fortunel, C., Hummel, I., et al. (2007). Let the concept of trait be functional. *Oikos* 116, 882–892. doi: 10.1111/j.0030-1299.2007.15559.x

Wen, D., Wei, P., Kong, G., Zhang, Q., and Huang, Z. (1997). Biomass study of the community of *Castanopsis chinensis* + *Cryptocarya concinna* + *Schima superba* in a southern China reserve. *Acta Ecol. Sin.* 19, 497–504.

Westoby, M., and Wright, I. J. (2006). Land-plant ecology on the basis of functional traits. *Trends Ecol. Evol.* 21, 261–268. doi: 10.1016/j.tree.2006.02.004

Wright, S. J., Kitajima, K., Kraft, N. J. B., Reich, P. B., Wright, I. J., Bunker, D. E., et al. (2010). Functional traits and the growth-mortality trade-off in tropical trees. *Ecology* 91, 3664–3674. doi: 10.1890/09-2335.1

Wright, I. J., Reich, P. B., Cornelissen, J. H. C., Falster, D. S., Groom., P. K., Hikosaka, K., et al. (2005). Modulation of leaf economic traits and trait relationships by climate. *Global Ecol. Biogeogr.* 14, 411–421. doi: 10.1111/j.1466-822x.2005.00172.x

Wright, I. J., Reich, P. B., Westoby, M., Ackerly, D. D., Baruch, Z., Bongers, F., et al. (2004). The worldwide leaf economics spectrum. *Nature* 428, 821–827. doi: 10.1038/nature02403

Wu, A., Tang, X., Li, A., Xiong, X., Liu, J., He, X., et al. (2022). Tree diversity, structure and functional trait identity promote stand biomass along elevational gradients in subtropical forests of southern China. *J. Geophys. Res. Biogeosci.* 127, e2022JG006950. doi: 10.1029/2022JG006950

Yang, J., Cao, M., and Swenson, N. G. (2018). Why functional traits do not predict tree demographic rates. *Trends Ecol. Evol.* 33, 326–336. doi: 10.1016/j.tree.2018.03.003

Yang, Y., Shi, Y., Sun, W., Chang, J., Zhu, J., Chen, L., et al. (2022). Terrestrial carbon sinks in China and around the world and their contribution to carbon neutrality. *Sci. China Life Sci.* 65, 861–895. doi: 10.1007/s11427-021-2045-5

Yee, A. T. K., Lai, H. R., Chong, K. Y., Neo, L., Koh, C. Y., Tan, S. Y., et al. (2019). Short-term responses in a secondary tropical forest after a severe windstorm event. *J. Veg. Sci.* 30, 720–731. doi: 10.1111/jvs.12753

Yin, X. H., Hao, G. Y., and Sterck, F. (2023). Ring-and diffuse-porous tree species from a cold temperate forest diverge in stem hydraulic traits, leaf photosynthetic traits, growth rate and altitudinal distribution. *Tree Physiol.* 43, 722–736. doi: 10.1093/treephys/tpad008

Yu, G., Chen, Z., Piao, S., Peng, C., Ciais, P., Wang, Q., et al. (2014). High carbon dioxide uptake by subtropical forest ecosystems in the East Asian monsoon region. *Proc. Natl. Acad. Sci. U.S.A.* 111, 4910–4915. doi: 10.1073/pnas.1317065111

Yu, M., Wang, Y., Jiang, J., Wang, C., Zhou, G., and Yan, J. (2019). Soil organic carbon stabilization in the three subtropical forests: importance of clay and metal oxides. *J. Geophys. Res. Biogeosci.* 124, 2976–2990. doi: 10.1029/2018JG004995

Zhao, X., Xie, H., Zhao, X., Zhang, J., Li, Z., Yin, W., et al. (2022). Combined inhibitory effect of Canada goldenrod invasion and soil microplastics on rice growth. *Int. J. Environ. Res. Public Health* 19, 11947. doi: 10.3390/ijerph191911947

Zhou, G., Houlton., B. Z., Wang, W. T., Huang, W., Xiao, Y., Zhang, Q., et al. (2014). Substantial reorganization of China's tropical and subtropical forests: based on the permanent plots. *Global Change Biol.* 20, 240–250. doi: 10.1111/gcb.12385

Zhou, G., Liu, S., Li, Z., Zhang, D., Tang, X., Zhou, C., et al. (2006). Old-growth forests can accumulate carbon in soils. *Science* 314, 1417–1417. doi: 10.1126/science.1130168

Zhou, G., Peng, C., Li, Y., Liu, S., Zhang, Q., Tang, X., et al. (2013). A climate change-induced threat to the ecological resilience of a subtropical monsoon evergreen broad-leaved forest in Southern China. *Global Change Biol.* 19, 1197–1210. doi: 10.1111/gcb.12128

Zhou, G., Wei, X., Wu, Y., Liu, S., Huang, Y., Yan, J., et al. (2011). Quantifying the hydrological responses to climate change in an intact forested small watershed in Southern China. *Global Change Biol.* 17, 3736–3746. doi: 10.1111/j.1365-2486.2011.02499.x

Zscheischler, J., Mahecha, M. D., von Buttlar, J., Harmeling, S., Jung, M., Rammig, A., et al. (2014). A few extreme events dominate global interannual variability in gross primary production. *Environ. Res. Lett.* 9, 035001. doi: 10.1088/1748-9326/9/3/035001

frontiers | Frontiers in Plant Science

TYPE Original Research
PUBLISHED 26 February 2024
DOI 10.3389/fpls.2024.1344883

OPEN ACCESS

EDITED BY
Runguo Zang,
Chinese Academy of Forestry, China

REVIEWED BY
Dongfeng Yan,
Henan Agricultural University, China
Ana Cristina Gonçalves,
University of Evora, Portugal

*CORRESPONDENCE
Bernard Roitberg
roitberg@sfu.ca

RECEIVED 26 November 2023
ACCEPTED 05 February 2024
PUBLISHED 26 February 2024

CITATION
Roitberg B, Li C and Lalonde R (2024) Tree adaptive growth (TAG) model: a life-history theory-based analytical model for post-thinning forest stand dynamics.
Front. Plant Sci. 15:1344883.
doi: 10.3389/fpls.2024.1344883

Tree adaptive growth (TAG) model: a life-history theory-based analytical model for post-thinning forest stand dynamics

Bernard Roitberg[1,2]*, Chao Li[2] and Robert Lalonde[3]

[1]Department of BioScience, Simon Fraser University, Burnaby, BC, Canada, [2]Canadian Wood Fibre Centre, Canadian Forest Service, Edmonton, AB, Canada, [3]Department of Biology, University of British Columbia, Kelowna, BC, Canada

Background: Understanding stand dynamics is essential for predicting future wood supply and associated ecosystem services for sustainable forest management. The dynamics of natural stands can be characterized by age-dependent growth and yield models. However, dynamics in managed stands appear somewhat different from that of natural stands, especially with difficulties in explaining the phenomenon of post-thinning overcompensation, based upon some long-term observations. Though overcompensation is an ideal outcome for the forest sector, it had been largely treated as an outlier and thus ignored or dismissed as "out-of-the-ordinary".

Methodology: We developed a life history theory-based, state-dependent model of Tree Adaptive Growth (TAG) to investigate this phenomenon and verified that overcompensation should be a common outcome in post-thinning forest stands when the stand growth over time is sigmoid shaped. TAG posits that individual trees will invest proportionately more into growth following thinning because it is evolutionarily adaptive to do so.

Results: Our investigation of the model's behavior unearthed diverse stand growth patterns similar to that which is observed in the empirical datasets and predicted by a statistics-based Tree's Compensatory Growth (TreeCG) model.

Conclusion: A simple, theory-driven, analytical model, TAG, can reproduce the diverse growth patterns in post-thinning stands and thus assist addressing silviculture-related issues. The model can be applied to various jurisdictions even without detailed regional growth and yield relationships and is capable of incorporating the effects of other time sensitive factors like fertilization, pruning, and climate change.

KEYWORDS

compensatory growth, thinning, life history theory, model, forestry, overcompensation

1 Introduction

Forests are extensively managed for the harvesting of wood, a material which provides many of the necessities of daily human life. In addition to this, forests are valued for their ecosystem services, which protect and maintain healthy environments. The dynamics of forests are a product of interactions between the growth of trees or forest stands and their environment, which includes physical site variables, natural disturbances such as fire and insect attack, as well as anthropogenic disturbances, which includes harvesting practices (Davis et al., 2001). Disturbances may result in immediate negative impacts on forests, which would compromise many of the benefits that forests provide. Our study focuses on the effect of thinning, a management practice that is a common anthropogenic disturbance, on forest stand dynamics.

Regional economic development often drives an increase in demand for wood materials and wood products (Buongiorno et al., 2003), and therefore presents a significant challenge to forest industries to maintain sufficient wood supply. To prevent over utilization of forest resources, a major component of forest management is to regulate harvest activities through annual allowable cut (AAC) for maintaining forest resources in a sustainable manner (Leuschner, 1984). An essential requirement for this AAC determination is a good understanding of long-term stand growth dynamics. Consequently, various growth functions have been estimated for natural stands of different tree species, site conditions, and geographical regions. However, the resulting growth curves necessarily are site-, and region-specific and lack generality, making prediction difficult as data acquisition on the local scale is logistically challenging. As a compromise, an assumption of same stand dynamics in natural and managed stands is generally made when developing management tools such as Woodstock of Remsoft (https://remsoft.com/woodstock-optimization-studio/) and Patchworks of Spatial Planning System (https://spatial.ca/patchworks/). Consequently, there is a need to improve our general understanding of stand dynamics in order to make accurate AAC estimation for managed stands in the context of anthropogenic disturbance.

A focus on disturbance tools for enhancing forest productivity will not only increase raw wood materials but also improve associated ecosystem services. This approach essentially addresses the question of "is it possible to increase natural growth of forest stands by judicious removal of some trees?" (Zeide 2011) that has attracted foresters for centuries. In forestry practice, a significant challenge for forest landowners and managers is the low productivity of forests which is a consequence of the slow growth rate of trees. Consequently, forest managers seek ways to speed up the growth and renewal of forest resources; tree removal or thinning is one such approach.

Disturbance ecology has elucidated how disturbances can affect tree and stand growth. However, the mechanistic responses of individual trees or stands of trees to disturbances remains poorly understood (McKenney, 2000). This presents significant challenges to sustainable forest management (SFM) decisions and carbon and GHG emission estimation because of the uncertainty involved in the post-thinning stand dynamics represented by the growth and yield relationships in managed stands. As an anthropogenic disturbance, thinning is a widely applied silviculture treatment for stand density management to produce the larger diameter trees that are desired by lumber industries. On one hand, thinning causes immediate loss of standing volume; and on the other hand, thinning promotes the accelerated growth of remaining trees (e.g., Bose et al., 2018).

There is a large literature focusing on thinning, in particular pre-commercial thinning (PCT) of smallest trees, the focus of this paper, which is mostly based on short-term observations as often required by guidelines (e.g., Reukema, 1975; Sohn et al., 2014; Elfstrom and Powers, 2023). A general conclusion Zeide (2011) reached as "after centuries of research and observations, we have learned that thinning, mostly from below, can increase merchantable but not total volume increment of trees per unit area", and he continued "this knowledge is valuable but not satisfactory". This summary reinforced Johnstone (1985) conclusion that "in all of the trials, the basal area and total volume of the thinned plots is well below that of the unthinned plots, but sufficient time has yet to elapse since treatment to indicate whether the thinned plots will ever catch up to their unthinned counterparts".

By contrast with outcomes from these short-term observations, investigation into long-term silviculture datasets demonstrated that gross volume in thinned stands could exceed that in unthinned stands. For example, Steele (1955) found that the volumes from a thinned stand exceeded that from the control stand for a 20-year dataset of two young Douglas-fir stands in Skamania County of Washington, United States. This was also demonstrated in balsam fir (*Abies balsamea* (L.) Mill.) stands 42 years after thinning operations in the Green River of New Brunswick, Canada (Pitt and Lanteigne, 2008), and coastal Douglas-fir (*Pseudotsuga menziesii* [Mirb.] Franco) stands 40 years after initial treatments in the Shawnigan Lake of British Columbia, Canada (Li et al., 2018). In general, not enough attention has been paid to such results due to the difficulties in incorporation with existing results. Although these findings are derived from single sites, they nonetheless support Zeide's (2011) suggestion that proper thinning can lead to enhanced stand productivity. To answer this question, a better understanding of the underlying mechanism(s) that generate this phenomenon is needed. This is where compensatory growth comes into play.

Compensatory growth (CG), a common cross-taxa phenomenon observed in both animals and plants, is defined as the accelerated growth of organisms after experiencing a period of unfavorable conditions (Mangel and Munch, 2005). CG has been well studied in crop and animal husbandry and is used to enhance productivity (Li et al., 2021), but it is a relatively new concept for forest practitioners. In forests, CG can be defined as accelerated forest stand growth after a stand experiences a loss of a proportion of the individual trees in a stand (Li et al., 2020). Li et al. (2018) used this concept to explain the enhanced costal Douglas-fir stand productivity in pre-commercial thinned stands 40-years after initial treatments. Recently, we described how CG following PCT has the potential to enhance forest yields (Li et al., 2020, 2021). We

followed those synthetic reviews with data analysis that confirms that CG can predictably enhance productivity in real world forests (Li et al., 2022a). A simulation model named TreeCG, standing for Tree's Compensatory Growth, was developed (Li et al., 2022b) to show how existing statistical growth and yield relationship from natural stands can be used to predict diverse stand growth curves in managed stands. As such, the observation of overcompensation, defined as the biomass in treated sites exceeds that in untreated sites, should not be seen as "out-of-the-ordinary", but an understandable and predictable phenomenon.

The development of the TreeCG model was based on the variable-density yield table of lodgepole pine (*Pinus contorta* Douglas) (Johnstone, 1976) and can, in theory, be calibrated to different tree species and geographical regions using detailed local growth and yield relationships. However, this calibration is limited by the fact that not every jurisdiction has such detailed information readily available. Therefore, a logical next step is to develop a simple analytical CG model to eliminate the need for extensive calibrated datasets in order to apply this method to a wide variety of tree species and habitats. The key feature that allows one to move beyond the data is the incorporation of life history theory (LHT).

Here, LHT is used to build and implement a PCT – CG model that follows growth of individual trees in stands. LHT attempts to elucidate how natural selection designs organisms to maximize reproductive success, given knowledge of how selective factors in the environment (i.e., extrinsic mortality) and factors intrinsic to the organism (i.e., trade-offs, constraints) affect survival and reproduction (e.g., Stearns, 2000; Del Giudice et al., 2015; Simon et al., 2016), from an evolutionary biology perspective. In other words, it predicts how individual trees should invest in growth and reproduction under different circumstances, for example following a disturbance, to maximize their evolutionary fitness. It has successfully explained phenomena such as mast fruiting in trees (Lalonde and Roitberg, 1992) that were difficult to interpret with other theories. Elucidating the LHT response of individual trees to their environment allows one to extrapolate to the growth dynamics at the stand level.

Here, we present such an LHT-based state-dependent forest growth model. It assumes that trees will vary their energy allocations to growth, reserves, and reproduction as a function of physiological state (age, size and current reserves) and ecological circumstances (e.g., crowded versus thinned sites) in an adaptive manner i.e., to maximize lifetime reproductive success. This paper provides a proof of concept, state-dependent LHT model that can generate stand dynamics that mimic those observed in nature. Once confirmed, we then use this type of model to examine how optimal intensity and timing of PCT can enhance forest productivity.

The objectives of this manuscript are: (1) to present the LHT-based state-dependent forest growth model to show that this simple model can generate dynamics that are like those observed in nature; (2) describe the model behavior through a series of sensitivity analyses, to show how different factors could influence the outcomes of post-thinning stand dynamics; and (3) discuss the trade-offs of different approaches of modeling stand dynamics and their management applications.

2 Materials and methods

2.1 Theory rationale

As discussed in the Introduction, our model of thinning-driven stand dynamics is based upon state dependent life history theory for individual trees, which are then extrapolated to the stand level. We focus on three trees states: size (S), reserves (R) and age (A) whose units are defined as kg, kg and years, respectively (in section 2.2, Equation 12, we transcribe size to volume to bring in line with traditional forestry approaches). A fourth state variable, competitive ability (ψ), enters into stand-level dynamics described in the following paragraph. How trees respond to A, S and R states is modelled via incorporation of four important life history assumptions: (i) innate tree growth follows a sigmoidal pattern (see Weiner and Thomas, 2001), (ii) based upon principles from evolutionary ecology, we assume that tree growth strategies have evolved to maximize lifetime reproductive success (Davies and Krebs, 1993), (iii) individual trees will acquire resources and modify their investment in growth in a state dependent manner according to (S), (R), (A) (see Equations 1-3 below) and (iv) there are no genetic constraints on the above i.e., we play the phenotypic gambit (Grafen, 1984), which assumes that selection on phenotypic variation translates directly into selection on heritable variation in the population. Finally, though we do not explicitly say so, we assume that there is an underlying tradeoff between growth and reproduction (e.g., Kassaby and Barclay, 1992) though we acknowledge that such a tradeoff is often not obvious (e.g., Harshman and Zera, 2007; Suzuki et al., 2019).

We assume that individual trees at a given combination of our three state values (S, R, A) will adopt a resource allocation strategy. Thus, a focal tree, n, in population of N trees with state variables S = s, R = r and A = a will grow in an adaptive manner as follows:

We expect that trees will mobilize reserves for growth and reproduction, at a rate that we define as alpha (α).

$$\alpha = \frac{r - R_{min}}{1 + e^{-(w_1 s + w_2 a)}} \tag{1}$$

Where: R_{min} is the minimum reserves value for a tree of size (s), with s, r and a defined as above and W values are weight constants for the state variables (see Table 1 for a list of variables and their values). For a tree of a given size (s), we expect that α will increase with size, reserves and age up to some maximum that never causes the focal tree to exceed its critical reserves state value (R_{crit}), which is the minimal level to maintain metabolic function. Here our reasoning is: (i) trees cannot forecast weather conditions for the current year and (ii) trees are risk averse and will never mobilize so many reserves so to put their survival at risk should the current year's weather turn out to be poor for energy harvesting (see Clark's asset protection principle, Clark, 1994).

We define beta (β) as the proportion of mobilized reserves that go to reproduction versus growth:

$$\beta(s, r, \alpha) = \begin{cases} 1 - e^{-(w_3 s + w_4 a)} & if r > \pi \\ 0 & otherwise \end{cases} \tag{2}$$

10.3389/fpls.2024.1344883

TABLE 1 List of parameters employed in life history functions and TAG simulation model.

Parameters and Functions	Interpretation	Range
S	Size (kg)	15, 2800
R	Reserves (kg)	0.75, 560
A	Time since monitoring (year)	0, 199
α	Reserves mobilization function	Equation 1
w_1	Size weight constant (α)	0.05
w_2	Age weight constant (α)	0.05
β	Reproduction vs growth function	Equation 2
w_3	Size weight constant (β)	0.007
w_4	Age weight constant (β)	0.015
φ	Growth vs reserves function	Equation 3
H	Risk aversion	1.2
γ	Growth increment function	Equation 4
ξ	Mobilization efficiency	0.8
Λ	Cone production function	2.000 seeds/kg
ς_s	Weather intensity vector	0.83, 1.2
ς_s	Weather frequency vector	0.05, 0.4
ρ	Intrinsic growth rate	1.12
θ	Tree growth rate shape parameter	0.6, 1.4
ζ	Tree senescence	0.004
τ'	Density dependence shape parameter	0.2, 0.4
N	Stand population size	0, 100/ 0.04 ha
ψ	Relative competitive ability function	Equation 6
K	Growth from reserves function	Equation 7
δ	Total maintenance costs function	Equation 8
ω	Maintenance costs per mass unit	0
π	Cost to initiating reproduction function	Equation 9
ϵ	Reproduction cost slope	0.05
ϵ'	Reproduction cost intercept	0.1
V	Volume	0, 6.15 m^3
D	Tree density	455 kg/m3

Where π is the start-up cost for initiating reproduction and the W's are weight constants for size and age states (Table 1).

Here, we assume two effects of size. First, it is necessarily true that small trees have small reserves such that R will rarely exceed π, meeting the $\beta = 0$ condition. Second, small trees are not efficient at producing seeds (e.g., Sherman et al., 2019) thus, we have set the size weight (W_3) low (Table 1). Regarding age weight (W_4), we further assume that older trees should strongly bias their mobilized reserves to reproduction because future discounting (e.g., Lee et al., 2011) will offset small gains from growth particularly if older trees are large, thus, we employed a small value for W_4.

We define phi (φ) as the allocation of harvested energy to growth versus reserves.

$$\phi = \begin{cases} \left(\frac{1}{\phi_s+\phi_r}\right)\phi_s & \text{if} \quad r' < s' R_{max} \quad \text{and} \quad r' < s' R_{min} \\ 1 - \frac{r-\alpha+\gamma-sR_{max}}{\gamma} & \text{if} \quad r' > s' R_{max} \\ 1 - \frac{(s+\gamma)R_{min}-r'}{\gamma} & \text{if} \quad r' < s' R_{min} \end{cases} \tag{3}$$

where: $\phi_s = 1 - \frac{s-s_{min}}{s}$ (Equation 3.1) and $\phi_r = 1 - ((r - (R_{min}))r)$ (Equation 3.2), based upon size and reserves, respectively. In addition, $s' = s + \gamma\left(\frac{1}{\phi_s+\phi_r}\right)\phi_s + (\alpha(1-\beta)\xi)$ (Equation 3.3) and $r' = r + \gamma\left(\frac{1}{\phi_s+\phi_r}\right)\phi_s - \alpha$ (Equation 3.4) are potential updated values for size and reserves, respectively and ξ is defined as the efficiency in mobilizing reserves to structure (see Equation 7).

Here, three conditions hold: Sufficient reserves remain after metabolic costs and reproduction start-up cost are paid and allocation to reserves does not exceed the maximum reserve level after adjusting for energy harvesting (γ). Otherwise, φ is adjusted to meet those minimum and maximum reserve levels, respectively with γ and π being functions of tree size. The rationale for the φ decision is: as trees increase in size, their growth rate decelerates (Weiner and Thomas, 2001) thus there is little gain from investing in growth vs building up reserves for reproduction (Lalonde and Roitberg, 1992).

All three of the above state-dependent strategies can be summarized as: invest in growth when that leads to accelerated returns but only when reserves are sufficiently high to avoid starvation i.e., metabolic reserves fall below critical level. When trees are large and growth is constrained, trees are assumed to invest in reproduction when it is safe to do so because of the greater return on investment for the latter. Also, future discounting means that future reproductive returns from current investment in growth will be constrained for older and larger trees (Equation 2).

We employed Equations 1-3 in simulations of stage-dependent tree growth, which we refer to as Tree Adaptive Growth or TAG. Details of the TAG model follow.

2.2 TAG model development

We developed an agent-based simulation model using C++ language, which is shown in flow chart form in Figure 1. Here, we

10.3389/fpls.2024.1344883

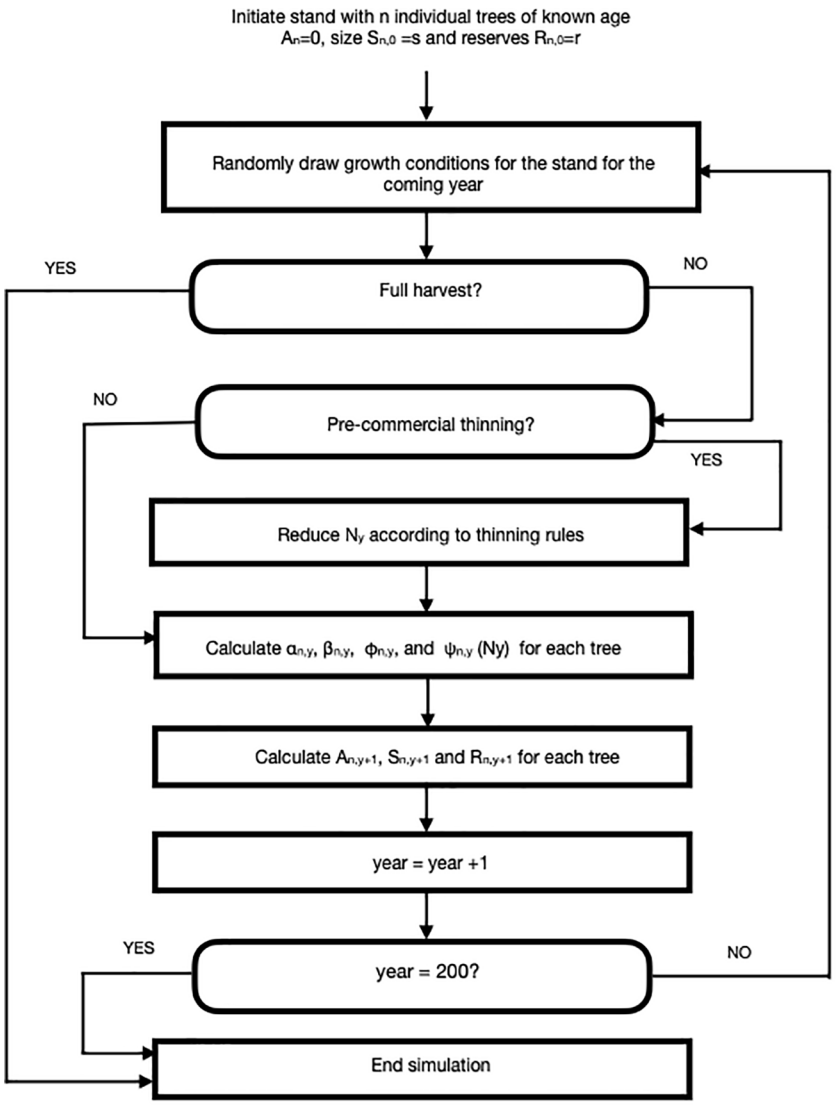

FIGURE 1
A flow chart for an agent-based Tree Adaptive Growth (TAG) simulation model. Description of parameters and their default values can be found in Table 1.

simulated small stands of (N = 100 giving a starting density of 2500 stems/ha) trees that were subjected to silvicultural practices including pre-commercial and commercial thinning. We assumed that each stand was comprised of lodgepole pine (*Pinus contorta*) though we expect that our model could be employed for any tree species with known growth parameters or, potentially, mixed stands. The TAG model is similar in spirit (but not detail) to the DESPOT model of Buckley and Roberts (2006) in that individual trees are assumed to maximize some goal, in their case carbon gain and in ours, lifetime reproductive success.

Each stand was planted with identically aged individuals at year=0. The size (mass in kg) of each tree was randomly generated from a normal distribution (x=15, sd=5). Tree reserves (mass in kg) were generated from a uniform distribution (1,5). The simulation tracks size (S), reserves (R) and cone production (Λ), if any, each year for 200 years.

We employed a 'weather' concept to describe conditions that impact growth i.e., energy and nutrients that are harvested by trees for growth and maintenance. Our weather concept was created for characterizing the distribution/spectrum of favorable to unfavorable environmental conditions and such causative agents as variation in hydrological factors, heat stress or insolation. As many (most) of these factors show strong autocorrelation, we chose to use a single parameter in this proof-of-concept model, rather than breaking 'weather' into component effects.

At the beginning of each year, weather is randomly drawn from two vectors ς_s and ς_f, which refer to weather intensity and frequency, respectively (see Table 1 for details). Tree growth for any individual tree is a product of growth potential (Equation 4) and weather intensity for that year. We assumed that, in a given year, weather intensity is identical for every tree in a stand i.e., our model is aspatial (see Discussion).

At the beginning of each year, each tree is subjected to a random mortality event by individually drawing from a uniform distribution (0,1). If the random number falls above a preset default- annual-survival value, then the tree dies. For our runs, the default value for annual survival was set at 0.998. While this survival value is a constant, it is also possible for a tree to die if its reserves fall below a critical value, R_{crit}, which would happen most frequently when an individual's R state is low, weather is poor (see Table 1) and the focal individual is a poor competitor (Equations 5 and 6), thus the assumption of risk averse investment and reproduction as above. In these simulations, we assumed that $R_{min} = R_{crit}$ H.

where: H describes the degree of risk aversion.

Following the mortality evaluation, the time counter for the current year was compared with the pre-determined time step for PCT (e.g., year = 15). If the current year was determined to be a PCT year, then individual trees were removed according to specific rules - in default simulations, the quartile of smallest trees were removed i.e., thinning from below; other thinning rules were also applied as discussed in section 2.3.vii. Late PCT was applied in a similar manner for trees later in the simulation.

Trees that survived random mortality and were not thinned were allowed to grow according to a modified logistic model where the potential growth increment for a tree of size (s) was:

$$\gamma = (\rho - 1)\left(1 - \left(\frac{s}{S_{max}}\right)^{\theta}\right)(e^{-\varsigma y}) \quad (4)$$

Where: ρ is the intrinsic growth rate, S_{max} is the maximum mass that an individual tree can realize (but see Bontemps and Duplat, 2012; Stephenson et al., 2014), θ is a shape parameter and ς is a senescence term that describes decreasing energy harvesting with age (e.g., Hubbard et al., 1999; Qiu et al., 2021 but see Lanner and Connor, 2001).

To determine our default value for ρ, we initiated simulations with ρ= 1.0 and then iterated a series (1.0, 1.20), increasing by 0.01 for each iteration and then plotting the stand volume against time from 0 to year 200. Since our goal was to produce a representative growth curve we visually confirmed that the TAG stand dynamics produced a sigmoidal plot as shown by existing growth and yield models like GYPSY (Huang et al., 2001, 2009) in Alberta (AB) and VDYP7 (British Columbia Ministry of Forests, Lands, Natural Resource Operations and Rural Development, 2019) in BC. Three features that we considered were, (i) the point of obvious acceleration in the growth curve, (ii) the inflection points (representing the change from the accelerating to the decelerating part of the growth curve) and (iii) maximum value of the growth curve for an unthinned (control) plot. In our case, the 15 m^3/ha, year 50 and 600 m^3/ha were used, respectively. Figure 2 shows the TAG output that that we used based upon these criteria. In the end, we chose ρ = 1.12, the value that gave good representation of stand dynamics. In the default model, we assumed that θ =1 i.e., there is a linear decline in per unit mass growth with tree size, yielding a classic symmetric growth increment curve. In some simulations, we modified θ to give right or left skew to the size performance curve.

We further modified an individual's potential growth increment from energy harvesting by including competitive performance.

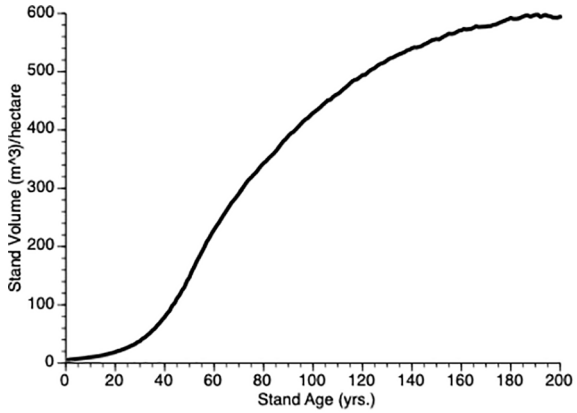

FIGURE 2
Mean stand volume over time from 5 TAG simulated unthinned (control) stands.

We assumed maximum performance for a tree with no competitors whose value declines with increasing density of competitors over time according to the function:

$$\tau = 1 - \left(\frac{N_y}{N_0}\right)^{\tau'}\psi \quad (5)$$

Where: N_0 is the number of trees at planting (year = 0) and N_y is the number of trees at year y and τ' is a shape parameter for the function and $\psi_{s,n,y}$ is relative competitive ability of a tree, n, of size s in year y, which is defined as:

$$\psi_{s,n,y} = \frac{s_{n,y}}{\bar{s}_y} \quad (6)$$

Where: $s_{n,y}$ is the size of a focal individual tree n at year y and S_y is mean tree size for a stand at year y.

Once the potential growth increment was calculated for a given tree of a given size (s) and reserve (r), new size and new reserve state values were calculated according to the three allocation rules (α, β and φ) as discussed in section 2.1.

A tree can also increase its structural mass by mobilizing reserves (β< 1 Equation 2). In doing so, we assume that there is some inefficiency in such mobilization, which we define as ξ i.e., ξ< 1.0. Thus, growth from reserves in year y is:

$$\kappa = R_y \beta_y \xi_y \alpha_y \quad (7)$$

Reserves are decremented when trees pay maintenance costs, which we assume are size dependent. Thus, for a tree of size S, maintenance costs are:

$$\delta_s = n_S \omega \quad (8)$$

Where: ω is the per unit mass cost of maintenance I n this version of our theory, we set ω to 0 based upon the assumption that maintenance costs are already subsumed in the growth function (Equation 4). Future work, may explicitly separate the two parameters.

In years in which an individual invests in reproduction, i.e., β > 0, we assume that there is a linear size dependent cost to reserves

from initiating reproduction, which we define for a tree n of size S in year y as:

$$\pi = \epsilon n_s + \epsilon' \quad (9)$$

Where: ϵ and ϵ' are the initiation slope and intercept, respectively.

From Equation 1 through 9, we can calculate (Equation 10) the size and reserves (Equation 11), respectively of an individual tree n in year y+1 based upon its size in year y as:

$$s_{n,y+1} = s_{n,y} + (\gamma\tau\varsigma\phi) + \kappa \quad (10)$$

and

$$r_{n,y+1} = \begin{cases} r_{n,y} + (\gamma\tau\zeta(1-\phi)) - (r_n\gamma\alpha) - \delta_{n,sy} - \pi & if\,\beta > 0 \\ r_{n,y} + (\gamma\tau\zeta(1-\phi)) - (r_n\gamma\alpha) - \delta_{n,sy} & otherwise \end{cases} \quad (11)$$

The simulation produces an even-aged stand of trees whose size distribution changes from year to year. There are several factors that generate individual size differences among trees. First, trees vary in size and reserves at initiation. From there, based upon absolute and relative size, and reserves, trees vary in their capacity to harvest energy but also in their tendency to allocate their harvest to growth, reserves and reproduction.

The process was repeated until either the year counter reached 200 and the entire stand was harvested, or no longer held any viable trees.

For each series of simulations described below, we replicated the treatment in 10 different even-aged stands, 5 stands for non-thinned controls and 5 stands for PCT. Each stand was originated using a unique set of random number seeds, however, identical random number seeds were employed for pairs of control and treatment stands. As such, each pair of stands generated identical dynamics up until PCT was implemented, confirming that any differences observed were due to treatment effects and not stochasticity.

To make our model relevant to forestry practices, we converted tree size to volume (V) by the following physical equation:

$$V = \frac{S}{D} \quad (12)$$

where: D = wood density, which is species specific, in this case, for pine, is 455 kg/m3 (https://www.thecalculatorsite.com/conversions/weighttovolume.php).

2.3 Model implementation

For each simulation, we considered two different management tactics: (i) no pre-commercial thinning (from here on referred to as Control) and (ii) PCT as described in section 2.2.

To demonstrate the utility of our approach we used the simulations in the following manner:

(i) We plotted mean volume for trees from both thinned and control plots to demonstrate that stand-level compensatory growth is determined by enhanced growth of remaining trees;

(ii) We plotted stand volume curves, over time, to show that overcompensation occurs relative to the Control stands;

(iii) We varied the size dependent growth rate shape parameter θ (Equation 4) to evaluate how it impacts the degree of overcompensation;

(iv) We varied (0.2, 0.25, 0.3, 0.35 and 0.4) the inter-tree competition shape parameter (τ') to evaluate how it impacts growth curves;

(v) We varied the timing of thinning (at years 15, 30, 45 and 60) to evaluate impact on overcompensation;

(vi) We varied the intensity of PCT (25, 50 and 75% removal) to evaluate their impact on overcompensation. The intensity of thinning is defined as the rate (or % of removal) at which the number of trees are removed: thinning intensity (%) = number of trees removed/stand density x 100. When the stand density is fixed in our model experiment, the absolute density can be directly calculated from the thinning intensity;

(vii) To evaluate the impact of thinning protocols we ran a further set of simulations wherein PCT was randomly applied to trees. In both sets of simulations (i.e., smallest quartile removal and random removal) the size of each of the culled trees was included to determine subsequent average tree size and thus impact on growth of remaining trees (Equation 6). However, since the model is aspatial, we did not calculate removal of any specific tree on growth of near neighbors.

2.4 Data analysis

Standardized relative growth (SRG) (Equation 13) is a proper indicator of the status of compensatory growth. We calculated RG to show the pattern of stand growth in thinned plots respect to control as follows:

$$SRG\,\% = \left(\frac{V_{Thinned} - V_{Control}}{V_{Control}}\right) x100 \quad (13)$$

Where $V_{thinned}$ and $V_{Control}$ are stand volumes for thinned and control plots, respectively. By definition, under compensation is denoted when SRG is less than 0, exact compensation happens when SRG equals to 0, and overcompensation is showed when SRG is greater than 0.

3 Results

i) Does PCT generate compensatory growth at the individual tree level?

Figure 3 shows the change in mean volume of trees over time. In this figure, thinning occurs at Year 15 in the thinned plots (see inset). Several features of this plot should be noted. First, as expected, trees in the thinned and control plots grew at an increasing rate for nearly 50 years. Second, following thinning,

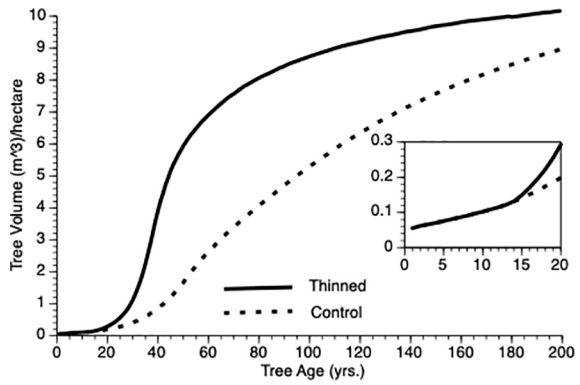

FIGURE 3
Mean tree volume over time from TAG simulated stands that were either subjected to pre-commercial thinning of 25% at year 15 (solid line) or left unthinned (stippled line).

mean volume of trees in thinned plots exceeded those from control plot trees for the length of the simulation. Third, the inflection point in the growth curve for trees in the thinned plot sits to the left of that for trees in the control plots (ca. year 40 vs 50). Eventually, however, both plots show trees approaching asymptotic size.

In the Introduction, we posited that compensatory growth could be generated by adaptive life history response to internal and external tree state. Equations 1 and 3 (α and φ, respectively) predict enhanced proportional investment in growth, primarily from harvested resources but also from reserves. Small trees that are released from intense competition due to thinning (natural or otherwise) should invest proportionately more in growth than do controls because increased harvest reduces their risk of reserve depletion. To test this supposition, we employed two metrics mean φ and coefficient of variation for φ (CV), which we evaluated for the 25 years following PCT. As expected, mean φ values for thinned trees exceeded those for controls (0.57 vs 0.44 m^3, N = 125 i.e., 5 replicates per treatment x 25 years). This confirms that overcompensation is due to thinned trees investing proportionately more of their harvested energy into growth as compensatory growth (Mangel and Munch, 2005) i.e., increased growth performance cannot simply be ascribed to reduced competition among trees. We noted one other feature of φ that was not obvious during theory development. Coefficient of variation was greatly reduced in thinned stands versus controls (0.15 vs 0.55, N = 125) (see Bose et al., 2018). Our interpretation is that thinned trees are unconstrained from consistently investing adaptively in growth whereas being risk adverse, control trees only do so in sufficiently good weather years (see Equation 3). As risk aversion (H) and variability in weather increases, so should the relative difference in φ mean and CV, initially and then they should converge as the perceived risk to thinned individuals impacts φ. However, it is important to recognize that both thinned and control trees do respond adaptively to their circumstances, however, control trees are constrained from expressing consistent investment as discussed here.

Finally, differential volume increases between thinned and control plot trees that we observed is not guaranteed; under some conditions we would expect individual trees to allocate increased resources (via reduced competition in thinned plots) to reserves instead of increased growth thus eliminating differences among trees between plots. This may be especially true if stress is severe or long lasting (e.g., Lv et al., 2022).

ii) Does the TAG model generate stand-level overcompensation?

Figure 4 compares stand-level output over time for (non-thinned) control and for stands pre-commercially thinned at 15 years after onset. Despite a 25% reduction in tree population size at that point, the thinned population stand volume exceeds that of the control population within 5 years of thinning, clearly demonstrating overcompensation, faster than has been found empirically (see Discussion for plausible biological explanations for this quantitative discrepancy). Note, the inflection point in the growth curves sits to the left (ca. year 40) for the thinned plot versus the control plot (ca. year 60). Also, note that given sufficient time, the TAG model predicts that control stand volume will meet and exceed that of the thinned stand as the smaller number of trees in the latter express asymptotic growth though we are not aware of any data sets that are followed over sufficiently long periods to confirm this prediction.

Another way to visualize the impact of PCT is to plot relative growth for each treatment (Equation 12). This is shown in Figure 5. It is obvious that soon after PCT is applied that the thinned stand shows overcompensation, eventually by 300%. Though this value is higher than is found in nature, the qualitative pattern holds i.e., initial performance of thinned plots falls below that controls, which is followed by overcompensation, which peaks at the inflection point in the thinned plot growth curve while the control plot continues to grow at an accelerated rate for another 20 years. Eventually, control plots show higher gross volume simply because they harbor more trees.

iii) How does the size dependent growth rate shape parameter θ impact stand level productivity?

We varied θ from 0.6 to 1.4 in steps of 0.2 and plotted stand volume (m^3)over maximum lifetime of stands (200 years) that were thinned by 25% at Year 15 (Figure 6). In response, every stand produced sigmodial growth. This is not surprising since the growth model for individual trees is based upon a logistic growth curve that

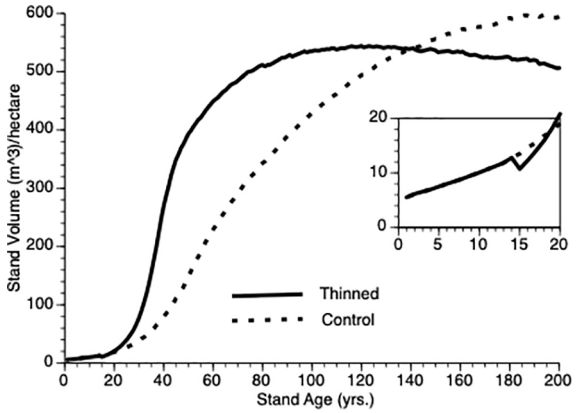

FIGURE 4
Stand volume over time from TAG simulated stands that were either subjected to pre-commercial thinning of 25% at year 15 (solid line) or left unthinned (stippled line).

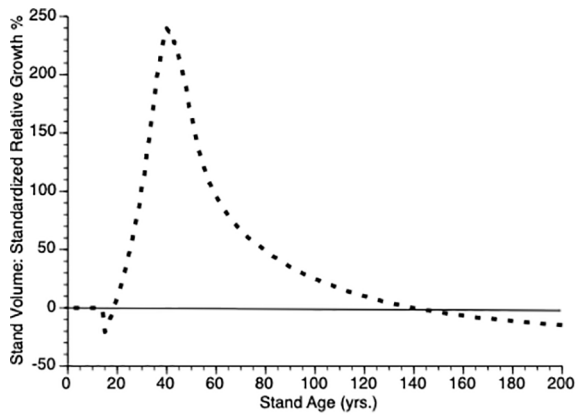

FIGURE 5
Standardized relative growth rates for stands over time from simulated stands that were either subjected to pre-commercial thinning of 25% at year 15 (stippled line) or left unthinned (solid line).

is modified by the aforementioned life history adjustments and changes in stand density. The best performing sites were those whose trees are relatively insensitive to their own tree size when such trees are small. When such trees are partially released from inter-tree competition via PCT, they gain more benefit than those trees whose growth is suppressed due to within tree competition for resources. It is not possible to directly compare the effect of this parameter for thinned trees against default control trees since the latter trees would also be affected by a change in this shape parameter. To get a sense of this parameter on the PCT effect, we compared stand volume for thinned versus control at Year = 50 for θ 0.6 vs 1.4 in both types of stands. We observed a nearly 200% increase in both cases (200% vs 190%, respectively) i.e., the PCT performance effect is relatively insensitive to the within-tree growth shape parameter though it impacts tree growth (Figure 6).

iv) Does inter-tree competition impact stand level productivity?

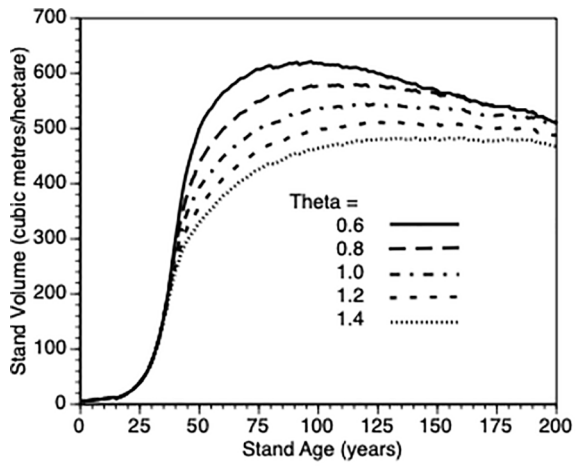

FIGURE 6
The impact of within-tree size dependent growth (θ = 0.6, 0.8. 1.0, 1.2, and 1.4) on stand volume from TAG simulated stands that were subjected to pre-commercial thinning of 25% at year 15.

To provide more insight into stand growth, the next plot (Figure 7) shows stand performance sensitivity to within-stand inter-tree competition when the shape parameter (τ') varied from 0.2 to 0.4. As expected, stand volume increased more rapidly when inter-tree competition was relaxed. As in 3.iii, it is not possible to compare directly with the default Control stands because their values would also be impacted by τ'. Further, as directly above, to get a sense of this parameter on the PCT effect, we compared stand volume for thinned versus control at Year = 50 for τ' 0.2 vs 0.4 in both types of stands. In both cases (3.0 vs 2.8., respectively) i.e., the PCT effect is relatively insensitive to the within-stand, inter-tree competition shape parameter.

v) Does the timing of thinning impact overcompensation?

Figures 8i, ii shows absolute and relative growth curves, respectively for stands at 5 levels of timing (Years 15, 30, 45, 60 and 0 (Control)). Several features can be seen: First, all plots show sigmoidal growth as expected (Figure 8i), second, all thinned plots show overcompensation (Figure 8ii) and third, plots thinned early, perform better than plots thinned late (e.g., compare year 15 vs year 45 thinned plots) both in absolute and relative terms.

vi) Does the thinning intensity impact overcompensation?

Figures 9i, ii shows absolute and relative stand level performance, respectively as a function of thinning intensity, which varies from 0 to 75% removal of the smallest trees at Year 15. Several features can be gleaned from these figures. First, as percentage culling increases there is an inverse response in terms of asymptotic value (Figure 9i). This is simply due to a smaller population of trees resulting from increased thinning, with all trees approaching their maximum size and thus the concomitant impact. Second, immediately following thinning, there is undercompensation, at the stand level, and it takes longer for stands to move into the overcompensation region under heavy thinning intensity (Figure 9ii). Finally, under heavy thinning intensity, there is a very short time window where overcompensation occurs (Figure 9ii). Again, this is due to the small number of trees in the thinned plots approaching their asymptotic size and, as such, gross volume declines slowly along with the occasional death of one of those trees.

vi) Does thinning protocol impact stand level growth?

Figure 10 compares growth in thinned and control plots when two different strategies were employed, the default removal of the smallest quartile of trees versus random removal of trees at the year of thinning. The resultant difference from these two approaches is minimal with both tactics outperforming the controls. Our reasoning for this non-obvious, minor-protocol effect is as follows: removing the smallest quartile of trees necessarily increases the mean size of the remaining trees thus reducing the competitive ability of survivors - recall that individual performance depends upon relative size (Equation 6 and section 3.iv).

4 Discussion

Compensatory growth is a well-known phenomenon for a wide variety of organisms from both the plant and animal kingdoms (e.g., lima beans (*Phaseolus lunatus*) - Bustos-Segura et al., 2022 and cattle (*Bos taurus*) - Keady et al., 2021). This includes trees both at the individual and stand level (e.g., Li et al., 2018). However, as has

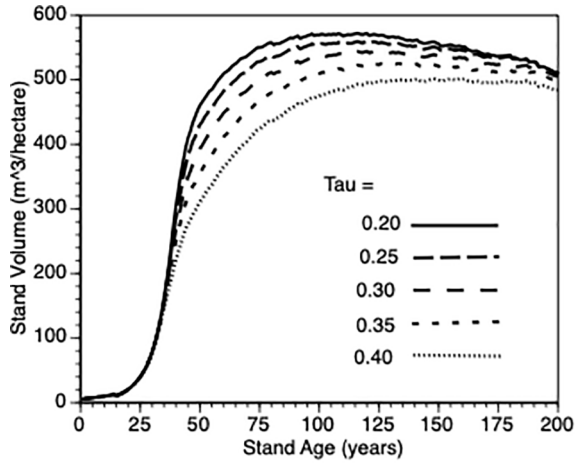

FIGURE 7
The impact of inter-tree competition when the shape parameter (τ') varied from (0.2, 0.25., 0.3, 0.35 and 0.4 - see Equation 5) on stand volume from TAG simulated stands that were subjected to pre-commercial thinning of 25%.

been noted on several occasions, the dynamics associated with compensatory growth of forests can vary dramatically depending upon intrinsic (i.e., species specific) aspects as well as site characteristics. Thus, there is a need to provide general models that can explain this phenomenon and can be used to optimize forest growth potential. In this paper, we developed a simple model of tree growth, TAG, that is based upon life history theory for long-lived trees and can be extrapolated to the forest level. Moreover, the TAG model can incorporate PCT to take advantage changes in growth in response stand density.

4.1 The model

The primary goals of this paper are: (i) as a proof of concept, develop a biologically-based theoretical model for tree and stand growth (TAG), (ii) demonstrate that the TAG model generates stand dynamics similar to that found in nature, (iii) demonstrate that stands that experience thinning can overcompensate under some conditions and (iv) explore the sensitivity of the compensatory growth to some easy-to-implement management tactics (e.g. intensity of thinning) as well as inherent characteristics of different tree species (e.g. sensitivity to crowding).

Based upon evaluation of the TAG model, the following insights emerged: (i) compensatory growth, following thinning (natural or otherwise) occurs readily especially early on in the life of a stand, (ii) the window for overcompensation narrows inversely with the intensity of PCT simply because increased performance by individuals is negated by reduced numbers of such, (iii) early PCT is beneficial because increased investment in growth is most readily observed during the accelerating part of the growth curve, (iv) results from the various sensitivity analyses were in line with expectations and (v) relative performance of thinned stands were higher than those observed in nature (see below). Finally, an important insight from employing individual trees was that the 'catching up' response of surviving trees, post-PCT (Figure 2), can be explained by such individuals gaining greater access to limiting resources and investing more of those resources into growth because it is safe to do so i.e., low risk of draining reserves. We would not have identified this crucial mechanism had we not employed an agent-based, life-history driven approach.

As shown in section 3ii, the overcompensation generated by the TAG model was nearly two to three times larger and two to five times faster, depending upon PCT treatments and site conditions, compared to observations from the Shawnigan Lake trial (Li et al., 2018), as has been observed in managed stands (Figure 4). There are several biologically plausible explanations for this discrepancy. First, values from the simple inverse relationship between crowding and growth (Equation 5) that we employed may have been too high. It is possible that other factors in the environment (Bennett et al., 2017) may ameliorate stress from crowding. Second, we employed an aspatial model, for heuristic reasons, but in doing so, we implicitly assumed a sized-biased, scramble competition for those resources that are forfeited by the now-culled trees (Kato et al., 2007). This might be a reasonable approximation for mobile organisms but it is too simplistic for sessile ones and would lead to overestimates of resource accrual within the stand (Husband and Barrett, 1996). Third, we assumed no limiting resources (e.g. nitrogen) to growth other than those competed for (e.g. energy,

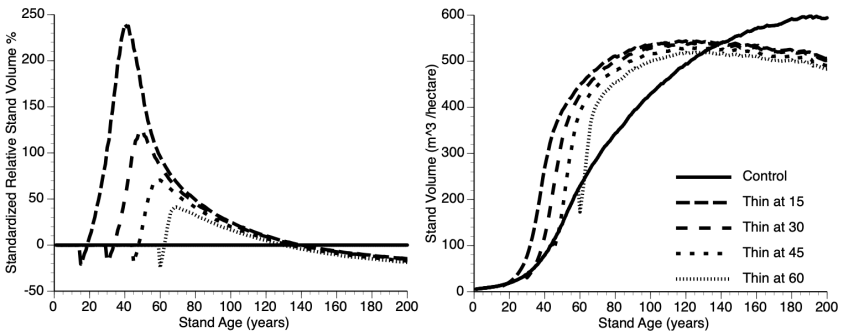

FIGURE 8
The relative (left) and absolute (right) impact of timing of thinning (Year - 15, 30, 45, 60 and Control) on stand volume from TAG simulated stands that were subjected to pre-commercial thinning of 25%.

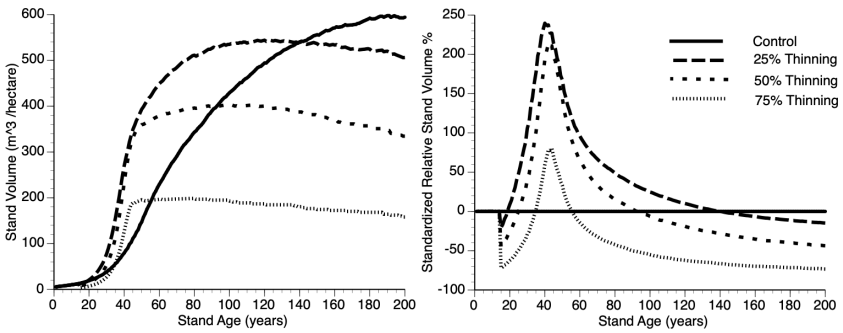

FIGURE 9
The absolute (left) and relative (right) impact of thinning (25%, 50%, 75% and Control (0%)), at Year = 15, on stand volume from TAG simulated stands that were subjected to pre-commercial thinning.

water, etc.) in the aforementioned competition. Fourth, as is often the case in heuristic models, we assumed near instantaneous access to resources that were freed up via the thinning process. Fifth, while there is an implicit effect of year-after-year stress in our model via Equations 1-3, there is no explicit assumption that long-term stress has cumulative effects, which would make compensatory response more difficult (e.g., Lv et al. 22). If any or all of the above assumptions were relaxed, that would lead to slower and less uptake of resources by trees in the thinned plots and would necessarily reduce resource harvest and the LTH allocation value for the parameter φ, which, in turn, would reduce magnitude and speed of overcompensation. Further, we assumed that survivorship would be equal in both thinned and control plots however, windthrow could increase soon after thinning, further reducing the number of trees and thus initial thinned stand productivity (Bose et al., 2018). Finally, again, for heuristic reasons, we employed simple baseline growth curves whereas further modification using specific allometric descriptors (e.g., Kramer et al., 2018) may have reduced the gap even further between thinned and control stands though we would still expect to observe the signature of overcompensation. All of these simplifications could be remedied without changing the tenor of our approach but that would reduce the generality of our model, which was the primary goal of this proof-of-concept exercise.

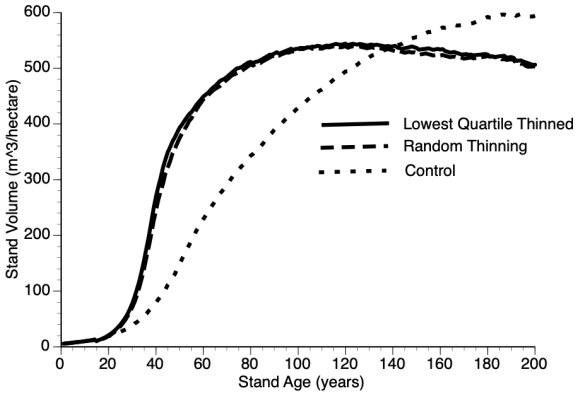

FIGURE 10
The impact of thinning protocols (smallest quartile, random removal of 25% of living trees and Control) on stand volume from TAG simulated stands that were subjected to pre-commercial thinning at year 15.

Further to the discussion above, it is possible to increase the reality of the TAG model without losing its generality however doing so would sacrifice some of its elegance. For example, suppose we wish to move from single-species to mixed-species stands; that would require that
we rewrite Equation 5 from the original

$\tau = 1 - (\frac{N_y}{N_0})^{\tau\prime}\psi$ (Equation 5) to $\tau = 1 - (\frac{\sum_{v=1}^{V} v_y}{\sum_{v=1}^{V} v_0})^{\tau\prime}\psi$ (Equation 5.1) and

Equation 6 from the original $\psi_{s,n,y} = \frac{s_{n,y}}{\bar{s}_y}$ (Equation 6) to $\psi_{s,v,n,y} = \frac{s_{v,n,y}}{\sum_{v=1}^{V} \bar{s}_{v,y}\lambda_v \frac{v}{N_y}}$ (equation 6.1).

The interpretation is that we now have accounted for those different species (or varieties) of trees of which there are V types (v = 1, 2, 3…V) each with average size s in a given year y which must be further weighted by both their interspecific competitive ability (λ_v) against the focal individual and their relative density. To account for different size classes would require another summation term that would cycle through those size classes within each tree variety.

As can be seen from this discussion, it is certainly possible to modify the TAG model to include diverse forests, however the complexity from doing so increases dramatically particularly with regard to statistical analysis and/or visualization given that we would have now added more dimensions to the problem. The same can be said for some of the other simplifications that we have employed, for example, the assumption of a non-spatial world. Even if spatial representation is included, there are practical limits to degree of resolution. For example, in Guignabert et al. (2023) spatially-explicit, forest dynamics model, seedlings were binned into size classes within $10m^2$ plots to reduce computational challenge.

At least two possible criticism of the TAG model need to be reconciled. First, TAG is generic and cannot be directly employed to make silvicultural decisions, for example, the exact amount of thinning that should be applied to a particular stand. We fully agree that this model is only the first step toward developing a comprehensive PCT silviculture system and as such we have

described it as proof of concept. At this point, we cannot say how broadly applicable TAG will be across a range of tree species an environments however most of the parameters that we employed are measurable thus it should yield testable predictions. Second, we have made a number of reasonable assumptions while deriving the TAG model some of which are untested. We hope that development of this novel theory will generate interest in parameters that until-now have garnered little attention.

On the other hand, the major contribution of the TAG model development is to confirm that a simple theoretical model can provide meaningful explanation and predict the compensatory growth phenomenon including overcompensation in post-thinning forest stands and the possibility of stand productivity enhancement. In particular, overcompensation has been difficult to understand and explain in the past but here it is seen as the simple outcome from enhanced resource access and disproportionate investment resource accrual into growth by trees in thinned plots. As we have noted, the simulation results are consistent with existing observations in both short and long term, without digging dept into very detailed physiological processes or waiting for corresponding empirical observations become available. The results presented in this paper reinforce the conclusions from the statistical approach of the TreeCG model with a verification from running the operational TASS model (Li et al., 2022b). These duel approaches can help speed up our understanding and predictability of complex forest dynamics in both natural and managed stands.

4.2 State dependence is key

A feature demonstrated in the TAG model development is the modeling approach of state-dependence (e.g., Li et al., 2020), which means that tree growth is determined by yearly changes in internal and external/environmental conditions/states, such as the internal states of tree size, age, and energy reserve, and the external states of available level of nutrients and fluctuations in weather variables. The advantage of this state-dependent modeling approach is the possible incorporation of adaptive growth/responses of trees during their long lifespan, with which the growth of trees is no longer a fixed function of tree age and site index as shown in many forest growth and yield models such as VDYP7 of BC and GYPSY of AB, Canada, but rather the results of a continuous trade-off process within a changing environment as indicated by the life-history theory. In this case, plant growth is closely related to resource capture and allocation over time (Thomas, 2002). In this paper, we finessed (i.e., no explicit optimization) state-dependent dynamic life history responses (Clark and Mangel, 2000) via the α, β and φ functions to describe the adaptive responses of individual trees to changing environment and this approach generates understandable, stand-level growth patterns. However, even using this finessed approach requires detailed calculations that take more time than that from conventional growth and yield models, but each simulation run can still be completed within a few seconds using a personal computer. The incorporation of these adaptive growth functions makes it suitable for exploring the effect of other time sensitive management operations such as fertilization and pruning, as well as addressing climate change related issues. (Note that our approach makes assumptions regarding the shape and direction of tree responses to their states. An assumption-free approach to calculating optimal response requires searching the fitness surface via backwards induction as explained by Mangel, Clark and others (Mangel and Clark 1986; McNamara and Houston, 1986). Another option for adding more realism and searching resultant complex fitness surfaces would be to employ genetic algorithms (e.g. Chubaty et al., 2013) again with the possible expense of losing some heuristics.

The state-dependent modeling approach is relatively new and unfamiliar to many foresters but promising in a sense of not only harmonizing the feature of conventional growth and yield modeling approach, but also opening the door for investigating how trees might respond to their changing environments, so as to be capable of addressing additional related issues. The state-dependent modelling approach has been widely employed in the field of behavioral ecology for representing how the behavior of animals could be explained as a result from response to specific environmental conditions. Many examples can be found from elucidating response to danger in tiny parasitoid wasps (*Asobara tabida*) (Roitberg et al., 2009) to explaining flexible torpor in insectivorous bats (Fjelldall et al., 2023) to evaluating impact of anthropogenic disturbance on adaptive foraging in beluga whales (*Delphinapterus leucas*) (McHuron et al., 2023). The research approach from behavioral ecology has recently been expanded to plants (Cahill, 2015; Simon et al., 2016), and this multi-disciplinary approach has demonstrated the benefits in enhancing our understanding of the dynamics of various ecosystems. Our current study is an example of this approach.

4.3 Future applications

The general stand growth patterns simulated by our TAG model can be widely applied as long as the growth curves from natural stands display a sigmoid shape. Thus, the calibration of this life history theory-driven TAG model could be much simplified compared to statistics-driven models such as TreeCG and hence widely applied to many jurisdictions without detailed stand growth relationships. This feature could serve as a complement to experimental approaches in a sense of providing a theoretical prediction even before implementing these experiments. As such, simulation results from carefully designed TAG model experiment could help address silviculture-effect related issues such as optimal thinning strategy leading to maximized productivity and optimal spacing in achieving the goals of stand density management, and could provide useful insights for improved field experiment designs, as well as for supporting forestry policy development and practical forest management decisions to mitigate the challenges from wood supply shortage. This modeling approach can also be applied to investigating the effect of other disturbances such as fire and insect pests, as well as other species of plants and animals with sigmoid growth pattern, especially those with long lifespans.

As an example of future applications of the TAG model, consider climate change. As a starting point, we envision the following in an

attempt to retain generality while focusing on specific problems: in our 'weather' parameter, we assumed that climate is stable and weather can be drawn from a likewise stable distribution. To deal with climate change, we would draw from two two-dimensional matrices ($\varsigma_{s,y}$ and $\varsigma_{f,y}$) based upon data from Coupled Model Intercomparison Project (CMIP6) (https://cds.climate.copernicus.eu/cdsapp#!/search?type=dataset&text=CMIP6) or similar, that assumes a changing climate rather than a stable one. The challenge in doing so will be to extrapolate change in tree growth performance as a function of changing climate.

Finally, as is the case with many theoretical studies, we have generated many new questions, especially those related to PCT and compensatory growth. A few of those include: (i) Since the adaptive compensatory growth response depends greatly up release from crowding stress, can this feature be generalized (see Equations 5 and 6) or will they be unique among species and sites? (ii) Similarly, will such stress show as simple additive functions or will they display emergent properties in mixed stands? (iii) Since climate will change necessarily advance much faster than the evolution of tree life history traits unlike short-lived plants (e.g. Acoca-Pidelle et al., 2023), can we employ models such as TAG that include contemporary tree life history values to navigate the many management obstacles that await us, at least in the near term? (iv) Can the post-thinning stand dynamics be extended to post-disturbance, including fire and post-pest-driven stand dynamics, especially if trees are incapable of distinguishing the causes of partial mortality from different types of disturbances? (Note that Arimura (2021) reviewed plants' response to herbivore elicitors that triggered plants unique defense mechanism that was identified as one of the compensatory growth mechanisms summarized by Prins and Verkaar (1992)). These are just a few of the challenges to sustainable forest management, however, the adaptive nature of tree growth presents an opportunity to develop effective dynamic strategies.

5 Conclusions

By including state dependence in an agent-based adaptive growth model (TAG), it was possible to demonstrate overcompensation by thinned stands in computer simulations. This is largely driven by thinned trees investing proportionately more of their increased resource allocation (due to reduced competition following thinning) because it adaptive to so. These results have implications for sustainable forest management.

Data availability statement

The raw data supporting the conclusions of this article will be made available by the authors, without undue reservation.

Author contributions

BR: Conceptualization, Formal analysis, Investigation, Methodology, Software, Visualization, Writing – original draft, Writing – review & editing. CL: Conceptualization, Data curation, Formal analysis, Investigation, Methodology, Project administration, Resources, Visualization, Writing – original draft, Writing – review & editing. RL: Conceptualization, Data curation, Formal analysis, Investigation, Methodology, Visualization, Writing – original draft, Writing – review & editing.

Funding

The author(s) declare financial support was received for the research, authorship, and/or publication of this article. This work was financially supported by Natural Resources Canada-Canadian Forest Service's Developing Sustainable Fibre Solutions Research Program.

Acknowledgments

The authors thank Marc Mangel for earlier discussions, Adam Dick for critical review and Dan Cooley for editorial suggestions.

Conflict of interest

The authors declare that the research was conducted in the absence of any commercial or financial relationships that could be construed as a potential conflict of interest.

Publisher's note

References

Acoca-Pidelle, S., Gauthier, P., Devresse, L., Merdrignac, A., Pons, V., and Cheptou, P.-O. (2023). Ongoing convergent evolution of a selfing syndrome threatens plant-pollinator interactions. *New Phytol.* doi: 10.1111/nph.19422

Arimura, G. (2021). Making sense of the way plants sense herbivores. *Trends Plant Sci.* 26, 288–298. doi: 10.1016/j.tplants.2020.11.001

Bennett, J. A., Maherali, H., Reinhart, K. O., Lekberg, Y., Hart, M. M., and Klironomos, J. (2017). Plant-soil feedbacks and mycorrhizal type influence temperate forest population dynamics. *Science* 355, 181–184. doi: 10.1126/science.aai8212.

Bontemps, J.-D., and Duplat, P. (2012). A non-asymptotic sigmoid growth curve for top height growth in forest stands. *Forestry*. 85, 353–368. doi: 10.1093/forestry/cps034

Bose, A. K., Weiskittel, A., Kuehne, C., Wagner, R. G., Turnblom, E., and Burkhart, H. E. (2018). Tree-level growth and survival following commercial thinning of four major softwood species in North America. *For. Ecol. Manage.* 427, 355–364. doi: 10.1016/j.foreco.2018.06.019

British Columbia Ministry of Forests, Lands, Natural Resource Operations and RuralDevelopment (2019) *Variable density yield projection*. Available online at: https://www2.gov.bc.ca/assets/gov/farming-natural-resources-and-industry/forestry/stewardship/forestanalysis-inventory/growth-yield/volume_1_vdyp_overview_2019.pdf.

Buckley, T. N., and Roberts, D. W. (2006). DESPOT, a process-based tree growth model that allocates carbon to maximize carbon gain. *Tree Phys.* 26, 129–144. doi: 10.1093/treephys/26.2.129.

Buongiorno, J., Zhu, S., Zhang, D., Turner, J., and Tomberlin, D. (2003). *The Global Forest Products Model* (Oxford, UK: Academic Press), 301. p.

Bustos-Segura, C., Gonzalez-Salaz, R., and Benrey, B. (2022). Early damage enhances compensatory responses to herbivory in wild lima bean. *Front. Plant Sci.* 13. doi: 10.3389/fpls.2022.1037047

Cahill, J. F. (2015). Introduction to the Special Issue: beyond traits: integrating behaviour into plant ecology and biology. *AoB Plants* 7, plv120. doi: 10.1093/aobpla/plv120

Chubaty, A., Ma, B. O., Stein, R. W., Gillespie, D. R., Henry, L. M., Phelan, C., et al. (2013). On the evolution of omnivory in a community context. *Ecol. Evol.* 4, 251–265. doi: 10.1002/ece3.923

Clark, C. W. (1994). Antipredator behavior and the asset-protection principle. *Behav. Ecol.* 5, 159–170. doi: 10.1093/beheco/5.2.159

Clark, C. W., and Mangel, M. (2000). *Dynamic state variable models in ecology—methods and applications* (New York: Oxford University Press). doi: 10.1093/oso/9780195122664.001.0001.

Davies, N. B., and Krebs, J. R. (1993). *An Introduction To Behavioural Ecology* (Cambridge, UK: Wiley-Blackwell Scientific Publications).

Davis, L. S., Johnson, K. N., Bettinger, P., and Howard, T. E. (2001). *Forest Management: To Sustain Ecological, Economic, and Social Values. 4th Edition* (Long Grove, Illinois: Waveland Press, Inc), 804. pp.

Del Giudice, M., Gangestad, S. W., and Kaplan, H. S. (2015). "Life history theory and evolutionary psychology," in *The handbook of evolutionary psychology –Vol 1: Foundations, 2nded*. Ed. M. Buss (Hoboken, New Jersey, USA: Wiley), 88–114.

Elfstrom, I. M., and Powers, M. D. (2023). Effects of thinning on tradeoffs between drought resistance, drought resilience, and wood production in mature Douglas-fir in western Oregon, USA. *Can. J. For. Res.* 53, 605–619. doi: 10.1139/cjfr-2022-0235.

Fjellddall, M. A., Muller, A. S., Ratikainen, I. I., Stawski, C., and Wright, J. (2023). The small-bat-in-summer behavioural routines of bats investigated through a stochastic dynamic model. *J. Anim. Ecol.* 92, 2078–2083. doi: 10.1111/1365-2656.13999

Grafen, A. (1984). *Behavioural ecology: an evolutionary approach. 2nd edn*. Eds. J. R. Krebs and N. B. Davies (Oxford: Blackwell Scientific Publications), 62–84).

Guignabert, A., Ponette,, André, F., Messier, C., Nolet, P., and Jonard, M. (2023). Validation of a new spatially explicit process-based model (HETEROFOR) to simulate structurally and compositionally complex forest stands in eastern North America. *Geosci. Model. Dev.* 16, 1661–1682. doi: 10.5194/gmd-16-1661-2023

Harshman, L. G., and Zera, A. J. (2007). The cost of reproduction: the devil in the details. *Trends Ecol. Evol.* 22, 80–86. doi: 10.1016/j.tree.2006.10.008

Huang, S., Meng, S. X., and Yang, Y. (2009). *A growth and yield projection system (GYPSY) for natural and post-harvest stands in Alberta* (Edmonton, Alberta, Canada: Alberta Sustainable Resource Development).

Huang, S., Morgan, D., Klappstein, G., Heidt, J., Yang, Y., and Greidanus, G. (2001). *GYPSY: A growth and yield projection system for natural and regeneratedstands within an ecologically based, enhanced forest management framework* (Edmonton, Alberta, Canada: Alberta Sustainable Resource Development). doi: 10.5962/bhl.title.116092.

Hubbard, R. M., Bond, B. J., and Ryan, M. G. (1999). Evidence that hydraulic conductance limits photosytnthesis in old *Pinus ponderosa* trees. *Tree Physiol.* 19, 165–172. doi: 10.1093/treephys/19.3.165.

Husband, B. C., and Barrett, S. C. H. (1996). A metapopulation perspective in plant population biology. *J. Ecol.* 84, 461–469. doi: 10.2307/2261207.

Johnstone, W. D. (1976). *Variable-density yield tables for natural stands of lodgepole pine in Alberta* Vol. 20 (Ottawa, ON: Can. For. Serv., Dept. Fish. Environ. For. Tech. Rep).

Johnstone, W. D. (1985). "Thinning lodgepole pine," in *Lodgepole Pine: the Species and its Management. Symposium Proceedings*. Eds. D. M. Baumgartner, R. G. Krebill, J. T. Arnott and G. F. Weetman (Washington State Univ., Pullman, WA), 253–262.

Kassaby, Y. A., and Barclay, H. J. (1992). Cost of reproduction in Douglas-fir. *Can. J. Bot.* 70, 1429–1432. doi: 10.1139/b92-179.

Kato, N., Oharu, S., and Shitaoka, K. (2007). Size-structured plant population models and harvesting problems. *J. Comp. Appl. Math.* 204, 114–123. doi: 10.1016/j.cam.2006.04.056.

Keady, S. M., Keane, M. G., Waters, S. M., Wylie, A. R., O'Riorda, E. G., Keough, K., et al. (2021). Effect of dietary restriction and compensatory growth on performance, carcass characteristics, and metabolic hormone concentrations in Angus and Belgian Blue steers. *Animal.* 15, 100215. doi: 10.1016/j.animal.2021.100215

Kramer, R. D., Sillett, S. C., and Van pelt, R. (2018). Quantifying aboveground components of *Picea sitchensis* for allometric comparisons among tall conifers in North American rainforests. *For. Ecol. Manage.* 430, 59–77. doi: 10.1016/j.foreco.2018.07.039

Lalonde, R., and Roitberg, B. (1992). On the evolution of masting behaviour in trees: Predation or weather? *Am. Nat.* 139, 1293–1304. doi: 10.1086/285387

Lanner, R. M., and Connor, K. F. (2001). Does bristelcone pine senesce? *Exper. Gerentol.* 36, 675–685. doi: 10.1016/S0531-5565(00)00234-5

Lee, W.-H. S., Metcalfe, N. B., Monaghan, P., and Mangel, M. (2011). A comparison of dynamic-state-dependent models of the trade-off between growth, damage, and reproduction. *Am. Nat.* 178, 774–786. doi: 10.1086/662671.

Leuschner, W. A. (1984). *Introduction to Forest Resource Management* (Malabar, Florida: John Wiley and S?os, Inc. Krieger Publishing Company), 298. pages.

Li, C., Barclay, H., Huang, S., Roitberg, B., Lalonde, R., and Thiffault, N. (2022a). Detecting compensatory growth in silviculture trials: empirical evidence from three case studies across Canada. *Front. Plant Sci.* 13. doi: 10.3389/fpls.2022.907598

Li, C., Barclay, H., Huang, S., Roitberg, B., Lalonde, R., Xu, W., et al. (2022b). Modelling the stand dynamics after a thinning induced partial mortality: A compensatory growth perspective. *Front. Plant Sci.* 13. doi: 10.3389/fpls.2022.1044637

Li, C., Barclay, H., Roitberg, B., and Lalonde, R. (2020). Forest productivity enhancement and compensatory growth: a review and synthesis. *Front. Plant Sci.* 11. doi: 10.3389/fpls.2020.575211

Li, C., Barclay, H., Roitberg, B., and Lalonde, R. (2021). Ecology and prediction of compensatory growth: from theory to application in forestry. *Front. Plant Sci.* 12. doi: 10.3389/fpls.2021.655417

Li, C., Huang, S., Barclay, H., and Filipescu, C. N. (2018). Estimation of compensatory growth of coastal Douglas-fir following pre-commercial thinning across a site quality gradient. *For. Ecol. Manage.* 429, 308–316. doi: 10.1016/j.foreco.2018.07.028

Lv, P., Rademacher, T., Huang, X., Zhang, B., and Zhang, X. (2022). Prolonged drought duration, not intensity, reduces growth recovery and prevents compensatory growth of oak trees. *Agric. For. Meteorol.* 326. doi: 10.1016/j.agrformet.2022.109183

Mangel, M., and Clark, C. W. (1986). Towards a unified forging theory. *Ecology* 67, 1127–1138. doi: 10.2307/1938669.

Mangel, M., and Munch, S. B. (2005). A life-history perspective on short- and long-term consequences of compensatory growth. *Am. Nat.* 166, E155–E176. doi: 10.1086/444439

McHuron, E. A., Castellote, M., Boor, H., Shelden, K. E. W., Warlick, A. J., MCGuire, T. L., et al. (2023). Modeling the impacts of a changing and disturbed environment on an endangered beluga whale population. *Ecol. Model.* 483, 110417. doi: 10.1016/j.ecolmodel.2023.110417

McKenney, D. W. (2000). What's the economics of intensive silviculture? *For. Chron.* 76, 275–281. doi: 10.5558/tfc76275-2.

McNamara, J. M., and Houston, A. I. (1986). The common currency for behavioral decisions. *Am. Nat.* 127, 358–378. doi: 10.1086/284489.

Pitt, D., and Lanteigne, L. (2008). Long-term outcome of precommercial thinning in northwestern New Brunswick: growth and yield of balsam fir and red spruce. *Can. J. For. Res.* 38, 592–610. doi: 10.1139/X07-132

Prins, A. H., and Verkaar, H. J. (1992). "Defoliation: do physiological and morphological responses lead to (over)compensation?," in *Pests and Pathogens: Plant Responses to Foliar Attack*. Ed. P. G. Ayres (The University of Michigan, Ann Arbor: Environmental plant biology). BIOS), 13–31. Available at: https://edepot.wur.nl/375837.

Qiu, T., Aravena, M., and Clark, J. S. (2021). Is there tree senescence? The fecundity evidence. *Proc. Nat. Acad. Sci.* 118, e2106130118. doi: 10.1073/pnas.2106130118

Reukema, D. L. (1975). *Guidelines for precommercial thinning of Douglas-fir. General Technical Report PNW 30* Vol. 10 (Portland, OR: USDA For. Serv., PNW, For. Rng. Exp. Sta. P).

Roitberg, B. D., Zimmerman, K., and Hoffmeister, T. H. (2009). Dynamic response to danger in a parasitoid wasp. *Behav. Ecol. Sociobiol.* 64, 627–637. doi: 10.1007/s00265-009-0880-9

Sherman, D. A., Dahlgren, J. P., Ehrlen, J., and Garcia, M. B. (2019). Sex and the cost of reproduction through the life course of an extremely long-lived herb. *Oecol.* 191, 369–375. doi: 10.1007/s00442-019-04491-0

Simon, F. W., Hodson, C. N., and Roitberg, B. D. (2016). State dependence, personality, and plants: light-foraging decisions in *Mimosa pudica* (L.). *Ecol. Evol.* 6, 6301–6309. doi: 10.1002/ece3.2340

Sohn, J. A., Brooks, J. R., Bauhus, J., Kohler, M., Kolb, T. E., and McDowell, N. G. (2014). Unthinned slow-growing ponderosa pine (Pinus ponderosa) trees contain muted isotopic signals in tree rings as compared to thinned trees. *Trees* 28, 1035–1051. doi: 10.1007/s00468-014-1016-z.

Stearns, S. C. (2000). Life history evolution: successes, limitations, and prospects. *Naturwiss.* 87, 476–486. doi: 10.1007/s001140050763.

Steele, R. W. (1955). Growth after precommercial thinning in two stands of Douglas-Fir. *USDA For. Serv. Res. Note PNW-117* 6, 1–4.

Stephenson, N. L., Das, A. J., and Zavala, M. A. (2014). Rate of tree carbon accumulation increases continuously with tree size. *Nature* 507, 90–93. doi: 10.1038/nature12914

Suzuki, M., Umeki, K., Orman, O., Shibata, M., Tanaka, H., Iida, S., et al. (2019). When and why do trees begin to decrease their resource allocation to apical growth? The importance of reproductive onset. *Oecol.* 191, 39–49. doi: 10.1007/s00442-019-04477-y

Thomas, H. (2002). Ageing in plants. *Mech. Ageing Dev.* 123, 747–753. doi: 10.1016/S0047-6374(01)00420-1.

Weiner, J., and Thomas, S. C. (2001). The nature of tree growth and the 'A'ge-related decline in forest productivity". *Oikos* 94, 374–376. doi: 10.1034/j.1600-0706.2001.940219.x.

Zeide, B. (2011). Thinning and growth: a full turnaround. *J. Forest.* 99, 20–25. doi: 10.1093/jof/99.1.20

Frontiers in Plant Science

Cultivates the science of plant biology and its applications

The most cited plant science journal, which advances our understanding of plant biology for sustainable food security, functional ecosystems and human health.

Discover the latest Research Topics

See more →

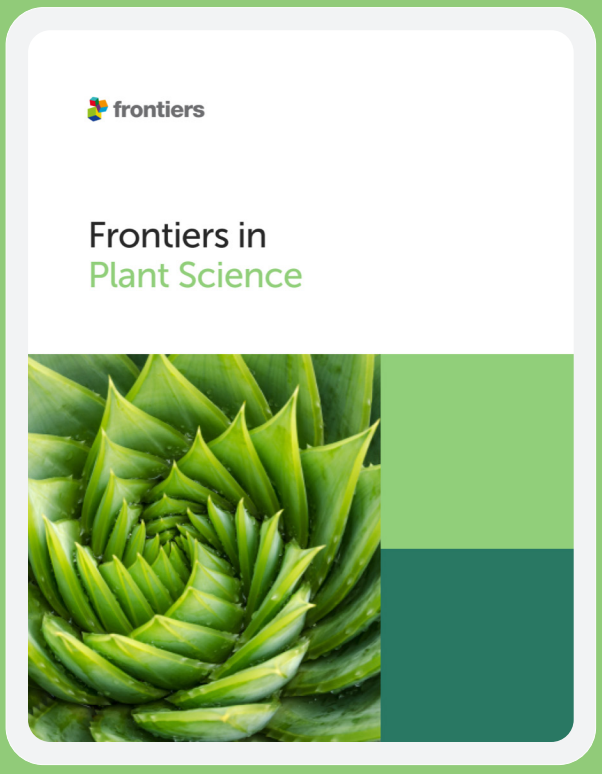

Frontiers

Avenue du Tribunal-Fédéral 34
1005 Lausanne, Switzerland
frontiersin.org

Contact us

+41 (0)21 510 17 00
frontiersin.org/about/contact